Interplay of Notch, BCR, and CD40 signaling during B cell differentiation, activation, and lymphomagenesis

Dissertation der Fakultät für Biologie

der Ludwig-Maximilians-Universität München

zur Erlangung des Doktorgrades

Franziska Hampel

April 2010

To Thomas

& my parents

Erklärung

Diese Dissertation wurde von Mai 2007 bis April 2010 am Institut für Klinische Molekularbiologie und Tumorgenetik des Helmholtz Zentrums München in der Arbeitsgruppe von PD Dr. Ursula Zimber-Strobl erstellt und von Prof. Dr. Dirk Eick betreut.

Eidesstattliche Versicherung

Hiermit erkläre ich, Franziska Hampel, geboren am 7. April 1982 in Fürstenfeldbruck, ehrenwörtlich, dass ich die vorliegende Arbeit selbständig und nur unter Verwendung der angegebenen Hilfsmittel und Quellen angefertigt habe.

München, den 13. April 2010

Franziska Hampel

Erstgutachter: Prof. Dr. Dirk Eick
Zweitgutachterin: Prof. Dr. Elisabeth Weiß

Tag der Einreichung: 13. April 2010
Tag der mündlichen Prüfung: 1. Oktober 2010

TABLE OF CONTENTS

Table of contents ..... **I**

List of figures ..... **V**

List of tables ..... **V**

List of abbreviations ..... **VI**

1 INTRODUCTION **1**

1.1. The immune system **1**

1.1.1 T cell development 1

1.1.2 Early B cell development 2

1.1.3 Late B cell development – Marginal zone versus follicular B cell differentiation 3

1.1.4 B cell activation 5

1.2 Central signaling pathways in B lymphocytes **6**

1.2.1 CD40 receptor signaling 7

1.2.2 NF-κB signaling 7

1.2.3 B cell receptor signaling 9

1.3 The role of the Notch pathway in lymphocytes **11**

1.3.1 The Notch signaling cascade 11

1.3.2 Notch signaling in lymphocytes 13

1.3.3 The role of Notch in marginal zone B cell development 13

1.3.4 Notch signaling in lymphomagenesis 15

1.4 Interplay of signaling pathways in B cell lymphomas **16**

1.5 Model systems **17**

1.5.1 The Notch1/2IC-expressing EREB2.5 cell lines 17

1.5.2 The LMP1/CD40-transgenic mouse strain 19

1.5.3 The Igβ-deficient mouse strain 19

2 GOAL **21**

3 RESULTS **22**

3.1 Comparison of Notch1IC, Notch2IC, and EBNA2 target genes in B cells *in vitro* **22**

3.1.1 The experimental setting 22

3.1.2 Notch1/2 lead to cell cycle entry due to the induction of cell cycle-associated genes 22

3.1.3 Differential expression of pro-apoptotic and anti-apoptotic genes in Notch1IC-, Notch2IC-, and EBNA2-expressing B cells 24

3.2 The role of Notch2 in B cell differentiation *in vivo* 27
3.2.1 Generation of a transgenic mouse line conditionally expressing Notch2IC 27
3.2.2 Notch2IC protein is translocated into the nucleus and is functional in B cells of Notch2IC//CD19Cre$^{+/-}$ mice 32
3.2.3 Early B cell development is blocked in Notch2IC//mb1Cre$^{+/-}$ mice 33
3.2.4 Notch2IC expression dependent on mb1-*Cre* causes an aberrant T cell-like differentiation in the bone marrow 34
3.2.5 Early B cell development is normal in Notch2IC//CD19Cre$^{+/-}$ mice 37
3.2.6 Marginal zone B cells are the dominant B cell population in Notch2IC//CD19Cre$^{+/-}$ mice 38
3.2.7 Notch2IC-expressing B cells are located in the marginal zone and display a pre-activated phenotype 43
3.2.8 Analysis of marginal zone B cell precursors in Notch2IC//CD19Cre$^{+/-}$ mice 45
3.2.9 Notch2IC//CD19Cre$^{+/-}$ B cells are hyper-responsive to LPS and α-CD40 stimulation *in vitro* but do not form germinal centers 47
3.2.10 Signaling pathways active in Notch2IC//CD19Cre$^{+/-}$ B cells 50
3.2.11 Constitutive Notch2 signaling overcomes CD19 deficiency during marginal zone B cell differentiation 53

3.3 The role of B cell receptor signaling in LMP1/CD40-activated B cells 58
3.3.1 Genetic ablation of Igβ in LMP1/CD40-transgenic mice 58
3.3.2 Constitutive CD40 signaling rescues Igβ-deficient B cells to a certain extent 59
3.3.3 LMP1/CD40//Igβ$^{\Delta GFP/\Delta}$ B cells display an activated phenotype 60
3.3.4 LMP1/CD40 expression prolongs the survival of Igβ-deficient B cells *in vitro* and *in vivo* 61
3.3.5 Analysis of signaling pathways in LMP1/CD40//Igβ$^{\Delta GFP/\Delta}$ B cells 63

4 DISCUSSION 67

4.1 Notch1/2IC activate proliferation-associated as well as pro-apoptotic genes in human B cells *in vitro* 67

4.2 Constitutive Notch2 signaling is instructive for marginal zone B cell differentiation *in vivo* 69
4.2.1 Notch2IC expression dependent on mb1-*Cre* blocks early B cell differentiation and leads to ectopic T cell development in the bone marrow 69
4.2.2 Notch2IC expression dependent on CD19-*Cre* induces marginal zone B cell differentiation at the expense of follicular B cells 71

4.2.3 The basal activity of the non-canonical NF-κB pathway is reduced in Notch2IC-expressing B cells 74
4.2.4 Notch2IC//CD19Cre$^{+/-}$ B cells display high c-Myc levels as well as enhanced MAPK and PI3K/Akt activity 75
4.2.5 Constitutive Notch2 signaling acts independently of CD19 during marginal zone B cell development 76
4.3 Activation of Notch signaling itself is not sufficient to induce B cell lymphomagenesis 77
4.4 Ablation of BCR signaling abrogates LMP1/CD40-mediated B cell expansion *in vivo* 79
5 SUMMARY 82
6 ZUSAMMENFASSUNG 84
7 MATERIAL 86
7.1 Plasmids 86
7.2 Bacteria 87
7.3 Cell lines 87
7.4 Mouse strains 88
7.5 DNA probes for Southern blotting 88
7.6 Oligonucleotides 89
7.7 Enzymes 90
7.8 Antibodies 91
7.9 Software 91
8 METHODS 92
8.1 Cell culture methods 92
8.1.1 Culture of EREB2.5 cells 92
8.1.2 Preparation of embryonic fibroblasts 92
8.1.3 Culture of embryonic fibroblasts 93
8.1.4 Culture of embryonic stem cells (ES cells) 93
8.1.5 Freezing and thawing of cells 94
8.1.6 Transfection of ES cells 94

8.1.7 Selection and expansion of stably transfected ES cell clones 95

8.2 Mice-associated methods 97

8.2.1 Mouse breeding 97

8.2.2 Isolation of primary lymphocytes 97

8.2.3 Flow Cytometry (FACS) 98

8.2.4 *In vitro* culture of primary lymphocytes 98

8.2.5 *In vivo* 5-bromo-2´-deoxyuridine (BrdU) assay 99

8.2.6 Immunization of mice 99

8.2.7 Enzyme-linked immunosorbent assay (ELISA) 99

8.2.8 Immunohistochemistry 100

8.3 Standard methods of molecular biology 101

8.3.1 DNA isolation 101

8.3.2 DNA analysis 103

8.3.3 Southern blotting (Southern *et al.*, 1997) 104

8.3.4 Cloning 105

8.3.5 RNA analysis 105

8.3.6 Protein detection 109

9 REFERENCES 111

10 APPENDIX 120

Supplementary Data 120

Acknowledgement 122

Curriculum Vitae 124

Publications 125

List of figures

Figure 1 Immunohistochemical analysis of a murine splenic cryosection ... 4
Figure 2 Simplified illustration of CD40 signaling ... 8
Figure 3 Simplified illustration of B cell receptor (BCR) signaling ... 10
Figure 4 Notch primary structure and signaling cascade ... 12
Figure 5 Generation of EBV-transformed B cell lines expressing doxycycline-regulable, human Notch1IC or Notch2IC (Kohlhof *et al.*, 2009) ... 18
Figure 6 Targeting strategy for the generation of the conditional Igβ-deficient mouse strain ... 20
Figure 7 Experimental design for kinetic experiments with Notch1IC/EREB, Notch2IC/EREB, and CAT/EREB cells ... 23
Figure 8 Differentially expressed cell cycle- and proliferation-associated genes in Notch1IC/EREB, Notch2IC/EREB, CAT/EREB, and EBNA2/EREB cells ... 25
Figure 9 Differential expression of pro-apoptotic and anti-apoptotic genes in Notch1IC/EREB, Notch2IC/EREB, CAT/EREB, and EBNA2/EREB cells ... 26
Figure 10 Targeting strategy for the generation of Notch2IC^{flSTOP} mice ... 28
Figure 11 Southern blot analyses of targeted and wild type ES cell clones ... 30
Figure 12 Functional testing of targeted ES cell clones for hCD2 expression ... 31
Figure 13 Blastocyst injection and establishment of the Notch2IC^{flSTOPP} mouse strain ... 32
Figure 14 Notch2IC protein is expressed, translocated into the nucleus, and functional in B cells of Notch2IC//CD19Cre$^{+/-}$ mice ... 33
Figure 15 Early B cell development is blocked in Notch2IC//mb1Cre$^{+/-}$ mice ... 34
Figure 16 hCD2^{+} bone marrow cells from Notch2IC//mb1Cre$^{+/-}$ display a CD8^{+}, CD4^{+}, CD43^{+}, CD5^{+}, Thy1.2^{+}, CD3^{low} phenotype ... 35
Figure 17 Notch2IC//mb1Cre$^{+/-}$ mice show T cell expansion in the bone marrow, but have reduced B cell numbers in the bone marrow and the spleen. ... 36
Figure 18 Early B cell development is normal in Notch2IC//CD19Cre$^{+/-}$ mice. ... 38
Figure 19 Slight splenomegaly, but normal splenic cell numbers in Notch2IC//CD19Cre$^{+/-}$ mice. ... 39
Figure 20 Marginal zone B cells are expanded in Notch2IC//CD19Cre$^{+/-}$ mice to the expense of the follicular B cell population ... 40
Figure 21 Notch2IC//CD19Cre$^{+/-}$ mice harbor reduced B cells in the peritoneal cavity and show a preferential loss of B1a cells ... 42
Figure 22 Notch2IC-expressing B cells are predominantly located in the marginal zone ... 44
Figure 23 Notch2IC//CD19Cre$^{+/-}$ B cells show an enhanced expression of marginal zone B cells markers and display an activated phenotype. ... 45
Figure 24 Analysis of marginal zone B cell precursor cells ... 47
Figure 25 Notch2IC//CD19Cre$^{+/-}$ B cells are hyper-responsive to LPS and α-CD40 stimulation *in vitro*. ... 48
Figure 26 Notch2IC//CD19Cre$^{+/-}$ B cells do not form germinal centers ... 50
Figure 27 Reduced basal non-canonical NF-κB activity in Notch2IC-expressing B cells ... 51
Figure 28 Notch2IC//CD19Cre$^{+/-}$ B cells show high c-Myc levels as well as an enhanced activation of Akt and the MAP kinases Erk and Jnk ... 52
Figure 29 Notch2IC induces marginal zone B development despite the absence of CD19 ... 54
Figure 30 CD19-deficient, Notch2IC-expressing B cells are pre-activated and hyper-responsive and show increased MAPK activation as well as c-Myc levels ... 57
Figure 31 Constitutive CD40 signaling rescues Igβ-deficient B cells to a certain extent ... 59
Figure 32 LMP1/CD40//Igβ$^{\Delta GFP/\Delta}$ B cells display an activated phenotype ... 60
Figure 33 Constitutive CD40 signaling prolongs the life-span of Igβ-deficient B cells ... 62
Figure 34 Enhanced non-canonical NF-κB activity is maintained LMP1/CD40//Igβ$^{\Delta GFP/\Delta}$ B cells ... 64
Figure 35 Activation of the MAPK Erk and Jnk is maintained LMP1/CD40//Igβ$^{\Delta GFP/\Delta}$ B cells ... 65
Figure 36 LMP1/CD40//Igβ$^{\Delta GFP/\Delta}$ B cells maintain basal phosphorylation of Akt kinase, but show reduced levels of c-Myc ... 66
Figure 37 A sequential model for marginal zone B cell development ... 72

List of tables

Table 1 B cell populations with deletion efficiencies in the bone marrow of Notch2IC//mb1Cre$^{+/-}$ and control mice ... 35
Table 2 Percentages of hCD2^{+} cells in organs of Notch2IC// mb1Cre$^{+/-}$ mice with respective percentages of B220^{+} B cells and Thy1.2^{+} T cells within the hCD2^{+} population ... 37
Table 3 B cell populations with deletion efficiencies in Notch2IC//CD19Cre$^{+/-}$ and control mice ... 41
Table 4 B cell populations with deletion efficiencies in Notch2IC//CD19Cre$^{+/+}$ and CD19Cre$^{+/+}$ control mice ... 56
Table 5 Deletion efficiencies measured from the percentage of GFP expression in B cells from spleen, inguinal lymph node, and peritoneal cavity ... 60

List of abbreviations

α	anti
A	adenine
AID	activation-induced cytidine deaminase
APC	allophycocyanin
APS	ammonium persulfate
BAFF	B cell-activating factor
B-CLL	B cell chronic lymphoblastic leukemia
BCR	B cell receptor
BrdU	5-bromo-2´-deoxyuridine
BM	bone marrow
bp	base pairs
BSA	bovine serum albumin
BTK	Burton's tyrosine kinase
C	cytosine
C-	carboxy
CCN	cyclin
CAT	chloramphenicol acetyl transferase
CD	cluster of differentiation
CDK	cyclin-dependent kinase
cDNA	copy DNA
CFSE	5-(and 6)-carboxyl fluorescein diacetate N-succinimidyl ester
CGG	chicken gamma globulin
CLP	common lymphoid progenitor
CMP	common myeloid progenitor
CMV	cytomegalovirus enhancer
cp.	compare
CP	crossing point
Cre	protein recombinase of the phage *P1* ("Causes Recombination")
Ctrl	control
d	day
D_H	diversity region of the immunoglobulin heavy chain locus
DMEM	Dulbecco's modified Eagle medium
DMSO	dimethyl sulfoxide
DN	double negative
DNA	deoxyribonucleic acid
DNAse	deoxyribonuclease
dNTP	deoxyribonucleotide triphosphate
DP	double positive
EBF	early B cell factor
EBNA	EBV nuclear antigen
EBV	Epstein-Barr virus
EC	extracellular
EDTA	ethylene diamine tetra acetate
ELISA	enzyme-linked immunosorbent assay
Erk	extracellular signal-regulated kinase
ES cells	embryonic stem cells
et al.	"et alii"
FACS	fluorescence-activated cell sorting
FCS	fetal calf serum
Fig.	figure
FITC	fluorescein isothiocyanate

Fo	follicular
FSC	forward scatter
G	guanine
g	gram
G418	geneticin
x g	x fold acceleration of gravity
GAPDH	glyceraldehyde 3-phosphate dehydrogenase
GC	germinal center
GFP	green fluorescent protein
h	hour
HEPES	4-2-hydroxyethyl 1-piperazine ethanesulfonic acid
HL	Hodgkin lymphoma
HRP	horseradish peroxidase
i	inguinal
IC	intracellular
ICAM	intercellular adhesion molecule
Ig	immunoglobulin
Igα/β	immunoglobulin-associated signaling molecule α and β, respectively
Igμ/δ	immunoglobulin heavy chain of class μ and δ, respectively
IgH	immunoglobulin heavy chain
IgL	immunoglobulin light chain
IκBα	inhibitor of NF-κBα
iLN	inguinal lymph node
IL	interleukin
IRES	internal ribosomal entry site
ITAM	immunoreceptor tyrosine-based activation motif
J_H	joining region of the immunoglobulin heavy chain locus
JAK	Janus kinase
Jnk	c-Jun N-terminal kinase
kb	kilobase
kDa	kilodalton
LIF	leukemia inhibitory factor
LMP	latent membrane protein
LPS	lipopolysaccharide
loxP	locus of crossing-over (x) of phage *P1*
m	murine
M	molar
MACS	magnetic cell separation
MAPK	mitogen-activated protein kinase
MHC	major histocompatibility complex
MINT	Msx2-interacting nuclear target protein
ml	milliliter
MOMA	monocytes, macrophages
MOPS	4-morpholino propanesulphonic acid
mRNA	messenger RNA
MZ	marginal zone
μF	microfaraday
N-	amino
NaAc	sodium acetate
NF-κB	nuclear factor κ B
NK cell	natural killer cell
NLS	nuclear localization sequence

nm	nanometer
NotchIC	intracellular part of the Notch receptor/activated Notch
NP	4-hydroxy-3-nitrophenylacetyl
n.s.	non-specific
nt	nucleotide
PAA	polyacrylamide
PAGE	polyacrylamide gel electrophoresis
PBS	phosphate-buffered saline
PCR	polymerase chain reaction
PE	phycoerythrin
PerCP	peridinin chlorophyll protein
PI	propidium iodide
Pten	phosphatase with tensin homology
PVDF	polyvinyliden fluoride
qPCR	quantitative real-time poly chain reaction
R	ratio
RBP-Jκ	recombination signal binding protein for immunoglobulin kappa J region
RNA	ribonucleic acid
RNAse	ribonuclease
rpm	rounds per minute
RT	room temperature
SA-AP	streptavidin-coupled alkaline phosphatase
SDS	sodium dodecyl sulfate
sec.	second
SHM	somatic hypermutation
SP	spleen
SSC	side scatter
T1, 2, 3	type 1, 2, 3
Tab.	table
TAE	Tris acetate EDTA
TCR	T cell receptor
TEMED	N,N,N`,N`-tetramethylene diamine
TD	T cell-dependent
TdT	terminal deoxynucleotidyl transferase
TE	Tris EDTA
T_H cell	helper T cell
TI	T cell-independent
TNFR	tumor necrosis factor receptor
TRAF	TNF receptor-associated factor
U	units
UTR	untranslated region
UV	ultraviolet light
V	volt
V_H	variable region of the immunoglobulin heavy chain locus
v/v	volume per volume
w	weeks
w/o	without
wt	wild type
w/v	weight per volume

1 Introduction

1.1. The immune system

Defense against a vast range of different pathogens encountering an individual during its lifetime is accomplished through the well coordinated action of the innate and adaptive branches of the immune system. Innate immunity provides a rapid and relatively unspecific first response to pathogens. In contrast, adaptive immunity contributes features as individual antigen specificity, self-non-self discrimination, receptor diversity, and immunological memory to a pathogen. In mammals, all cells of the immune system are derived from pluripotent stem cells and they develop during hematopoiesis in the bone marrow in adults. Hematopoietic stem cells differentiate either into myeloid or lymphoid progenitor cells. Myeloid progenitors are the precursors of granulocytes and macrophages, which play a major role within the innate branch of the immune system. Common lymphoid progenitors either give rise to B and T lymphocytes or to natural killer (NK) cells. Whereas NK cells are also considered to be part of innate immunity, B and T cells are key players of the adaptive arm of the immune system. Via a series of sequential differentiation steps and selection processes, B and T lymphocytes acquire unique variants of antigen receptors that are not self-reactive, but highly specific for a certain antigen. Thus, the lymphocyte population of an individual harbors a large repertoire of receptors that are highly diverse in their antigen binding site. An adaptive immune response is subdivided into humoral and cell-mediated immunity. The latter is performed by specialized cytotoxic T cells and is risen against intracellular pathogens, such as viruses, as well as against aberrant cells of the body, like tumor cells. Humoral immune response is based on the effect of antigen-specific antibodies, which are secreted by antigen-activated B cells. Additionally, a set of plasma proteins known as the complement system enhances recognition and destruction of encountered pathogens. As the expansion of cell populations in response to antigens followed by subsequent downregulation of the response occur permanently in the immune system, a tight control of these processes is essential to prevent dangerous developments such as autoimmunity or cellular transformation.

1.1.1 T cell development

Lymphocyte development is initiated in the bone marrow with the commitment of a hematopoietic stem cell to a common lymphoid precursor cell (CLP), which may give rise to B and T lymphocytes or NK cells. CLPs that receive signals via the Notch1 receptor are committed to the T cell lineage and migrate to the thymus, where they further develop into T cells before emigrating to the periphery. The earliest stages of immature T cells are designated as double negative (DN), as these cells lack the expression of both the T cell receptor (TCR) and the co-

receptor molecules CD4 and CD8. Via a series of sequential differentiation steps, the rearrangement of the TCR genes occurs over four stages (DN1-4) that are differentiated based on their CD25 and CD44 surface expression. T lymphocytes are distinguished into αβ or γδ T cells, depending on whether their TCR is formed by αβ or γδ chains. The β, γ, and δ TCR loci rearrange almost simultaneously during DN2 to 3 stages and the decision that a precursor commits to the αβ or γδ lineage is thought to depend on whether a functional γδ receptor is produced before a functional β chain, which can pair with a pTα to form the pre-TCR (βpTα). Mostly, αβ T cells are generated. At a checkpoint known as β-selection, only DN3 cells that express a functional pre-TCR in association with CD3 are selected to mature to proliferating DN4 cells. These pass through a transient immature $CD8^+$ single positive (ISP) stage before maturing into $CD4^+CD8^+$ double positive (DP) T cells. At the DP stage, TCR α chain rearrangement is completed, resulting in the expression of the TCR. The TCR binds its cognate antigen exclusively when it is presented via a major histocompatibility complex (MHC) molecule on an antigen-presenting cell. DP thymocytes are then subjected to a serial selection process ultimately yielding single positive (SP) T cells. These thymocytes either express CD4 or CD8 in combination with a TCR that displays a moderate affinity to self-MHC. Mature, SP T cells exit the thymus and migrate to the periphery, where they operate either as $CD8^+$ cytotoxic T cells in cellular immunity or provide antigen-activated B cells during humoral immunity with additional signals as $CD4^+$ helper T cells (T_H).

1.1.2 Early B cell development

During embryogenesis, B cell development starts in the fetal liver, and is continued in the bone marrow in adults. Thereby, B lymphocytes are generated via a series of sequential differentiation steps, yielding the surface expression of a functional, non-self-reactive B cell receptor (BCR). The BCR complex consists of an immunoglobulin heavy chain (IgH), an immunoglobulin light chain (IgL), and two associated signaling molecules, Igα and Igβ (cp. Fig. 3). Whereas antigen specificity and binding are provided by the variable regions of IgH and IgL, Igα and Igβ mediate downstream BCR signaling into the cell (reviewed in Janeway, 2007).

B cell development is initiated with the commitment of lymphoid precursor cells to the B cell lineage, what critically depends on the transcription factors E2A, EBF, and Pax5. While E2A and EBF activate B cell-specific gene expression and induce the initiation of immunoglobulin (Ig) gene rearrangement, Pax5 restricts any further development to the B cell lineage by repressing lineage-inappropriate genes like Notch1 and simultaneously activating the expression of B cell signaling molecules (Busslinger, 2004). In the earliest B lineage cells, known as pro-B cells, expression of two enzymes encoded by the recombination-activated genes *rag-1* and *rag-2* induces

the rearrangement of the Ig heavy chain locus. This process is known as somatic recombination and involves the rearrangement of variable (V), diversity (D), and joining (J) gene segments encoding for the variable Ig regions. By individual VDJ joining, each B cell acquires a unique receptor specificity and thus a limited number of inherited gene segments can give rise to a greatly divers antibody repertoire. D_H to J_H joining at the early pro-B cell stage is followed by V_H to D_H joining at the late pro-B cell stage (Tonegawa, 1993). Another enzyme, terminal deoxynucleotidyl transferase (TdT), contributes to the diversity of the BCR by adding N-nucleotides at the rearrangement joints (Gilfillan *et al.*, 1993). Following successful rearrangement of the Ig heavy chain locus, a pre-BCR is expressed on the cell surface of large pre-B cells. The pre-BCR complex consists of the rearranged Igμ heavy chain and a surrogate Ig light chain, which is composed of VpreB and λ5. Pre-BCR signaling promotes light chain rearrangement in small pre-B cells. As soon as an Ig light chain has been successfully rearranged and can pair with the heavy chain, it replaces the surrogate light chain to form a complete IgM molecule. Once a B cell expresses the BCR on its surface, the cell is defined as an immature B cell (Bossy *et al.*, 1991). As soon as one Ig heavy or one Ig light chain allele has been productively recombined, a mechanism known as allelic exclusion prevents further rearrangements of the second Ig allele to guarantee that a single B cell only expresses Ig molecules of a single specificity (Alt *et al.*, 1984). Cells lacking a productive Ig heavy or light chain rearrangement after the first recombination process have the possibility to undergo a further rearrangement process of the second Ig allele. In case of a still unproductive rearrangement, cells undergo apoptosis. A series of selection events in the bone marrow guarantees that only B cells that have gained a non-self-reactive BCR enter the peripheral B cell pool. Cells that are self-reactive are eliminated by clonal deletion, become anergic or are reprogrammed through a mechanism known as receptor editing. The latter changes the BCR specificity by further rearrangements to ablate autoreactivity (Edry and Melamed, 2004). Anergic cells can enter the periphery but cannot be further activated and possess only a short half-live. Cells that are autoreactive but escape this negative selection in the bone marrow can cause autoimmune diseases. While about $2x10^4$ IgM^+ immature B cells are generated daily in the murine bone marrow, only about 10 % of these cells are able to survive these series of selection events (Gay *et al.*, 1993; Radic *et al.*, 1993; Tiegs *et al.*, 1993). Those B cells exit the bone marrow, enter the circulation, and migrate to the spleen to undergo further maturation.

1.1.3 Late B cell development – Marginal zone versus follicular B cell differentiation

The spleen is divided into two compartments known as red and white pulp. The splenic lymphocytes are mainly harbored in the white pulp, which is organized in follicles with respective B and T cell areas, surrounded by the marginal sinus and the marginal zone. A detailed scheme of

the follicular microarchitecture is illustrated in figure 1. Immature B cells that are "in transit" from the bone marrow to the periphery are referred to as "transitional" B cells when entering the spleen. These cells comprise a distinct short-lived developmental transition from immature into mature B cells. Thereby these cells develop via several differentiation stages (1 to 3). Transitional type 1 (T1) B cells are subjected to an additional selection process, allowing only about one third of T1 transitional B cells to further differentiate via the T2 and T3 transitional stage, ultimately giving rise to mature B cells (Chung *et al.*, 2003). At all stages, B cell survival critically depends on signals of the BCR (Lam *et al.*, 1997; Kraus *et al.*, 2004), delivered presumably in a tonic (ligand-independent) fashion in the periphery when no antigen is encountered. From the T2 transitional B cell stage, also survival signals via the B cell activating factor (BAFF) receptor are required (Moore *et al.*, 1999; Hsu *et al.*, 2002). Only cells that gain excess to the splenic follicles within days have the ability to develop into long-lived B cells.

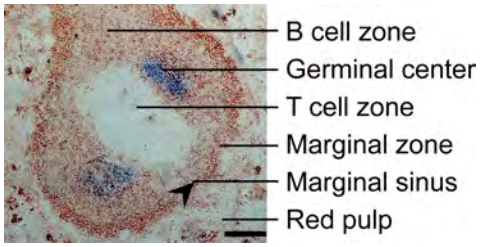

Figure 1 Immunohistochemical analysis of a murine splenic cryosection. Follicular B cells (bright red) form the follicular B cell zone, which is located next to the T cell zone (white). Germinal centers (blue) as hallmark structures of a T cell-dependent (TD) immune response are formed at the border between B and T cell zone by proliferating B cells upon TD activation. A splenic follicle is surrounded by the marginal sinus (indicated by an arrowhead), which is lined by specialized macrophages and marginal zone B cells (dark red), forming the marginal zone. Follicles form the white pulp of the spleen. These are surrounded by the splenic red pulp that consists mainly out of connective tissue and vasculature. In this compartment, filtration of the blood and removal of old erythrocytes are accomplished. Staining: α-IgM (red), PNA (blue); 14 days after TD immunization; Bar: 250 μm.

In the spleen, two major subsets of mature B cells, follicular (Fo) and marginal zone (MZ) B cells are discriminated. With about 75 %, Fo B cells constitute the majority of peripheral B cells in adults. Circulating with the blood stream, Fo B cells continuously pass the peripheral lymphoid tissues. With about 5 %, MZ B cells are less abundant. Together with specialized macrophages, MZ B cells line the marginal sinus at its outer border and form the marginal zone, separating the red from the white pulp. In contrast to Fo B cells, MZ B cells do not circulate to other lymphoid organs and can therefore exclusively be found in the spleen. The marginal zone is constantly exposed to large amounts of blood that exit the circulation through the marginal sinus. By trapping pathogens that have reached the blood stream, MZ B cells provide a first and rapid immune response to various blood-borne bacteria. For that specialized function, MZ B cells are pre-activated and highly express special surface receptors like the complement receptors CD21/35. Whereas homing of B cells to the follicular B cell zone is dependent on the

engagement of the CXCR5 receptor by the chemokine CXCL13, which is expressed by follicular dendritic cells, B cells are attracted to the MZ by the engagement of their $S1P_1$ and $S1P_3$ receptors through lysophospholipid-shingosine-1-phosphate, which is available in the blood. MZ B cells highly express these receptors in comparison to Fo B cells. Adhesion of MZ B cells within the MZ is further mediated through the interaction with MARCO receptors, expressed on MZ macrophages, and via binding of integrins like LFA-1 and α4β1 on MZ B cells to adhesion molecules on stroma cells (Pillai and Cariappa, 2009).

A third population of mature B cells that has not been discussed yet is known as B1 B cells. These cells do not conform to the developmental pathway that is described above and have to be distinguished from the conventional B2 cells, like Fo and MZ B cells. The main parts of the B1 B cells are thought to arise early in ontogeny and to be derived from stem cells in the fetal liver. B1 cells form the predominant B cell population in the peritoneal and pleural cavities and share both some phenotypic and functional analogies with MZ B cells. Both populations have the capacity for self-renewal (Tarakhovsky, 1997) and express only a restricted primary antibody repertoire. MZ and B1 B cells are regarded as major source of IgM antibodies and are thus rather considered as players of innate immunity (Martin and Kearney, 2002; Martin *et al.*, 2001).

1.1.4 B cell activation

Mature B cells are referred to as resting and naïve, until they interact with their specific antigen and become activated. Depending on the nature of the antigen, B cell activation can either occur with or without the involvement of helper T cells (T_H cells), known as T cell-dependent (TD) and -independent (TI) immune response, respectively. Cross-linking of the BCR by TI antigens, for example bacterial polysaccharides, initiates clustering of the BCR and subsequently signaling, leading to B cell activation without T cell help. In this way, activated B cells undergo clonal expansion and form extrafollicular foci, where they differentiate into plasma cells, secreting low-affinity IgM or IgG1 antibodies (Gray *et al.*, 1996). In contrast to TD antigens, TI antigens neither trigger affinity maturation of the BCR nor the generation of memory B cells. The TI immune response is predominantly accomplished by MZ B cells and B1 B cells and leads to a prompt, but rather unspecific immune response.

TD immune responses are mainly performed by Fo B cells, though they also have the ability to respond to TI antigens (Rajewsky, 1996). After the binding of a TD antigen by the BCR, the antigen is internalized, processed, and presented on major histocompatibility complex (MHC) II molecules. $CD4^+$ T_H cells that express a TCR specific for the same antigen and have been activated by dendritic cells before interact with these B cells at the border between follicular B and T cell zone. The TCR binds to both the MHC class II molecule and the presented antigen,

initiating internal signaling in both B and T cells. Thus, B cells are provided with co-stimulatory signals, which include the interaction between CD40 receptors on B cells and the CD40 ligand, displayed on activated T_H cells, as well as the stimulation by cytokines, which are released by T_H cells. Those activated B cells undergo clonal expansion and can either take part in the germinal center reaction or migrate to extrafollicular foci, where they differentiate into low affinity antibody-secreting plasma cells.

Germinal center (GC) formation is the hallmark of a TD immune response and is a prerequisite for the generation of high affinity antibodies. GCs are structures that are formed by proliferating B cells in the follicles of secondary lymphoid tissues like the spleen, lymph nodes, and Peyer's patches within days upon contact with TD antigens. In the GC, B cells undergo somatic hypermutation and Ig class switch recombination. Thereby, the enzyme activation-induced cytidine deaminase (AID) plays an essential role during both processes (Revy *et al.*, 2000; Muramatsu *et al.*, 2000). Somatic hypermutation changes the immunoglobulin variable region genes with a mutation rate of 10^{-3}/nt, increasing the antigen specificity of the BCR (Liu *et al.*, 1997). B cells accomplishing high affinity binding to antigens, displayed on the surface of follicular dendritic cells, and simultaneously receiving survival signals from antigen-specific T_H cells are positively selected. Cytokines released by T_H cells induce Ig class switch recombination in B cells, leading to the replacement of the μ and δ constant regions with further constant regions as γ, ε, and α, while maintaining the same antigen specificity. This process is known as isotype switching and leads to the production of IgG1, IgG2a, IgG2b, IgG3, IgE, and IgA antibodies, which possess different effector properties and operate at different sites. Central functions of secreted immunoglobulins are the neutralization and the opsonization of pathogens, followed by phagocytosis through macrophages or lysis mediated by the complement system.

B cells that have been positively selected during the GC reaction leave the follicle and enter the peripheral circulation either as long-lived antibody-secreting plasma cells or memory B cells. Plasma cells migrate to the bone marrow, where they reside and secrete high affinity antibodies that bind to the specific antigen. Memory B cells remain resting in the peripheral lymphatic tissues until they are activated again by a second antigen challenge, allowing a rapid and specific secondary immune response and thus long-lasting protective immunity. Interestingly, MZ B cells have also been reported to show the ability to form GC structures in splenic follicles after TD activation (Song and Cerny, 2003).

1.2 Central signaling pathways in B lymphocytes

B cell activation during TD immune response is based on BCR signaling upon binding of cognate antigen and on additional signals provided by the contact with $CD4^+$ T_H cells. This B-T cell

interaction is commonly referred to as "immunological synapse" and includes contacts of various cell surface molecules, eliciting internal signaling in both B and T cells. Binding of CD40 ligand by the CD40 receptor on B cells is a crucial interaction within that immunological synapse to allow B cell activation during a TD immune response.

1.2.1 CD40 receptor signaling

CD40 is a member of the tumor necrosis factor receptor (TNFR) family. Its expression was initially noted on B cells, but is also found on other antigen-presenting cells like monocytes or dendritic cells as well as on non-hematopoietic cells such as epithelial or endothelial cells. The engagement of CD40 by the CD40 ligand (CD40L, CD154) triggers clustering of the receptor and the recruitment of a set of adaptor proteins known as TNFR-associated factors (TRAFs). TRAF proteins interact with the cytoplasmic domain of CD40 and mediate signaling into the cell, most prominently by activating the canonical and non-canonical NF-κB pathway as well as the mitogen-activated protein (MAP) kinases p38, extracellular signal-regulated kinase (Erk), and c-Jun N-terminal kinase (Jnk). In addition, JAK-STAT (Janus-activated kinase - signal transducer and activator of transcription) as well as phosphoinositol 3-kinase (PI3K) and phospholipase Cγ2 (PLCγ2) signaling can be triggered in response to CD40 activation (Hanissian and Geha, 1997; Harnett, 2004) (Fig. 2). CD40 ligation on B cells *in vitro* promotes B cell activation, reflected in the upregulation of activation and adhesion molecules, and promotes proliferation, survival, and cytokine secretion (Dallman *et al.*, 2003; Harnett, 2004). In concert with certain cytokines such as IL4, CD40 stimulation of B cells *in vitro* induces class switch recombination. *In vivo,* the CD40-CD40L interaction is essential for a TD immune response. This became evident with the finding that patients with "X-linked hyper IgM syndrome" who suffer from diminished generation of IgG, IgE, and IgA antibodies including memory B cells harbor mutations in their CD40L gene (DiSanto *et al.*, 1993; Korthauer *et al.*, 1993). Later it was shown that mice with inactivated CD40 or CD40L do neither form GCs nor perform class switch recombination after TD immunization, underlining the important role of the CD40-CD40L interaction for the GC reaction (Kawabe *et al.*, 1994; Xu *et al.*, 1994).

1.2.2 NF-κB signaling

NF-κB/Rel is a family of inducible transcription factors with essential functions during lymphocyte development, activation, proliferation, and survival. In mammals, the NF-κB family consists of five genes coding for NF-κB1 (p105/p50), NF-κB2 (p100/p52), RelA (p65), RelB, and c-Rel (Bonizzi and Karin, 2004). In resting cells, NF-κB dimers are retained in the cytoplasm by the interaction with proteins of the inhibitor of the NF-κB (IκB) family, which mask

respective nuclear localization sequences and prevent nuclear transport of NF-κB components. In B cells, the canonical NF-κB pathway is rapidly but only transiently activated in response to a wide range of stimuli inducing signaling of different receptors including the BCR, Toll-like receptors, the IL1 receptor, as well as members of the TNFR family. Upon activation, IκBα, which is the most prominent inhibitor of the canonical NF-κB pathway, is phosphorylated and ubiquitin-dependently proteasomally degraded, followed by nuclear translocation of p50/c-Rel or p50/p65 heterodimers. Activation of non-canonical NF-κB signaling is kinetically slower but more sustained. In B cells, its activation is triggered predominantly by engagement of CD40, BAFF, or lymphotoxin β receptors and depends on the proteolytic cleavage of the inhibitory precursor p100, releasing mainly p52/RelB heterodimers for nuclear translocation (cp. Fig. 2).

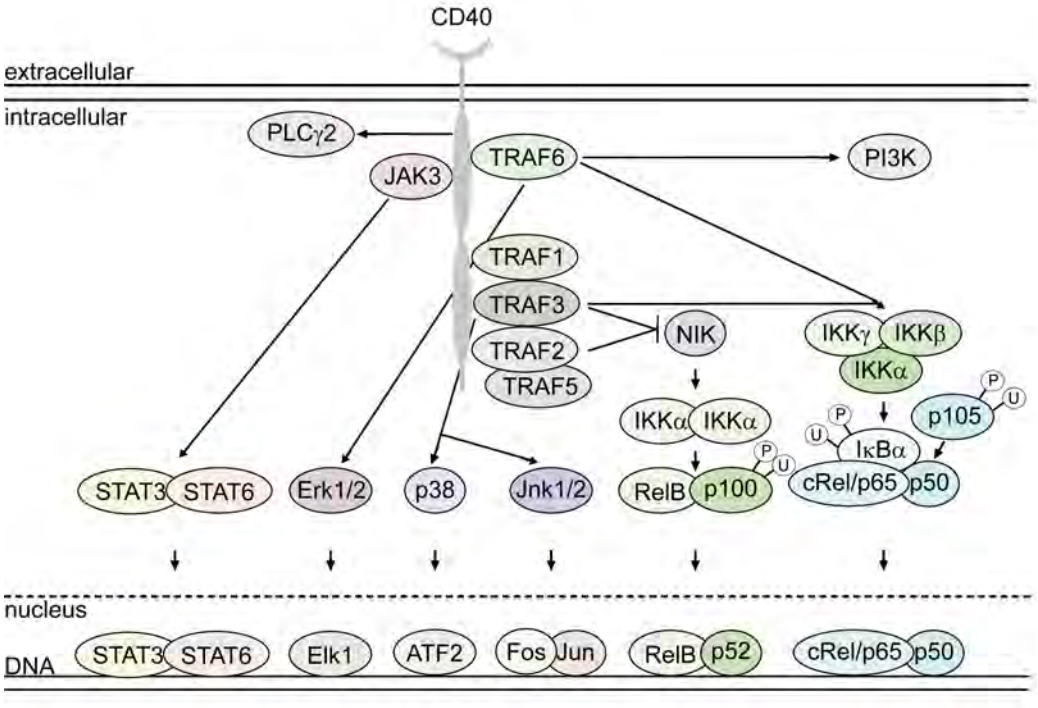

Figure 2 Simplified illustration of CD40 signaling, modified from (van Kooten and Banchereau, 2000; Elgueta *et al.*, 2009). Upon engagement of the CD40 receptor, TRAFs1,2,3,5, and 6 as well as JAK3 are recruited to the cytoplasmic tail of CD40 and drive the activation of the MAPKs Erk, p38, and JNK, the canonical and non-canonical NF-κB pathways, PI3K, PLCγ2, as well as JAK-STAT-signaling. MAPKs activate transcription factors like Elk1, ATF2, or Jun/Fos that activate gene transcription in the nucleus. Activation of canonical and non-canonical NF-κB signaling is initiated with the activation of specific kinases (IKKs, NIK), mediating phosphorylation and subsequent ubiquitin-dependent proteasomal degradation of inhibitors of NF-κB (IκBα, p100). p50 is constitutively generated by processing of p105. NF-κB dimers (RelB:p52, cRel/p65:p50) translocate into the nucleus to activate gene transcription. Of note, recruitment of TRAF2 and 3 to CD40 releases otherwise cooperatively degraded NIK, allowing NIK accumulation and subsequent activation of non-canonical NF-κB signaling. PLCγ2 (phospholipase Cγ2), JAK (Janus kinase), TRAF (tumor necrosis factor receptor-associated factor), PI3K (phosphoinositol 3-kinase), STAT (signal transducer and activator of transcription), Erk (extracellular signal-regulated kinase), Jnk (c-Jun N-terminal kinase), NIK (nuclear factor κB-inducing kinase), IKK (IκB kinase), IκBα (inhibitor of NF-κBα), P (phosphorylation), U (ubiquitination).

In summary, canonical and non-canonical NF-κB signaling cause the formation and nuclear translocation of distinct NF-κB heterodimers that activate NF-κB target genes (Bonizzi *et al.*, 2004; Dejardin *et al.*, 2002; Derudder *et al.*, 2003).

1.2.3 B cell receptor signaling

The successful generation of a functional, non-self-reactive B cell receptor (BCR) is the prerequisite for positive selection and survival of B cells during early development in the bone marrow. But also the survival of resting, peripheral B cells critically depends on signals delivered by the BCR (Lam *et al.*, 1997; Kraus *et al.*, 2004). However, these signals are considered to be mediated ligand-independently, and thus to be of a "tonic" nature. During immune response, B cells become activated by binding of the cognate antigen to their BCR, initiating BCR signaling within minutes. In the BCR complex, a surface Ig molecule that binds an antigen is associated with two transmembrane molecules, Igα and Igβ that harbor immunoreceptor tyrosine-based activation motives (ITAMs) in their cytoplasmic tails to mediate BCR signaling downstream. Upon BCR ligation by antigens, signaling is initiated by phosphorylation of these ITAMs via various Src family tyrosine kinases, most prominently through Lyn (Kurosaki, 1999). This allows SH2 domain-containing proteins such as Syk to bind to the phosphorylated ITAMs (Rowley *et al.*, 1995). Syk in turn recruits and phosphorylates SLP65 as well as other adaptor proteins that mediate further downstream signaling (Wienands *et al.*, 1998). Thereby, PLCγ2 and PI3K are crucial effector molecules. BCR signaling results in the activation of the MAP kinases Erk, Jnk, and p38, as well as of canonical NF-κB and Akt signaling (Marshall *et al.*, 2000) (Fig. 3).

On the cell surface, BCR complexes are constitutively localized in lipid rafts (Bannish *et al.*, 2001; Guo *et al.*, 2000). In addition, the BCR is associated with co-receptors that positively or negatively influence BCR signaling. CD19 functions as a positive co-receptor, since it lowers the threshold of BCR signaling (Pezzutto *et al.*, 1987; Carter *et al.*, 1991). CD19 is present on the cell surface with two other transmembrane proteins, CD21 and CD81. CD21 is the complement receptor 2, which can be co-ligated with the BCR by complement-coated antigens. CD81 is required to stabilize the co-receptor complex, whereas CD19 mediates signaling. PI3K, Lyn, and Vav were shown to interact directly with the cytoplasmic tail of CD19 and transmit signaling to PLCγ2, Akt, and the MAP kinase Erk (Buhl *et al.*, 1997; Otero *et al.*, 2001; Li and Carter, 1998; Wang *et al.*, 2002). As deficiency for Pten, which is a negative regulator of PI3K, was shown to fully restore the phenotype of CD19 knock-out mice (Anzelon *et al.*, 2003), CD19 is suggested to signal most prominently via PI3K. PI3K/Akt signaling is widely known to promote B cell survival and proliferation (Harnett *et al.*, 2005). Recently, PI3K was identified as key mediator of tonic BCR signaling (Srinivasan *et al.*, 2009).

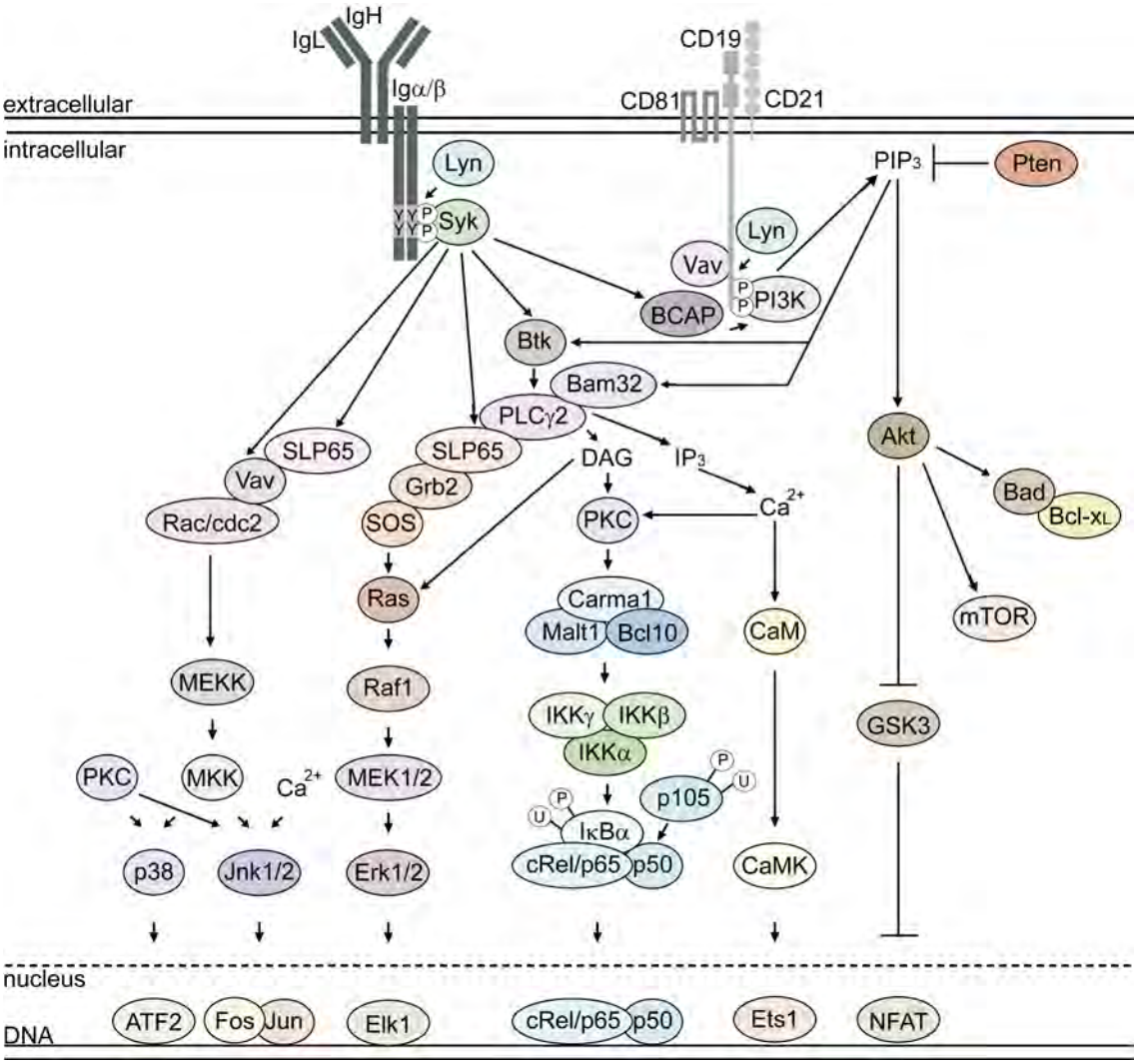

Figure 3 Simplified illustration of B cell receptor (BCR) signaling, modified from (Dal Porto *et al.*, 2004). The BCR complex consists of an Ig surface molecule associated with the signaling proteins Igα and Igβ and is linked to a co-receptor complex of CD81, CD19, and CD21. Upon BCR engagement, Src family tyrosine kinase Lyn is recruited and phosphorylates the ITAMs of Igα and Igβ, thereby creating docking sites for SH2 domain-containing proteins such as Syk. Syk mediates downstream signaling via the adaptor proteins SLP65, Vav, and BCAP and activates Btk. Through Vav and Rac, the MAPK cascade MEKK-MEK-p38/Jnk is activated, while PKC and Ca^{2+} also contribute to p38/Jnk activation. A complex of SLP65, Grb2, and SOS activates the Ras-Raf-MEK-Erk signaling cascade. MAPKs p38, Jnk, and Erk activate transcription factors that activate gene transcription in the nucleus. The lipid-mobilizing enzyme PI3K generates PIP_3, serving as substrate for PLCγ2 to generate DAG and IP_3. Latter induces Ca^{2+} release from the endoplasmatic reticulum and results in the activation of Calmodulin and PKC, which is also activated by DAG. PKC activates a complex of Carma1, Malt1, and Bcl10, which activates in turn an IKK complex mediating degradation of the inhibitor IκBα, allowing the nuclear translocation of canonical NF-κB dimers (c-Rel/p65:p50) to activate gene transcription. PI3K activation is mostly triggered by the co-receptor CD19, which binds in addition Vav and Lyn through phosphorylated tyrosine residues in its cytoplasmic domain. PIP_3 generated by PI3K activates Akt, Btk, Bam 32, and PLCγ2. Akt kinase activates Bcl-X_L and mTor and inhibits GSK3, an inhibitor of NFAT. Btk kinase activates PLCγ2. The adaptor protein Bam32 integrates PI3K and PLCγ2 signaling. Pten negatively regulates PI3K activity by degrading PIP_3. Ig (Immunoglobulin), H (heavy chain), L (light chain), BCAP (B cell adaptor for PI3K), Btk (Burton's tyrosine kinase), PIP_3 (Phosphatidylinositol-trisphosphate), DAG (Diacylglycerol), IP_3 (Inositol-trisphosphate), PKC (protein kinase C), CaM (Calmodulin), CaMK (Calmodulin-dependent kinase), GSK3 (Glycogen synthase kinase 3), Pten (phosphatase with tensin homology), P (phosphorylation), U (ubiquitination).

1.3 The role of the Notch pathway in lymphocytes

1.3.1 The Notch signaling cascade

In 1917, Thomas Hunt Morgan described fruit flies with notches at the edges of their wing blades (Morgan, 1917). Decades later, haploinsufficiency in the *Drosophila Notch* gene, which was cloned in the mid eighties, was taken as the basis for that phenotype (Kidd *et al.*, 1986; Wharton *et al.*, 1985). Notch signaling is an evolutionarily conserved pathway, which is involved in the regulation of cell fate decisions, differentiation processes, cell survival, and proliferation in a wide variety of biological systems. In mammals, the Notch family of transmembrane receptors comprises four different members, Notch1, 2, 3, and 4 that are bound by different ligands of the Delta-like (Dll) or Jagged family (Dll1, 3, 4, Jagged1, 2). Receptor-ligand interaction results in the activation of the Notch signaling pathway.

Notch receptors are heterodimers that are encoded by one gene and that consist of a N-terminal extracellular and C-terminal transmembrane and intracellular domain, which are non-covalently linked to each other (Blaumueller *et al.*, 1997; Logeat *et al.*, 1998). The extracellular part harbors epidermal growth factor (EGF)-like repeats that mediate ligand binding, followed by cysteine rich Lin12/Notch repeats (LIN) that prevent ligand-independent activation. A hydrophobic stretch of amino acids mediates heterodimerization. The intracellular part contains diverse elements that mediate signal transduction. These include the RAM domain and ankyrin repeats, necessary for the interaction with downstream effector proteins, nuclear localization signals, and a transactivation domain. Furthermore, a PEST (proline-glutamine-serine-threonine-rich) sequence, regulating protein stability, is located at the C-terminus (Fig. 4A). Ligand binding to the extracellular domain of Notch (NotchEC) results in a regulated set of proteolytic cleavage events, liberating the Notch intracellular fragment (NotchIC). Firstly, metalloproteases of the ADAM family cleave Notch extracellularly. Shed NotchEC is endocytosed together with the ligand by the ligand-expressing cell. A multiprotein complex with γ-secretase activity induces a second cleavage of Notch within the transmembrane region. Released NotchIC translocates into the nucleus, where it complexes with the DNA binding protein CSL/RBP-Jκ (CBF in human, Suppressor of Hairless in *Drosophila*, Lag1 in *C. elegans,* RBP-Jκ in mice) and induces the recruitment of co-activators such as Mastermind. Thus, CSL/RBP-Jκ is converted from a transcriptional repressor to a transcriptional activator, ultimately triggering the transcription of Notch target genes (Fig. 4B). These include most prominently members of the Hes and Hey family (Kopan and Ilagan, 2009).

Notch signaling is regulated at multiple levels. Downstream, the Notch activation complex is short-lived, as the PEST domain targets nuclear NotchIC for ubiquitin-dependent proteasomal

degradation. In addition, negative regulators as the MINT (Msx2-interacting nuclear target) protein can compete with NotchIC for complexing with CSL/RBP-Jκ (Kuroda *et al.*, 2003). At the level of ligand binding, the Fringe glycosyltransferase modifies NotchEC by adding sugar moieties, in a way that preferentially Delta-like (Dll), but not Jagged ligands will initiate Notch signaling (Moloney *et al.*, 2000). Recently, it was discovered that the pairing of Notch receptors to different ligands influences the outcome of Notch signaling (Besseyrias *et al.*, 2007; Santos *et al.*, 2007). Moreover, cell type-specific and spatial expression of Notch receptors and Notch ligands can limit Notch signaling to a certain cell population and determine its nature.

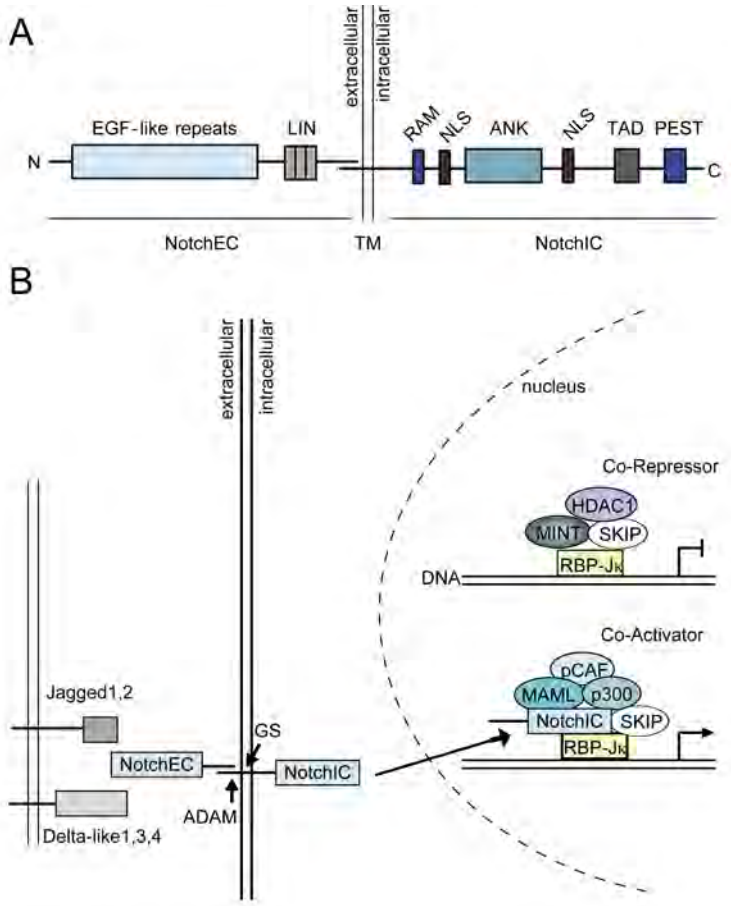

Figure 4 Notch primary structure and signaling cascade. (A) The N-terminal, extracellular part of Notch (NotchEC) contains 29 to 36 epidermal growth factor (EGF)-like repeats and three cysteine-rich Lin12/Notch repeats (LIN). The intracellular part of Notch (NotchIC) harbors a RAM domain (RAM), six ankyrin repeats (ANK), two nuclear localization signals (NLS), a transactivation domain (TAD), and a proline-glutamine-serine-threonine-rich (PEST) sequence at the C-terminus. NotchEC and NotchIC are non-covalently linked; TM (transmembrane); **(B)** The interaction of NotchEC with ligands of the Delta-like or Jagged family induces sequential proteolytical cleavages. Notch is extracellularly cleaved by members of the ADAM family of metalloproteases, while γ-secretase (GS) cleaves Notch within the transmembrane region. Liberated NotchIC translocates into the nucleus to interact with RBP-Jκ (recombination signal binding protein for Ig kappa J region) and to recruit a co-activator complex containing besides others MAML (mastermind-like), p300 and pCAF (p300-associated factor). SKIP can be part of both the co-activator and the co-repressor complex, while the latter contains MINT (Msx2-interacting nuclear target protein), HDAC1 (histone deacetylase 1) and is displaced from RBP-Jκ by the co-activator complex to ultimately activate the transcription of Notch target genes.

The outcome of Notch signaling is diverse. While Notch regulates lineage decisions at developmental branch points in some circumstances, Notch may maintain cells in undifferentiated states or promote differentiation of cells in other contexts. Thus, the outcome of Notch signaling is thought to be dependent not only on the nature of ligand pairing, but also on the cellular context and signaling strength.

1.3.2 Notch signaling in lymphocytes

Both Notch1 and Notch2 have been shown to be expressed on lymphocytes, where they function non-redundantly. The essential role of Notch in T cell lineage commitment and development is the best-characterized function of Notch in hematopoiesis, whereas the impact of Notch on B cell development is not so accurately defined. In bone marrow progenitors, ablation of Notch1 or RBP-Jκ results in a block of T cell development and the appearance of ectopic B cells in the thymus (Han *et al.*, 2002; Radtke *et al.*, 1999). In contrast, retroviral expression of Notch1IC causes a block in B cell development at the pre-/pro-B cell stage and the simultaneous development of ectopic T cells in the bone marrow (Pui *et al.*, 1999). These data evidence that Notch1 signaling is necessary and sufficient to induce T cell development. Once the T cell lineage has been committed, Notch1 is thought to influence the choice of αβ or γδ T cell fates (Washburn *et al.*, 1997). Whereas γδ T cells appear to develop Notch-independently, Notch1 signaling is continuously required for the development of αβ T cells up to the DN3 stage (Wolfer *et al.*, 2002). Thereby, Notch1 seems to cooperate with pre-TCR signaling for successful β-selection (Ciofani *et al.*, 2006; Maillard *et al.*, 2006; Allman *et al.*, 2001a). Notch2 is in contrast dispensable for T cell development, but influences lineage commitment during peripheral B cell development. While both Notch1 and Notch2 are expressed on early B cell subsets in the bone marrow, mainly Notch2 is expressed in mature B cells (Walker *et al.*, 2001; Saito *et al.*, 2003; Witt *et al.*, 2003b). In detail, Notch2 expression is predominantly found in transitional type 1 (T1) and marginal zone (MZ) B cells (Tan *et al.*, 2009). Since these data revealed Notch expression during different stages of B cell development, several groups attempted to study the impact of Notch on B cell development and proliferation. Retroviral expression of Notch2IC in all hematopoietic stem cells was shown to block B cell differentiation at the large pre-B cell stage and to induce ectopic T cell development in the bone marrow. In addition, enhanced B1 B cell differentiation was found in the spleen when Notch2IC was expressed at lower levels (Witt *et al.*, 2003b).

1.3.3 The role of Notch in marginal zone B cell development

It is well established that Notch2 signals influence the cell fate decision between follicular (Fo) and MZ B cells. This has been demonstrated by the B cell-specific inactivation of Notch2 or

RBP-Jκ that results in the loss of MZ B cells, while Fo B cells develop in a Notch-independent manner (Saito *et al.*, 2003). In addition, the deletion of MINT, a negative regulator of Notch signaling, leads to increased MZ B cell development (Kuroda et al 2003), whereas the inactivation of MAML1, a co-activator component within the Notch-RBP-Jκ complex, results in defective MZ B cell generation (Wu *et al.*, 2007). The crucial Notch ligand for MZ B cell development is Dll1 (Hozumi *et al.*, 2004)). Thus, commitment to the MZ B cell compartment is thought to depend upon the non-redundant, competitive interaction between the Notch2 receptor on T1 transitional B cells with the Dll1 ligand, expressed in a limited nature on non-hematopoietic, in particular endothelial cells located in the splenic red pulp and MZ. The Dll1-Notch2 interaction is presumably weak and is assumed to be strengthened by modifications of NotchEC through the glycosyltransferases Lunatic and Manic Fringe (Tan *et al.*, 2009). The precise mechanism, how Notch2 signaling contributes to the generation and/or maintenance of MZ B cells is still elusive. It is not known whether Notch2 signaling truly drives MZ B cell differentiation or rather provides survival signals for these cells.

Moreover, it is still controversially discussed at which developmental B cell stage Fo and MZ B cells branch from each other. Recent studies indicate that the vasculature of the splenic red pulp provides a microenvironmental niche, in which T1 transitional B cells, entering the spleen, are committed to the MZ B cell lineage (Tan *et al.*, 2009) by receiving Notch2 signals. T1 transitional B cells may thus develop to MZ B cell precursor cells ($IgM^{high}IgD^{high}CD21/35^{high}CD1d^{high}CD23^{+}$) and finally to MZ B cells ($IgM^{high}IgD^{low}CD21/35^{high}CD1d^{high}CD23^{-}$) (Allman and Calamito, 2009). T1 transitional B cells, which do not receive Notch2 signals are thought to develop to T2 transitional B ($IgM^{high}IgD^{high}CD21/35^{int}CD1d^{low}CD23^{+}$) and Fo B ($IgM^{low}IgD^{high}CD21/35^{int}CD1d^{low}CD23^{high}$) cells. However, previous studies in the rat point to an origin of MZ B cells from the Fo B cell pool (Dammers *et al.*, 1999), suggesting that each B cell including T2 transitional and Fo B cells, receiving respective signals as from the Notch2 receptor, may adopt a MZ B cell phenotype.

Besides Notch2, a number of gene ablations in the BCR and NF-κB-linked signaling pathways display defects of MZ B cell development in parallel with normal Fo B cell development. Particularly S. Pillai and A. Cariappa have postulated that the BCR signaling strength is a critical determinant for the MZ vs. Fo B cell lineage decision. While strong BCR signals are supposed to induce commitment to the Fo B cell pool, weak BCR signals may allow MZ B cell differentiation. This hypothesis is supported by various mouse mutants displaying decreased or increased BCR signaling strength (Pillai and Cariappa, 2009). Additionally, PI3K signaling seems to be critically involved in the generation of MZ B cells. Thus, the deletion of CD19, which signals mainly through PI3K, as well as the ablation of the PI3K signaling component p110δ lead to decreased

numbers of MZ B cells (Otero *et al.*, 2001; Clayton *et al.*, 2002), whereas enhanced MZ B cell formation is observed in mice deficient for Pten, a negative regulator of PI3K signaling (Suzuki *et al.*, 2003). Moreover, the inactivation of various NF-κB components, predominantly of the canonical NF-κB pathway, resulted in impaired MZ B cell generation (Pillai *et al.*, 2005). Various cross-talks between Notch and NF-κB signaling either enhancing or inhibiting NF-κB activity have been described (Osipo *et al.*, 2008). However, it is unclear how Notch2, BCR, and NF-κB signals are integrated during the commitment of a Fo or MZ B cell fate. It is still in question whether Notch2 signaling could be sufficient for the generation of MZ B cells or requires the involvement of further signaling pathways.

1.3.4 Notch signaling in lymphomagenesis

Notch has been linked to cancer for the first time almost 20 years ago, when a chromosomal translocation was identified in T cell acute lymphoblastic leukemia (T-ALL) patients that resulted in the overexpression of a constitutive active Notch1 receptor (Ellisen *et al.*, 1991). That translocation was later named TAN1 (translocation-associated Notch homologue) and its oncogenic effect was proven when bone marrow reconstitution with progenitors expressing TAN1 rapidly caused T-ALL in mice (Pear *et al.*, 1996). Meanwhile, deregulated Notch signaling has been associated with diverse malignancies (Koch and Radtke, 2007). In the hematopoietic system, aberrant Notch signaling is preferentially oncogenic for T cells since constitutive activation of Notch1, 2, or 3 have been shown to induce T cell leukemia (Pui *et al.*, 1999; Bellavia *et al.*, 2000; Rohn *et al.*, 1996). Moreover, more than 50 % of human T-ALLs suffer from activating mutations within the Notch1 gene (Weng *et al.*, 2006). However, the effect of deregulated Notch signaling in B lymphocytes in regard to the development of B cell malignancies is still controversial. Notch1 and Notch2 are highly expressed in B cell chronic lymphatic leukemia and Hodgkin lymphomas and were suggested to promote proliferation and survival of these tumors (Hubmann *et al.*, 2002; Jundt *et al.*, 2002a; Jundt *et al.*, 2004; Rosati *et al.*, 2009). Recently, gain-of-function mutations of Notch2 have been reported in marginal zone and diffuse large B cell lymphomas (Troen *et al.*, 2008; Lee *et al.*, 2009). Nevertheless, a direct oncogenic effect of activated Notch in B cells has not been described so far. Other studies even indicate that Notch itself may rather induce apoptosis in B cells (Morimura *et al.*, 2000; Romer *et al.*, 2003; Zweidler-McKay *et al.*, 2005). However, activated Notch has been recently reported to synergize with CD40 and BCR signaling to induce proliferation of primary B cells *in vitro* (Thomas *et al.*, 2007). Therefore, the kind of interplay between Notch and other signaling cascades is likely to determine the outcome of active Notch signaling in B cells, leading potentially either to apoptosis or tumor initiation.

1.4 Interplay of signaling pathways in B cell lymphomas

Notch, CD40, and BCR signaling are all involved in B cell activation and may support B cell expansion. Deregulated activation of such signaling cascades may maintain proliferation or survival signals inappropriately and may ultimately lead to lymphomagenesis. Therefore, this section will pull together the role of these receptors during the development of B cell lymphomas. Interestingly, these three signaling molecules are linked to an oncogenic virus, the Epstein-Barr virus (EBV). This herpes virus mainly infects human B cells and leads to the transformation of B cells *in vitro*. Thereby, EBV induces the expression of a set of viral latency genes in the context of different latency programs. Off note, some of those viral proteins mimic constitutive active cellular receptors, including EBNA2, mimicking a constitutive active Notch receptor, LMP1, mimicking a constitutive active CD40 receptor, and LMP2A, mimicking a constitutive active B cell receptor (BCR).

Aberrant Notch signaling is clearly transforming for T cells, and the still controversial contribution of Notch to B cell malignancies has been described in detail above. More obvious, CD40 is involved in the development of B cell tumors. CD40 is not only highly expressed in B cell lymphomas like the Hodgkin lymphoma (HL) and B cell chronic lymphatic leukemia (O'Grady *et al.*, 1994; Westendorf *et al.*, 1994), but was shown to lead to B cell transformation when it is constitutive active (Homig-Holzel *et al.*, 2008). BCR dependency is a main determinant of B cell survival over all stages of development including peripheral existence. Many B cell lymphomas also seem to be reliant on survival signals mediated by the BCR, thus retaining BCR expression.

One exception is the HL, implicating the interplay of Notch, CD40, and BCR signaling in B cell lymphomas. Malignant cells in the HL arise from germinal center B cells and have lost their B cell-specific expression pattern including BCR surface expression in the majority of cases (Kanzler *et al.*, 1996). To persist, these cells must have activated other survival pathways. In fact, constitutive NF-κB activity is a hallmark of HLs (Bargou *et al.*, 1997). Enhanced CD40 and CD30 signaling have been suggested to contribute to strong NF-κB activity in the malignant cells of this tumor. Beside TNFRs, also Notch1 and 2 were reported to be highly expressed in HLs and were suggested to promote proliferation and survival of HL cell lines *in vitro* (Jundt *et al.*, 2002; Jundt *et al.*, 2004). Whether HL cells are completely independent of BCR expression is not absolutely clear, since all HLs that are truly BCR-negative are infected with EBV and express LMP2A, a viral homolog of an active BCR that may substitute for survival signals usually delivered by the BCR. EBV-negative HL cells show at least low levels of BCR expression (Kuppers *et al.*, 2005). Thus, it is still in question whether these malignant B cells still depend on survival signals from the BCR or whether other survival pathways can actually compensate for it.

1.5 Model systems

In this work, various model systems, including transgenic mice and cell lines, were used. In this section, the establishment of these systems and previous results will be explained.

1.5.1 The Notch1/2IC-expressing EREB2.5 cell lines

The Epstein-Barr (EBV) virus-encoded nuclear antigen 2 (EBNA2) is an important transcription factor of EBV, which is not only essential for initiation but also for maintenance of B cell immortalization by EBV (Kempkes *et al.*, 1995a). Since EBNA2 is also tethered to promoter regions by the interaction with CSL/RBP-Jκ, it is regarded as functional homologue of an activated Notch receptor (Henkel *et al.*, 1994; Grossman *et al.*, 1994; Zimber-Strobl *et al.*, 1994). Whereas transactivation of genes by Notch depends on previous ligand-receptor interaction, EBNA2-mediated transactivation is autonomous and thus constitutive active. Therefore, it is in question whether EBNA2 uses the Notch signaling pathway to contribute to B cell immortalization.

To compare the function of NotchIC and EBNA2 in B cells, pRTS-1 expression vectors (Bornkamm *et al.*, 2005) encoding for the intracellular parts of human Notch1 and human Notch2, respectively, under the control of a doxycycline-inducible, bidirectional promoter were generated and stably introduced into human EREB2.5 cells (Kempkes *et al.*, 1995a). EREB2.5 is a conditionally EBV-immortalized, human B cell line, in which EBNA2 function and thus the EBV program depends on the presence of estrogen. As negative control, the bacterial *CAT* (chloramphenicol acetyl transferase) gene was introduced instead of *Notch1IC* or *Notch2IC* (*Notch1/2IC*). These stably transfected cell lines are referred to as Notch1IC/EREB, Notch2IC/EREB, and CAT/EREB. In order to identify and sort transgene expressing cells, a cDNA coding for a truncated human nerve growth factor receptor (Δ*NGFR*) was cloned in all three cases in the opposite transcriptional orientation. The generation of EREB2.5 cells and respective Notch1/2IC- or CAT-expressing cell lines is illustrated in figure 5. In this cell system, EBNA2 and Notch1/2IC can be activated separately by adding estrogen and doxycycline, respectively. Comparing the kinetics of doxycycline and estrogen induction revealed that in EREB2.5 cells, the EBNA2 protein is functionally active and translocated into the nucleus 20 minutes after the addition of estrogen. In contrast, full expression of Notch is reached four hours after the induction through doxycycline. Thus, cells were analyzed at different time points after adding estrogen or doxycycline.

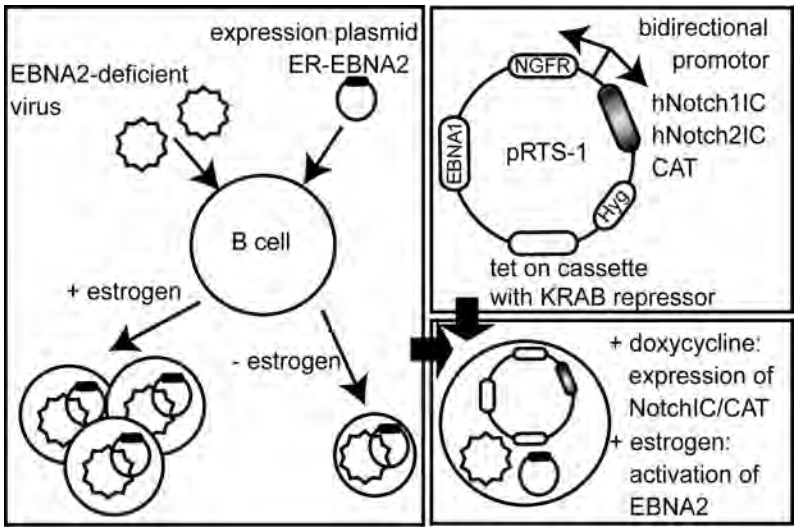

Figure 5 Generation of EBV-transformed B cell lines expressing doxycycline-regulable, human Notch1IC or Notch2IC (Kohlhof *et al.*, 2009). EREB2.5 is a conditionally immortalized lymphoblastoid cell line that was established by infecting human primary B cells with an *ebna2*-deficient strain of EBV, while the EBNA2 defect is complemented by an ER-EBNA2 expression plasmid (Kempkes *et al.* 1995a). Thus, EBNA2 function depends on the presence of estrogen. Without functional EBNA2, cells exhibit a resting phenotype, while cells proliferate in the presence of estrogen. *Notch1IC*, *Notch2IC*, and *CAT* (Chloramphenicol acetyl transferase) were cloned downstream of a bidirectional, doxycycline-dependent (Tet-O7) promoter. Transfection of the expression plasmids into EREB2.5 cells resulted in the cell lines Notch1IC/EREB, Notch2IC/EREB, and CAT/EREB. ΔNGFR (truncated nerve growth factor receptor) serves as marker in order to detect or sort transgene-expressing cells; EBNA1 (EBV nuclear antigen 1) ensures episomal maintenance of the expression plasmids; the tet-on cassette is coding the reverse transactivator (rtTA) and the KRAB repressor; Hyg (hygromycin expression cassette for selection of stably transfected cell clones); ER (estrogen receptor).

Using these cell lines, an Affymetrix GeneChip® analysis was performed by H. Kohlhof, revealing that Notch1/2IC and EBNA2 exhibit profound differences in the regulation of target genes. Whereas EBNA2 turned out to be more efficient in upregulating genes involved in proliferation, survival, and chemotaxis, Notch1IC and Notch2IC were more potent inducing genes associated with development and differentiation. Only a small group of not specifically classified genes was similarly upregulated by EBNA2 and NotchIC. Since this group contained various genes associated with the regulation of cell cycle and proliferation, the question whether Notch1/2IC can replace EBNA2 in its function to maintain B cell immortalization, was addressed. *In vitro* studies revealed that Notch1/2IC were not able to maintain survival of cultured EREB cells, in contrast to EBNA2. However, Notch1/2IC/EREB cells were still able to incorporate BrdU, unlike the negative control CAT/EREB. This indicated that Notch1/2IC can drive some cells into the S-phase of the cell cycle although numbers of cultured cells did not increase. In addition, annexin staining revealed higher percentages of apoptotic cells in Notch1/2IC- compared to CAT- or EBNA2-expressing cells, suggesting that in the absence of EBNA2, Notch1/2IC actively induces apoptosis in EBV-infected B cells (Kohlhof *et al.*, 2009).

In this work, these cell lines were used to study target genes of Notch1/2 in B cells *in vitro* in comparison to gene regulation by EBNA2.

1.5.2 The LMP1/CD40-transgenic mouse strain

CD40 plays an essential role during T cell-dependent immune response and is widely expressed on tumor cells of diverse B cell malignancies. To study constitutive CD40 signaling *in vivo*, C. Hömig-Hölzel generated a conditional transgenic mouse strain expressing a constitutive active CD40 protein in a *Cre*/loxP-dependent manner. Constitutive activity of CD40 was achieved by fusing the signaling domain of human CD40 and the transmembrane domain of the EBV-encoded latent membrane protein 1 (LMP1/CD40). LMP1 is regarded as a functional equivalent of CD40 except that LMP1 signals ligand-independently by self-aggregation of its membrane domain. The LMP1/CD40 transgene was targeted into the murine *rosa26* genomic locus to establish the LMP1/CD40-transgenic mouse strain. LMP1/CD40 signaling in mature B cells dependent on CD19-*Cre* resulted in splenomegaly with a 3.5 fold increase of splenic weight in LMP1/CD40 mice compared to controls. Splenic B and T cell numbers of LMP1/CD40 mice were strongly increased. LMP1/CD40-expressing B cells displayed an activated phenotype from their size and surface expression of activation markers and showed prolonged survival and spontaneous cell division *in vitro*. With one year of age, more than 50 % of LMP1/CD40-transgenic mice developed B cell lymphomas. C. Hojer further analyzed the activation profile and respective importance of signaling pathways in LMP1/CD40-expressing B cells, revealing a selective activation of non-canonical NF-κB signaling in LMP1/CD40-transgenic B cells. In addition, constitutive CD40 signaling induced the activation of the MAP kinases Jnk and Erk, while the increased survival properties of LMP1/CD40-expressing B cells could be assigned to this constitutive Erk activation (Homig-Holzel *et al.*, 2008). In this work, these transgenic mice were used to study the role of tonic BCR signaling in pre-malignant LMP1/CD40-expressing B cells *in vivo*.

1.5.3 The Igβ-deficient mouse strain

The survival of resting, peripheral B cells depends on the expression of a functional BCR. This has been initially revealed by the lab of K. Rajewsky, showing that deletion of the BCR or of one of its signaling molecules, indeed Igα, lead to a severe diminished mature B cell compartment (Lam *et al.*, 1997; Kraus *et al.*, 2004). To investigate the importance of Igβ in the BCR complex for mediating survival of mature B cells, N. Uyttersprot generated a knock-out mouse strain based on the *Cre*/loxP system that is conditional deficient for the Igβ C-terminus. The targeting strategy she used is detailed in figure 6.

In this mouse strain the deletion of the Igβ signaling domain, containing the ITAMs, can be traced by concomitant expression of GFP. To allow normal early B cell development and to delete Igβ *Cre*-dependently only in mature B cells, CD21-*Cre*-transgenic mice were used, deleting only from the T2 transitional B cell stage (Kraus *et al.*, 2004). It is not clear, whether the deletion of BCR-associated signaling components like Igα or Igβ only severely impairs or entirely abrogates tonic BCR signaling. However, such Igβ-deficient mice showed strongly diminished peripheral B cell numbers, indicating that the maintenance signal delivered through the BCR requires the signaling function of both Igα and Igβ subunits (N. Uyttersprot, personal communication). In this work, this mouse strain was used to ablate Igβ and thus to severely impair BCR signaling in pre-malignant LMP1/CD40-expressing B cells *in vivo*.

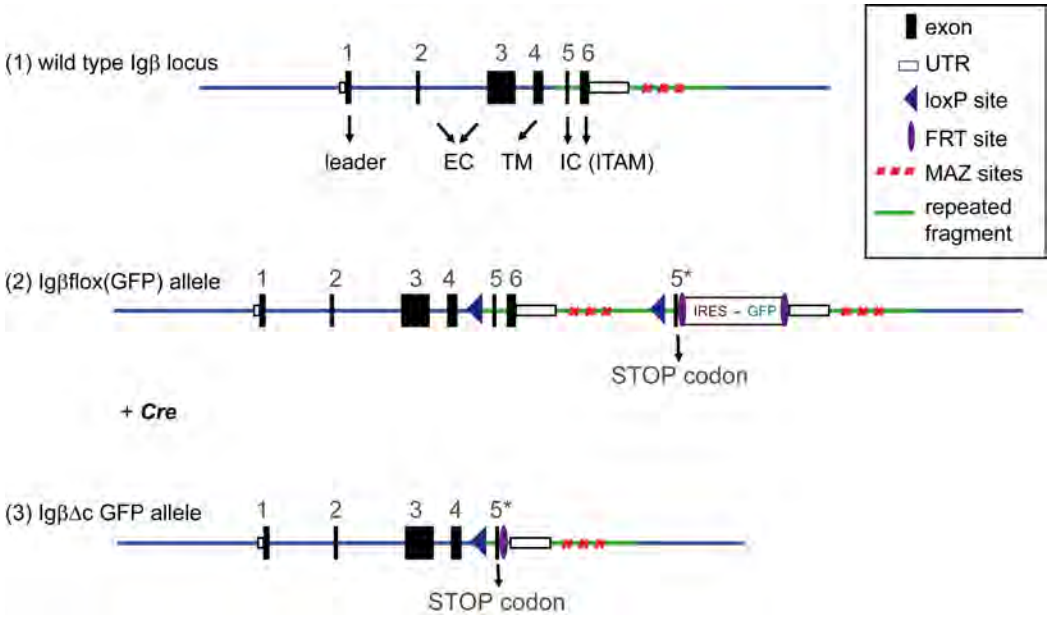

Figure 6 Targeting strategy for the generation of the conditional Igβ-deficient mouse strain (adapted from N. Uyttersprot). (1) The wild type Igβ locus contains 6 exons, while exon 1 encodes the leader sequence, exon 2 and 3 the extracellular (EC) domain, exon 4 the transmembrane (TM) region, and exon 5 and 6 the intracellular (IC) domain, containing the ITAMs for signaling. In the 3´ UTR of the Igβ gene, a termination sequence is located that contains MAZ (Myc-associated zinc finger) sites. (2) During gene targeting, exon 5, 6, and the 3´ UTR region were flanked with loxP sites and a cassette containing a truncated exon 5 (5*), an *IRES-GFP* coding sequence flanked with frt sites, and the wild type 3´ UTR sequence including the MAZ sites was placed downstream of the Igβ gene (Igβflox(GFP)). (3) *Cre*-mediated excision of the loxP sites-flanked region results in splicing from exon 4 to the truncated exon 5, removing the Igβ signaling domain, and ultimately leading to the concomitant expression of a truncated Igβ molecule and GFP via the IRES (IgβΔc GFP allele).

2 Goal

Peripheral B cells are resting until they encounter their cognate antigen. Binding of antigens to the B cell receptor (BCR) and the interaction with ligands on other cells via specific receptors like CD40 or Notch trigger internal signaling, resulting in B cell activation and expansion. Moreover, B cell differentiation may be influenced by those signals. Deregulated expression or activation of such receptors may inhibit expanding cells to terminate proliferation properly, and may implicate cellular transformation. Notch signaling crucially influences lymphocyte differentiation. Whereas Notch1 signaling is instructive for T cell development, Notch2 signals are essential for the generation of marginal zone (MZ) B cells. However, the precise mechanism how Notch2 signaling contributes to the generation and/or maintenance of these cells, particularly in interplay with other signaling pathways, has not been defined jet. Deregulated Notch signaling is clearly transforming for T cells and enhanced Notch expression is also found in divers B cell lymphomas. However, the role of Notch in those tumors is still controversial as aberrant Notch signaling has been proposed to promote survival and proliferation, but also apoptosis in B cells. A viral homologue of Notch interacting as well with RBP-Jκ is EBNA2, an important transcription factor of the Epstein-Barr virus (EBV). EBV immortalizes human B cells *in vitro*, while EBNA2 contributes essentially to that process. Since EBNA2 interacts with similar factors as an activated Notch receptor to activate its target genes, EBNA2 is suspected to make use of the Notch signaling pathway to contribute to B cell immortalization.

To further specify the role of Notch in B cells, we firstly intended to study target genes of Notch1/2 in B cells *in vitro* in comparison to gene regulation by EBNA2, using a cell culture system that allows the conditional regulation of EBNA2 and activated Notch. Secondly, we aimed to investigate the influence of constitutive Notch2 signaling (Notch2IC) on B cell differentiation, activation, and lymphomagenesis *in vivo*. For that purpose, a conditional transgenic mouse strain allowing B cell-specific Notch2IC expression should be generated in this work. To study the role of Notch2 in early B cells, Notch2IC expression should by activated by mb1-*Cre*. To analyze the function of Notch2 predominantly in mature B cells, CD19-*Cre* should be used for activation. In the latter approach, the attention should be particularly turned to the impact of Notch2 on the generation of MZ B cells.

The CD40 receptor provides B cells with crucial costimulatory signals during TD immune response. Moreover, CD40 is highly expressed on divers B cell lymphomas and leads to B cell transformation *in vivo* when it is constitutive active. In developing as well as in mature, peripheral B cells, functional BCR signaling is essential for survival. However, it is in question whether aberrantly activated or malignant B cells also depend on this tonic BCR signal. In the last part of this work, we therefore ablated the BCR-associated signaling molecule Igβ in mature B cells displaying constitutive CD40 signaling, to study the requirement of tonic BCR signaling in pre-malignant B cells *in vivo*.

3 Results

3.1 Comparison of Notch1IC, Notch2IC, and EBNA2 target genes in B cells *in vitro*

We were able to show previously that neither Notch1IC nor Notch2IC (Notch1/2IC) can replace EBNA2 in its function to maintain B cell immortalization. Although in the absence of EBNA2, Notch1/2IC were able to drive EREB2.5 cells into the S-phase of the cell cycle, cell numbers did not increase, presumably due to an increased apoptosis rate in Notch1/2IC-expressing cells (Kohlhof *et al.*, 2009). To examine whether these biological differences between Notch1/2IC and EBNA2 are reflected in the regulation of target genes, mRNA levels of cell cycle- and apoptosis-related genes were analyzed by quantitative real-time (q) PCR.

3.1.1 The experimental setting

Based on previous kinetic studies, we designed the following experimental approach. In Notch1IC/EREB, Notch2IC/EREB, and CAT/EREB cells, EBNA2 function depends on the presence of estrogen while the expression of Notch1/2IC or CAT is dependent on doxycycline (see 1.5.1 for details). Thus, the cell lines were kept in the absence of estrogen for three days to completely abort the effect of EBNA2 on its target gene regulation, before doxycycline or estrogen was added. Doxycycline-induced cells were harvested eight and 24 hours and estrogen-induced cells four and 24 hours after induction (Fig. 7 I.). Since the viability of EREB2.5 cells strongly declines after three days of estrogen withdrawal, a modified experimental approach had to be applied to analyze long-term effects of Notch signaling. Therefore, cells were induced immediately after estrogen withdrawal and were kept in the presence of doxycycline for three days before cells were harvested or analyzed (Fig. 7 II.). Sorting of $\Delta NGFR^+$ cells by magnetic cell separation (MACS) yielded a purity of 87 to 98 % of cells expressing the respective transgenes in response to doxycycline. Subsequently, RNA or whole-protein cell extracts were isolated for further analyses. To accomplish gene expression monitoring, mRNA was reversely transcribed into cDNA.

3.1.2 Notch1/2 lead to cell cycle entry due to the induction of cell cycle-associated genes

Firstly, we investigated the regulation of cell cycle- and proliferation-associated genes by Notch1/2IC in comparison to EBNA2. Genes to be tested by qPCR were chosen based on an Affymetrix GeneChip® analysis performed by H. Kohlhof (Kohlhof *et al.*, 2009). To get further insight into the regulation of cell cycle- and proliferation-associated genes, she clustered all

differentially expressed genes that had been assigned to these functional groups. Genes were arranged in four gene clusters (1 to 4).

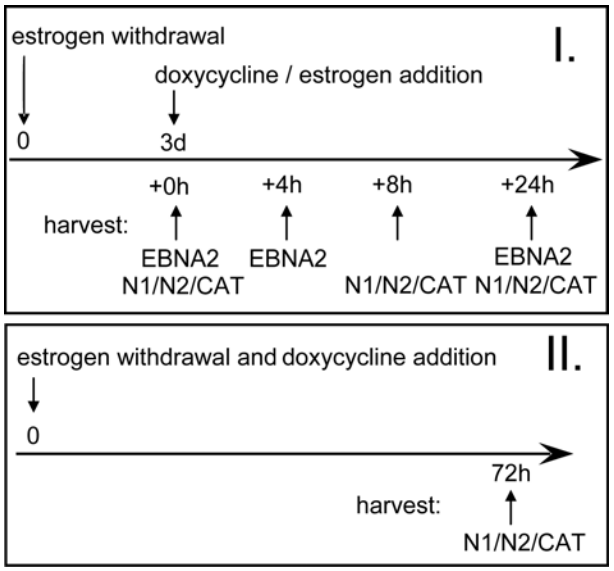

Figure 7 Experimental design for kinetic experiments with Notch1IC/EREB, Notch2IC/EREB, and CAT/EREB cells. Schematic illustration of the experimental design that was valid for all kinetic experiments. I.) Prior to induction, cells were deprived of estrogen for three days. Cells were harvested directly after estrogen withdrawal (0 hours), eight, and 24 hours after doxycycline addition (Notch1IC, Notch2IC, CAT), and four and 24 hours after estrogen addition to CAT/EREB cells (EBNA2). II.) To examine the effects of constitutive Notch signaling over a period of three days, doxycycline was added immediately after estrogen withdrawal and cells were harvested three days later. The control cell line CAT/EREB was treated in the same way as Notch1IC/EREB and Notch2IC/EREB cells. Prior to the preparation of RNA or to protein isolation, ΔNGFR$^+$ cells were purified by MACS separation to enrich the cells with a transcriptional response to doxycycline.

Clusters 1 and 2 contained cell cycle-associated genes that were upregulated late by EBNA2, suggesting an indirect regulation. Notch1IC and Notch2IC were able to induce most of these genes, however to a lower extent than EBNA2. *CCNE1* (*CyclinE1*), *CCNE2* (*CyclinE2*), *CCNA2* (*CyclinA2*), and *CDK6* from cluster 1 and *CDK4* from cluster 2 were selected to confirm their regulation by qPCR (Fig. 8A). All genes tested revealed a clear induction 24 hours and three days after Notch1/2IC induction as well as 24 hours after EBNA2 activation. In all cases, mRNA levels were significantly higher in EBNA2-expressing cells than in Notch1/2IC-expressing cells 24 hours after induction. Clusters 3 and 4 contained genes which were strongly activated already four hours after EBNA2 activation, including some known EBNA2 target genes like *CCND2* (*CyclinD2*), *c-MYC, PIK3R1*, and *CDK2*. qPCR confirmed that regulation by Notch1/2IC behaved heterogeneously in clusters 3 and 4. Whereas *CCND1*, *CCND*2, and *CDK2* were upregulated comparably by EBNA2 and Notch1/2IC (Fig. 8B), *c-MYC* and *PIK3R1* were much stronger upregulated by EBNA2 than by Notch1/2IC (Fig. 8C). In accordance with the mRNA expression data, PIK3R1 protein was detected in EBNA2- but not in Notch1/2IC-expressing cells. c-MYC protein expression was induced by Notch2IC and to a higher extent by Notch1IC, but did not reach the high peak of c-MYC protein levels as observed early after EBNA2 induction (Fig. 8D). From that data we draw the conclusion that the entry of Notch1/2IC-

expressing B cells into the S-phase of the cell cycle may be attributed to the induction of several cell cycle- and proliferation-associated genes by Notch1/2IC. However, that induction is obviously in general lower as the induction by EBNA2, except in case of *CCND2*, *CDK2*, and *CCND1*.

3.1.3 Differential expression of pro-apoptotic and anti-apoptotic genes in Notch1IC-, Notch2IC-, and EBNA2-expressing B cells

Since we observed an increased percentage of apoptotic cells in Notch1IC- and Notch2IC-expressing cell cultures compared to the negative control CAT/EREB, we were interested in the regulation of genes associated with apoptosis. Genes whose expression should be further tested were chosen from cluster analysis of apoptosis-related genes, which were at least two-fold regulated in the Affymetrix GeneChip® analysis (performed by H. Kohlhof). The cluster analysis revealed four different clusters. Cluster 1 contained genes that are mainly induced by Notch1/2IC, cluster 2 genes that are regulated by Notch1/2IC and EBNA2, and cluster 3 and 4 genes that are primarily regulated by EBNA2. Whereas cluster 1 mostly comprised pro-apoptotic genes, interestingly we found pro- as well as anti-apoptotic genes in clusters 2 to 4. By qPCR, we confirmed that several pro-apoptotic genes like *DNASE1L3, BID*, and *BCL2L11 (BIM)* were induced by Notch1/2IC and EBNA2 (Fig. 9A). In contrast, most anti-apoptotic genes like *BCL2A1 (BFL-1), BCL2L1,* and *BIRC5* (*Survivin*) were more intensely upregulated by EBNA2 than by Notch1/2IC (Fig. 9B). Since most of these anti-apoptotic genes are known as LMP1 target genes (Dirmeier *et al.*, 2005), their high expression in EBNA2-expressing cells is most likely due to the high amount of LMP1 protein in EBNA2/EREB compared to Notch1/2IC/EREB cells. These data show that Notch1/2IC as well as EBNA2 induce pro-apoptotic genes, implying that EBNA2 as well as Notch1/2IC lead to the induction of apoptosis in B cells as long as anti-apoptotic stimuli, for instance via LMP1, are missing (Kohlhof *et al.*, 2009).

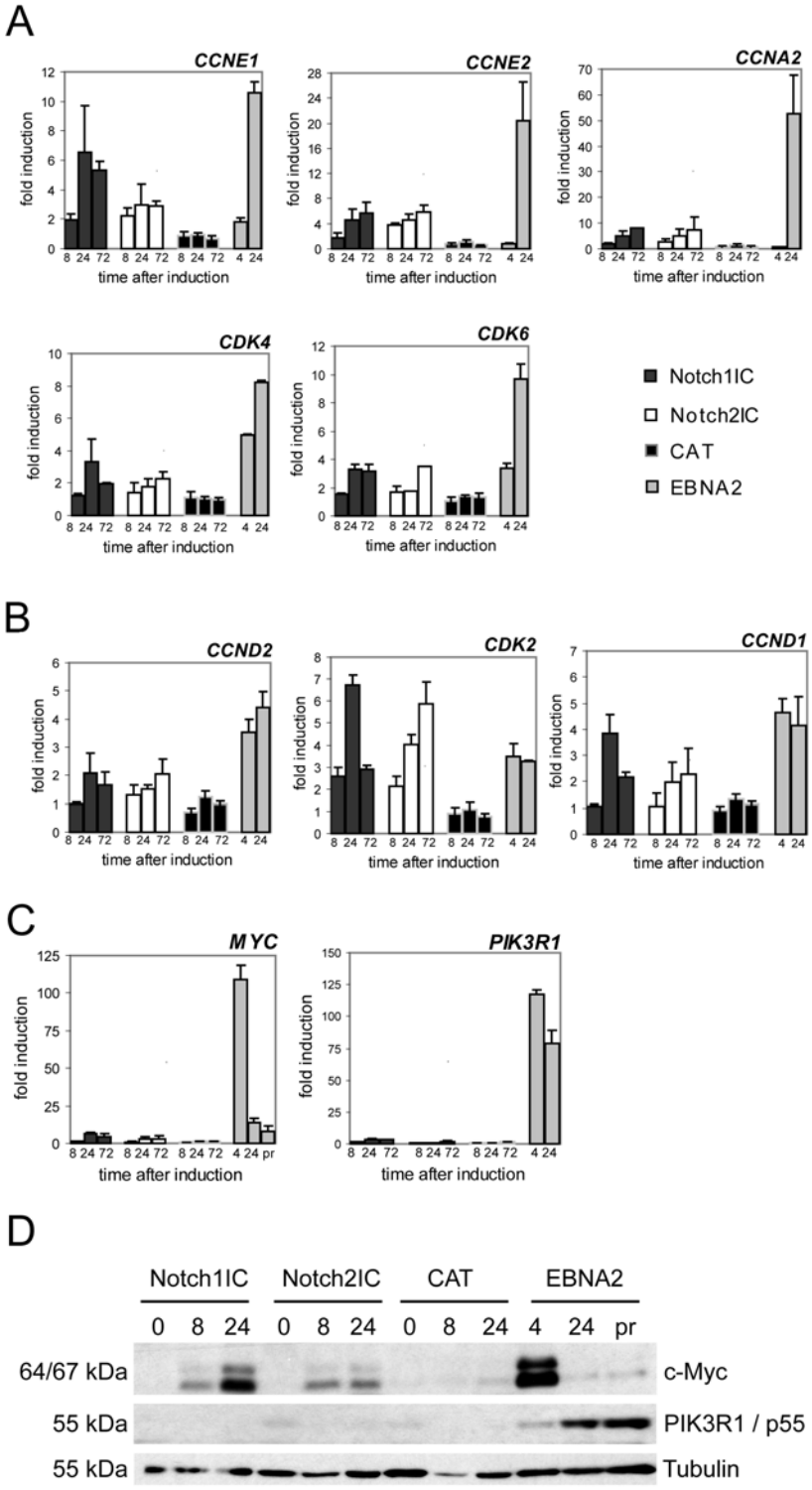

Figure 8 Differentially expressed cell cycle- and proliferation-associated genes in Notch1IC/EREB, Notch2IC/EREB, CAT/EREB, and EBNA2/EREB cells. Cells were treated as outlined in figure 7 and were harvested at indicated time points. mRNA levels were quantified by qPCR and are normalized to the expression of ribosomal protein genes. Values represent the fold induction of mRNA levels compared to the mRNA levels at 0 hours, which were set to 1. Data represent the average of triplicate samples with SD as shown. Coding of the graphs is explained beside the diagram; Notch1IC (Notch1IC/EREB), Notch2IC (Notch2IC/EREB), CAT (CAT/EREB), EBNA2 (CAT/EREB after the addition of estrogen); The analyzed genes are indicated above each diagram; CCN (cyclins); CDK (cyclin-dependent kinases); A-C show the results of qPCR analyses of **(A)** Cell cycle-associated genes, which were upregulated late but stronger by EBNA2 than by Notch1/2IC. **(B)** *CCNs* and *CDKs*, which were

upregulated early by EBNA2 and similarly by Notch1/2IC. **(C)** *PIK3R1* and *c-MYC,* which were upregulated early and strongly by EBNA2, and only marginally by Notch1/2IC. **(D)** Protein expression of c-MYC and PIK3R1 by Notch1/2IC and EBNA2. Notch1IC/EREB, Notch2IC/EREB, and CAT/EREB cells were deprived of estrogen for three days. Whole-cell lysates were harvested from growth-arrested cells (0 hours), from cells which were stimulated with doxycycline for eight or 24 hours (Notch1IC, Notch2IC, CAT), or from CAT/EREB cells, which were stimulated with estrogen for four or 24 hours (EBNA2). Additionally, whole-cell extracts were prepared from CAT/EREB cells continuously growing in the presence of estrogen (pr). Membranes were stained with antibodies raised against indicated proteins. Equal protein loading was controlled by staining with an α-Tubulin antibody.

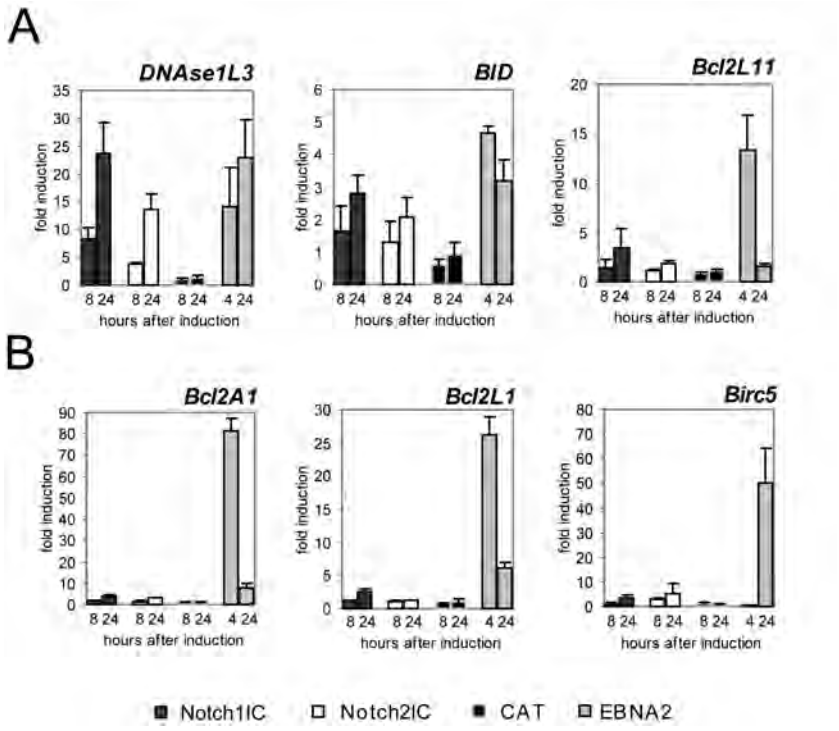

Figure 9 Differential expression of pro-apoptotic and anti-apoptotic genes in Notch1IC/EREB, Notch2IC/EREB, CAT/EREB, and EBNA2/EREB cells. qPCR analysis of apoptotic **(A)** and anti-apoptotic **(B)** genes. Cells were treated as outlined in figure 7 and were harvested at the indicated time points. mRNA levels were quantified by qPCR and are normalized to the expression of ribosomal protein genes. Values represent fold induction of mRNA levels compared to the mRNA levels at 0 hours, which was set to 1. Data represent the average of triplicate samples with SD as shown. The analyzed genes are indicated above the diagrams; The coding of the graphs is elucidated below the diagram; Notch1IC (Notch1IC/EREB), Notch2IC (Notch2IC/EREB), CAT (CAT/EREB), EBNA2 (CAT/EREB after the addition of estrogen).

3.2 The role of Notch2 in B cell differentiation *in vivo*

3.2.1 Generation of a transgenic mouse line conditionally expressing Notch2IC

To further investigate, how Notch2 influences normal B cell development *in vivo* and whether constitutive Notch2 signaling itself promotes B cell lymphomagenesis or rather induces apoptosis of mature B cells *in vivo*, a conditional transgenic mouse strain expressing a constitutive active Notch2 receptor (Notch2IC) based on the *Cre*/loxP system was generated. As we were particularly interested to explore the role of Notch in mature B cells, Notch2 was chosen to be investigated instead of Notch1, since Notch2 is the Notch family member mainly expressed in mature B cells (Saito *et al.*, 2003).

3.2.1.1 Targeting strategy

To generate the conditional Notch2IC-transgenic mouse strain, murine *notch2IC* cDNA was targeted into the murine *rosa26* locus (Fig. 10, 1). An endogenous ATG-Kozak sequence, located at the 5´-end of the *notch2IC* coding sequence, was used as translational start site. *Rosa26* is a commonly used locus for transgene expression, as *rosa26* is ubiquitously expressed, but can be homozygously deleted without phenotypic alterations.

The used targeting strategy is illustrated in figure 10. The *notch2IC* cDNA was placed under the control of the CAGGS (CMV early enhancer/chicken β-actin/rabbit globin) promoter, which is known as very strong and constitutive active promoter, achieving high expression levels in all tissues *in vivo* with the exception of erythrocytes and hair (Niwa *et al.*, 1991; Daly *et al.*, 1999b; Daly *et al.*, 1999a). The CAGGS expression module comprises at the 3´-end a short intron sequence, flanked by a splice donor and acceptor side, enhancing the transcription rate of the otherwise non-spliced transgene cDNA. To restrict the expression of *notch2IC* in a cell type-specific manner, a loxP-flanked transcription and translation termination sequence (STOP cassette) was placed upstream of the *notch2IC* coding sequence. To identify cells expressing the Notch2IC protein, an IRES-hCD2 cassette was placed downstream of the *notch2IC* coding sequence, leading to the simultaneous expression of a truncated human CD2 (hCD2) molecule and Notch2IC. Flanked with frt sites, the *IRES-hCD2* sequence may be excised by crossing the Notch2IC mouse strain to *Flp* recombinase-expressing mice, to exclude any alteration of the phenotype due to the concomitant expression of hCD2. In the targeting vector, the described expression cassette is flanked by rosa26 homologous arms, allowing the insertion into the *XbaI* restriction site of the murine *rosa26* genomic locus by homologous recombination (Fig. 10, 2). After *Cre*-mediated excision of the STOP cassette, the *notch2IC* transgene will be expressed under the control of the CAGGS promoter (Fig. 10, 3).

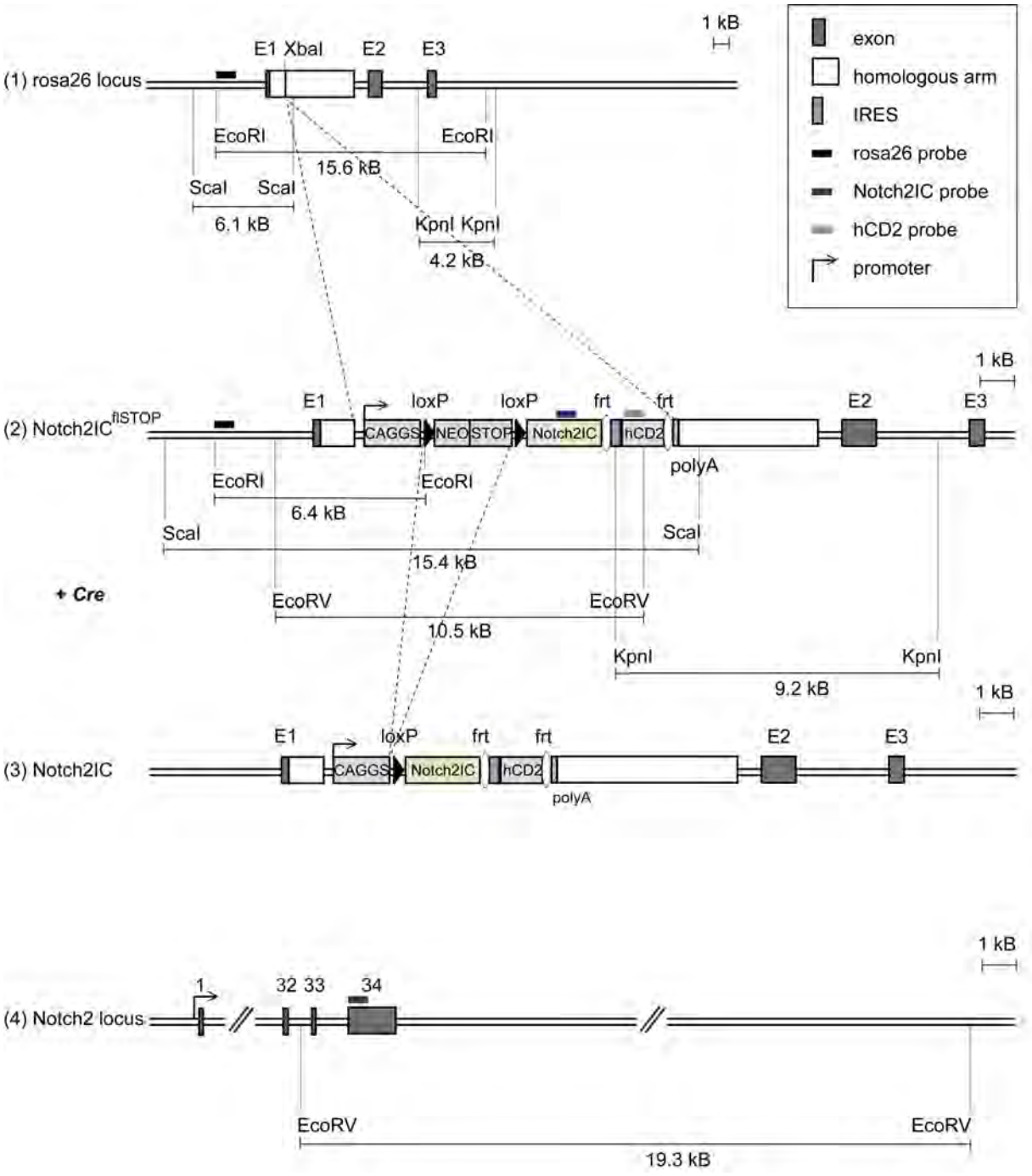

Figure 10 Targeting strategy for the generation of Notch2IC^{flSTOP} mice. The conditional *notch2IC* allele *(notch2IC^{flSTOP})* was inserted together with an *IRES-hCD2* coding sequence into the murine *rosa26* locus. (1) Wild type *rosa26* locus with its three exons and the *XbaI* restriction site in the first intron, where the transgene was inserted; (2) *Rosa26* locus after homologous recombination of the targeting construct (Notch2IC^{flSTOP}); (3) *Rosa26* locus after homologous recombination and deletion of the STOP cassette upon *Cre*-mediated recombination (Notch2IC), what leads to the expression of the *notch2IC* transgene under the transcriptional control of the constitutive active CAGGS promoter. The dotted lines illustrate the homologous recombination and the excision by *Cre*. The scheme shows the restriction sites (*EcoRI*, *ScaI*, *KpnI*, *EcoRV*) used for Southern blot digest and the location of the respective probes. The expected fragments after the respective digestion and hybridization with the labeled probe are indicated by the thin lines. *XbaI* (site of insertion); CAGGS (CMV early enhancer/chicken β-actin/rabbit globin promoter); STOP (STOP cassette); hCD2 (truncated human CD2); NEO (neomycin-geneticin resistance gene); *Cre* (*Cre* recombinase).

For the generation of the transgenic mouse strain, four consecutive steps were required. (1) Cloning of the targeting construct; (2) Transfection of the construct in murine embryonic stem cells and screening to identify clones, which have inserted the expression cassette into the *rosa26* locus by homologous recombination; (3) Injection of correctly targeted ES cell clones into blastocysts followed by implantation into foster mothers; (4) Breeding of resulting chimeric offspring with wild type mice to achieve germline transmission of the transgene.

3.2.1.2 ES cell targeting

After cloning as described in 8.3.4, the linearized Notch2IC targeting construct was transfected into murine IDG2.3 ES cells by electroporation. IDG2.3 is a F1-hybrid cell line that was established from a male C57BL/6Jx129/SV (F1) blastocyst (Hitz *et al.*, 2007). 384 G418-resistant cell colonies were picked and expanded for further analyses. To identify clones with correct, homologous, and single recombination, different Southern blot analyses were performed. The different Southern blot strategies are outlined in figure 10. To screen for homologous recombination of the targeting vector with the *rosa26* locus, *EcoRI*-digested DNA was hybridized to the rosa26 probe, which is externally located at the 5´-end of the targeting vector. This probe detects the wild type *rosa26* locus as a 15.6 kb fragment and the homologous recombined locus as a 6.4 kb fragment (Fig. 11A). 29 out of the 384 screened clones showed homologous integration at one *rosa26* allele, and out of these, six clones were subjected to further analyses. Non-targeted IDG2.3 ES cells were used as negative control. The integration of the entire 9.3 kb expression cassette into the *rosa26* locus was further confirmed with a *ScaI* digest and hybridization with the rosa26 probe, detecting a 15.4 kb fragment in the recombinant clones and the wild type allele as a 6.1 kb fragment (Fig. 11B). To prove the complete integration not only from the 5´-site, as accomplished by *EcoRI* and *ScaI* digests, but also from the 3´-site, a probe recognizing sequences of hCD2 was hybridized to *KpnI*-digested DNA, detecting a 9.2 kb fragment after complete integration at the 3´-end (Fig. 11C). To exclude multiple integrations, a probe recognizing a sequence of *notch2IC* was used in combination with *EcoRV*-digested DNA (Fig. 11D), revealing a 10.5 kb fragment in the correctly targeted clones and an additional 19.3 kb fragment in all examined samples, resulting from the hybridization of the probe with the endogenous *notch2* locus. Moreover, a non-specific signal at the fragment size of 15.0 kb was detected in all examined samples including the non-targeted control, what might be due to an unknown restriction polymorphism of the *notch2* gene in IDG2.3 cells.

From the Southern blot analyses we concluded that all further examined clones carry the Notch2IC expression cassette correctly integrated exclusively in the *rosa26* locus. Three out of these six clones (NIA5, NIC6, NIIID8) were subjected to sequencing of the *notch2IC* transgene

to exclude any mutations. For this purpose, the transgene was amplified from genomic ES cell DNA in two parts by PCR and the sequence integrity of the obtained products was confirmed in all clones by BLAST analysis of the sequencing data with the original sequence.

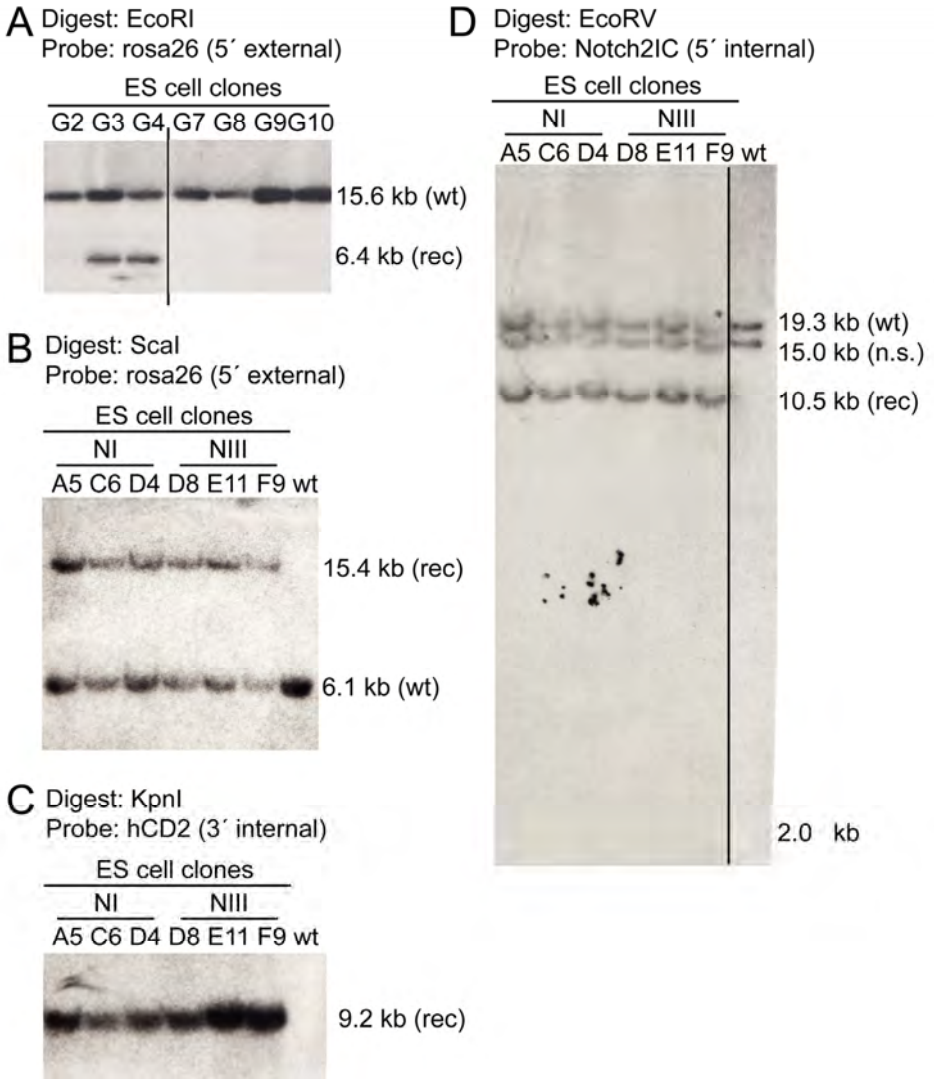

Figure 11 Southern blot analyses of targeted and wild type ES cell clones. Southern blot analyses showing the correct and single integration of the Notch2IC expression cassette in the *rosa26* genomic locus of targeted IDG2.3 ES cells. Genomic DNA from targeted and wild type ES cells was digested with the indicated restriction enzymes and subjected to Southern blot analyses with the stated radioactively labeled probes; (wt) fragments detect the wild type alleles; expected (rec) fragments are detected after homologous recombination. **(A)** After an *EcoR1* digest, a 15.6 kb (wt) and a 6.4 kb (rec) fragment are detected by the rosa26 probe. **(B)** After a *ScaI* digest, a 15.4 kb (rec) and a 6.1 kb (wt) fragment are detected by the rosa26 probe. **(C)** After a *KpnI* digest, a 9.2 kb (rec) fragment and no signal in wild type ES cells are detected by the hCD2 probe. **(D)** After an *EcoRV* digest, the Notch2IC probe detects a 10.5 kb (rec) fragment, a 19.3 kb (wt) fragment from hybridization with the endogenous *notch2* locus, and a non-specific 15.0 kb (n.s.) fragment in all lanes. No additional signal down to the size of 2 kb was detected, excluding any multiple integrations.

Furthermore, the expression of hCD2 was tested by deleting the loxP sites-flanked STOP cassette *in vitro*. For that purpose, targeted ES cells were transiently transfected with a *Cre* recombinase expression plasmid and hCD2 expression was analyzed by flow cytometry after 48 hours (Fig. 12). 11 to 16 % of $hCD2^+$ cells were detected in the different clones after *Cre* expression, what corresponds approximately to the expected transfection efficiency. Only very few (0.35 %) $hCD2^+$ cells were found in the non-transfected control. Thus, we concluded that the STOP cassette does not exhibit any leakiness and can be successfully excised via *Cre*-mediated recombination at the loxP sites leading to hCD2 expression via the IRES element in the targeted IDG2.3 ES cells.

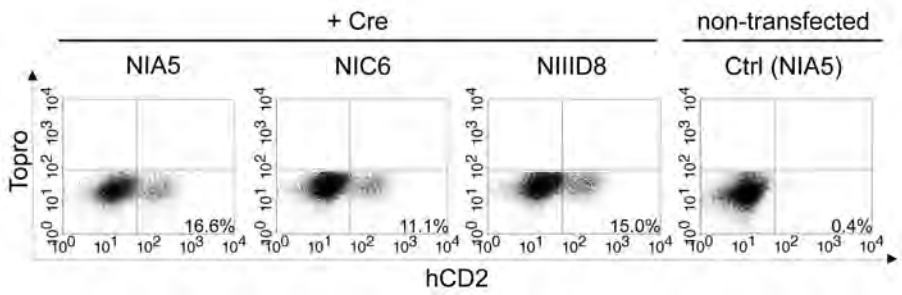

Figure 12 Functional testing of targeted ES cell clones for hCD2 expression. Flow cytometric analysis of targeted ES cell clones (N1A5, NIC6, NIIID8) 48 hours after transient transfection of a *Cre* recombinase expression plasmid (+ *Cre*). Non-transfected cells of clone NIA5 served as negative control. Numbers display the percentages of $TOPRO^-$-gated, $hCD2^+$ cells.

3.2.1.3 Establishment of the Notch2IC^{flSTOP} mouse line

In cooperation with the Institute of Developmental Genetics of the Helmholtz Center Munich, the clones NIA5 and NIIID8 were injected into C57BL/6-derived blastocysts and were implanted into C57BL/6 foster mothers (Fig. 13A). Clone NIA5 gave rise to seven chimeras (Fig. 13B), showing 95 to 100 % of chimerism, while clone NIIID8 gave rise to four chimeras of 95 % of chimerism. To establish the Notch2IC^{flSTOP} mouse strain, chimeras of each clone were bred with C57BL/6 mice. Since the *notch2IC* transgene was passed to the offspring in all cases according to Mendelian segregation, 100 % germline transmission of the transgene was obtained for each chimera (Fig. 13C).

As we aimed to investigate the role of Notch2 in B cells, Notch2IC expression was activated specifically in B lymphocytes at certain differentiation stages. Notch2IC^{flSTOP} mice were either crossed to CD19-*Cre* (Rickert *et al.*, 1997) or mb1-*Cre* (Hobeika *et al.*, 2006) mice. Both *Cre*-strains induce deletion of the STOP cassette from the pro-B cell stage on. Whereas the deletion efficiency mediated by mb1-*Cre* is already high in pro-B cells, CD19-*Cre* leads to a gradual increase in *Cre*-mediated recombination as B cells proceed through their differentiation (Rickert *et*

al., 1997). For simplicity, mice carrying one *notch2IC* knock-in allele, and one CD19-*Cre* or mb1-*Cre* allele, respectively, are referred to as Notch2IC//CD19Cre$^{+/-}$ and Notch2IC//mb1Cre$^{+/-}$ mice, respectively. As controls, either Notch2IC^{flSTOP} and CD19Cre$^{+/-}$, or Notch2IC^{flSTOPP} and mb1Cre$^{+/-}$ mice, were used despite otherwise stated, since these control strains showed an identical phenotype.

Figure 13 Blastocyst injection and establishment of the Notch2IC^{flSTOPP} mouse strain. (A) IDG2.3 ES cell colonies, cultured on an embryonic feeder cell layer, on the day of injection into blastocysts. ES cell colonies are indicated by an arrow. **(B)** Chimeric mouse with 95 to 100 % of chimerism, resulting from the blastocyst injection of clone NIA5. The extent of chimerism is judged from the ratio of black and brown coat color. A ratio of 25:75 (brown:black) corresponds to a chimerism of 100 % after injection of C57BL/6Jx129/SV (F1) ES cells in C57BL/6-derived blastocysts. **(C)** Genotyping PCR to prove germline transmission of the *notch2IC* transgene detected by a 560 bp PCR product. Transgene detection in about 50 % of offspring corresponds to 100 % germline transmission since 50 % was the expected transmission of this breeding according to Mendelian segregation. Genomic DNA from clone NIA5 and targeting vector DNA served as positive controls for PCR; (1-7) offspring after germline breeding of chimeras from clone NIIID8.

3.2.2 Notch2IC protein is translocated into the nucleus and is functional in B cells of Notch2IC//CD19Cre$^{+/-}$ mice

To prove the functionality of the established transgenic mouse strain, the expression of the Notch2IC protein after removal of the STOP cassette was analyzed by Western blots of whole-cell extracts from splenic B cells (Fig. 14A). High expression levels of Notch2IC protein were detected in splenic B cells isolated from Notch2IC//CD19Cre$^{+/-}$ mice but not in B cells of Notch2IC^{flSTOP} control mice, evidencing that Notch2IC is expressed *in vivo* after *Cre*-mediated recombination and proving a tight control exerted by the STOP cassette on transgene expression. Since nuclear translocation of Notch is a prerequisite for the interaction with RBP-J$\varkappa$ and the activation of target genes, we studied next whether the transgenic Notch2IC protein can be translocated into the nucleus. To this end, we separated protein lysates of splenic B cells isolated from Notch2IC//CD19Cre$^{+/-}$ and control mice in cytoplasmic and nuclear fraction and analyzed the Notch2IC protein level by Western blot (Fig. 14B). Notch2IC protein was detected in large amounts in the nuclear fraction of Notch2IC-expressing B cells as multiple bands of slightly different molecular weight. A very low level of Notch2IC, but only the variant of higher

molecular weight was found in Notch2IC^{flSTOP} or CD19Cre$^{+/-}$ control B cells. In Notch2IC//CD19Cre$^{+/-}$ B cells, the detection of multiple signals for Notch2IC slightly differing in size could be due to either lacking posttranslational modifications in comparison to wild type Notch2IC or to partial degradation.

To confirm the functionality of the transgenic Notch2IC protein, we examined the expression of *hes1* and *deltex1* in the mutant mice, as both are classical Notch target genes. Both Hes1 and Deltex1 levels were significantly increased in whole-cell extracts from Notch2IC-expressing B cells compared to controls (Fig. 14C). These data show that the transgenic Notch2IC protein is expressed specifically in B cells at high levels upon *Cre*-mediated deletion of the STOP cassette, and can be translocated into the nucleus, where it exhibits its function in the transcriptional regulation of target genes, as shown for *hes1* and *deltex1*.

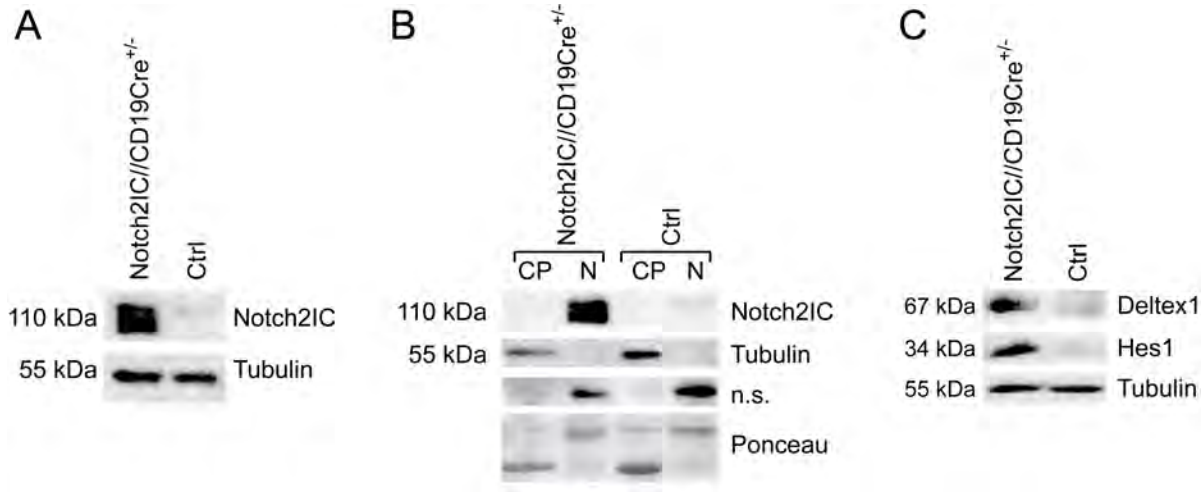

Figure 14 Notch2IC protein is expressed, translocated into the nucleus, and functional in B cells of Notch2IC//CD19Cre$^{+/-}$ mice. Splenic B cells were purified from Notch2IC//CD19Cre$^{+/-}$ and control mice. For experiments shown in A-C, both Notch2IC^{flSTOP} and CD19Cre$^{+/-}$ control mice were used and showed an identical phenotype. **(A)** Whole-cell extracts were subjected to immunoblot analysis with an antibody raised against Notch2. Equal protein loading was controlled by an α-Tubulin staining. The result is representative for five independent experiments. **(B)** Cytoplasmic (CP) and nuclear (N) levels of Notch2IC were analyzed by immunoblot. The purity of cytoplasmic and nuclear extracts was verified by an α-Tubulin staining and by an non-specific (n.s.) signal arising only in the nucleus after staining with an α-Bcl3 antibody. Equal protein loading was controlled by a Ponceau S staining. The experiment was performed three times. **(C)** Whole-cell extracts were subjected to immunoblot analysis with antibodies raised against murine Deltex1 and Hes1. Equal protein loading was controlled by an α-Tubulin staining. The experiment was performed five times.

3.2.3 Early B cell development is blocked in Notch2IC//mb1Cre$^{+/-}$ mice

Retroviral high-level expression of Notch2IC in hematopoietic stem cells has been shown to block B cell development at the large pre-B cell stage and to result in the development of T cell leukemia, whereas lower-level expression of Notch2IC selectively promoted B1 B cell differentiation (Witt *et al.*, 2003a). To assess what phenotype is achieved when transgenic

Notch2IC is expressed from the early pro-B cell stage on, we analyzed the lymphoid compartment of Notch2IC//mb1Cre$^{+/-}$ mice by flow cytometry.

B cells in the bone marrow can be distinguished in B220^{+}CD43^{+} pro- and large pre-B cells, B220^{+}CD43^{-} small pre- and immature B cells, and B220^{high}CD43^{-} mature B cells, recirculating to the bone marrow from the periphery. B220^{+}CD43^{+} B cells can be further divided into Hardy Fraction A (BP1^{-}CD24^{low}), Fraction B (BP1^{-}CD24^{+}), Fraction C (BP1^{+}CD24^{low}), and Fraction C´ (BP1^{+}CD24^{+}) (Allman *et al.*, 2001b). Lymphoid cells were isolated, stained for the expression of various surface markers, and subsequently subjected to flow cytometric analysis.

Notch2IC expression induced by mb1-*Cre* resulted in a complete block of B cell development in the bone marrow. No immature and mature B cells were detected and even the B220^{+}CD43^{+} pro-/large pre-B cell population was strongly reduced compared to control mice (Fig. 15, upper panel and Tab. 1). A more detailed analysis of the remaining B cell population revealed that almost all B220^{+}CD43^{+} B cells are BP1^{-} and CD24^{low} (Hardy Fraction A). The BP1^{-}CD24^{+} population (Hardy Fraction B) was slightly reduced, whereas the BP1^{+} fractions C and C´ were strongly diminished in Notch2IC//mb1Cre$^{+/-}$ mice compared to controls (Fig. 15, lower panel). These results indicate that Notch2IC expression blocks B cell development already at Hardy Fractions A and B. Analysis of hCD2 expression showed that only around 15 % of B220^{+}CD43^{+} B cells carry a deletion of the STOP cassette (Tab. 1) suggesting that B cell development is blocked as soon as Notch2IC is expressed.

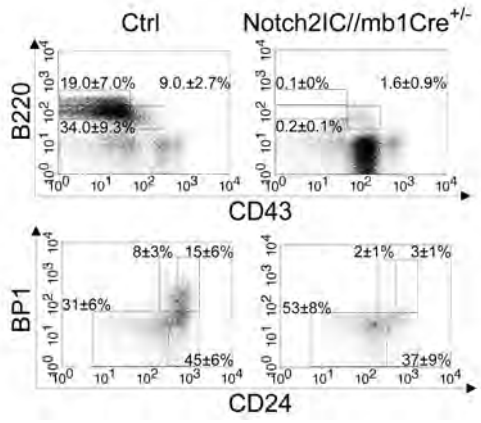

Figure 15 Early B cell development is blocked in Notch2IC//mb1Cre$^{+/-}$ mice. FACS dot blots from representative experiments characterizing B cell populations in the bone marrow of Notch2IC//mb1Cre$^{+/-}$ and control mice. Numbers display the mean percentages and SD of lymphocyte-gated pro- and large pre-B cells (B220^{+}CD43^{+}), immature and small pre-B cells (B220^{+}CD43^{-}), and mature, recirculating B cells (B220^{high}CD43^{-}) (upper panel) or of lymphocyte-gated, B220^{+}CD43^{+} Hardy Fraction A (BP1^{-}CD24^{low}), Fraction B (BP1^{-}CD24^{+}), Fraction C (BP1^{+}CD24^{low}), and Fraction C´ (BP1^{+}CD24^{+}) (Allman *et al.*, 2001b) (lower panel). Values were calculated from 10 analyzed mice per genotype.

3.2.4 Notch2IC expression dependent on mb1-*Cre* causes an aberrant T cell-like differentiation in the bone marrow

In Notch2IC//mb1Cre$^{+/-}$ mice, 72 % of lymphocyte-gated bone marrow cells expressed hCD2, although less than 2 % of these cells were B220^{+} (Tab. 2). Further analyses of this hCD2^{+} bone marrow population showed that up to 99 % of these cells were CD8^{+}, CD4^{+}, CD43^{+}, CD5^{+}, Thy1.2^{+}, CD3^{low} but T cell receptor β^{-} (Fig. 16A and data not shown). Thus, the phenotype of

this cell population is clearly reminiscent of T cells. Forward/side scatter analysis of the hCD2$^+$ bone marrow population showed that the major percentage of cells is located in the lymphocyte gate. Thereby, a notable fraction of cells displayed an activated phenotype, visible from an enlarged size in the forward scatter (Fig. 16B).

Table 1

B cell populations with deletion efficiencies in the bone marrow of Notch2IC//mb1Cre$^{+/-}$ and control mice.

Mice (n)	5-12			
Gated on:	IgM$^-$ B220^{low} CD43$^+$ Pro B	IgM$^-$ B220^{low} CD43$^-$ Pre B	B220$^+$ IgM$^+$ IgD$^-$ Immature B	B220$^+$ IgM$^+$ IgD$^+$ Mature B
% of:				
Ctrl	8.4±2.2	33.9±6.6	11.4±4.1	20.8±7.9
Notch2IC//mb1Cre$^{+/-}$	1.6±0.7***	0.2±0.1***	0.2±0.3***	0.5±0.6***
[x 10^5]				
Ctrl	14.9±2.5	13.7±6.3	5.2±3.0	8.4±3.4
Notch2IC//mb1Cre$^{+/-}$	1.2±0.7***	0.2±0.1***	0.03±0.04***	0.05±0.05***
% hCD2$^+$				
Notch2IC//mb1Cre$^{+/-}$	14±4	22±11	n.s.	n.s.

Bone marrow cells were isolated from two tibia bones per mouse. Percentages within the lymphocyte gate are shown. Values represent the mean ± SD. *** P<0.001, in comparison to Ctrl; n.s. (non-specific).

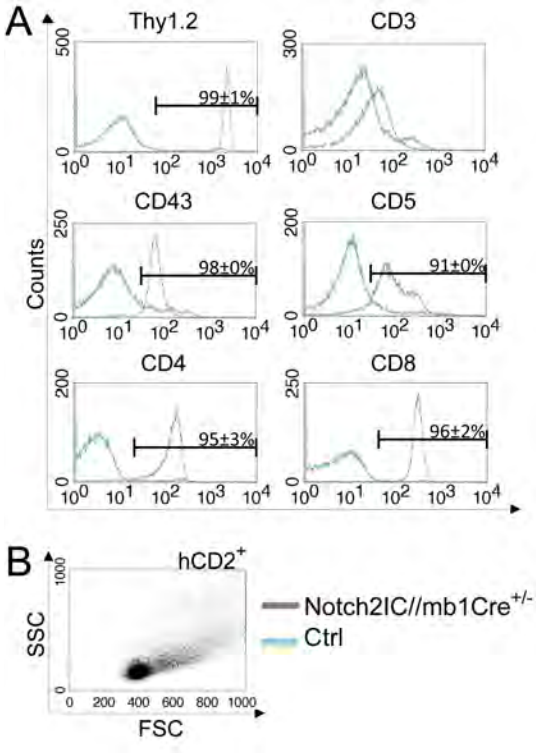

Figure 16 hCD2$^+$ bone marrow cells from Notch2IC//mb1Cre$^{+/-}$ display a CD8$^+$, CD4$^+$, CD43$^+$, CD5$^+$, Thy1.2$^+$, CD3^{low} phenotype. (A) Bone marrow single cell suspensions were stained and analyzed by flow cytometry for the expression of indicated surface markers. Histograms show overlays of the surface expression of the respective molecules on lymphocyte-gated, hCD2$^+$ cells from Notch2IC//mb1Cre$^{+/-}$ mice (grey line) and lymphocyte-gated bone marrow cells from control mice (blue line). Mean percentages and SD were calculated from 10 independent experiments. **(B)** Forward/side scatter (FSC/SSC) characterization of hCD2$^+$ bone marrow cells of Notch2IC//mb1Cre$^{+/-}$ mice. The blot displays FSC/SSC distribution of TOPRO-3$^-$, hCD2$^+$ cells representative for 15 independent experiments.

In total, B220$^+$ B cell numbers were severely reduced in the bone marrow, while Thy1.2$^+$ T cell numbers were extremely increased, leading in summary to an increased number of total lymphocytes in the bone marrow compared to control animals (Fig. 17A). B220$^+$ B cells in the spleen, lymph nodes, and the peritoneal cavity of Notch2IC//mb1Cre$^{+/-}$ mice were drastically reduced (Fig. 17B, Tab. S1, and data not shown). The remaining B220$^+$ lymphocyte population of these organs did not express IgM, IgD, CD21, or CD23 (data not shown), pointing to a rather immature state of these peripheral B cells. T cell development in the thymus of Notch2IC//mb1Cre$^{+/-}$ mice was not altered (data not shown) and also T cell numbers in the spleen, lymph nodes, and the thymus were comparable to control mice (Fig. 17B and Tab. S1).
The aberrant hCD2$^+$ population was found only in small amounts in other secondary lymphoid organs including the blood of Notch2IC//mb1Cre$^{+/-}$ mice, displaying in 50 to 98 % the described immune phenotype (data not shown). The percentages of lymphocyte-gated, hCD2$^+$ cells in the various organs with percentages of Thy1.2$^+$ T cells and B220$^+$ B cells within this population are displayed in table 2, and do rather not point to an established leukemic disease at the time point of analysis. Mice of six, eight, 10, and 11 weeks of age were analyzed and all showed an identical phenotype. Mice died with 10 to 12 weeks of age of unknown cause of death. In summary, the expression of Notch2IC dependent on mb1-*Cre* blocked early B cell maturation at the pro-B cell stage for unknown reasons and led to the formation of an aberrant Notch2IC-expressing population with a T cell-like surface phenotype, mainly located in the bone marrow.

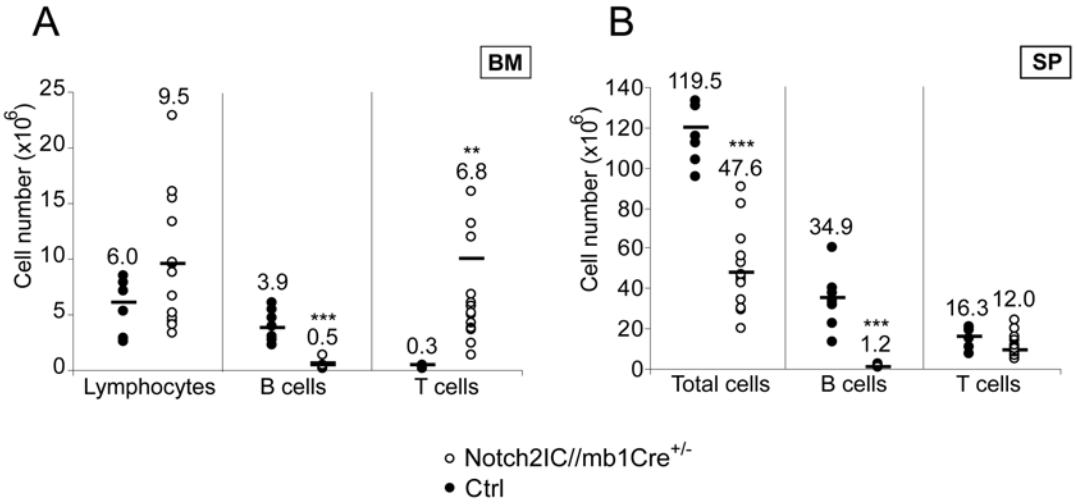

Figure 17 Notch2IC//mb1Cre$^{+/-}$ mice show T cell expansion in the bone marrow, but have reduced B cell numbers in the bone marrow and the spleen. Absolute numbers of lymphocytes or total counted cells, lymphocyte-gated, B220$^+$ B cells, and Thy1.2$^+$ T cells in bone marrow (BM) **(A)** and spleen (SP) **(B)** of Notch2IC//mb1Cre$^{+/-}$ (blank circle) and control (filled circle) mice. Points represent data from individual mice and horizontal bars mark the mean value, indicated in numbers above each point column. ** P<0.01, *** P<0.001, as calculated by the two-tailed student's t-test in comparison to control.

Table 2

Percentages of hCD2$^+$ cells in organs of Notch2IC//mb1Cre$^{+/-}$ mice with respective percentages of B220$^+$ B cells and Thy1.2$^+$ T cells within the hCD2$^+$ population.

			hCD2$^+$	
	Mice (n)	% hCD2$^+$	% B220$^+$	% Thy1.2$^+$
Bone Marrow	15	71.6±8.4***	1.8±0.6	98.9±0.6
Thymus	14	2.3±2.0*	n.d.	99.3±1.1
Spleen	15	1.3±0.9**	57.0±9.7	66.3±20.5
Peripheral Blood	11	1.0±0.7*	n.d.	95.3±1.1
Peritoneal Cavity	11	0.3±0.3	2.3±0	n.s.
i Lymph Node	15	0.1±0.1*	n.s.	94.6±5.7

Percentages within the lymphocyte gate are shown. Values represent the mean ± SD.
* P<0.1, ** P<0.01, *** P<0.001 in comparison to Ctrl; (n.s.) non-specific; (n.d.) not defined.

3.2.5 Early B cell development is normal in Notch2IC//CD19Cre$^{+/-}$ mice

To overcome the block of early B cell development, Notch2IC^{flSTOP} mice were bred with CD19-*Cre* mice. CD19-*Cre* initiates deletion of the STOP cassette from the pro-B cell stage on, but leads to a gradual increase in *Cre*-mediated recombination as B cells proceed through their differentiation. Thereby, negative selection of transgene-expressing cells during early B cell development may be overcome by delayed recombination. Expression of *Cre* recombinase under the control of the endogenous CD19 promoter has been reported to result in a deletion efficiency of 75 to 80 % in bone marrow B cells and > 95 % in B cells of the periphery (Rickert *et al.*, 1997). The analysis of hCD2 expression revealed the deletion of the STOP cassette in 17 % of all bone marrow, and in 79 % of all splenic B cells in Notch2IC//CD19Cre$^{+/-}$ mice (Fig. 18A). The very low deletion efficiency in B cells of the bone marrow indicates a negative selection of developing B cells that express Notch2IC, though the percentages and total cell numbers of pro-, pre-, and immature B cells were comparable in mutant and control mice. Only percentages and total numbers of mature, recirculating B cells were significantly diminished in Notch2IC//CD19Cre$^{+/-}$ mice compared to controls (Fig. 18B and Tab. 3).

In summary, we observed normal early B cell development in Notch2IC//CD19Cre$^{+/-}$ mice in contrast to Notch2IC//mb1Cre$^{+/-}$ mice. In addition, high percentages of peripheral B cells expressing the transgene were detected. From these results we concluded that the block of B cell development can obviously be overcome by the delayed activation of Notch2IC expression dependent on CD19-*Cre*.

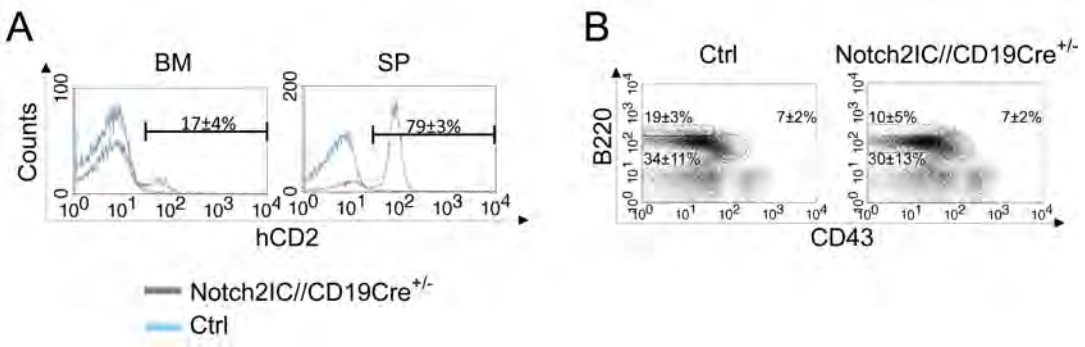

Figure 18 Early B cell development is normal in Notch2IC//CD19Cre$^{+/-}$ mice. (A) Deletion efficiency of the STOP cassette measured by flow cytometric analysis of hCD2 expression on bone marrow (BM) and splenic (SP) B cells from Notch2IC//CD19Cre$^{+/-}$ (grey line) and control (blue line) mice. Numbers indicate mean percentages and SD of hCD2 expression on lymphocyte-gated, B220^{+} B cells. Values were calculated from 10 independent experiments. **(B)** Flow cytometric analysis of bone marrow single cell suspensions. Numbers display the mean percentages and SD of lymphocyte-gated pro- and large pre-B cells (B220^{+}CD43^{+}), immature and small pre-B cells (B220^{+}CD43^{-}), and mature, recirculating B cells (B220^{high}CD43^{-}). Values were calculated from twelve analyzed mice per genotype.

3.2.6 Marginal zone B cells are the dominant B cell population in Notch2IC//CD19Cre$^{+/-}$ mice

As the genetic deletion of Notch2 or components of its signaling pathway result in the abolishment of the MZ B cell population with normal maintenance of the Fo B cell population, we were particularly interested, how the peripheral B cell compartment of Notch2IC//CD19Cre$^{+/-}$ mice will be affected by the expression of constitutive active Notch2. For that purpose, cell populations, in particular B cell subsets, were analyzed in secondary lymphoid organs as the spleen, inguinal lymph nodes, and the peritoneal cavity of Notch2IC//CD19Cre$^{+/-}$ and control mice.

3.2.6.1 Notch2IC//CD19Cre$^{+/-}$ mice show a slight splenomegaly, but normal splenic cell numbers

Conditional expression of Notch2IC induced by CD19-*Cre* resulted in a slight, but statistically significant splenomegaly in eight to 16 week-old mice (Fig. 19A), while the splenic weight of Notch2IC//CD19Cre$^{+/-}$ mice was increased on average by 1.5-fold compared to control mice (Fig. 19B). B and T cell numbers were normal in Notch2IC-expressing mice compared to age-matched controls (Fig. 19C and Tab. 3).

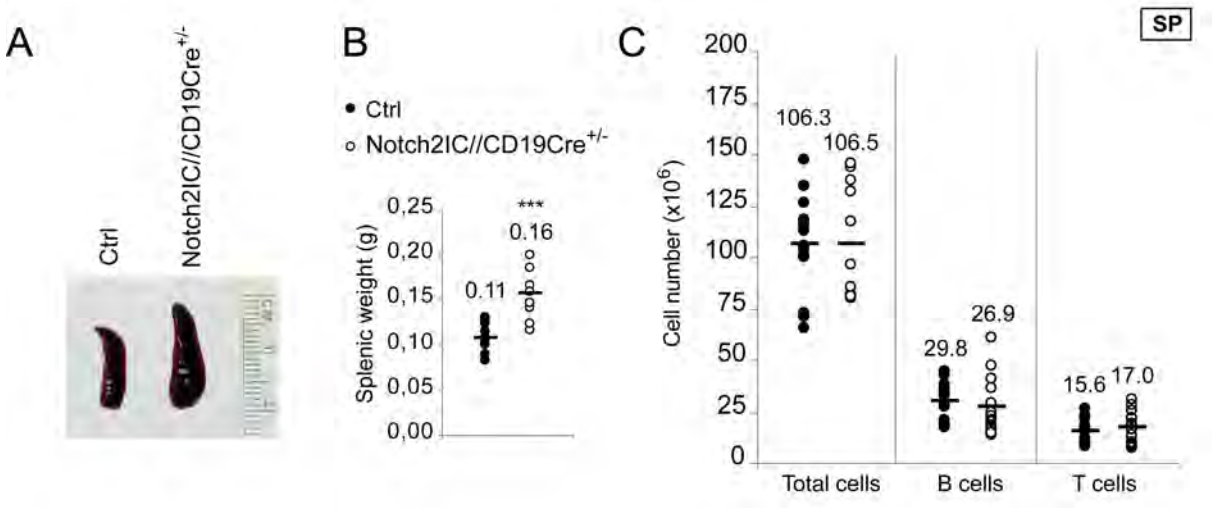

Figure 19 Slight splenomegaly, but normal splenic cell numbers in Notch2IC//CD19Cre$^{+/-}$ mice. **(A)** Splenic size of eight week-old Notch2IC//CD19Cre$^{+/-}$ mice and littermates. The ruler indicates the size of the organs. **(B)** Splenic weight and **(C)** absolute numbers of total counted cells, B220^{+} B cells, and CD3^{+} T cells in the spleen (SP) of Notch2IC//CD19Cre$^{+/-}$ (blank circle) and control (filled circle) mice. Points represent data from individual mice and horizontal bars mark the mean value, indicated in numbers above each point column. *** $P < 0.001$, in comparison to control, as calculated by the two-tailed student's t-test.

3.2.6.2 Marginal zone B cells are expanded in Notch2IC//CD19Cre$^{+/-}$ mice to the expense of the follicular B cell population

To determine the distribution of different B cell subsets in the spleen, splenic cells were stained with different antibody combinations and were subsequently analyzed by flow cytometry. By staining cells with α-IgM and α-IgD antibodies, immature and MZ B cells (IgM^{+}IgD^{low}) can be distinguished from Fo B cells (IgM^{+}IgD^{+}). As shown in the dot plots in figure 20A (upper panel), the percentage of IgM^{+}IgD^{low} B cells was significantly increased in Notch2IC//CD19Cre$^{+/-}$ mice. As a consequence, the percentage of the IgM^{+}IgD^{+} B cell population was dramatically decreased. However, the remaining Fo B cell population expressed higher overall levels of IgM. Moreover, the analysis of CD21 and CD23 expression revealed that the majority of the mature B cell fraction in Notch2IC//CD19Cre$^{+/-}$ mice has adopted a MZ B cell phenotype (CD21^{high}CD23^{-}), while the percentage of CD21^{int}CD23^{+} Fo B cells was dramatically decreased (Fig. 20B, upper panel). The absolute B cell numbers of Fo and MZ B cells were five times lower and seven times higher, respectively, in Notch2IC//CD19Cre$^{+/-}$ mice than those of controls (Tab. 3). These data suggest a strong shift of mature B cells to the MZ B cell compartment at the expense of Fo B cells upon constitutive Notch2 signaling.

3.2.6.3 B cell subsets are altered in the inguinal lymph nodes of Notch2IC//CD19Cre$^{+/-}$ mice

Fo B cells form the pool of mature B cells that recirculate with the blood through the body and the peripheral lymphoid organs. In contrast, MZ B cells are sessile at the margin of splenic follicles and can thus exclusively be found in the spleen, but not in other secondary lymphoid compartments like the lymph nodes. Therefore, we were interested to investigate how the intensive generation of MZ instead of Fo B cells affects the B cell subsets in the inguinal lymph nodes of Notch2IC//CD19Cre$^{+/-}$ mice.

Mainly cells that had not deleted the STOP cassette were found in the inguinal lymph nodes of Notch2IC//CD19Cre$^{+/-}$ mice, since only 24 % of B cells expressed hCD2 (data not shown). Applying an IgM/IgD as well as a CD21/CD23 staining revealed that the predominant B cell population in the inguinal lymph nodes is still formed by Fo B cells. However, percentages and numbers of this population were reduced compared to the control, while percentages and numbers of B cells displaying a MZ B cell phenotype were significantly elevated (Fig. 20A and B, lower panel, Fig. S1, right panel). In addition, a slightly increased CD21^{-}CD23^{-} immature B cell population was observed. Total B cell numbers were slightly, but not significantly reduced, whereas T cell numbers were almost doubled compared to the wild type (Fig. S1, left panel). The diminished B cell number and percentage of Fo B cells may be the consequence of reduced numbers of circulating Fo B cells in Notch2IC//CD19Cre$^{+/-}$ mice and is in line with the reduction of recirculating B cells in the bone marrow as described in 3.2.5.

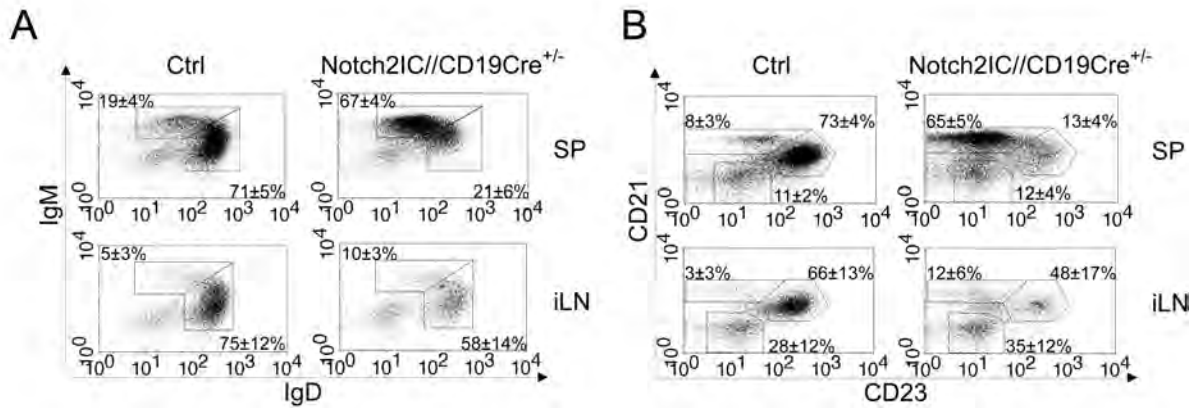

Figure 20 Marginal zone B cells are expanded in Notch2IC//CD19Cre$^{+/-}$ mice to the expense of the follicular B cell population. (A) Lymphocytes of the spleen (SP) and inguinal lymph nodes (iLN) were analyzed by flow cytometry for the expression of IgM and IgD. Numbers indicate mean percentages and SD of lymphocyte-gated populations of B220^{+} B cells displaying a Fo (IgM^{+}IgD^{+}) or MZ and transitional (IgM^{+}IgD^{low}) B cell phenotype. **(B)** Flow cytometric analysis of Fo (CD21^{int}CD23^{+}) and MZ B cells (CD21^{high}CD23^{-}) in the spleen (SP) and inguinal lymph nodes (iLN). Numbers indicate mean percentages and SD of lymphocyte-gated, B220^{+} B cells displaying the respective phenotypes. The calculations are based on eleven independent experiments.

Table 3

B cell populations with deletion efficiencies in Notch2IC//CD19Cre$^{+/-}$ and control mice.

	Bone marrow				Spleen					
Mice (n)	7				10					
Gated on:	IgM$^-$ B220^{low} CD43$^+$ Pro B	IgM$^-$ B220^{low} CD43$^-$ Pre B	B220$^+$ IgM$^+$ IgD$^-$ Immature B	B220$^+$ IgM$^+$ IgD$^+$ Mature B	AA4.1$^+$ IgM$^+$ T B	AA4.1$^+$ IgM^{high} CD23$^-$ T1 B	AA4.1$^+$ IgM^{high} CD23$^+$ T2 B	AA4.1$^+$ IgM^{low} CD23$^+$ T3 B	B220$^+$ CD21^{int} CD23$^+$ Fo B	B220$^+$ CD21^{high} CD23$^-$ MZ B
% of:										
Control	8±2	36±12	15±3	20±3	17±8	23±5	40±6	19±3	73±4	8±3
Notch2IC//CD19Cre$^{+/-}$	8±2	29±13	18±2	7±3***	17±5	39±9***	34±10*	11±3***	13±4***	65±5***
[x 10^5]										
Control	1.8±0.6	7.9±2.9	3.1±1.0	4.2±0.5	4.3±1.6	1.4±0.6	2.3±0.7	1.1±0.4	22.0±8.5	2.4±1.2
Notch2IC//CD19Cre$^{+/-}$	1.4±0.6	5.2±2.1	2.3±0.8	0.9±0.2***	5.9±2.6	2.6±1.4*	2.1±0.9	0.7±0.2*	4.2±3.0***	17.6±7.8***
% hCD2$^+$										
Notch2IC//CD19Cre$^{+/-}$	9±2	9±2	42±4	57±9	58±7	70±9	58±12	49±7	26±8	95±2

Bone marrow cells were isolated from one tibia bone per mouse. Percentages within the lymphocyte gate are shown.
Values represent the mean ± SD. * P<0.05,** P<0.01, *** P<0.001, in comparison to Ctrl.

3.2.6.4 Notch2IC//CD19Cre$^{+/-}$ mice harbor reduced B cells in the peritoneal cavity, with a preferential loss of B2 and B1a cells

In the peritoneal cavity, B1 cells are found besides the common IgM^{+}B220^{high}CD5^{-} B2 cells. B1 cells are a self-renewing IgM^{+}B220^{low} B cell population that can be divided into B1a (CD5^{+}) and B1b (CD5^{low}) cells. B1 cells are also located in the spleen in low numbers (Martin and Kearney, 2000). Recently, Witt and colleagues have suggested that Notch2 plays a determining role in the generation of B1 B cells, as they found selective B1 B cell generation in the presence of constitutive Notch2 signals in the spleen, and a reduction of peritoneal B1 B cells upon Notch2 haploinsufficiency (Witt *et al.*, 2003a; Witt *et al.*, 2003b). Thus, we aimed to analyze the different B cell subsets in the peritoneal cavity. Peritoneal cells were isolated from mutant and control mice and stained with α-IgM, α-B220, α-CD5, and α-hCD2 antibodies, followed by flow cytometric analysis. In the peritoneal cavity of Notch2IC-expressing mice, total B cell numbers were reduced to less than 25 % of wild type (Fig. 21A). Whereas the percentage of B1a cells was strongly diminished, the percentage of B1b cells was slightly increased in Notch2IC//CD19Cre$^{+/-}$ mice compared to controls (Fig. 21B), resulting in strongly reduced B1a cell numbers whereas total numbers of B1b cells were less affected. The percentages of B2 cells were normal in Notch2IC//CD19Cre$^{+/-}$ mice, but total numbers were reduced to about 20 % of wild type. Collectively, these results not only reflect again the strongly diminished pool of circulating Fo B cells in Notch2IC//CD19Cre$^{+/-}$ mice, but indicate normal B1b cell differentiation with a preferential loss of B1a cells in the peritoneal cavity under constitutive Notch2 signaling.

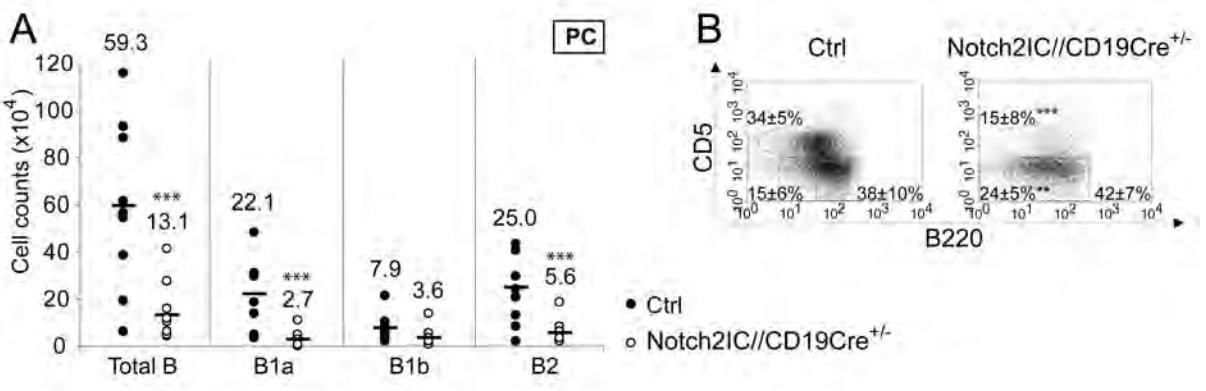

Figure 21 Notch2IC//CD19Cre$^{+/-}$ mice harbor reduced B cells in the peritoneal cavity and show a preferential loss of B1a cells. (A) Absolute numbers of total counted cells, IgM^{+} B1a (B220^{low}CD5^{+}), B1b (B220^{low}CD5^{low}), and B2 (B220^{high}CD5^{-}) cells in the peritoneal cavity of Notch2IC//CD19Cre$^{+/-}$ (blank circle) and control (filled circle) mice. Points represent data from individual mice and horizontal bars mark the mean value, indicated in numbers above each point column. **(B)** Flow cytometric analysis of cells isolated from the peritoneal cavity. Numbers display the mean percentages and SD of lymphocyte-gated, IgM^{+} B1a (B220^{low}CD5^{+}), B1b (B220^{low}CD5^{low}), and B2 (B220^{high}CD5^{-}) cells. Values were calculated from nine independent experiments. ** P<0.01, *** P<0.001, calculated by the two-tailed student's t-test, in comparison to control.

3.2.7 Notch2IC-expressing B cells are located in the marginal zone and display a pre-activated phenotype

MZ B cells are characterized by their location in the MZ, the expression of characteristic surface markers as well as by a pre-activated phenotype, allowing rapid responses particularly to T cell-independent antigens. To further characterize if Notch2IC-expressing B cells display the biological behavior as real MZ B cells, various assays were performed.

3.2.7.1 Notch2IC-expressing B cells are predominantly located in the marginal zone

To assess the location of Notch2IC-expressing B cells and to examine whether the overall structure of splenic follicles may still be maintained in the presence of an extremely enlarged MZ B cell population, we performed immunohistochemical analyses of the spleen. Splenic cryosections were prepared and stained with different antibodies, using α-IgM to detect B cells in the follicular B cell zone and MZ, α-CD3 to detect T cells in the T cell zone, and α-MOMA-1 to detect metallophilic macrophages located at the inner border of the MZ. Immunohistochemistry revealed that the overall follicular structure with the respective B and T cell zones as well as the MZ was retained in Notch2IC//CD19Cre$^{+/-}$ mice (Fig. 22A). The size of the MZ was strongly increased and the follicular B cell zone was significantly diminished, while the T cell zone was retained normal in size. Furthermore, we investigated whether Notch2IC-expressing B cells can be found exclusively in the MZ. For that purpose, a hCD2-specific antibody was used for immunohistochemistry in combination with α-MOMA-1 and α-CD3 antibodies. Immunohistochemical analysis showed that transgene-expressing cells are predominantly located in the splenic MZ, but can also partially be found at the outer border of the Fo B cell zone (Fig. 22B, upper panel). Moreover, no clusters of hCD2^{-} B cells were detected within the follicle (Fig. 22B, lower panel).

3.2.7.2 Notch2IC//CD19Cre$^{+/-}$ B cells show an enhanced expression of MZ B cell markers and display an activated phenotype

A pre-activated phenotype as well as the expression of characteristic surface markers is a hallmark of MZ B cells (Pillai *et al.*, 2005). Therefore, splenic cells were stained with antibodies directed against further characteristic markers of MZ B cells (CD1d, CD36, CD9, and CD25) as well as against activation and adhesion molecules (CD80, CD86, ICAM-1, and MHCII). The surface expression level of these markers was analyzed by FACS. Respective histograms are displayed in figure 23. Flow cytometric analysis demonstrated an increased expression of CD1d, CD36, CD9, and CD25 on Notch2IC-expressing B cells, confirming the MZ B cell phenotype. Furthermore, these cells displayed an enhanced expression of the activation markers CD25, CD80, and CD86,

and of the adhesion molecule ICAM-1, suggesting an activated phenotype. Moreover, MHCII surface expression was significantly reduced on Notch2IC-expressing B cells compared to controls. The analysis of the forward scatter revealed an increased cell size of Notch2IC-expressing B cells compared to control B cells, being in accordance with the pre-activated status as well as the MZ B cell phenotype of these cells and explaining the increase in splenic size and weight of Notch2IC//CD19Cre$^{+/-}$ mice compared to wild type mice.

In summary, these data show that Notch2IC-expressing B cells are MZ B cells not only from their immune phenotype and activation status, but also with regard to their localization predominantly in the splenic MZ.

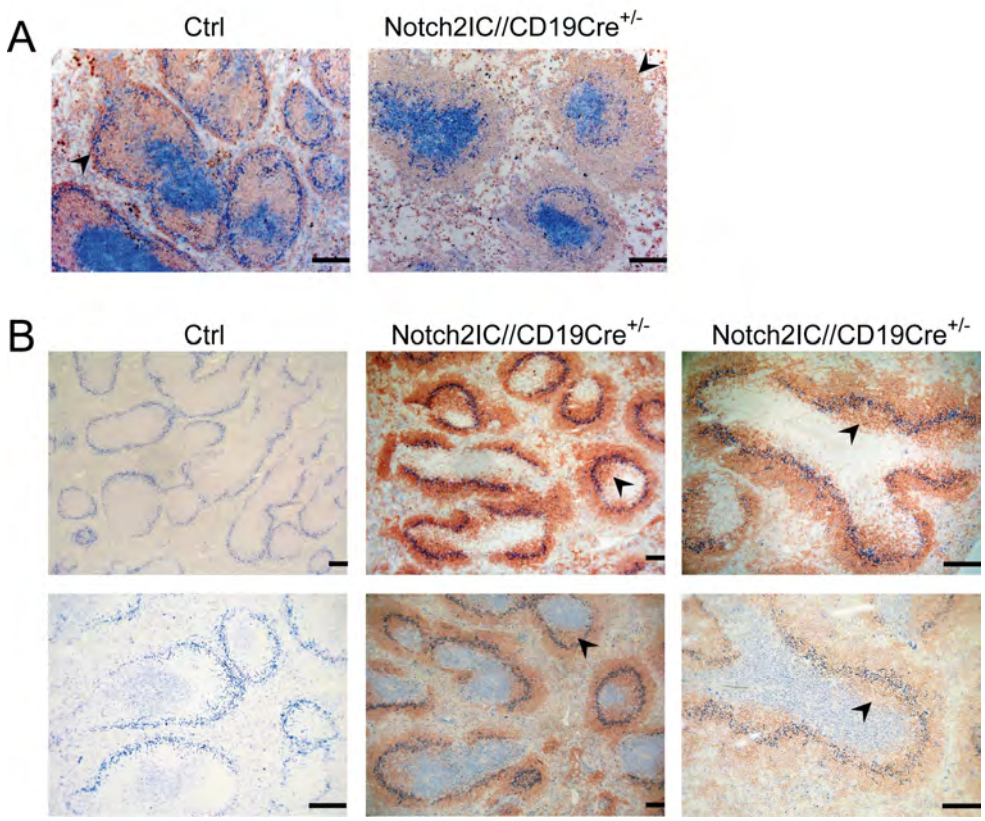

Figure 22 Notch2IC-expressing B cells are predominantly located in the marginal zone. (A) Immunohistochemical staining of splenic cryosections from Notch2IC//CD19Cre$^{+/-}$ and control mice for MOMA-1^{+} metallophilic macrophages (α-MOMA-1 – blue), lining the marginal zone at the sinus, IgM^{+} B cells (α-IgM – red), and CD3^{+} T cells (α-CD3 – blue). The MZ is indicated by arrows. Bar: 250 μm. **(B)** Splenic cryosections from mice with indicated genotype were stained for metallophilic macrophages (α-MOMA-1 – marine blue) and hCD2 (α-hCD2 – red). In the upper row, the white, unstained region within the follicle represents the T cell zone and potential hCD2^{-} B cells. Sections in the lower row were additionally stained for CD3^{+} T cells (α-CD3 – pigeon blue). Arrowheads indicate hCD2^{+} B cells within the follicle. Bar: 250 μm.

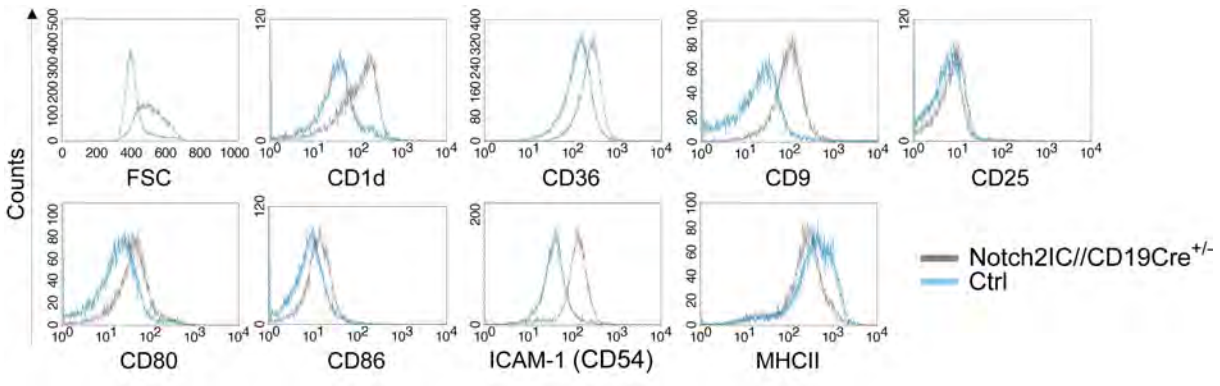

Figure 23 Notch2IC//CD19Cre$^{+/-}$ B cells show an enhanced expression of marginal zone B cells markers and display an activated phenotype. Splenocytes were stained with antibodies specific for CD1d, CD36, CD9, CD25, CD80, CD86, ICAM-1, and MHCII and were analyzed by FACS. Histograms show overlays of cell size (FSC) or overlays of surface expression of the indicated molecules on lymphocyte-gated, B220^{+}, hCD2^{+} B cells from Notch2IC//CD19Cre$^{+/-}$ mice (grey line) and on lymphocyte-gated, B220^{+} B cells from control mice (blue line). Data are representative for five independent experiments; FSC (forward scatter).

3.2.8 Analysis of marginal zone B cell precursors in Notch2IC//CD19Cre$^{+/-}$ mice

Since we confirmed a MZ B cell phenotype for Notch2IC-expressing B cells *in vivo*, we aimed to investigate the generation of MZ B cells in the mutant mice in detail. Immature B cells, emerging from the bone marrow, enter the spleen from the blood stream to undergo further maturation by differentiating through the T1 (IgM^{high}CD23^{-}), T2 (IgM^{high}CD23^{+}), and T3 (IgM^{low}CD23^{+}) transitional B cell stage. Finally, this differentiation yields Fo or MZ B cells. It is still elusive, at which differentiation stage transitional B cells are committed to adopt either a Fo or MZ B cell phenotype, and in detail how Notch2 contributes to that lineage decision. Recent studies indicate that the Fo versus MZ B cell fate decision is already made at the T1 transitional B cell stage (Tan *et al.*, 2009). But also commitment from the T2 transitional B cells stage and even from Fo B cells has been postulated (Pillai and Cariappa, 2009). To get further insight into the generation of MZ B cells, we analyzed the immature/transitional B cell population in Notch2IC//CD19Cre$^{+/-}$ mice in more detail.

Firstly, we investigated the deletion efficiency of the STOP cassette in the different B cell subsets. Deletion efficiencies were determined from the percentages of hCD2^{+} cells in the respective populations and are displayed in table 3. While only poor deletion efficiency in pro- and pre-B cells was achieved (< 10 %), more than 40 % of immature B cells in the bone marrow showed hCD2 expression. In AA4.1^{+} transitional B cells, the deletion efficiency peaked with 70 % in T1 transitional B cells, then decreasing in T2 and T3 transitional B cells to less than 50 %, finally reaching > 95 % deletion in MZ and 26 % in Fo B cells. While the T1 transitional B cell population was significantly increased in Notch2IC//CD19Cre$^{+/-}$ mice, the T2 and T3 transitional B cell populations were obviously diminished (Tab. 3). The higher deletion efficiency

in T1 as compared to T2 transitional B cells suggests that T1 transitional B cells expressing Notch2IC develop to MZ B cells, whereas undeleted cells preferentially proceed to T2 transitional B cells. The gradual decrease of the deletion efficiency from T2 transitional to Fo B cells might indicate that B cells deleting the STOP cassette at the T2 transitional stage might still develop to MZ B cells.

To analyze the MZ B cell precursors in more detail, we examined the splenic B cell compartment of Notch2IC//CD19Cre$^{+/-}$ mice in comparison to control mice according to an approach previously applied by Allman and colleagues (Srivastava *et al.*, 2005; Calamito *et al.*, 2009). For that purpose, splenic B cells were purified and stained with antibodies directed against the complement receptors CD21/35 as well as IgM, AA4.1, and CD23. As shown in figure 24A, three fractions can be defined (Frs. I to III). These three populations were further subdivided based on differential AA4.1 and CD23 levels. Fr. I (IgM^{high}CD21/35$^{low/int}$ cells) is divided in T1 (AA4.1^{+}CD23^{-}) and T2 (AA4.1^{+}CD23^{+}) transitional B cells (Fig. 28B, left). Within Fr. II, (IgM$^{low/int}$CD21/35^{int} cells) T3 transitional (AA4.1^{+}CD23^{+}) and Fo (AA4.1^{-}CD23^{+}) B cells can be found (Fig. 24B, middle). Fr. III (IgM^{high}CD21/35^{high} cells) is divided in MZ B cells (AA4.1^{-} CD23^{-}) and MZ B cell precursors (AA4.1^{low}CD23^{+}) (Fig. 24B, right).

As expected, the Fr. III harboring MZ B cells and MZ B cell precursors was extremely enlarged, while Fr. II, containing mainly Fo B cells, was respectively diminished in Notch2IC//CD19Cre$^{+/-}$ mice compared to the control. Fr. I was found in normal percentages, but contained significantly more T1 transitional B cells than in the control. Furthermore, Fr. III almost exclusively comprised MZ B cells but nearly no MZ B cell precursors, in contrast to the control. The increased T1 transitional B cell pool is in line with results described above. However, the absence of conventional MZ B cell precursors raised the question whether MZ B cell differentiation in Notch2IC//CD19Cre$^{+/-}$ mice does not follow the common way as described previously in the literature. In case of intensive MZ B cell commitment already at the T1 transitional B cell stage, we suspected another kind of MZ B cell precursor with an IgM$^{int/high}$CD21/35$^{int/high}$ AA4.1^{low}CD23^{-} phenotype. Indeed, such cells were found in large percentages predominantly in Fr. II, but also in Fr. III of Notch2IC//CD19Cre$^{+/-}$ mice but not of control mice. Those cells were designated as MZ Pre* in figure 24. In summary, our data suggest that in Notch2IC//CD19Cre$^{+/-}$ mice, transitional B cells are committed to the MZ B cell pool subsequently after receiving Notch2 signals. Commitment might be preferentially achieved from the T1 transitional stage, involving a new IgM$^{int/high}$CD21/35$^{int/high}$AA4.1^{low}CD23^{-} MZ B cell intermediate, which has not been described so far. T2 cells might still differentiate into MZ B cells via the conventional IgM^{high}CD21/35^{high}AA4.1^{low}CD23^{+} MZ B cell precursor stage, which is still present in Notch2IC//CD19Cre$^{+/-}$ mice to some extent.

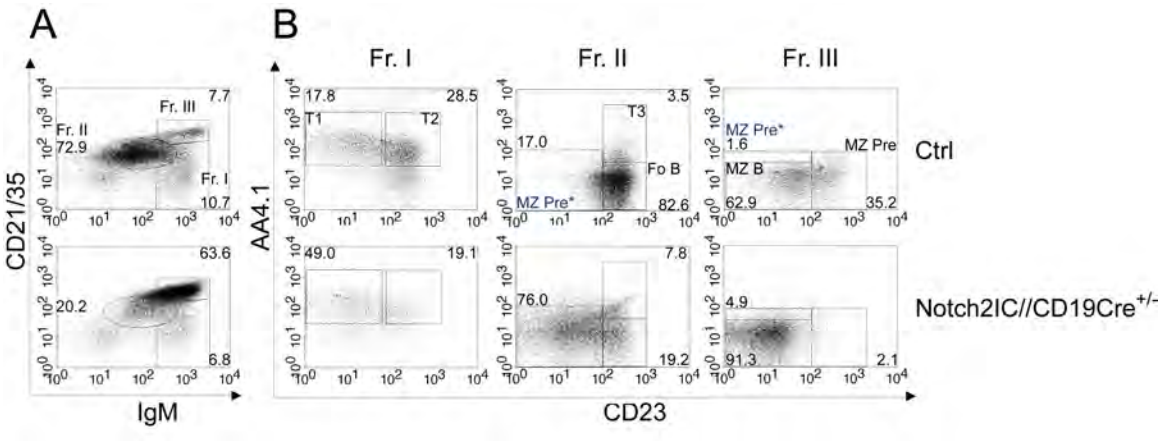

Figure 24 Analysis of marginal zone B cell precursor cells. Flow cytometric analysis of splenic B cells isolated from mice with indicated genotypes by depletion of $CD43^+$ cells. B cells were stained with antibodies specific for CD21/35, IgM, CD23, and AA4.1 and were analyzed by FACS. **(A)** Blots are lymphocyte-gated and display percentages of cells belonging to fraction I to III (Fr. I, II, III) according to Allman and colleagues; $IgM^{high}CD21/35^{low/int}$ cells (Fr. I); $IgM^{low/int}CD21/35^{int}$ cells (Fr. II); $IgM^{high}CD21/35^{high}$ cells (Fr. III); **(B)** Numbers display the frequency of events as function of the indicated parent gate, which is stated above. Fr. I harbors T1 and T2 transitional B cells, Fr. II T3 transitional and Fo B cells as well as potential MZ B cell precursors* (MZ Pre*), and Fr. III MZ B cells and conventional MZ B cell precursors as well as further MZ B cell precursors*. Data are representative for three independent experiments.

3.2.9 Notch2IC//CD19Cre$^{+/-}$ B cells are hyper-responsive to LPS and α-CD40 stimulation *in vitro* but do not form germinal centers

Additionally, we tested whether Notch2IC-expressing B cells are hyper-responsive like real MZ B cells in response to certain stimuli. Robust induction of proliferation to lipopolysaccharide (LPS) or CD40 ligation is known as hallmark of MZ B cells (Allman *et al.*, 2001b; Oliver *et al.*, 1997). To determine the proliferation of Notch2IC-expressing B cells in comparison to control B cells, such cells were isolated from the spleen, labeled with carboxyl fluorescein succinimidyl ester (CFSE), and were cultured with or without α-CD40 or LPS. CFSE is a fluorescent dye that binds to proteins of the inner cell membrane and that can be used to monitor proliferation, due to the progressive decline of CFSE fluorescence intensity within daughter cells following each cell division. Proliferation profiles were recorded after 72 hours with or without α-CD40 or LPS stimulation (Fig. 25A). Notch2IC-expressing B cells showed similar proliferation as control B cells without stimulation, but displayed a higher proliferation rate in response to α-CD40 or LPS. Besides, cell numbers and percentages of living cells declined similarly to the control over five days in culture without stimulation (Fig. 25B and C).

To test whether the pre-activated status of Notch2IC-expressing B cells also results in enhanced class switch recombination upon stimulation, splenic primary B cells were cultured in the presence of α-CD40 plus IL4, LPS plus IL4, or without any stimulus, and were stained for surface IgG1 before as well as after 48 and 72 hours of culture (Fig. 25D).

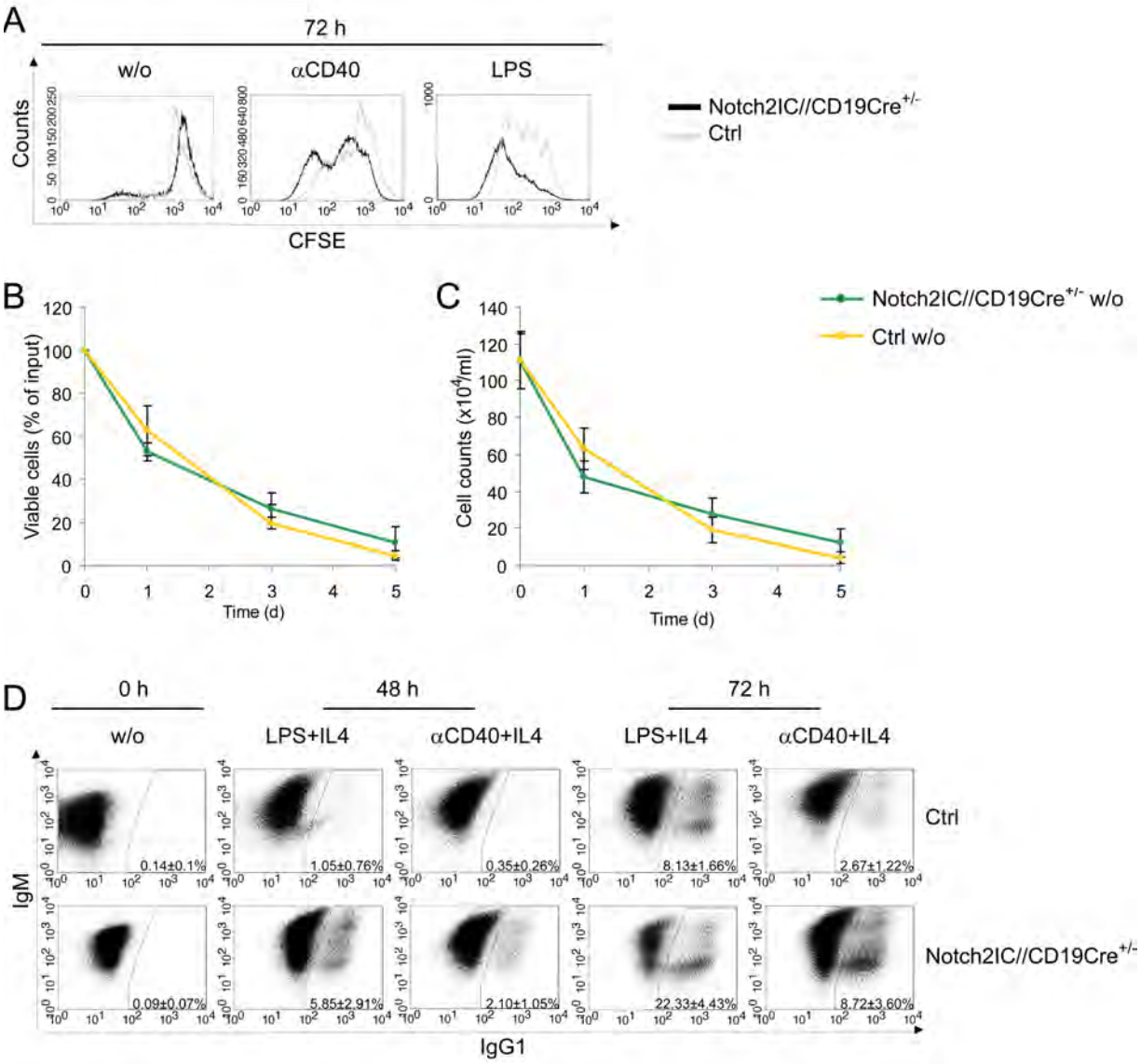

Figure 25 Notch2IC//CD19Cre$^{+/-}$ B cells are hyper-responsive to LPS and α-CD40 stimulation *in vitro.* Splenic B cells of Notch2IC//CD19Cre$^{+/-}$ and control mice were enriched by depletion of CD43^{+} cells. **(A)** Cells were labeled with CFSE and cultured with or without the indicated stimuli (LPS concentration: 10 μg/ml). After 72 hours, proliferation profiles of propidium iodide negative cells were assessed by flow cytometric analysis and are displayed in the histogram overlays as black (Notch2IC//CD19Cre$^{+/-}$) and grey (control) graphs. Notch2IC-expressing B cells were identified by re-gating histograms additionally on hCD2^{+} cells. Shown proliferation profiles are representative for four independent experiments. **(B, C)** Cells were cultured up to five days without (w/o) stimulation and their viability was analyzed on day 0, 1, 3, and 5 after incubation with propidium iodide. Notch2IC-expressing B cells were identified by staining additionally for hCD2. (B) Percentages of viable (propidium iodide negative) cells were determined by FACS. Percentages of viable control cells and percentages of viable Notch2IC-expressing cells at day 0 were each set to 100 %. (C) Total numbers of viable cells were determined using FACS by uptaking all cells of one well and excluding dead (propidium iodide positive) cells. The graphs show the mean results with SD of three independent experiments either of living cell numbers (C) or of viable cells in relation to the input at day 0. Color coding is indicated beside the diagrams. **(D)** Cells were cultured with α-CD40 and IL4, LPS and IL4, or without stimulation (w/o) (LPS concentration: 25 μg/ml). After indicated culture times, cells were stained for IgM, IgG1, and hCD2. Numbers indicate mean percentages and SD of IgG1^{+} control B cells and IgG1^{+}, hCD2^{+} Notch2IC-expressing B cells of three independent experiments. Only propidium iodide negative cells were included in the analysis.

In cultures of Notch2IC-expressing B cells, an enlarged fraction of IgG1 class-switched cells was detected compared to control cultures, both upon α-CD40/IL4 and LPS/IL4 stimulation. In summary, these data show that Notch2IC-expressing B cells are MZ B cells also with regard to their biological behavior, as these cells are hyper-responsive to LPS and α-CD40 stimulation. In addition, proliferation and survival *in vitro* without stimulation were not obviously improved, underlining that constitutive Notch2 activity in mature B cells impacts only lineage decision but not survival and proliferation properties of mature B cells.

Next, we tested the responsiveness of Notch2IC-expressing B cells *in vivo* to different antigens. MZ B cells have been reported to secrete more IgM and IgG3 than other immunoglobulins isotypes (Oliver *et al.*, 1997). During immune response, MZ B cells rapidly differentiate into plasmablasts in response to blood-borne bacteria (Oliver *et al.*, 1999; Phan *et al.*, 2005), and are thus considered as major source of IgM upon interaction with T cell-independent (TI) antigens (Martin and Kearney, 2000; Martin *et al.*, 2001). Nevertheless, MZ B cells have been also shown to respond to T cell-dependent (TD) antigen and to form germinal centers (Attanavanich and Kearney, 2004; Song and Cerny, 2003).

To analyze the responsiveness of Notch2IC-expressing B cells *in vivo*, we firstly examined total titers of the different immunoglobulin isotypes in the sera of non-immunized Notch2IC//CD19Cre$^{+/-}$ and control mice by ELISA. As shown in the diagram of figure S3A, IgG3 titers of Notch2IC-expressing mice were slightly but statistically significantly decreased compared to littermate controls, while IgM, IgG1, IgG2b, IgG2a, and IgA titers were unaltered. Thus, Notch2IC-expressing MZ B cells were not observed to secrete more IgG3 as suggested previously (Oliver *et al.*, 1997).

Secondly, we aimed to investigate the immune response of Notch2IC//CD19Cre$^{+/-}$ mice upon challenge with TD and TI antigens. For that purpose, we immunized mutant and control mice with 4-hydroxy-3-nitrophenylacetyl (NP) conjugated to TD chicken gamma globulin (CGG) or to TI type 1 LPS, and determined serum titers of NP-specific antibodies by ELISA 14 days after immunization. In case of TD immunization, the presence of splenic germinal centers (GC) was revealed 14 days after immunization with flow cytometric and immunohistochemical analyses. Following TD immunization, the fraction of CD95^{high}PNA^{high} GC B cells was drastically reduced in the spleen of Notch2IC//CD19Cre$^{+/-}$ mice in comparison to control mice (Fig. 26A) and GC structures were almost not detected by immunohistochemistry (Fig. 26B). As a consequence, only low levels of NP-specific IgM and IgG1 antibodies were measured by ELISA in the sera of Notch2IC//CD19Cre$^{+/-}$ mice immunized with TD antigen (Fig. S3B). In contrast, immunization with the TI type 1 antigen NP-LPS resulted in a similar immune response in Notch2IC//CD19Cre$^{+/-}$ mice like in controls. Thus, seven days after immunization, levels of

NP-specific immunoglobulin titers were comparable to control levels in the serum of Notch2IC//CD19Cre$^{+/-}$ mice (Fig. S3C). Only titers of NP-specific IgG3 were lower.

In summary, these data indicate that Notch2IC-expressing MZ B are especially impaired in their immune response to TD antigen, including GC formation and class switch recombination, but are not in general detained in plasma cell differentiation as these cells respond to the TI type 1 antigen LPS.

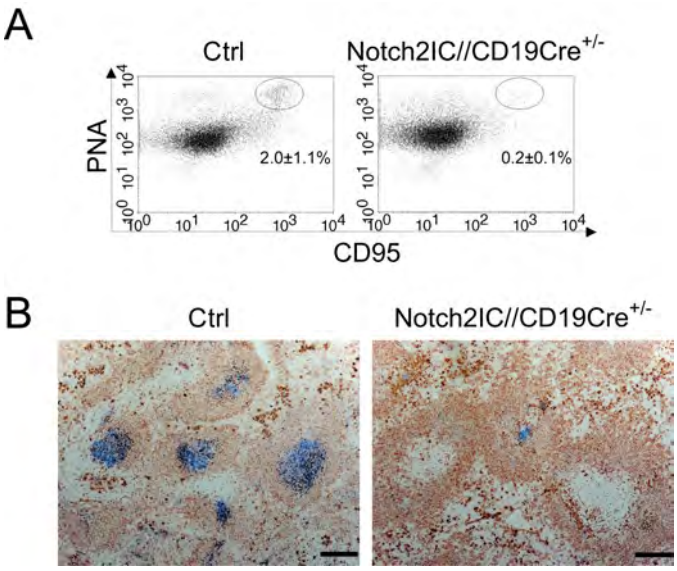

Figure 26 Notch2IC//CD19Cre$^{+/-}$ B cells do not form germinal centers. (A) Flow cytometry to identify germinal center (GC) B cells (CD95^{+}PNA^{high}) in the spleen of Notch2IC//CD19Cre$^{+/-}$ and control mice 14 days after immunization with 100 µg NP-CGG. Cells are gated on B220^{+} lymphocytes. Numbers indicate the mean percentages of GC B cells with SD. Three mice were analyzed per group. **(B)** Immunochemical analysis of GC formation in the spleen, 14 days post-immunization with 100 µg NP-CGG. Cryosections were stained for B cells (α-IgM – red) and for GC B cells (PNA – blue). Bar: 250 µm.

3.2.10 Signaling pathways active in Notch2IC//CD19Cre$^{+/-}$ B cells

Since we confirmed that Notch2IC-expressing B cells display a pre-activated phenotype as it is described for MZ B cells, we studied whether this phenotype is accompanied with the activation of certain signaling pathways like NF-κB, MAP kinase, or PI3K/Akt signaling as well as c-Myc expression. Until now, the basal activity of these signaling pathways in MZ B cells has not been investigated in detail. Moreover, it is not clear how constitutive Notch2 activity impacts the activation of these pathways in B cells *in vivo*. Recently, enhanced basal phosphorylation of Akt kinase as well as higher basal levels of c-Myc has been reported for murine primary MZ B cells in comparison to Fo B cells *in vitro* (Meyer-Bahlburg *et al.*, 2009). Furthermore, it has been described that IκBα mRNA levels are diminished in MZ B cells (Zhang *et al.*, 2007).

3.2.10.1 Notch2IC-expressing B cells display reduced basal non-canonical NF-κB activity

Several reports have described a cross-talk between Notch and NF-κB signaling, resulting either in the stimulation or inhibition of NF-κB activity (Osipo *et al.*, 2008). In addition, Notch2 and NF-κB1/p50 have been suggested to synergize during MZ B cell development (Moran *et al.*, 2007). Therefore, we were interested to analyze the basal activity of the canonical and non-

canonical NF-κB pathways in non-stimulated Notch2IC-expressing B cells. Canonical NF-κB signaling requires the phosphorylation and subsequent degradation of IκBα, leading to the nuclear translocation of p50/p65 and p50/c-Rel heterodimers. Non-canonical NF-κB signaling includes the processing of the precursor protein p100 to p52, resulting in the nuclear translocation of p52/RelB heterodimers.

Western blots of whole-cell extracts showed decreased levels of both phosphorylated and non-phosphorylated IκBα in mutant B cells compared to control B cells (Fig. 27A). To analyze whether the decreased IκBα levels influence the nuclear translocation of canonical NF-κB components, we performed nuclear fractionation experiments and analyzed the protein levels of p50, p65, and c-Rel in the cytoplasm and the nucleus (Fig. 27B). However, a similar basal activation of the canonical NF-κB pathway as in the control was observed in Notch2IC-expressing B cells.

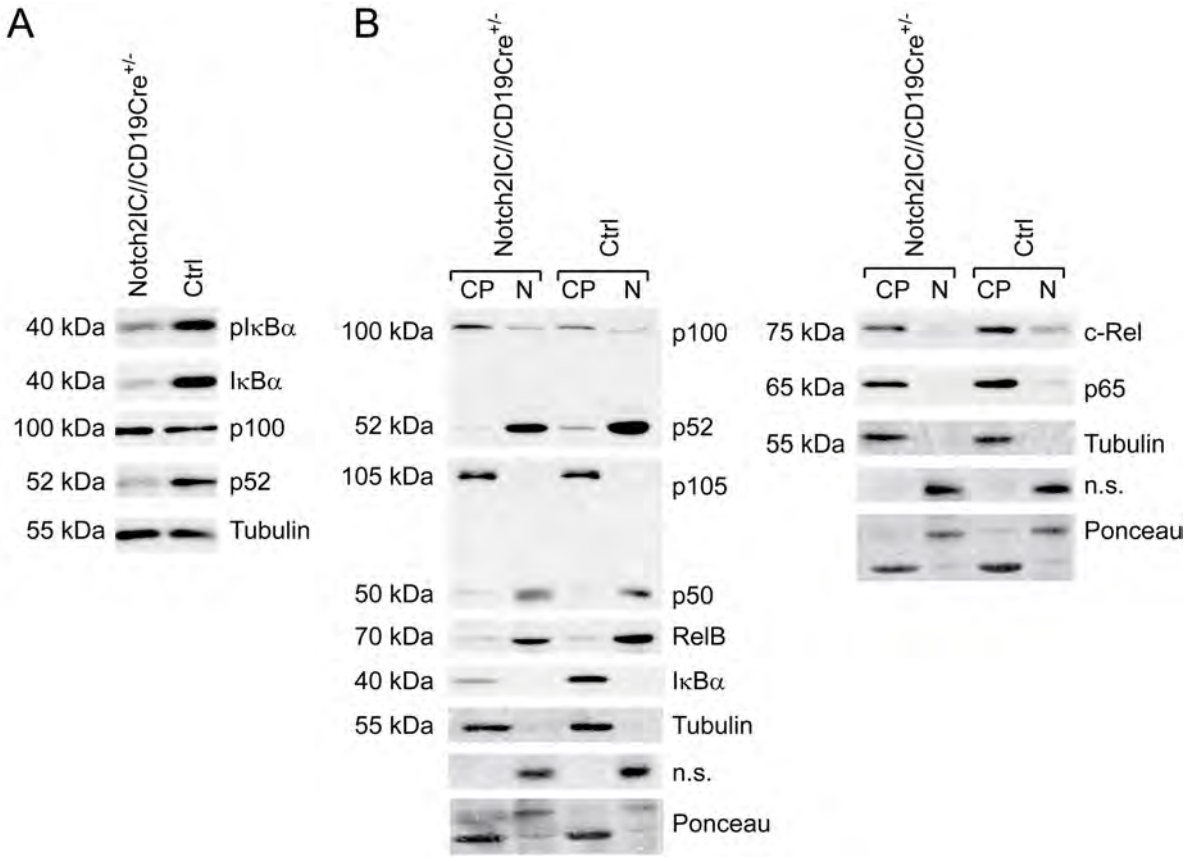

Figure 27 Reduced basal non-canonical NF-κB activity in Notch2IC-expressing B cells. (A) Splenic B cells were purified from Notch2IC//CD19Cre$^{+/-}$ and control mice and whole-cell extracts from non-stimulated B cells were subjected to immunoblot analysis using antibodies specific for p100/p52, pIκBα (Ser32/36), and IκBα. Equal protein loading was controlled by an α-Tubulin staining. The result is representative for five independent experiments. **(B)** Cytoplasmic (CP) and nuclear (N) levels of NF-κB components of splenic B cells from Notch2IC//CD19Cre$^{+/-}$ and control mice were analyzed by immunoblot. The purity of cytoplasmic and nuclear extracts was verified by an α-Tubulin staining and by an non-specific (n.s.) signal arising only in the nucleus after staining with an α-Bcl3 antibody. Equal protein loading was controlled by Ponceau S staining. The experiment was performed two times.

Furthermore, we investigated the basal activity of non-canonical NF-κB signaling. In Western blot analyses, we detected decreased p52 and marginally increased p100 protein levels in mutant B cells compared to control B cells, indicating a diminished processing of p100 to p52, and thus a reduced activation of non-canonical NF-κB signaling (Fig. 27A). To corroborate these findings, we analyzed the distribution of RelB and p52 in the cytoplasm and nucleus. In accordance with the previous result, levels of RelB and p52 were diminished in nuclear fractions of Notch2IC-expressing B cells compared to control B cells, pointing to a decreased basal activity of the non-canonical NF-κB pathway (Fig. 27B). These data suggest that constitutive Notch2 activity in B cells reduces rather than activates canonical and non-canonical NF-κB signaling.

3.2.10.2 Notch2IC//CD19Cre$^{+/-}$ B cells show enhanced PI3K/Akt activity and high c-Myc levels

Furthermore, we wondered whether the pre-activated status of Notch2IC-expressing B cells is reflected in an enhanced basal phosphorylation of Akt and the MAP kinases Erk and Jnk as well as in increased levels of c-Myc. The transcription factor c-Myc is a prominent target of Notch signaling and is associated with proliferation, cell growth, and apoptosis. MAP kinases are known to mediate proliferation and survival in immune cells, including B cells. Akt kinase promotes cell survival and its basal phosphorylation reflects the activity of PI3K, which acts upstream of Akt. Thus, we investigated the basal phosphorylation and the total protein amount of these kinases as well as protein levels of c-Myc by subjecting whole-cell extracts from Notch2IC-expressing and control B cells to Western blot analyses (Fig. 28).

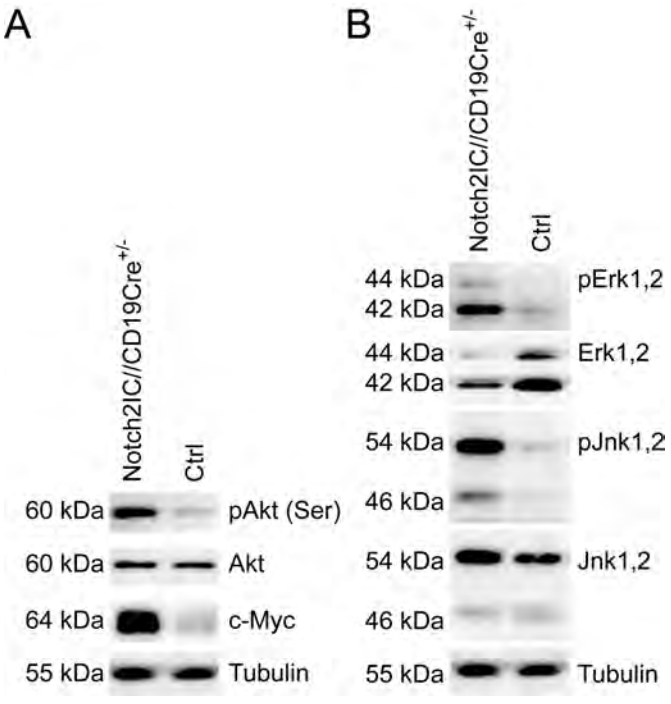

Figure 28 Notch2IC//CD19Cre$^{+/-}$ B cells show high c-Myc levels as well as an enhanced activation of Akt and the MAP kinases Erk and Jnk. Splenic B cells were purified from Notch2IC//CD19Cre$^{+/-}$ and control mice and whole-cell extracts from non-stimulated cells were subjected to Western blot analyses using antibodies specific for pAkt (pS473) and the corresponding non-phosphorylated form as well as for c-Myc **(A)**, pJnk1/2 (Thr183/Tyr185), pErk1/2 (Thr202/ Tyr204), and the corresponding non-phosphorylated forms **(B)**. Equal protein loading was controlled by an α-Tubulin staining. The result is representative for four (A) and seven (B) independent experiments.

We found that the phosphorylated forms of Akt and of the MAP kinases Erk and Jnk were strongly increased in non-stimulated Notch2IC-expressing B cells compared to control cells, pointing to a constitutive activity of these kinases. Additionally, increased Akt phosphorylation indicates enhanced PI3K activity in the mutant cells. Furthermore, Western blot analyses showed that c-Myc levels were strongly increased in Notch2IC-expressing B cells in comparison to the control (Fig. 28A). In summary, we observed that the pre-activated state of Notch2IC-expressing B cells is reflected in an enhanced activation of the PI3K/Akt and MAPK signaling cascades as well as in high basal levels of c-Myc protein.

3.2.11 Constitutive Notch2 signaling overcomes CD19 deficiency during marginal zone B cell differentiation

CD19 functions as a co-receptor of the BCR and was shown to be required for the generation of MZ B cells, as these cells are absent in CD19-deficient mice (Pezzutto *et al.*, 1987; Carter *et al.*, 1991; Engel *et al.*, 1995; Rickert *et al.*, 1995). Since CD19 signals most prominently via PI3K (Buhl *et al.*, 1997), diminished PI3K signaling might be responsible for the lack of MZ B cells in CD19-deficient mice. This is in accordance with further observations that also the lack of the PI3K isoform p110δ has been described to result in defective MZ B cell generation (Clayton *et al.*, 2002). The capacity of constitutive Notch2 signaling to induce constitutive phosphorylation of Akt, the main downstream target of PI3K signaling, prompted us to investigate whether constitutive Notch2 signaling can restore MZ B cell development in the absence of CD19. In CD19Cre$^{+/-}$ mice, *Cre* is placed into and disrupts one CD19 locus, thereby resulting in the knock-out of one endogenous CD19 allele. Thus, CD19 deficiency was achieved by generating CD19-*Cre* homozygous mice (CD19Cre$^{+/+}$). These mice were crossed to Notch2IC-transgenic mice to obtain Notch2IC-expressing, CD19-deficient mice (Notch2IC//CD19Cre$^{+/+}$). Flow cytometric analyses of the B cell compartment of Notch2IC//CD19Cre$^{+/+}$ mice demonstrated by a CD21/CD23 staining that also in the absence of CD19 the MZ B cell population is enlarged comparable to Notch2IC//CD19$^{+/-}$ mice up to 70 %, while the Fo B cell fraction is even stronger reduced to less than 10 % (Fig. 29A, upper panel). This was confirmed by an additional IgM/IgD staining, showing an increased percentage of IgM^{+}IgD^{low} MZ and immature B cells, while the IgM^{+}IgD^{+} Fo B cell population was dramatically diminished (Fig. 29A, lower panel). Immunohistochemistry of splenic sections from Notch2IC//CD19Cre$^{+/+}$ mice revealed a similar follicular organization as found in the spleen of Notch2IC//CD19Cre$^{+/-}$ mice (cp. Fig. 22A), including an enlarged MZ. In contrast to Notch2IC-expressing, CD19-proficient mice, B cells were not detected inside the follicle, most likely due to the lower numbers of Fo B cells. Sections

are illustrated in comparison to sections of CD19Cre$^{+/+}$ mice, which harbor no MZ but only Fo B cells (Fig. 29B).

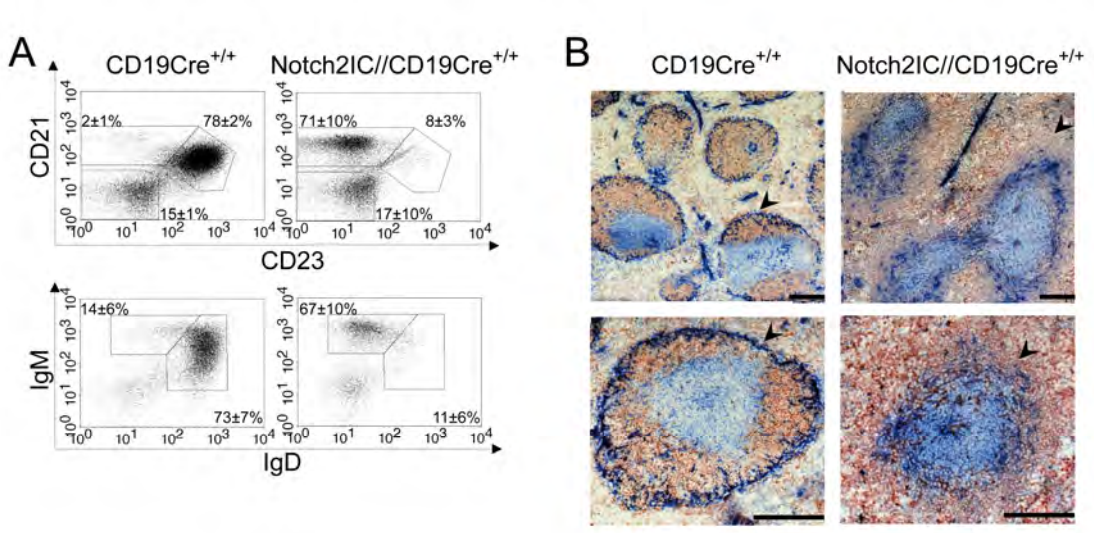

Figure 29 Notch2IC induces marginal zone B development despite the absence of CD19. (A) Splenic lymphocytes from mice of the indicated genotypes were analyzed by flow cytometry for the expression of CD21 and CD23 (upper panel) or IgM and IgD (lower panel); Fo B cells (CD21^{int}CD23^{+}) and MZ B cells (CD21^{high}CD23^{-}) (upper panel); Fo B cells (IgM^{+}IgD^{+}), MZ and transitional B cells (IgM^{+}IgD^{low}) (lower panel); Numbers indicate mean percentages and SD of lymphocyte-gated populations of B220^{+} B cells displaying the respective phenotype. The calculation is based on four independent experiments. **(B)** Immunohistochemical staining of splenic cryosections from mice of the indicated genotypes for MOMA-1^{+} metallophilic macrophages (α-MOMA-1 – blue), lining the marginal zone at the sinus, IgM^{+} B cells (α-IgM – red), and CD3^{+} T cells (α-CD3 – blue). The MZ B cell zone is indicated by arrows. Bar: 250 μm.

Total splenic B cell numbers of Notch2IC//CD19Cre$^{+/+}$ mice were reduced to about the half of CD19Cre$^{+/+}$ mice, which already suffer from a strongly reduced B cell compartment (Fig. S2A). The reduction of mature B cells was traced back to a slightly defective early B cell development that was observed in Notch2IC//CD19Cre$^{+/+}$ mice, mirrored in lower percentages of pre-B cells in the bone marrow and less transitional B cells (Tab. 4). This defect can be due to the doubled amount of *Cre* in Notch2IC//CD19Cre$^{+/+}$ mice because of the CD19-*Cre* homozygosity, what was reflected in a higher deletion efficiency already in the bone marrow compared to Notch2IC//CD19Cre$^{+/-}$ mice, yielding 70 % of hCD2^{+} immature B cells in Notch2IC//CD19Cre$^{+/+}$ mice in comparison to 42 % in Notch2IC//CD19Cre$^{+/-}$ mice. In addition, higher percentages of Thy1.2^{+} cells within the hCD2^{+} lymphocyte population of the bone marrow were observed in Notch2IC//CD19Cre$^{+/+}$ mice compared to Notch2IC//CD19Cre$^{+/-}$ mice (Fig. S2B). Since CD19-*Cre* expression is known as highly B cell-specific (Rickert *et al.*, 1997), this may suggest a trans-differentiation of already committed pro-B

cells to the T cell lineage as a consequence of an earlier or more intense onset of Notch2IC expression due to the CD19-*Cre* homozygosity.

Investigating the transitional B cell compartment, an increased T1, but decreased T2 and T3 transitional B cell populations were found in Notch2IC//CD19Cre$^{+/+}$ mice in comparison to CD19Cre$^{+/+}$ mice, similarly as observed in Notch2IC//CD19Cre$^{+/-}$ mice. T1 transitional B cells displayed again the highest deletion efficiency, suggesting again MZ B cell commitment at that stage. Off note, hCD2 expression was found in almost 95 % of T1 transitional B cells, indicating that at that stage roughly no B cells are left to escape Notch2-induced MZ B cell commitment. All cell numbers and deletion efficiencies of the respective sub-populations are stated in table 4.

To test whether these CD19-deficient MZ B cells show also a pre-activated phenotype and are hyper-responsive to stimulation *in vitro*, surface expression of activation molecules and MZ B cell markers as well as proliferation in response to α-CD40 stimulation were examined. B cells isolated from Notch2IC//CD19Cre$^{+/+}$ mice showed an even larger size than Notch2IC//CD19Cre$^{+/-}$ B cells and displayed an increased expression of the markers CD86 and CD36 compared to the control (Fig. 30A). In response to stimulation with α-CD40, Notch2IC-expressing, CD19-deficient B cells showed a higher proliferation rate than control cells, comparable to Notch2IC-expressing B cells proficient for CD19 (Fig. 30B). Consequently, a pre-activated and hyper-responsive phenotype of Notch2IC-expressing B cells was also observed in the absence of CD19. Ultimately, Western blot analyses evidenced an increased activation of the MAP kinases Erk and Jnk as well as elevated levels of c-Myc protein in Notch2IC-expressing B cells also in the absence of CD19 (Fig. 30C). However, preliminary results of first analyses indicated only normal activation of Akt in Notch2IC//CD19Cre$^{+/+}$ B cells (data not shown).

In summary, constitutive Notch2 signaling was shown to overcome CD19 deficiency, demonstrating that constitutive Notch2 signaling acts independently of CD19 in the generation of MZ B cells. Increased activation of PI3K/Akt due to constitutive Notch2 signals could form the basis to compensate for CD19 ablation.

Table 4

B cell populations with deletion efficiencies in Notch2IC//CD19Cre$^{+/+}$ and CD19Cre$^{+/+}$ control mice.

	Bone marrow				Spleen					
Mice (n)	4				4					
Gated on:	IgM$^-$ B220^{low} CD43$^+$ Pro B	IgM$^-$ B220^{low} CD43$^-$ Pre B	B220$^+$ IgM$^+$ IgD$^-$ Immature B	B220$^+$ IgM$^+$ IgD$^+$ Mature B	AA4.1$^+$ IgM$^+$ T B	AA4.1$^+$ IgM^{high} CD23$^-$ T1 B	AA4.1$^+$ IgM^{high} CD23$^+$ T2 B	AA4.1$^+$ IgM^{low} CD23$^+$ T3 B	B220$^+$ CD21^{int} CD23$^+$ Fo B	B220$^+$ CD21^{high} CD23$^-$ MZ B
% of:										
CD19Cre$^{+/+}$	10±2	43±14	16±4	20±4	27±5	21±0	49±1	12±2	78±2	2±1
Notch2IC//CD19Cre$^{+/+}$	9±2	21±12*	13±1	3±1***	17±5	38±4***	25±8**	11±2**	8±3***	71±10***
[x 10^5]										
CD19Cre$^{+/+}$	1.9±0.5	7.9±3.5	3.0±1.6	3.4±0.1	3.3±1.9	0.9±0.5	2.1±1.1	0.5±0.2	12.8±5.4	0.4±0.4
Notch2IC//CD19Cre$^{+/+}$	2.1±1.3	3.1±1.8	1.2±0.3	0.3±0.1**	1.7±0.9	1.0±0.1	0.6±0.1***	0.3±0.1**	0.6±0.2***	7.0±1.1***
% hCD2$^+$										
Notch2IC//CD19Cre$^{+/+}$	17±11	33±3	70±2	74±10	69±9	94±3	88±8	68±7	48±15	94±5

Bone marrow cells were isolated from one tibia bone per mouse. Percentages within the lymphocyte gate are shown.
Values represent the mean ± SD. * P<0.05,** P<0.01, *** P<0.001, in comparison to Ctrl.

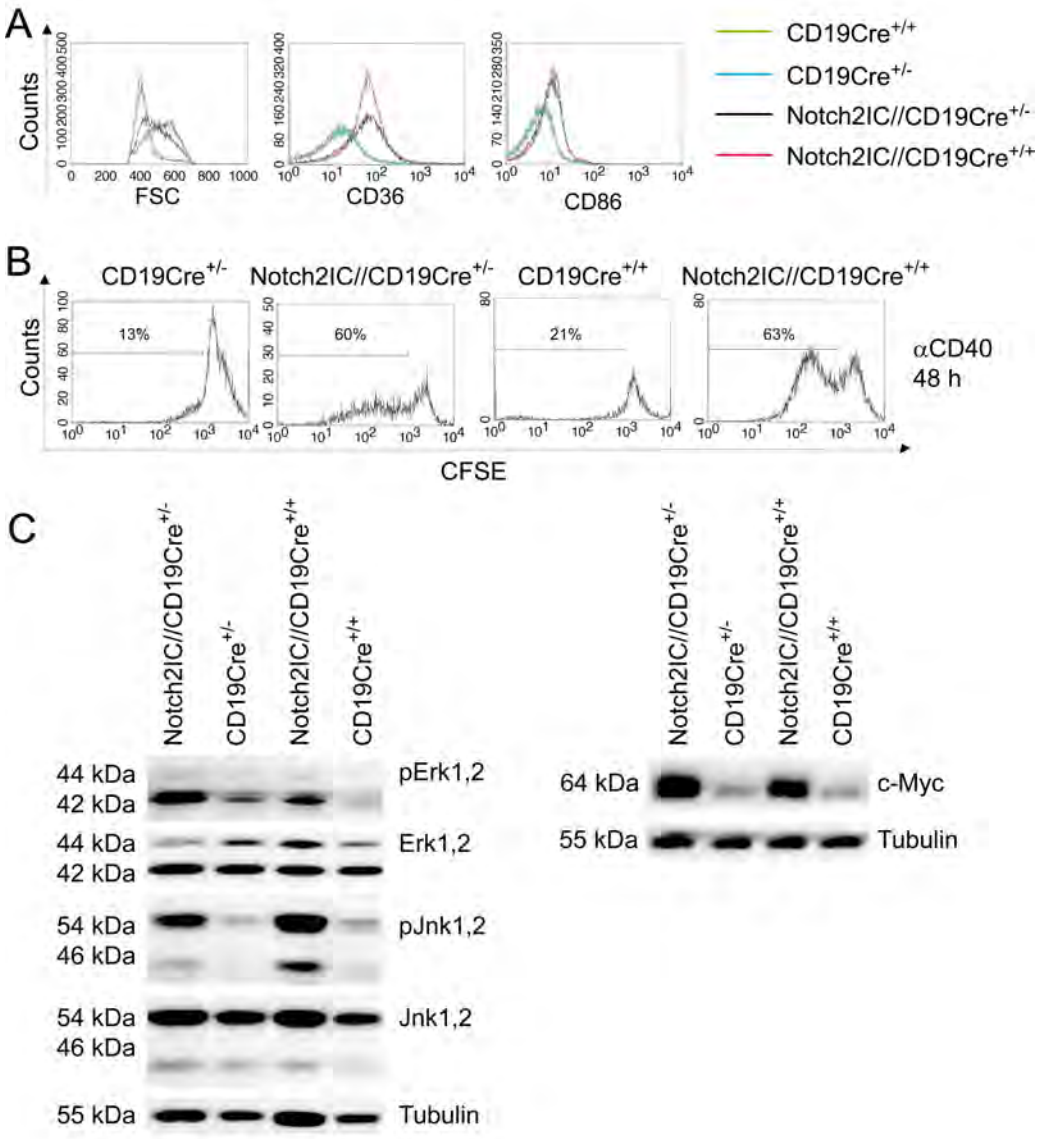

Figure 30 CD19-deficient, Notch2IC-expressing B cells are pre-activated and hyper-responsive and show increased MAPK activation as well as c-Myc levels. (A) To examine the immune phenotype of Notch2IC//CD19Cre$^{+/+}$ B cells, splenocytes were stained with antibodies specific for the indicated surface markers. Histograms show overlays of cell size (FSC) or overlays of the surface expression of the indicated molecules on lymphocyte-gated, B220^{+} B cells from the indicated genotypes. Data are representative for three independent experiments; FSC (forward scatter). **(B)** To test whether Notch2IC//CD19Cre$^{+/+}$ B cells are hyper-responsive, splenic B cells from mice of the indicated genotypes were enriched by depletion of CD43^{+} cells and were labeled with CFSE before cells were cultured with α-CD40 antibody. After 48 hours, the proliferation profiles were assessed by flow cytometric analysis and are displayed in the histograms. Numbers indicate percentages of lymphocyte-gated, propidium iodide-negative cells of one representative analysis. Notch2IC-expressing B cells were identified by gating on hCD2^{+} cells. The experiment was performed twice. **(C)** To investigate whether the pre-activation of Notch2IC//CD19Cre$^{+/+}$ B cells is also reflected in the activation of certain signaling pathways, splenic B cells were purified from mice of indicated genotypes and whole-cell extracts from non-stimulated cells were subjected to Western blot analysis using antibodies specific for pErk1/2 (Thr202/Tyr204), pJnk1/2 (Thr183/Tyr185), and the corresponding non-phosphorylated forms (left panel) as well as c-Myc (right panel). Equal protein loading was controlled by an α-Tubulin staining. The result is representative for three independent experiments.

3.3 The role of B cell receptor signaling in LMP1/CD40-activated B cells

In a second project of this work, we were interested in the role of B cell receptor (BCR) signaling in pre-malignant B cells *in vivo*. Survival of resting, peripheral B cells critically depends on the expression of a functional BCR. It is believed that BCR-mediated survival signals occur ligand-independently and are thus of "tonic" nature. Recently, these signals were shown to be mediated by PI3K (Srinivasan *et al.*, 2009). Until now, it is in question whether aberrantly activated or malignant B cells also depend on this tonic BCR signal. This brought us to the question whether constitutive CD40 signaling can overcome the need for a functional BCR. To investigate this hypothesis, we have genetically abrogated Igβ, one signaling molecule of the BCR complex, in pre-malignant B cells *in vivo* that underlie constitutive CD40 signaling.

3.3.1 Genetic ablation of Igβ in LMP1/CD40-transgenic mice

A former member of our laboratory, C. Hömig-Hölzel, established a conditional transgenic mouse strain, in which a LMP1/CD40 chimeric protein is B cell-specifically expressed based on the *Cre*/loxP system and mediates constitutive CD40 signaling. This resulted in B cell activation, leading to B cell expansion as well as to enhanced proliferation and survival properties *in vitro*, ultimately followed by the development of B cell lymphomas at high incidence with a latency of 12 to 19 months (Homig-Holzel *et al.*, 2008) (see 1.5.2 for details). In this mouse strain, BCR signaling was to be impaired in mature B cells by deleting the ITAM-containing domain of Igβ in a *Cre*/loxP-dependent manner. For that purpose, we made use of a conditional Igβ-deficient mouse strain, which was established by N. Uyttersprot, a former member of our department. In the conditional Igβ-deficient mouse strain (fl(GFP)), deletion of Igβ can be traced by GFP expression (ΔGFP) (see 1.5.3 for details). Since the ablation of Igβ during early B cell differentiation in the bone marrow leads to a block of B cell development, Igβ deletion was achieved by using CD21-*Cre* mice (Kraus *et al.*, 2004), expressing *Cre* recombinase under the control of the CD21 promoter and thus deleting the floxed alleles efficiently only from the T2 transitional B cell stage on. $Ig\beta^{fl(GFP)/\Delta c}$//CD21Cre mice carry one deleted Igβ allele in all body cells ($Ig\beta^{\Delta c}$), while the second Igβ allele ($Ig\beta^{fl(GFP)}$) can be *Cre*-mediated and GFP-traced deleted, to receive homozygous Igβ deficiency. Whether the deletion of BCR-associated signaling components like Igα or Igβ only severely impairs or entirely abrogates tonic BCR signaling is not clear. However, as the deletion of Igα (Kraus *et al.*, 2004), ablation of Igβ resulted in a strongly diminished Fo B cell compartment and the disappearance of the MZ B cell population in $Ig\beta^{fl(GFP)/\Delta c}$//CD21Cre mice (N. Uyttersprot, personal communication), indicating that both signaling molecules are essential for tonic BCR signaling and thus for the survival of peripheral B cells. By mouse crossings, the $Ig\beta^{fl(GFP)/\Delta c}$, the CD21-*Cre*, and the LMP1/CD40 alleles were

combined. Upon CD21-*Cre*-mediated deletion of the floxed allele and concomitant GFP expression, the fl(GFP) allele is referred to as ΔGFP. Thus, LMP1/CD40//Igβ$^{fl(GFP)/\Delta c}$//CD21Cre (referred to as LMP1/CD40//Igβ$^{\Delta GFP/\Delta}$) mice were established and were analyzed in comparison to Igβ$^{fl(GFP)/wt}$//CD21Cre (referred to as Igβ$^{\Delta GFP/wt}$), Igβ$^{fl(GFP)/\Delta c}$//CD21Cre (referred to as Igβ$^{\Delta GFP/\Delta}$), and LMP1/CD40//Igβ$^{fl(GFP)/wt}$//CD21Cre (referred to as LMP1/CD40//Igβ$^{\Delta GFP/wt}$) mice. As the heterozygous deletion of Igβ does not negatively impact B cell development and activation, controls were also maintained to a heterozygous background, in order to monitor the deletion efficiency from the respective GFP expression.

3.3.2 Constitutive CD40 signaling rescues Igβ-deficient B cells to a certain extent

C. Hojer has shown that the deletion of Igβ in LMP1/CD40 B cells leads to the ablation of B cell expansion. However, LMP1/CD40 expression can rescue Igβ-deficient B cells to a certain extent as LMP1/CD40//Igβ$^{\Delta GFP/\Delta}$ mice harbor about the same numbers of B cells in the peripheral lymphatic organs like Igβ$^{\Delta GFP/wt}$ control mice (Fig. 31A). In addition, the deletion efficiency in LMP1/CD40//Igβ$^{\Delta GFP/\Delta}$ B cells is roughly as high as in Igβ$^{\Delta GFP/wt}$ B cells, indicating that LMP1/CD40//Igβ$^{\Delta GFP/\Delta}$ B cells are almost not counter-selected, in contrast to Igβ-deficient B cells that do not express LMP1/CD40 (Igβ$^{\Delta GFP/\Delta}$) (Tab. 5).

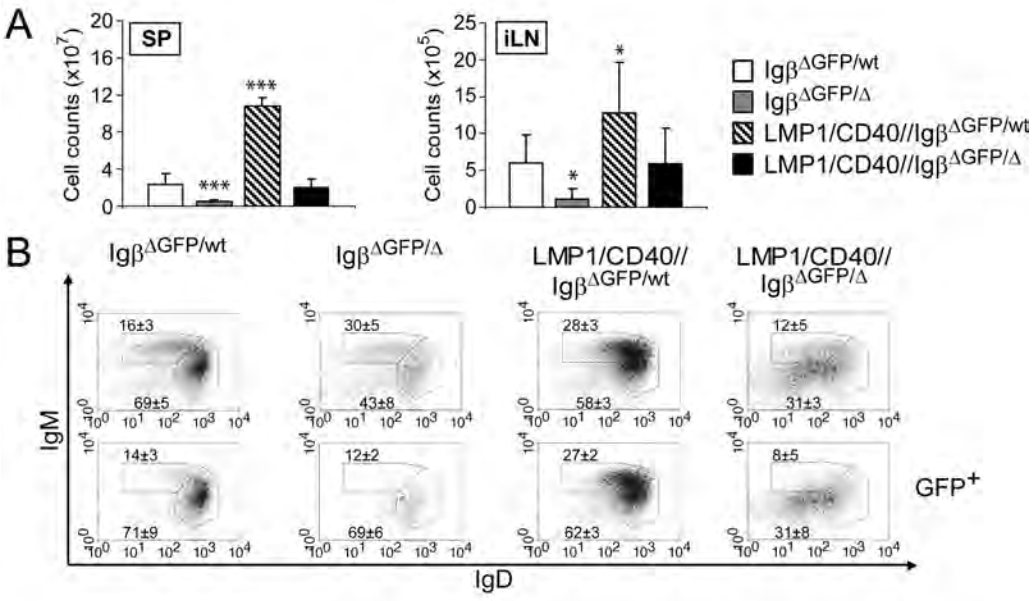

Figure 31 Constitutive CD40 signaling rescues Igβ-deficient B cells to a certain extent (adapted from C. Hojer). **(A)** Absolute numbers of B220$^+$ B cells in spleen (SP) and inguinal lymph node (iLN) of mice with genotypes as indicated besides the diagrams; * $P<0.05$, *** $P<0.001$, calculated by the two-tailed student's t-test compared to Igβ$^{\Delta GFP/wt}$ control mice. **(B)** Splenic lymphocytes were analyzed for the expression of IgM/IgD by flow cytometry. The upper panel is only gated on living, B220$^+$ lymphocytes, whereas the lower panel is additionally gated on GFP, thus depicting only Igβ-deleted cells. Numbers represent mean percentages and SD of gated populations from three independent experiments. Data were collected by C. Hojer as content of her PhD thesis and were confirmed by myself in further analyses.

Furthermore, the analysis of Ig surface expression revealed that the deletion of Igβ results in the downregulation of the BCR molecules IgM and IgD (Fig. 31B) (Hojer *et al.*, in preparation).
In this work, LMP1/CD40-expressing, Igβ-deficient B cells were further characterized according to their activation status as well as their proliferation and survival properties in comparison to Igβ-deficient B cells that do not express LMP1/CD40 ($Ig\beta^{\Delta GFP/\Delta}$).

Table 5 (adapted from C. Hojer)

Deletion efficiencies measured from the percentage of GFP expression in B cells from spleen, inguinal lymph nodes, and peritoneal cavity.

	Mice (n)	SP	iLN	PC
$Ig\beta^{\Delta GFP/wt}$	2	88±11	86±12	87±14
$Ig\beta^{\Delta GFP/\Delta}$	5	26±7***	30±12**	9±4***
LMP1/CD40//$Ig\beta^{\Delta GFP/wt}$	6	90±5	90±2	92±4
LMP1/CD40//$Ig\beta^{\Delta GFP/\Delta}$	3-4	75±5	84±4	66±11

Percentages of GFP^+cells within the B lymphocyte gate are shown. Values represent the mean ± SD. ** P<0.01, *** P<0.001, in comparison to $Ig\beta^{\Delta GFP/wt}$.

3.3.3 LMP1/CD40//$Ig\beta^{\Delta GFP/\Delta}$ B cells display an activated phenotype

An activated phenotype, displayed by high expression of CD95 or CD80 on the cell surface, is a hallmark of LMP1/CD40-transgenic B cells. Thus, we were interested whether constitutive CD40 signaling may also lead to an activation of Igβ-deficient B cells. Therefore, splenic B cells were isolated from all four genotypes, and cells were stained with respective antibodies before surface expression levels of respective activation molecules and the forward scatter was analyzed by FACS (Fig. 32). Flow cytometry revealed an increased expression of CD95 and CD80 on LMP1/CD40//$Ig\beta^{\Delta GFP/\Delta}$ B cells compared to $Ig\beta^{\Delta GFP/\Delta}$ and $Ig\beta^{\Delta GFP/wt}$ B cells, similar as detected on LMP1/CD40-expressing B cells proficient for Igβ. In addition, a significant larger size than control B cells was detected in the forward scatter analysis. These results show that constitutive CD40 signaling leads to an activated B cell phenotype also in the absence of Igβ.

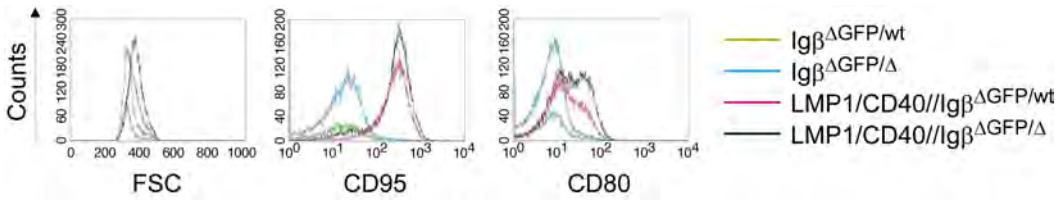

Figure 32 LMP1/CD40//$Ig\beta^{\Delta GFP/\Delta}$ B cells display an activated phenotype. Splenocytes were stained with antibodies specific for CD95 and CD80 and were subjected to flow cytometric analysis. Histograms show overlays of cells size (FSC) or overlays of surface expression of the indicated molecules on lymphocyte-gated, $B220^+$, GFP^+ B cells from mice with genotypes as indicated besides the histograms. Data are representative for three independent experiments; FSC (forward scatter).

3.3.4 LMP1/CD40 expression prolongs the survival of Igβ-deficient B cells *in vitro* and *in vivo*

Constitutive CD40 signaling in B cells via LMP1/CD40 expression leads to prolonged survival and spontaneous cell division *ex vivo* (Homig-Holzel *et al.*, 2008). In Igβ-deficient mice, constitutive CD40 signaling restores the peripheral B cell compartment to comparable B cell numbers as found in wild type mice (Hojer *et al.*, in preparation). Consequently, we aimed to characterize the survival properties of LMP1/CD40//Igβ$^{\Delta GFP/\Delta}$ B cells *in vitro* and *in vivo*.

3.3.4.1 LMP1/CD40//Igβ$^{\Delta GFP/\Delta}$ B cells show a prolonged survival *in vitro*

To test whether constitutive CD40 signaling prolongs the survival of Igβ-deficient B cells *in vitro*, splenic B cells from all four genotypes were isolated and cultured for five days without additional stimulation. At day 1, 2, 3, and 5 of the culture, cells were stained with the vital dye TOPRO-3 and were subjected to flow cytometric analysis. From beginning of the culture, the survival of LMP1/CD40//Igβ$^{\Delta GFP/\Delta}$ B cells declined much slower than of the rapidly dropping Igβ$^{\Delta GFP/\Delta}$ B cells, and thus similarly to Igβ$^{\Delta GFP/wt}$ control B cells (Fig. 33A). While monitoring the percentage of GFP$^+$ cells over five days in culture, the percentages of GFP$^+$ cells in the Igβ$^{\Delta GFP/\Delta}$ culture dropped rapidly, indicating a negative selection of Igβ-deficient B cells (Fig. 33B). LMP1/CD40 expression was observed to counteract that negative selection, as the percentages of GFP$^+$ cells in the LMP1/CD40//Igβ$^{\Delta GFP/\Delta}$ culture remained rather constant, similarly as in the culture of Igβ$^{\Delta GFP/wt}$ control B cells. All together these results show that LMP1/CD40 expression prolongs the survival of Igβ-deficient B cells *in vitro,* and indicate that constitutive CD40 signaling is able to rescue Igβ-deficient B cells from cell death to a certain extent.

3.3.4.2 Constitutive CD40 signaling enlarges the life-span of Igβ-deficient B cells *in vivo*

To confirm a prolonged life-span of LMP1/CD40//Igβ$^{\Delta GFP/\Delta}$ B cells also *in vivo*, we performed bromodeoxyuridine (BrdU) pulse chase experiments. BrdU is a thymidine analog that is incorporated into replicating cells during the S-phase of the cell cycle by substituting for thymidine in all newly synthesized DNA strands. By applying BrdU to cell cultures or experimental animals (pulse), and subsequently detecting BrdU in the DNA with a specific antibody, cells that have entered the S-phase can be identified. After the pulse, the life-span of labeled cells can be monitored over a period of time without further labeling (chase). Since peripheral B cells are resting and barely proliferate, BrdU$^+$ B cells in the periphery are derived from transitional B cells emerging from the bone marrow, where they underwent several cycles of cell division during early B cell development (Forster and Rajewsky, 1990). For the *in vivo* assay, mice were fed with BrdU in the drinking water for 14 days (pulse) and were further observed

over a period of 56 days until day 70 (chase). Mice were analyzed on day 14 at the end of the pulse, and on day 42 and 70 during the chase. The percentages of $BrdU^+$ splenic B cells were determined by flow cytometry. The respective values are displayed with the graphs in figure 33C.

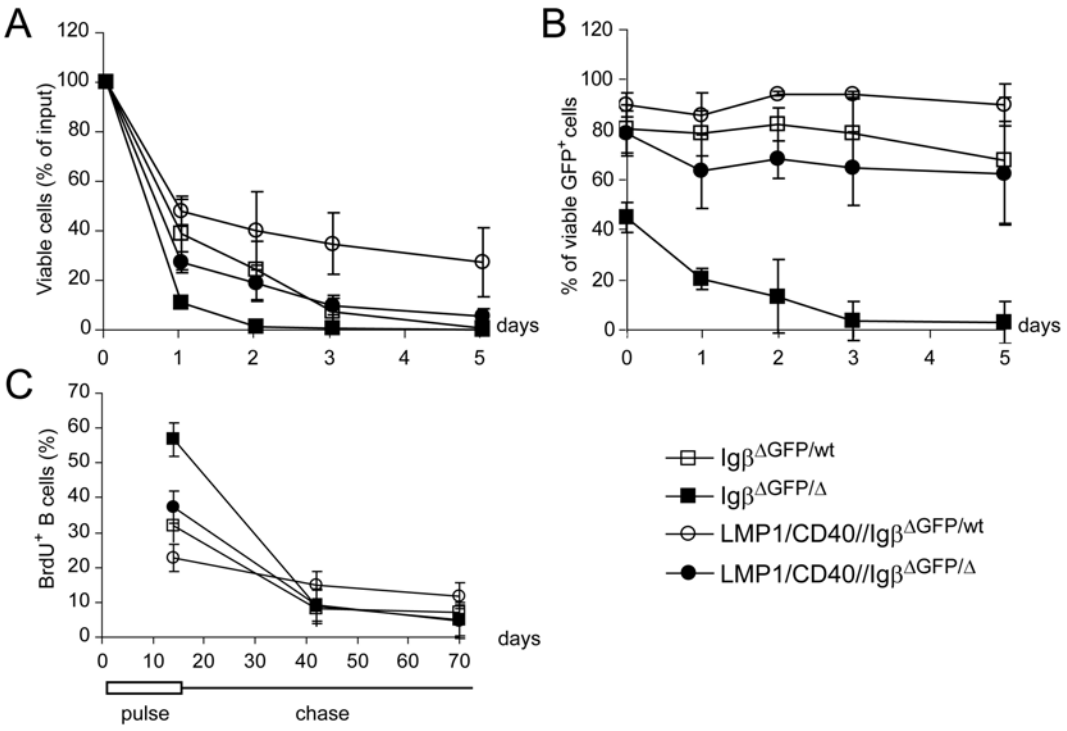

Figure 33 Constitutive CD40 signaling prolongs the life-span of Igβ-deficient B cells. (A, B) Splenic B cells of the indicated genotypes were enriched by depletion of $CD43^+$ cells. Cells were cultured up to five days without stimulation and were analyzed for viability with TOPRO-3 incubation on day 0, 1, 2, 3, and 5 by flow cytometry. Percentages of viable ($TOPRO\text{-}3^-$) cells were determined and mutant cells were identified by re-gating on GFP^+. The graphs show (A) mean percentages of viable GFP-expressing cells with SD of three independent experiments in relation to the input at day 0, which were set as 100 % or (B) mean percentages of viable GFP^+ cells of the respective genotypes over the time of the culture. **(C)** Mice were fed with 0.8 mg/ml BrdU in their drinking water for 14 days during the pulse period and $BrdU^+$ B cells were tracked until day 70 during the chase period. Splenic samples were taken at day 14, 42, and 70. Percentages of $BrdU^+$, $B220^+$ B cells were determined by flow cytometry. The graphs show the mean results (symbols) with SD of three different BrdU pulse chase experiments. The four different genotypes are indicated besides.

At day 14 of the pulse period, $Ig\beta^{\Delta GFP/\Delta}$ mice showed high percentages of $BrdU^+$ B cells (57 %). In contrast, percentages of $BrdU^+$ B cells in LMP1/CD40//$Ig\beta^{\Delta GFP/\Delta}$ mice were much lower (37 %) and similar to $Ig\beta^{\Delta GFP/wt}$ control mice (32 %). During the chase period, Igβ-deficient B cells showed a rapid decline of BrdU-labeled cells (5 % at day 70), whereas LMP1/CD40//$Ig\beta^{\Delta GFP/\Delta}$ mice cells showed a similar decline of $BrdU^+$ B cells (5 % at day 70) as $Ig\beta^{\Delta GFP/wt}$ control mice (7 % at day 70). The similar kinetics of BrdU labeling and decline in B cells of LMP1/CD40//$Ig\beta^{\Delta GFP/\Delta}$ mice like in B cells of $Ig\beta^{\Delta GFP/wt}$ control mice indicates a similar survival of LMP1/CD40//$Ig\beta^{\Delta GFP/\Delta}$ B cells as control $Ig\beta^{\Delta GFP/wt}$ B cells. LMP1/CD40//$Ig\beta^{\Delta GFP/wt}$ mice

showed not only the lowest percentage of $BrdU^+$ B cells after the pulse (23 %), but also the slowest decline of labeled cells during the chase (12 % at day 70), evidencing a prolonged survival of peripheral LMP1/CD40-expressing B cells *in vivo*.

The increased percentage of $BrdU^+$ B cells in Igβ-deficient mice at day 14 as well as the fast decline during the chase period is most likely caused by a high influx of immature B cells from the bone marrow to the periphery, due to the diminished life-span of peripheral B cells deficient for Igβ (N. Uyttersprot, personal communication). By constitutive CD40 signaling, the survival of Igβ-deficient B cells was approximated to the survival of wild type B cells *in vivo*. Therefore, these results strengthen again the observations we made *in vitro*, namely that constitutive CD40 signaling is able to rescue Igβ-deficient B cells from cell death to a certain degree. However, this data also show that the ablation of Igβ results in the drop of survival of LMP1/CD40-expressing B cells to wild type level, evidencing that though constitutive CD40 signaling, pre-malignant B cells are still susceptible to the impairment of tonic BCR signals.

3.3.5 Analysis of signaling pathways in LMP1/CD40//Igβ$^{\Delta GFP/\Delta}$ B cells

LMP1/CD40-transgenic B cells show a selective activation of the non-canonical NF-κB pathway and the MAP kinases Erk and Jnk (Homig-Holzel *et al.*, 2008). Since these signaling pathways are associated with survival and proliferation in B cells, we were interested whether the improved survival of Igβ-deficient B cells due to constitutive CD40 signaling is somehow reflected in the activation of these signaling pathways in LMP1/CD40//Igβ$^{\Delta GFP/\Delta}$ B cells. Since Igβ$^{\Delta GFP/\Delta}$ mice have strongly reduced peripheral B cell numbers, showing less than 30 % deletion efficiency in the spleen, the analysis of signaling pathways was technically not feasible in Igβ$^{\Delta GFP/\Delta}$ B cells. Thus, only B cells from LMP1/CD40//Igβ$^{\Delta GFP/\Delta}$, Igβ$^{\Delta GFP/wt}$, and LMP1/CD40//Igβ$^{\Delta GFP/wt}$ mice were subjected to further analyses.

3.3.5.1 LMP1/CD40 expression leads to increased non-canonical NF-κB activity despite Igβ deficiency

Firstly, we examined the basal activity of the canonical and non-canonical NF-κB pathways in non-stimulated B cells by Western blot with or without nuclear fractionation experiments. Canonical NF-κB signaling includes the phosphorylation and subsequent degradation of IκBα, resulting in the nuclear translocation of p50/p65 and p50/c-Rel heterodimers. Non-canonical NF-κB signaling requires the processing of the precursor protein p100 to p52, leading to the nuclear translocation of p52/RelB heterodimers. In Western blots of whole-cell extracts, an increased level of p52 protein was detected in LMP1/CD40//Igβ$^{\Delta GFP/\Delta}$ B cells, similar as found in LMP1/CD40//Igβ$^{\Delta GFP/wt}$, but not in Igβ$^{\Delta GFP/wt}$ control B cells (Fig. 34A). Besides, less

phosphorylated IκBα was detected in LMP1/CD40//Igβ$^{\Delta GFP/\Delta}$ B cells compared to Igβ$^{\Delta GFP/wt}$ control B cells, reminiscent of LMP1/CD40 B cells proficient for Igβ, indicating that LMP1/CD40 leads to the selective activation of the non-canonical NF-κB pathway also in the absence of Igβ. To corroborate these findings, we performed nuclear fractionation experiments and analyzed the protein levels of NF-κB components in the cytoplasm and the nucleus (Fig. 34B). In accordance with the previous results, the levels of RelB, p52, and p50 were increased in the nuclear fraction of LMP1/CD40//Igβ$^{\Delta GFP/\Delta}$ B cells compared to Igβ$^{\Delta GFP/wt}$ control B cells, to a similar extent as seen in LMP1/CD40//Igβ$^{\Delta GFP/wt}$ B cells. An increased level of p105 like in LMP1/CD40 B cells was not observed after the deletion of Igβ (cp. Homig-Holzel *et al.*, 2008). These data show that constitutive CD40 signaling still activates the non-canonical NF-κB pathway, despite the Igβ deficiency.

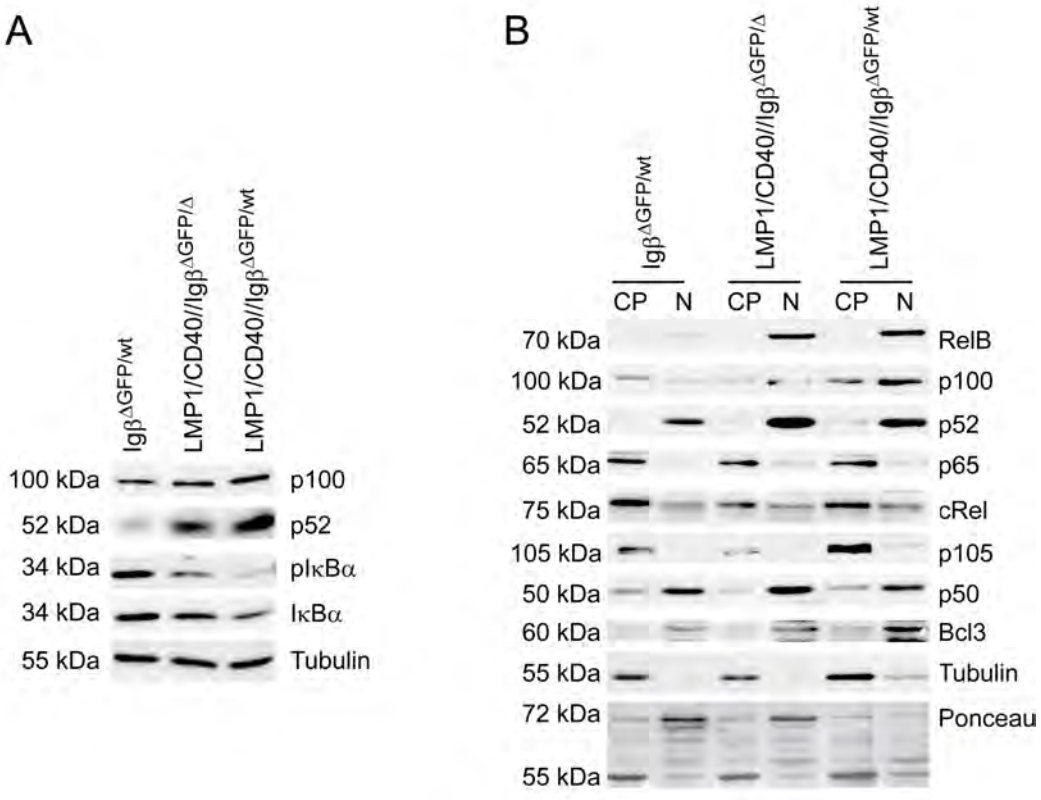

Figure 34 Enhanced non-canonical NF-κB activity is maintained in LMP1/CD40//Igβ$^{\Delta GFP/\Delta}$ B cells. (A) Splenic B cells were purified from the indicated genotypes and whole-cell extracts from non-stimulated cells were subjected to immunoblot analysis using antibodies specific for p100/p52, pIκBα (Ser32/36), and IκBα. Equal protein loading was controlled by an α-Tubulin staining. The result is representative for three independent experiments. **(B)** Cytoplasmic (CP) and nuclear (N) levels of NF-κB components in non-stimulated splenic B cells from the indicated genotypes were analyzed by immunoblot. The purity of cytoplasmic and nuclear extracts was verified by α-Tubulin and α-Bcl3 stainings, respectively. Equal protein loading was controlled by a Ponceau S staining. The experiment was performed three times.

3.3.5.2 Enhanced activation of the MAPK Erk and Jnk is maintained in LMP1/CD40//Igβ$^{\Delta GFP/\Delta}$ B cells

Secondly, we investigated the activation status of the MAP kinases Erk and Jnk. For that purpose, whole-cell extracts from splenic B cells were prepared and the phosphorylation state of these proteins as well as the total protein amounts were analyzed by Western blotting (Fig. 35). In LMP1/CD40//Igβ$^{\Delta GFP/\Delta}$ B cells, we observed an increased phosphorylation of Erk and Jnk compared to Igβ$^{\Delta GFP/wt}$ control B cells. The phosphorylation was similarly enhanced as in LMP1/CD40-expressing B cells proficient for Igβ. Therefore, we concluded that constitutive CD40 signaling activates Erk and Jnk irrespective of Igβ deficiency.

This result is moreover important for another study of our laboratory showing that the phosphorylation of Erk is mediated through CD19 in LMP1/CD40-expressing B cells and is critically involved in the survival of these cells. Since phosphorylation of Erk is not abrogated in LMP1/CD40//Igβ$^{\Delta GFP/\Delta}$ B cells, but in LMP1/CD40-expressing B cells deficient for CD19, this result indicates that the requirement of CD19 for Erk activation by constitutive CD40 signaling is independent of the BCR (Hojer *et al.*, in preparation).

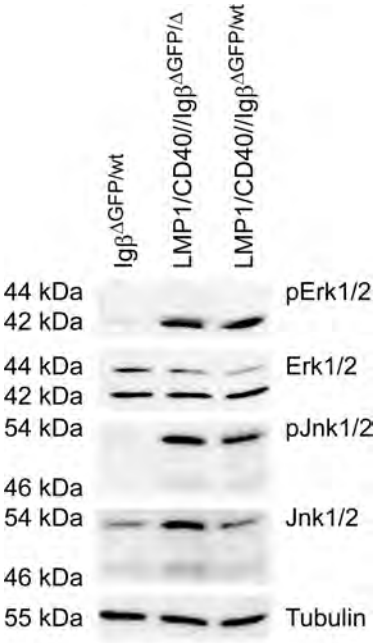

Figure 35 Enhanced activation of the MAPK Erk and Jnk is maintained LMP1/CD40//Igβ$^{\Delta GFP/\Delta}$ B cells. Whole-cell extracts were isolated from non-stimulated splenic B cells of mice with indicated genotypes and were subjected to immunoblot analysis using antibodies specific for pJnk1/2 (Thr183/Tyr185) and pErk1/2 (Thr202/Tyr204), as well as for the corresponding non-phosphorylated forms. Equal protein loading was controlled by an α-Tubulin staining. The result is representative for three independent experiments.

3.3.5.3 LMP1/CD40//Igβ$^{\Delta GFP/\Delta}$ B cells maintain basal phosphorylation of Akt

PI3K is most prominently activated upon BCR engagement but has also been shown to be essential for prolonged survival of LMP1/CD40 B cells *in vitro* (Hojer *et al.*, in preparation). PI3K activity is reflected in the phosphorylation of Akt kinase. However, LMP1/CD40 B cells show normal basal phosphorylation of Akt (Hojer *et al.*, in preparation). Thus, we were interested

whether basal phosphorylation of Akt is maintained in non-stimulated LMP1/CD40//Igβ$^{\Delta GFP/\Delta}$ B cells. In Western blot analyses, comparable phosphorylation of Akt like in Igβ$^{\Delta GFP/wt}$ and LMP1/CD40//Igβ$^{\Delta GFP/wt}$ B cells was detected in LMP1/CD40//Igβ$^{\Delta GFP/\Delta}$ B cells (Fig. 36A), evidencing that Igβ deficiency does not abrogate basal Akt activation in LMP1/CD40-expressing B cells.

3.3.5.4 Ablation of Igβ reduces c-Myc levels in LMP1/CD40 B cells

c-Myc is a major target of the Erk pathway and is both phosphorylated and transcriptionally regulated by the Erk cascade (McCubrey *et al.*, 2007; Z. Hao, personal communication). Furthermore, c-Myc is highly expressed in LMP1/CD40-expressing B cells and may partially account for the phenotype of these cells (Hojer *et al.*, in preparation). As basal phosphorylation of Erk is maintained in LMP1/CD40//Igβ$^{\Delta GFP/\Delta}$ B cells, we were interested whether high c-Myc expression would still be found in these cells. Western blot analyses showed that c-Myc levels are significantly reduced in LMP1/CD40//Igβ$^{\Delta GFP/\Delta}$ B cells in comparison to LMP1/CD40//Igβ$^{\Delta GFP/wt}$ B cells (Fig. 36B). Thus, a diminished c-Myc level might explain that LMP1/CD40 is only partially able to rescue Igβ-deficient B cells, but cannot maintain B cell expansion and survival as found in LMP1/CD40-expressing B cells proficient for Igβ.

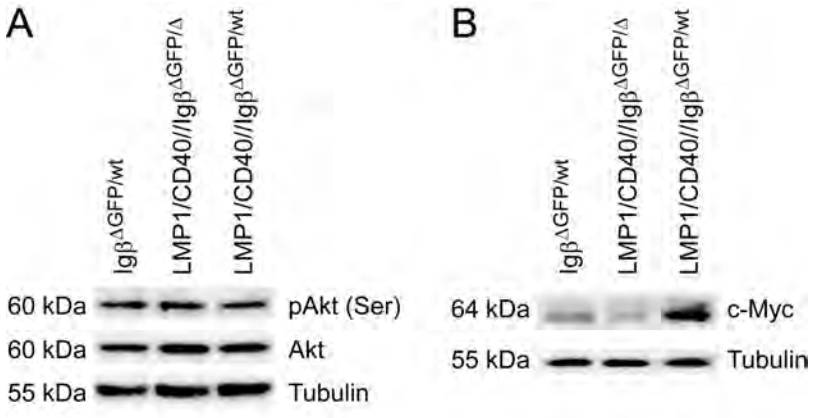

Figure 36 LMP1/CD40//Igβ$^{\Delta GFP/\Delta}$ B cells maintain basal phosphorylation of Akt kinase, but show reduced levels of c-Myc. Whole-cell extracts were isolated from non-stimulated splenic B cells of mice with indicated genotypes and were subjected to immunoblot analysis using antibodies specific for **(A)** pAkt (pS473) and its corresponding non-phosphorylated form, **(B)** c-Myc. Equal protein loading was controlled by an α-Tubulin staining. The result is representative for three independent experiments.

4 Discussion

Notch signaling influences cell fate decisions during differentiation processes of a wide range of tissues, including lymphocyte development. In the hematopoietic system, Notch1 signals are required for T cell development and T effector class decisions (Han *et al.*, 2002; Radtke *et al.*, 1999; Pui *et al.*, 1999; Schmitt *et al.*, 2004). In mature B cells, Notch2 is the Notch family member that is mainly expressed and is essential for MZ B cell differentiation (Saito *et al.*, 2003). Constitutive activation of Notch is clearly transforming for T cells and induces T cell leukemia (Ellisen *et al.*, 1991; Pear *et al.*, 1996; Bellavia *et al.*, 2000; Rohn *et al.*, 1996). However, the effect of deregulated Notch signaling in B lymphocytes in regard to the development of B cell malignancies is still controversial. In this work, we provide deeper insights into the role of Notch2 signaling in B cell differentiation, activation, and B cell lymphomagenesis.

4.1 Notch1/2IC activate proliferation-associated as well as pro-apoptotic genes in human B cells *in vitro*

Through the interaction with RBP-Jκ, Notch and the Epstein-Barr-viral protein EBNA2 use the same signaling cascade to activate their target genes. Therefore, it is in discussion whether EBNA2 makes use of the Notch signaling pathway to contribute to B cell immortalization. However, previous work has shown that neither constitutive active Notch1 nor Notch2 (Notch1/2IC) can replace EBNA2 in its function to maintain B cell immortalization. Although Notch1/2IC expression drove some B cells into the S-phase of the cell cycle, cell numbers did not increase, presumably due to an increased apoptosis rate in Notch1/2IC-expressing cells (Kohlhof *et al.*, 2009). Based on mRNA expression analyses, we investigated whether the biological differences between Notch1/2IC and EBNA2 can be traced back to differences in the regulation of genes associated with proliferation or survival.

We show that both Notch1/2IC and EBNA2 induce the expression of cell cycle- and proliferation-associated genes, but only EBNA2 leads to the strong induction of anti-apoptotic genes in parallel. Like EBNA2, Notch1/2IC induced the expression of cyclins and CDKs, although most of them were less intensely upregulated as by EBNA2. Exceptionally, a small group of genes containing *CCND2*, *CCND1*, and *CDK2* was comparably induced by Notch1/2IC and EBNA2. This observation corroborates previous studies, reporting that Notch1IC can upregulate *CCND1* and *CDK2,* leading to S-phase entry (Ronchini and Capobianco, 2001; Stahl *et al.*, 2006). The profound differences between Notch1/2 and EBNA2 in maintaining B cell proliferation might be partially attributed to the diverse regulation of PI3K and c-MYC expression by EBNA2 and Notch1/2IC. *PI3KR1* and *c-MYC* are both direct target genes of EBNA2 and were rapidly and intensively upregulated solely by EBNA2. These genes

play an essential role in the proliferation of immortalized cell lines in concert with the Epstein-Barr-viral genes *LMP1* and *LMP2A* (Dirmeier *et al.*, 2005; Kilger *et al.*, 1998). Whereas Notch1/2 did not induce the expression of PI3K, c-MYC expression levels were upregulated to a certain degree. This is in line with previous observations showing that *c-MYC* is a direct target gene of Notch1IC in T cell acute lymphoblastic leukemia (T-ALL) (Weng *et al.*, 2006; Palomero *et al.*, 2006; Sharma *et al.*, 2006), as well as with our own observations that constitutive Notch2 signaling elevates c-Myc levels in B cells *in vivo*. However, Notch1/2IC were not able to induce the high peak of c-MYC levels in EREB2.5 cells as observed early after EBNA2 induction. High c-MYC expression itself can induce hyperphosphorylation of Rb, activation of CDK2, and entry into the cell cycle (Schuhmacher *et al.*, 1999). Thus, high c-MYC levels as induced by EBNA2 might be essential to drive EBV-infected cells into the cell cycle. As soon as EBV-infected cells express all viral latency genes, which drive B cell proliferation and activation, c-MYC expression may significantly decrease to an even lower level than in Notch1/2IC-expressing cells. One reason for a different nature of gene regulation by EBNA2 and Notch1/2IC may be attributed to differences in their structures. This might lead to different binding affinities of EBNA2- and NotchIC-containing complexes to certain RBP-Jκ binding sites, or to qualitative differences in the interactions with other transcription factors that bind additionally within EBNA2- or Notch-responsive promoters. Moreover, EBNA2 and NotchIC cooperate very exclusively with viral and cellular proteins that modulate their transcriptional activity (Zimber-Strobl and Strobl, 2001).

Furthermore, we concluded that the increased percentages of apoptotic cells in cultures of Notch1/2IC/EREB cells may be traced back to the predominant induction of pro-apoptotic genes by Notch1/2IC in comparison to EBNA2. Strikingly, both Notch1/2IC and EBNA2 upregulated the expression of several pro-apoptotic genes, whereas only EBNA2 led to the intensive induction of anti-apoptotic genes. Since most of these anti-apoptotic genes are known as target genes of LMP1 (Dirmeier *et al.*, 2005), their high expression in EBNA2-expressing cells is most likely due to the high amount of LMP1 in EBNA2/EREB compared to Notch1/2IC/EREB cells. As this observation implied the presence of anti-apoptotic signals as a prerequisite that Notch1/2IC may induce proliferation in B cells, we aimed to analyze whether a similar interplay of Notch with such signaling pathways can be found also in human B cell tumors. Using the recently established human transcriptome data base "GeneSapiens" (Kilpinen *et al.*, 2008), an expression analysis across a wide range of tumor samples revealed a very high *DTX1* expression in certain B cell lymphomas, suggesting that Notch signaling is active in these tumors. Interestingly, high *DTX1* expression was in most cases correlated with high expression of anti-apoptotic genes like *BCL2A1* and *BIRC5*, indicating that active Notch signaling is present in certain B cell lymphomas, in which anti-apoptotic signals are provided by other stimuli

(Kohlhof *et al.*, 2009). These data underline the hypothesis that deregulated Notch signaling induces proliferation of B cells only in the presence of anti-apoptotic stimuli. Thus, this implication contributes to the understanding of the role of Notch in B cell lymphomas, as further discussed in section 4.3.

4.2 Constitutive Notch2 signaling is instructive for marginal zone B cell differentiation *in vivo*

To further investigate the importance of Notch2 during normal and malignant B lymphopoiesis *in vivo*, we have established a transgenic mouse strain, allowing the conditional expression of a constitutive active form of Notch2 (Notch2IC) in a *Cre*/loxP-dependent manner. The concomitant expression of a truncated human CD2 molecule enables the tracing of Notch2IC-expressing cells. To study the function of Notch2 in early and late B cell development, Notch2IC expression was activated in B cells *in vivo* either dependent on mb1-*Cre* (Hobeika *et al.*, 2006) or on CD19-*Cre* (Rickert *et al.*, 1997).

4.2.1 Notch2IC expression dependent on mb1-*Cre* blocks early B cell differentiation and leads to ectopic T cell development in the bone marrow

Constitutive Notch2 activity dependent on mb1-*Cre* completely blocked B cell development beyond the pro-B cell stage and led to the formation of an aberrant T cell population in the bone marrow, reminiscent of the T cell population detected after the transplantation of Notch1IC-transduced bone marrow progenitors into irradiated mice (Pui *et al.*, 1999). Unlike normal T cells, only low CD3 and no T cell receptor (TCR) expression were detected on these Notch2IC-expressing T cells, which is in contrast to the abovementioned study of Pui *et al.* (1999), reporting intermediate αβ TCR levels on bone marrow-derived, Notch1IC-expressing T cells. Successful transition through the β-selection as a prerequisite for differentiation to the $CD4^+CD8^+$ double positive (DP) stage requires the cooperative action of both Notch and pre-TCR signaling (Starr *et al.*, 2003; Wolfer *et al.*, 2002; Ciofani *et al.*, 2006; Maillard *et al.*, 2006; Allman *et al.*, 2001a). Thus, the DP phenotype of Notch2IC-expressing T cells despite the absence of TCR β expression is somehow surprising. Either constitutive Notch2 signaling mimics pre-TCR-derived signals as it has been recently suggested for Notch1IC (Michie *et al.*, 2007), or the aberrant T cell phenotype is induced by the ectopic expression of T cell-specific genes such as *gata3*, which encodes an important T cell transcription factor, and has been recently identified as target gene of Notch in T cells *in vivo* (Amsen *et al.*, 2007; Fang *et al.*, 2007). The bone marrow-derived Notch2IC-expressing T cells failed to further mature to CD4 or CD8 single positive T cells, what might be due to the lack of thymus-specific factors in the bone marrow (Carlyle and Zuniga-Pflucker,

1998) and/or to a Notch-induced block of terminal T cell differentiation. Thus, after successful β-selection during thymic T cell development, pre-TCR signaling mediates the downregulation of Notch1 expression (Taghon *et al.*, 2006; Yashiro-Ohtani *et al.*, 2009). This mechanism is presumed to be essential to avoid oncogenic effects of Notch (Weng *et al.*, 2006) and may explain the block of further T cell differentiation when high levels of Notch signaling are maintained beyond the DN4 stage.

In Notch2IC//mb1Cre$^{+/-}$ mice, B cell maturation was arrested at Hardy fractions A and B and no peripheral, mature B cells were found. This is in contrast to a former study performed by Witt and colleagues, reporting that retroviral high-level expression of Notch2IC blocked B cell development at the large pre-B cell stage (Hardy fraction C/C´), whereas lower-level expression of Notch2IC selectively promoted B1 B cell differentiation in the spleen (Witt *et al.*, 2003a). In our case, the very few B cells found in the spleen of Notch2IC//mb1Cre$^{+/-}$ mice did not display a B1 cell but rather an immature phenotype. The differences of these two experimental settings might be due to a different expression level of Notch2IC.

In contrast to previous studies, expressing NotchIC retrovirally in all hematopoietic stem cells (HSC), Notch2IC expression should be restricted to the B cell lineage in our approach. The mb1-*Cre*-mediated recombination was described as primarily B cell-specific (Hobeika *et al.*, 2006). Therefore, it was surprising to observe a very similar phenotype concerning the build-up of bone marrow-derived T cells also upon mb1-*Cre*-dependent Notch2IC expression. The reason might be that *Cre*-mediated recombination already occurs occasionally in single CLPs. Using transgenic reporter mice, mb1-*Cre* was reported to lead to a low frequency (< 1 %) of T cells having deleted the STOP cassette (Hobeika *et al.*, 2006). These T cells may arise from CLPs, which have already deleted the STOP cassette and have further developed into normal T cells, as the expression of the reporter transgene had not interfered with T cell development. However, strong and constitutive Notch2 signaling in CLPs might enforce T cell commitment at the expense of B cells, prompting ectopic T cell development in the bone marrow environment as it has been previously described for retrovirally expressed Notch1/2IC (Pui *et al.*, 1999; Witt *et al.*, 2003a). Alternatively, the aberrant T cell-like population in Notch2IC//mb1Cre$^{+/-}$ mice may arise from already committed pro-B cells starting to express Notch2IC and therefore trans-differentiating to the T cell lineage. Constitutive Notch2 signaling might suppress the induction of B cell-specific transcription factors like Pax5, EBF, and E2A and may simultaneously upregulate the expression of T cell-specific factors, thus leading to the trans-differentiation of early B cell progenitors. Our assumption is corroborated by findings of F. Jundt and colleagues, showing that in Hodgkin lymphoma cells Notch1 signaling antagonizes the key transcription factors EBF and E2A, leading to the suppression of B cell lineage genes and induction of lineage-inappropriate genes (Jundt *et*

al., 2008). Moreover, our own, unpublished data demonstrated that in a human B cell line, Notch1/2IC negatively regulate the expression of B cell-specific genes as *Igα*, *Igβ*, *E2A*, and *Igμ*, whereas T cell-specific factors like *CD3* and *GATA3* are positively regulated (H. Kohlhof, personal communication).

In contrast to former investigations, our data do not point to an established T cell leukemic disease at the time point of analyses, which was six to 12 weeks of age. It has been previously shown that weak gain-of-function Notch1 alleles, which induce relatively weak Notch signaling activity, were only able to induce ectopic T cell development, but failed to initiate T cell leukemia (Chiang *et al.*, 2008). Assuming that transgenic expression of Notch2IC might result in a lower Notch2 protein level or activity as in previous retroviral approaches, this might explain the induction of only ectopic, but not malignant T cells in our experimental system. Notch2IC//mb1Cre$^{+/-}$ mice died with nine to 12 weeks of age for unknown reasons. Therefore, we cannot exclude that these mice would have developed T cell leukemia at an age beyond.

4.2.2 Notch2IC expression dependent on CD19-*Cre* induces marginal zone B cell differentiation at the expense of follicular B cells

Negative selection of early Notch2IC-expressing B cells was counteracted by delayed activation of Notch2IC dependent on CD19-*Cre*, resulting in normal percentages and numbers of developing B cells in the bone marrow. Mature B cells of Notch2IC//CD19Cre$^{+/-}$ mice exhibited a strong shift to the MZ B cell compartment at the expense of Fo B cells. However, also the remaining B cells at the outer border of the follicular B cell zone were observed to express Notch2IC and high levels of IgM. Recently, Cariappa and colleagues have described two distinct Fo B cell populations, namely IgM^{low} Fo-I and IgM^{high} Fo-II B cells (Cariappa *et al.*, 2007). Thus, the remaining Fo B cell population of Notch2IC//CD19Cre$^{+/-}$ mice is reminiscent of the Fo-II B cells, which have been postulated to serve as a reservoir for replenishing the MZ B cell compartment (Pillai and Cariappa, 2009). Based on the current data, we can only hypothesize about the nature of the Notch2IC-expressing B cells within the follicle. In theory, those cells could be (i) MZ B cells that have migrated into the follicle potentially as a consequence of an overcrowded MZ, (ii) transitional or Fo B cells that have just initiated Notch2IC expression and thus start to migrate towards the MZ, or (iii) MZ B cell precursors. While MZ B cells can exclusively be found in the spleen in wild type mice, Notch2IC//CD19Cre$^{+/-}$ mice harbored significant amounts of MZ-like B cells also in the inguinal lymph nodes. These cells may originate either from (i) splenic MZ B cells that have migrated to the lymph nodes, (ii) transitional B cells that have started to express Notch2IC in the blood stream and migrated to the lymph nodes

rather than to the spleen, or (iii) Fo B cells that were already located in the lymph nodes before starting to express Notch2IC and to differentiate into MZ B cells.

It is still unclear, at which developmental stage immature B cells are committed to adopt either a Fo or MZ B cell phenotype, and in detail how Notch2 contributes to that lineage decision. Previous reports suggest that MZ B cell commitment occurs at the T1 transitional B cell stage upon the interaction of Notch2, expressed on these cells, with the ligand Dll1, expressed on endothelial cells located in the splenic red pulp and MZ (Tan *et al.*, 2009). However, other studies in the rat suggest an origin of MZ B cells also from the Fo B cell pool (Dammers *et al.*, 1999), indicating that each B cell, including T2 and Fo B cells, receiving a Notch2 signal may adopt a MZ B cell phenotype. In Notch2IC//CD19Cre$^{+/-}$ mice, we observed a higher deletion efficiency in T1 as in T2 transitional B cells as well as diminished T2 and T3 transitional B cell populations, suggesting that in Notch2IC//CD19Cre$^{+/-}$ mice, MZ B cells mainly develop from the T1 transitional B cell stage. This differentiation step might most likely involve a so far non-characterized MZ B cell precursor displaying a CD21/35$^{int/high}$IgM$^{int/high}$AA4.1^{low}CD23^{-} phenotype. Cells undeleted at the T1 transitional stage may preferentially mature to T2 transitional B cells, which might still differentiate into MZ B cells upon Notch2IC expression via the conventional MZ B cell precursor stage displaying a CD21/35^{high}IgM^{high}AA4.1^{low} CD23^{+} phenotype. A sequential model for MZ B cell development involving those kinds of MZ B cell precursors is illustrated in figure 37.

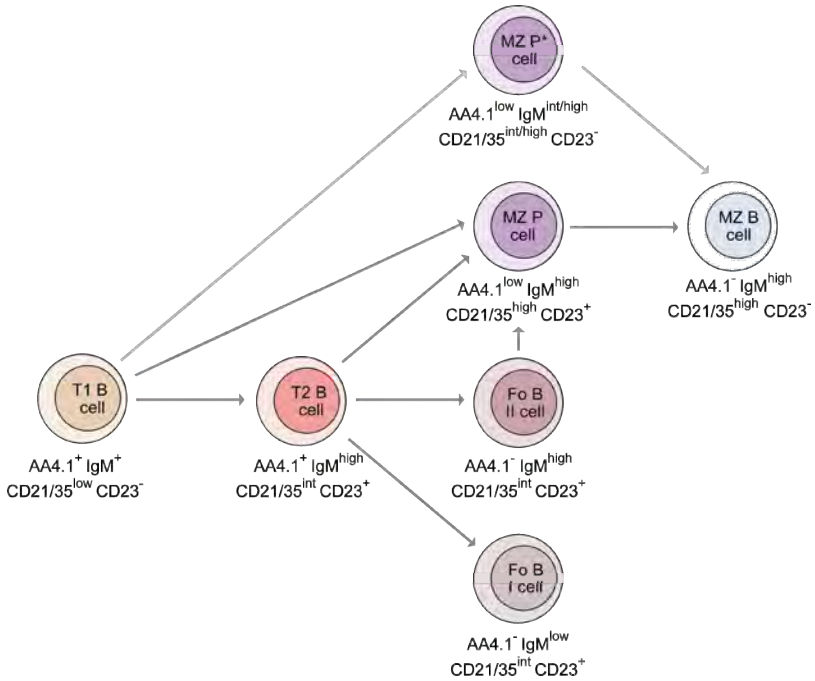

Figure 37 A sequential model for marginal zone B cell development (modified from Pillai and Cariappa, 2009). Transitional (T1 or T2) B cells can develop either into follicular (Fo) I B cells forming the major mature B cell population, or into Fo II B cells, potentially serving as reservoir for marginal zone (MZ) B cells. Transitional (T1 or T2) B cells that are committed to the MZ B cell compartment develop into MZ B cell precursors (MZ P) before maturing to MZ B cells. Upon constitutive Notch2 signals, MZ B cell commitment is enforced in transitional B cells, but appears to predominantly involve another variant of MZ B cell precursor (MZ P*) when commitment is achieved from the T1 B cell stage (shown in bright grey arrows).

Our data clearly evidence that Notch2 mediates differentiation of MZ B cells. Whether it is also required for MZ B cell survival and whether Notch2IC can also induce MZ B cell differentiation in Fo B cells may be studied particularly with a conditional and inducible Notch2IC-transgenic mouse strain that will allow switching off Notch2IC expression in an established MZ B cell compartment or activating Notch2IC expression in an existing Fo B cell population.

B cells of Notch2IC//CD19Cre$^{+/-}$ mice were hyper-responsive to LPS and α-CD40 stimulation *in vitro*. Robust proliferation to LPS or CD40 ligation is known as hallmark of MZ B cells (Allman *et al.*, 2001b; Oliver *et al.*, 1997). Moreover, α-IgM stimulation resulted in increased cell death of Notch2IC-expressing B cells (data not shown), consistent with previous reports showing that α-IgM treatment induces apoptosis in MZ B cells (Oliver *et al.*, 1997; Meyer-Bahlburg *et al.*, 2009). Hence, the localization in the MZ, the surface marker expression, and the biological behavior of Notch2IC//CD19Cre$^{+/-}$ B cells is perfectly reminiscent of MZ B cells. Thus, entire lineage characteristics of MZ B cells are maintained in Notch2IC-expressing B cells, confirming these cells as real MZ B cells. Despite their pre-activated phenotype, Notch2IC-expressing B cells were impaired in germinal center (GC) formation and class switch recombination after challenging mice with the TD antigen NP-CGG. Not only NP-specific IgG1 but also IgM antibodies were diminished, suggesting a general defect of these cells to respond to TD antigens. However, Notch2IC-expressing B cells were not generally detained in plasma cell differentiation, indicated by their normal response to the TI type 1 antigen LPS. The impaired TD immune response of Notch2IC-expressing B cells might either be due to their MZ B cell phenotype or to the influence of constitutive Notch2 signaling. Previously, MZ B cells have been suggested to participate also in TD immune response, since they were fully capable to initiate GC formation and to undergo somatic hypermutation following activation by TD antigens in cell transfer studies (Song and Cerny, 2003). Most likely, constitutive Notch2 expression in MZ B cells inhibits the migration of these cells towards the follicular T cell zone upon antigen contact, where B cells receive costimulatory signals provided by T_H cells. Members of our laboratory have recently shown in human B cells *in vitro* that Notch1/2IC represses the expression of various genes encoding for chemokines their selves or their receptors (H. Kohlhof, personal communication). Signals mediated via such components influence cellular migration properties profoundly. Thus, a migration defect of Notch2IC-expressing MZ B cells may explain the impaired immune response to TD antigen. Future studies, allowing Notch2IC expression specifically in activated B cells dependent on γ1-*Cre* or using a conditional and inducible Notch2IC-expressing mouse strain, have been initiated to investigate the role of Notch2 in B cell activation and immune response *in vivo* in more detail.

4.2.3 The basal activity of the non-canonical NF-κB pathway is reduced in Notch2IC-expressing B cells

An interplay of NF-κB and Notch signaling has been described in various cellular systems. These interactions are partially based on the identification of NF-κB components as Notch1 target genes, as well as on physical interactions between Notch and NF-κB components (Osipo *et al.*, 2008). Previously, it has been reported that soluble Notch ligand triggers IκBα phosphorylation (Jang *et al.*, 2004) and that IκBα is a Notch1 target gene (Oakley *et al.*, 2003). However, in Notch2IC-expressing B cells, both the levels of phosphorylated and non-phosphorylated IκBα were significantly reduced. Since p50, p65, and c-Rel levels were not increased in the nucleus of Notch2IC-expressing B cells, we suggest that the reduced levels of IκBα do not reflect an enhanced activity of the canonical NF-κB pathway. However, it might be possible that other IκB members are able to partially replace IκBα in its function in Notch2IC-expressing B cells.

Compared to wild type cells, both nuclear p52 and RelB levels were reduced in Notch2IC-expressing B cells, whereas p100 levels were increased, indicating a selective reduction of basal non-canonical NF-κB signaling. This could indicate that constitutive Notch2 signaling might render the cell generally less dependent on signaling cascades that activate the non-canonical NF-κB pathway, such as signaling upon engagement of the BAFF receptor.

In this regard, we cannot differentiate whether the NF-κB status in Notch2IC-expressing B cells reflects the common NF-κB status of MZ B cells or is due to an interplay between NF-κB and constitutive Notch2 signaling in B cells. Indeed, diminished IκBα expression in MZ B cells has been already reported (Zhang *et al.*, 2007), suggesting that reduced IκBα levels as observed in Notch2IC-expressing B cells could be assigned to their MZ B cell phenotype. In general, MZ B cell maintenance, and potentially MZ B cell commitment may be less dependent on NF-κB signaling in the presence of constitutive active Notch2. This might indicate that Notch2 has to be regarded downstream of NF-κB signaling during MZ B cell differentiation under normal circumstances. Since the Notch2 gene harbors a NF-κB binding site in its promoter region appearing to be conserved over different organisms (L.J. Strobl, personal communication), the NF-κB signaling strength may determine the surface expression level of Notch2 on transitional B cells. Already haploinsufficiency of Notch2 results in the absence of MZ B cells (Witt *et al.*, 2003b, U. Zimber-Strobl, personal communication), indicating that NF-κB signaling may critically influence the MZ B cell lineage decision by modulating the Notch2 surface expression level. To further investigate this hypothesis, we will cross conditional Notch2IC-transgenic mice with conditional MALT1-deficient mice, which are defective in their MZ B cell generation due to an impaired canonical NF-κB activity (Ruland *et al.*, 2003). This will shed light on the hierarchy of

these signaling pathways and will clarify whether constitutive Notch2 signaling may act independently of canonical NF-κB signaling during MZ B cell differentiation.

4.2.4 Notch2IC//CD19Cre$^{+/-}$ B cells display high c-Myc levels as well as enhanced MAPK and PI3K/Akt activity

The pre-activated state of Notch2IC-expressing B cells is mirrored in an increased activation of PI3K/Akt and the MAP kinases Erk and Jnk as well as in higher basal levels of c-Myc protein.

Akt is broadly known to promote cell survival by a variety of mechanisms including the direct inhibition of pro-apoptotic proteins like Bad, caspase-9, or Bax as well as the indirect inhibition of the tumor suppressor gene p53 (Khwaja, 1999; Tsuruta *et al.*, 2002; Brazil *et al.*, 2002). Phosphorylation of Akt is thought to directly reflect PI3K activity. In Notch2IC-expressing B cells, enhanced PI3K/Akt activity is most likely the result of an increased expression of Hes1. In T-ALL and other Notch-regulated malignancies, Hes1 as target of Notch1 has been shown to mediate transcriptional downregulation of Pten, which negatively regulates PI3K activity by inactivating PIP3 (Palomero *et al.*, 2007; Katso *et al.*, 2001; Sulis and Parsons, 2003; Cully *et al.*, 2006; Samuels and Ericson, 2006; Hay, 2005; Sarbassov *et al.*, 2005). Besides, increased levels of *TCL1* gene product are suggested to be involved in the activation of Akt in many B cell malignancies (Gold, 2003). In human B cells *in vitro*, *TCL1* mRNA expression has been shown to be particularly induced by Notch2IC (H. Kohlhof, personal communication). Therefore, it remains to be further investigated whether a reduced expression of Pten or an enhanced expression of TCL1 can also be found in Notch2IC-expressing B cells *in vivo*, contributing to enhanced Akt activity.

Additionally, Erk was found to be strongly phosphorylated in Notch2IC-expressing B cells. Erk is commonly activated via the Ras-Raf-MEK-Erk cascade. Also PI3K is involved in Erk activation in association with PLCγ2 (Jacob and Kelsoe, 1992), acting upstream of that cascade. Activated Raf kinases phosphorylate MEK1/2, ultimately resulting in the activation of Erk1/2. Erk in turn modulates the activity of a wide range of substrates that are critically involved in the regulation of cell proliferation and survival. However, neither Raf (B-Raf or Raf-1) nor MEK1/2 showed an increased activation in Notch2IC-expressing B cells. Moreover, Raf-1 protein levels were of unknown reasons consistently reduced in Notch2IC//CD19Cre$^{+/-}$ B cells (data not shown). Probably, the enhanced activation of Erk and Akt depends on PI3K. Analysis of the basal activation of these kinases in the presence of chemical inhibitors that target PI3K activity might shed light on the signaling cascade leading to the activation of Erk and Akt.

In Notch2IC//CD19Cre$^{+/-}$ B cells, we found moreover significantly elevated c-Myc levels. Both active Akt and Erk were reported to lead to the upregulation of c-Myc protein levels (Grumont *et*

al., 2002, Z. Hao, personal communication). Additionally, c-Myc is a known target gene of Notch1 not only in T-ALL (Palomero *et al.*, 2006; Weng *et al.*, 2006; Sharma *et al.*, 2006), but also in other cells including B lymphocytes (Gordadze *et al.*, 2001; Kohlhof *et al.*, 2009). Enhanced basal phosphorylation of Akt kinase as well as higher basal levels of c-Myc have been recently reported for MZ B cells *in vitro* in comparison to Fo B cells (Meyer-Bahlburg *et al.*, 2009). Thus, it can not be discriminated whether the activation state/protein level of these signaling molecules in Notch2IC-expressing B cells is due to the MZ B cell phenotype itself or to constitutive Notch2 signaling.

In this context, it is still in question whether the phenotype of MZ and Fo B cells is mainly regulated by the presence and absence of Notch2 signaling. Comparing the gene expression profiles and activity of signaling pathways in Notch2IC-expressing vs. wild type MZ B cells as well as in Notch2-deficient vs. wild type Fo B cells might clarify this issue. Furthermore, it is from a special interest to reveal target gene regulation by Notch2 in B cells *ex vivo*, as Notch target genes in B cells have so far only been studied *in vitro*. Since the $IgM^{high}CD23^{-}$ phenotype of Notch2IC//$CD19Cre^{+/-}$ B cells did not reflect the repression of *Igμ* and the induction of *CD23* expression, which has been described after *in vitro* induction of NotchIC in mature B cells (Strobl *et al.*, 2000; Hubmann *et al.*, 2002), this already indicates that the *ex vivo* analysis will reveal differences in the gene regulation by Notch2 in B cells compared to data collected *in vitro*.

4.2.5 Constitutive Notch2 signaling acts independently of CD19 during marginal zone B cell development

Current data suggest that BCR signaling is involved in the cell fate decision between MZ and Fo B cells. Thereby, PI3K signaling seems to play a crucial role. Like the deficiency for the BCR co-receptor CD19, mutations in the PI3K isoform p110δ result in defective MZ B cell development (Rickert *et al.*, 1997; Clayton *et al.*, 2002), whereas in mice deficient for Pten, a negative regulator of PI3K signaling, enhanced MZ B cell formation is observed (Suzuki *et al.*, 2003). In this work, we show that Notch2IC expression in CD19-deficient B cells (Notch2IC//$CD19Cre^{+/+}$) can overcome the defect in MZ B cell differentiation. Enhanced PI3K/Akt signaling upon constitutive Notch2 activity as it has been discussed in 4.3.4 is likely to compensate for the deficiency for CD19, which signals most prominently via PI3K (Buhl *et al.*, 1997). Thus, our results are reminiscent of studies of Anzelon and colleagues, showing that Pten deficiency, what results in constitutive activation of PI3K activity, can rescue CD19 deficiency *in vivo* (Anzelon *et al.*, 2003). Notch2IC//$CD19Cre^{+/+}$ B cells showed again elevated levels of c-Myc protein as well as enhanced activation of the MAP kinases Erk and Jnk, indicating that constitutive Notch2

signaling acts independently of CD19 in the activation of these signaling cascades and in the generation of MZ B cells.

Our data also shed a critical light on the hypothesis that the BCR signaling strength is an important determinant for MZ B cell lineage commitment. Based on the results of a variety of gain- or loss-of-function studies *in vivo*, particularly S. Pillai and A. Cariappa have been postulating over the last years that a strong BCR signal in transitional B cells induces commitment to the Fo B cell pool, while weak BCR signals render the cell sensitive for Notch2 signals and allow MZ B cell commitment (Pillai and Cariappa, 2009). Since the probability of a maturing B cell to receive a strong or a weak BCR signal can be assumed to be the same in a wild type or a Notch2IC-expressing mouse, we think that any dependency on this signaling strength is overcome in case of constitutive Notch2 activity as demonstrated by the extensive MZ B cell formation in Notch2IC//CD19cre$^{+/-}$ mice. Our data indicate that constitutive Notch2 signaling acts independently of BCR signaling during the induction of MZ B cell differentiation. Furthermore, we demonstrate that Notch2 signals are sufficient for MZ B cell differentiation, also in the absence of CD19, similarly as Notch1 signals are instructive for T cell lineage commitment.

4.3 Activation of Notch signaling itself is not sufficient to induce B cell lymphomagenesis

The role of Notch in the development of B cell lymphomas is still controversially discussed. Notch2 is highly expressed in B-CLL and both Notch1 and Notch2 are overexpressed in Hodgkin lymphoma (HL) cells. Engagement of Notch receptors resulted in an increased proliferation of HL and multiple myeloma cell lines and prolonged the survival of B-CLL cell lines (Hubmann *et al.*, 2002; Jundt *et al.*, 2002b; Jundt *et al.*, 2004; Rosati *et al.*, 2009). However, our results as discussed above in 4.1 indicate that Notch itself may induce apoptosis in B cells as long as anti-apoptotic stimuli, for instance LMP1 or CD40 signals, are missing (Kohlhof *et al.*, 2009). This corroborates other studies, reporting the inhibition of cell growth and the induction of apoptosis by NotchIC in avian, murine, and human B cell lines (Morimura *et al.*, 2000; Romer *et al.*, 2003; Zweidler-McKay *et al.*, 2005). Moreover, this is in line with recently published data showing a proliferative effect of Notch signaling in murine primary B cells in cooperation with BCR and CD40 stimulation and with the observation of our own laboratory that Notch1IC induces proliferation only in combination with LMP1 in B cells (Thomas *et al.*, 2007; Hofelmayr *et al.*, 2001).

The conditional Notch2IC-expressing mouse line allowed analyzing whether constitutive Notch2 signaling itself promotes rather B cell differentiation and expansion or the induction of apoptosis

in B cells *in vivo*. In Notch2IC//mb1Cre$^{+/-}$ mice, B cell development was blocked at the pro-B cell stage. The block in B cell development was accompanied by the development of ectopic T cells in the bone marrow, indicating that Notch2IC interferes with further B cell differentiation beyond the pro-B cell stage, forcing T cell development instead. In HLs, which derive from germinal center (GC) B cells and have lost their B cell phenotype, Notch1 has been recently suspected to contribute to the suppression of B lineage-specific genes and to the induction of B lineage-inappropriate genes by antagonizing the key B cell transcription factors E2A and EBF (Jundt *et al.*, 2008). This suggests that Notch signaling may be able to interfere with the B cell phenotype when it is activated at certain differentiation stages as in pro-B cells or GC B cells.

Activation of Notch2IC in immature B cells dependent on CD19-*Cre* did not result in a loss of the B cell phenotype but strongly induced MZ B differentiation. B cell numbers were normal in comparison to wild type mice and neither prolonged survival, increased proliferation, nor enhanced apoptosis of Notch2IC//CD19Cre$^{+/-}$ B cells was observed during *in vitro* cultures in comparison to control B cells. Since MZ B cells are described as very long-lived (Hao and Rajewsky, 2001), Notch2IC-expressing B cells may be suspected to exhibit a similar longevity *in vivo*. Therefore, it will be interesting to study the survival of Notch2IC//CD19Cre$^{+/-}$ B cells also *in vivo*. Strikingly, the increased levels of c-Myc as well as the enhanced activation of Akt and Erk were not reflected in an increased proliferation of Notch2IC//CD19Cre$^{+/-}$ B cells *in vitro*. In T-ALL, *c-MYC* is a direct transcriptional target downstream of oncogenic Notch1 (Palomero *et al.*, 2006; Weng *et al.*, 2006; Sharma *et al.*, 2006) and the Notch1/c-Myc transcriptional regulatory loop is regarded as the core mechanism mediating T cell transformation by oncogenic Notch1. Besides, PI3K/Akt signaling is known as further mechanism how Notch1 regulates cell growth in immature T cells (Gutierrez and Look, 2007). Also in B cells, the c-Myc and PI3K/Akt cascade are associated with cell growth and proliferation (Wade and Wahl, 2006; Harnett *et al.*, 2005). Thus, constitutive activation of c-Myc in B cells *in vivo* causes B cell transformation (Adams *et al.*, 1985). Moreover, Erk signaling is associated with proliferation of mature B cells and constitutive active Erk is found in HL cells (Kuppers, 2009). Therefore, it is tempting to speculate whether B cell lymphomas will develop in Notch2IC//CD19Cre$^{+/-}$ mice with an increased incidence over time when other mutations are acquired during the life-time of these animals, ultimately leading – in concert with already activated signaling cascades – to the transformation of these cells.

To finally address the question whether constitutive activity of Notch2 and CD40 cooperate in terms of B cell lymphomagenesis, Notch2IC-transgenic mice will be crossed to LMP1/CD40-transgenic mice, expressing a constitutive active CD40 receptor.

The differences received based on the activation of Notch2IC expression at various stages of B cell development by using different *Cre* strains underline that the biological outcome of Notch

signaling highly depends on the cellular background, the developmental stage, and the present co-stimulatory signals. Longevity of MZ B cells and the intense activation of growth- and survival-associated signaling pathways in Notch2IC-expressing B cells make it conceivable that B cell lymphomas will develop with a longer latency. Thus, further studies will be necessary to explore whether Notch2 signaling contributes in fact mechanistically to B cell lymphomagenesis. This will shed light on the question whether Notch2 may serve as a potential target for the treatment of certain B cell malignancies.

4.4 Ablation of BCR signaling abrogates LMP1/CD40-mediated B cell expansion *in vivo*

B cells are permanently selected for the expression of a functional BCR during all stages of their development. Also resting, peripheral B cells critically require signals delivered by the BCR for their survival (Lam *et al.*, 1997; Kraus *et al.*, 2004). However, it is still unclear whether aberrantly activated or malignant B cells also depend on this tonic BCR signal. To address this question, we genetically abolished the BCR-associated signaling component Igβ in pre-malignant B cells *in vivo* that express a constitutive active CD40 receptor. Members of our laboratory have recently shown that deregulated CD40 signaling in B cells provided by a LMP1/CD40 fusion protein prolongs survival as well as induces spontaneous cell division *ex vivo* and ultimately leads to the development of B cell lymphomas (Homig-Holzel *et al.*, 2008). Furthermore, it has been previously demonstrated in normal B cells that ablating of BCR-associated signaling molecules like Igα or Igβ results in strongly diminished peripheral B cell numbers, indicating that both signaling subunits are essential for the maintenance signal delivered through the BCR (Kraus *et al.*, 2004, N. Uyttersprot, personal communication).

By deleting Igβ in mature LMP1/CD40-expressing B cells, LMP1/CD40-mediated B cell expansion was abrogated, demonstrating that also pre-malignant B cells displaying constitutive CD40 signaling are not independent of tonic BCR signals. However, B cell numbers of LMP1/CD40//Igβ$^{\Delta GFP/\Delta}$ mice were elevated to wild type level, indicating that LMP1/CD40 expression can rescue Igβ-deficient B cells to some degree (Hojer *et al.*, in preparation). This was confirmed by analyzing the survival and proliferation of these cells *in vitro* and *in vivo* revealing that the survival and proliferation properties of LMP1/CD40//Igβ$^{\Delta GFP/\Delta}$ B cells are similar to those of wild type B cells, in contrast to rapidly dying Igβ-deficient B cells. Moreover, constitutive CD40 signaling induced an activated B cell phenotype despite the Igβ deficiency. Both the non-canonical NF-κB pathway and the MAP kinases Erk and Jnk, which are highly activated in LMP1/CD40 B cells, were still active in LMP1/CD40-expressing B cells deficient for Igβ. The activity of these signaling pathways might enhance the survival and proliferation of

LMP1/CD40//Igβ$^{\Delta GFP/\Delta}$ B cells, in contrast to Igβ-deficient B cells without LMP1/CD40 expression.

However, constitutive CD40 signaling could not entirely overcome the need of a functional BCR, as the ablation of Igβ resulted in a drop of the survival of LMP1/CD40-expressing B cells to wild type level. Therefore, we suspected that the Igβ deficiency must be reflected at least partially in changes of activated signaling cascades compared to LMP1/CD40 B cells proficient for Igβ. Tonic BCR signals are considered to occur ligand-independently, and were recently shown to be mediated by PI3K (Srinivasan *et al.*, 2009), though their entire nature is not known so far. Although PI3K/Akt signaling is most prominently activated upon BCR signaling, it can also be triggered by CD40 engagement (Harnett, 2004). PI3K-dependent Erk activation has been shown to be crucial for the survival of LMP1/CD40 B cells (Hojer *et al.*, in preparation). Surprisingly, basal phosphorylation of Akt was completely maintained in LMP1/CD40 B cells also in the absence of Igβ. Based on the crucial role of PI3K in mediating tonic BCR signaling (Srinivasan *et al.*, 2009), retained PI3K activation in LMP1/CD40//Igβ$^{\Delta GFP/\Delta}$ B cells may be regarded as one potential mechanism how constitutive CD40 partially compensates the impairment of tonic BCR signals. c-Myc is highly expressed in LMP1/CD40 B cells and elevated c-Myc levels are suggested to be at least partially responsible for the LMP1/CD40-induced phenotype of B cell expansion (Hojer *et al.*, in preparation). High c-Myc levels in LMP1/CD40 B cells are thought to depend on the Erk pathway as the latter is able to control c-Myc levels both transcriptionally and posttranslationally. Although basal activation of Erk is still maintained in LMP1/CD40//Igβ$^{\Delta GFP/\Delta}$ B cells, c-Myc expression was reduced to wild type levels. Thus, diminished c-Myc levels may at least partially account for the fact that LMP1/CD40 can only rescue Igβ-deficient B cells to a certain extent, but cannot maintain B cell expansion and prolonged survival as found in LMP1/CD40-expressing B cells proficient for Igβ.

However, we still aim to characterize Igβ-deficient cells with or without LMP1/CD40 expression in more detail. To analyze how the impairment of BCR signaling affects B cell functionality, we will test whether these cells are still sensitive to α-IgM treatment or CD40 ligation *in vitro*. As increased Erk phosphorylation was inconsistently detected also in Igβ-deficient cells without LMP1/CD40 expression, we have moreover to absolutely rule out that maintained Erk phosphorylation in LMP1/CD40//Igβ$^{\Delta GFP/\Delta}$ B cells is triggered by stress-induced activation during preparation. Therefore, further attempts to characterize activated signaling pathways in Igβ-deficient cells without LMP1/CD40 expression by intracellular flow cytometric analysis will be done. To further approve the survival properties of B cells from LMP1/CD40 B cells proficient or deficient for Igβ, survival of these cells will be monitored *in vivo*. For that purpose, the percentages of peripheral, GFP^{+} B cells will be followed while blocking the influx of newly

generated B cells from the bone marrow to the periphery by administering an α-IL7R antibody that blocks early B cell development in the bone marrow (Sudo *et al.*, 1993).

In summary, the observation that the ablation of Igβ results in a drop of survival of LMP1/CD40-expressing B cells to wild type level evidences that pre-malignant B cells are still susceptible to the impairment of tonic BCR signals. Unfortunately, the development of lymphomas could not be investigated over a longer period of time since CD21-*Cre* mediates ectopic recombination also in other tissues than mature B cells as in the forehead (Schmidt-Supprian and Rajewsky, 2007). This might lead to unspecific LMP1/CD40 expression and did not allow keeping mice longer than six months. Any lymphoma development in LMP1/CD40//Igβ$^{\Delta GFP/\Delta}$ mice was not observed up to that age and is also not expected based on both *in vitro* and *in vivo* survival studies. Although deregulated BCR expression has not been described in B cell lymphomas so far, the tonic survival signals that are constantly delivered by the BCR are suspected to contribute to tumor initiation or maintenance. This is corroborated by the observation that most B cell lymphoma cells still express the BCR and seem to be positively selected for BCR expression (Kuppers *et al.*, 2005). Therefore, targeting tonic BCR signaling, for instance by inhibiting Syk, is regarded as promising new treatment of Non-Hodgkin lymphomas (Gururajan *et al.*, 2006; Young *et al.*, 2009; Chen *et al.*, 2008). Our data even more encourage such approaches, as we provide evidence that tonic BCR signaling is crucial for the survival of pre-malignant B cells *in vivo* and most likely a prerequisite to allow their malignant transformation.

transformation.

5 Summary

Notch2 is known to be essential for the development of marginal zone (MZ) B cells. However, the precise mechanism leading to the generation of these cells is still elusive. In divers B cell lymphomas, enhanced Notch expression is moreover found, but the role of deregulated Notch signaling in the development of B cell malignancies is still unclear. In this work, we aimed to investigate the role of Notch signaling in B cell development, activation, and lymphomagenesis in more detail.

Using a human B cell line, we observed that the expression of constitutive active Notch1 or Notch2 (Notch1/2IC) initiates cell cycle entry, but also appears to actively induce apoptosis, potentially due to the absence of appropriate survival signals. In the current study, these biological effects were assigned to the induction of several cell cycle- and proliferation-associated genes as well as to the predominant upregulation of pro- but not anti-apoptotic genes by Notch1/2IC. Thus, we conclude that a sudden, constitutive Notch signal in B cells rather induces apoptosis than proliferation, as long as anti-apoptotic stimuli are missing (Kohlhof *et al.*, 2009).

In order to analyze the influence of constitutive Notch2 signaling on B cell development and lymphomagenesis *in vivo*, a conditional transgenic mouse strain that expresses a constitutive active Notch2 receptor (Notch2IC) based on the *Cre*/loxP system was generated and characterized. Notch2IC expression from the pro-B cell stage on mediated by mb1-*Cre* blocked early B cell development, and led to ectopic T cell development in the bone marrow. In contrast, delayed activation of Notch2IC in B cells dependent on CD19-*Cre* did not interfere with early B cell development. However, mature B2 cells were strongly shifted to the MZ B cell compartment at the expense of follicular B cells. Thereby, most MZ B cells appeared to branch from the T1 transitional B cell stage. Compared to wild type B cells, Notch2IC-expressing B cells displayed enhanced PI3K/Akt and MAPK signaling as well as increased c-Myc protein levels, while the basal activity of non-canonical NF-κB signaling was reduced. Of note, exclusive generation of MZ B cells was achieved even in the absence of CD19, which has been shown to be essential for MZ B cell development. However, B cell expansion or lymphoma development has been not observed until the current age of mice (six month). Our findings not only underline the differences in the outcome of Notch2 signaling depending on the B cellular developmental stage, but point to an instructive role of Notch2 signals during MZ B cell lineage decision.

Previously, our group was able to demonstrate that the expression of a constitutive active CD40 receptor, LMP1/CD40, in B cells *in vivo* results in B cell expansion and lymphomagenesis (Homig-Holzel *et al.*, 2008). To determine whether such pre-malignant B cells still require tonic BCR signals for their survival as normal, resting B cells do, tonic BCR signaling was impaired in mature LMP1/CD40-expressing B cells by deleting Igβ. Constitutive CD40 signaling prolonged

the survival of Igβ-deficient B cells, most likely due to a maintained activation of the MAP kinases Erk and Jnk as well as of the non-canonical NF-κB pathway by LMP1/CD40. However, in comparison to expanded LMP1/CD40-expressing B cells, the ablation of Igβ was accompanied by a drop of survival to a similar level as of wild type B cells, which was at least partially assigned to severely reduced basal c-Myc levels. Thus, these data indicate that pre-malignant B cells are still sensitive to the impairment of tonic BCR signaling.

6 Zusammenfassung

Notch2-Signale spielen bei der Bildung von Marginalzonen (MZ) B-Zellen eine essentielle Rolle. Allerdings ist der Mechanismus wie Notch2 zur MZ B-Zellgenerierung beiträgt noch weitgehend unbekannt. Des Weiteren findet man in verschiedenen B-Zelllymphomen eine verstärkte Notch-Expression, wobei die Bedeutung der deregulierten Notch-Signale bei der Entstehung dieser Tumore noch unklar ist. Deshalb wurde in dieser Arbeit die Rolle des Notch-Signalweges während der B-Zellentwicklung, -aktivierung und -lymphomentstehung genauer untersucht.

Vorausgegangene Arbeiten zeigten, dass die Expression eines konstitutiv-aktiven Notch1- oder Notch2-Rezeptors (Notch1/2IC) in einer humanen B-Zelllinie zwar den Eintritt in den Zellzyklus initiiert, aber vermutlich mangels entsprechender Überlebenssignale auch zur aktiven Apoptoseinduktion führt. Diese Arbeit zeigte, dass jene biologischen Befunde auf der Induktion verschiedener zellzyklus- und proliferations-assoziierter Gene, sowie vor allem pro- aber nicht anti-apoptotischer Gene basieren. Daraus schließen wir, dass ein dereguliertes, konstitutives Notch-Signal in B-Zellen eher Apoptose als Proliferation induziert, sofern es an anti-apoptotischen Stimuli mangelt (Kohlhof *et al.*, 2009).

Um den Einfluss von konstitutiven Notch2-Signalen auf die B-Zellentwicklung und -lymphomentstehung *in vivo* zu untersuchen, wurde des Weiteren auf Basis des *Cre*/loxP-Systems ein transgener Mausstamm generiert und charakterisiert, in dem ein konstitutiv-aktiver Notch2-Rezeptor (Notch2IC) konditional exprimiert wird. Notch2IC-Expression ab dem pro-B-Zellstadium durch mb1-*Cre* blockierte die frühe B-Zellentwicklung und induzierte ektopische T-Zellentwicklung im Knochenmark. Im Gegensatz dazu beeinträchtigte eine im Verlauf der B-Zellentwicklung etwas spätere Aktivierung von Notch2IC mittels CD19-*Cre* die frühe B-Zellentwicklung nicht, führte aber im reifen B2-Zellkompartiment zu einer stark vermehrten Generierung von MZ B-Zellen, zu Lasten der sehr verringerten follikulären B-Zellpopulation. Dabei schienen sich die meisten MZ B-Zellen aus T1 transitionellen B-Zellen zu entwickeln. Im Vergleich zur Wildtypkontrolle zeigten die Notch2IC-exprimierenden B-Zellen eine verstärkte Aktivierung des PI3K/Akt- und des MAPK-Signalwegs sowie ein erhöhtes Proteinlevel von c-Myc, während die basale Aktivität des nicht-kanonischen NF-κB Signalweges vermindert war. Interessanterweise konnte zudem in Abwesenheit von CD19, welches für die MZ B-Zellentwicklung unter normalen Umständen essentiell ist, eine ausschließliche Generierung von MZ B-Zellen bewirkt werden. Eine Expansion der B-Zellen oder gar die Entstehung von B-Zelllymphomen wurde bis zum jetzigen Alter der Tiere von sechs Monaten nicht beobachtet. Die Ergebnisse verdeutlichen zum einen die unterschiedlichen Effekte von Notch2-Signalen in Abhängigkeit des Differenzierungsstadiums der B-Zellen, und unterstreichen zum anderen, dass Notch2-Signale bei der MZ B-Zellentwicklung instruktiv wirken.

In Vorarbeiten zu einem weiteren Projekt konnte unsere Gruppe zeigen, dass die Expression eines konstitutiv-aktiven CD40-Rezeptors, LMP1/CD40, in B-Zellen *in vivo* zur B-Zellexpansion und Lymphomentstehung führt (Homig-Holzel *et al.*, 2008). Um zu untersuchen, ob das Überleben solch prämaligner B-Zellen immer noch von tonischen B-Zellrezeptor-(BCR)-Signalen abhängig ist, so wie es für normale, ruhende B-Zellen der Fall ist, wurde in reifen LMP1/CD40-exprimierenden B-Zellen Igβ deletiert, was zu einer starken Beeinträchtigung der tonischen BCR-Signale führt. Konstitutive CD40-Signale verbesserten die Überlebensfähigkeit von Igβ-defizienten B-Zellen, was auf eine aufrechterhaltene Aktivierung der MAP-Kinasen Erk und Jnk sowie der nicht-kanonischen NF-κB-Aktivität durch LMP1/CD40 zurückgeführt wurde. Im Gegensatz zu den expandierten LMP1/CD40-exprimierenden B-Zellen führte die Igβ-Deletion allerdings zu einer verminderten Überlebensfähigkeit ähnlich dem Überleben von Wildtyp-B-Zellen, was zumindest zum Teil einem stark verringertem c-Myc-Level durch die Igβ-Defizienz zugeschrieben wurde. Diese Befunde zeigen deutlich, dass das Überleben von prämalignen B-Zellen durch die Abschwächung von tonischen BCR-Signalen beeinträchtigt werden kann.

7 Material

7.1 Plasmids

I) DCR26CAGp-IRESCD2 (provided by M. Schmidt-Supprian)

Modified pROSA26-1 vector (Zambrowicz *et al.*, 1997), allowing homologous recombination with the murine *rosa26* locus via a short (1 kb) and a long (4 kb) homologous arm. Between the two homologous arms, a constitutive active CAGGS (CMV early enhancer/chicken β-actin/rabbit globin) promoter is located, followed by a loxP sites-flanked STOP cassette, containing a transcription and translation termination site and a neomycin-geneticin resistance gene, mediating resistance against G418 (Geneticin). Using the *AscI* site downstream of this region, a gene of interest may be inserted that will be followed by a frt sites-flanked IRES-hCD2 coding sequence, allowing the concomitant expression of a truncated human CD2 molecule.

II) pHprt_Notch2IC (provided by C. Hojer)

Plasmid containing *notch2IC* cDNA, initially isolated from the pTracer-CMV-Notch2cDNA vector (Shimizu *et al.*, 2000), harboring the sequence of full length murine *notch2* cDNA.

III) DCR26CAGp-IRESCD2-Notch2IC

DCR26CAGp-IRESCD2 plasmid, containing *notch2IC* cDNA within the *AscI* restriction site. The *notch2IC* cDNA corresponds to cDNA 5253 to 7583 of NCBI NM_010928 and was isolated from pHprt_Notch2IC. The vector was cloned as described in 8.3.4 and was used to target the abovementioned expression cassette containing *notch2IC* cDNA into the *rosa26* locus of murine IDG2.3 embryonic stem cells, in order to establish the Notch2IC^{flSTOPP}-transgenic mouse strain.

IV) puc18 (provided by G. Laux)

High copy number plasmid, used to subclone *notch2IC* cDNA.

V) pGK-Cre-bpA (provided by K. Fellenberg)

Plasmid encoding for *Cre* recombinase, controlled by the pGK promoter. This plasmid was used for transient transfection of recombinant ES cell clones to delete the loxP sites-flanked STOP cassette, in order to test clones for transgene expression.

VI) pRTS-1-N1, pRTS-1-N2, pRTS-1-CAT (Kohlhof *et al.*, 2009)

pRTS-1 vectors (Bornkamm *et al.*, 2005), containing coding sequences for the full length intracellular part of the human Notch1 receptor from position 5278 to 7668 of NM_0176173 (Notch1IC) and of the human Notch2 receptor from position 5362 to 7672 of NM_024408.2

(Notch2IC), respectively, including the PEST domain, but excluding the 3´ untranslated regions. Notch1IC and Notch2IC (Notch1/2IC) are under the control of a doxycycline-inducible bidirectional Tet-O7 promoter, which also controls the expression of a truncated nerve growth factor receptor (ΔNGFR). pRTS-1 also encodes for EBV nuclear antigen 1 (EBNA1). Chloramphenicol acetyl transferase (CAT) was inserted instead of Notch1/2IC to generate the control vector. Vectors are referred to as pRTS-1-N1, pRTS-1-N2, and pRTS-1-CAT, respectively. The plasmids were stably transfected into EREB2.5 cells, in order to identify Notch-regulated genes in B cells. Cloning and stable transfection were performed by H. Kohlhof.

7.2 Bacteria

DH5α (*E. coli*)

Genotype: F- endA1 glnV44 thi-1 recA1 relA1 gyrA96 deoR nupG Φ80d *lacZ* ΔM15 Δ(*lacZYA-argF*) U169 hsdR17 (r_K^- m_K^+), λ- .

7.3 Cell lines

I) IDG2.3 embryonic stem cells (ES) (Hitz *et al.*, 2007)

Murine ES cell line, derived from a male C57BL/6Jx129/SV (F1) blastocyst. Cells were used for gene targeting to generate the Notch2IC^{flSTOPP}-transgenic mouse strain.

II) Embryonic feeder (EF) cells

EF cells were prepared from pSV2neo, PEP-IL4 C57BL/6 embryos at day 13.5 as described in 8.1.2 and were used until the third passage for ES cell culture.

III) Notch1/2IC/EREB and CAT/EREB cells (Kohlhof *et al.*, 2009)

EREB2.5 is a conditionally EBV-immortalized, lymphoblastoid cell line that encodes an EBNA2 estrogen receptor (ER) fusion protein (ER-EBNA2). Thus, the function of EBNA2 depends on the presence of estrogen in EREB2.5 cells (Kempkes *et al.*, 1995a). In the absence of functional EBNA2, cells exhibit a resting phenotype, similar to mature, naive B cells, before having encountered antigen. In the presence of estrogen, EBNA2 is functional and able to transactivate not only the viral *LMP1* and *LMP2A* promoters, but also cellular target genes (Kempkes *et al.*, 1995a; Kempkes *et al.*, 1995b). This results in cell activation and proliferation, reminiscent of mature B cells after antigen-dependent activation. The cell lines Notch1IC/EREB, Notch2IC/EREB, and CAT/EREB were established by stably transfecting the pRTS-1-N1, pRTS-1-N2, and pRTS-CAT vectors, respectively (Kohlhof *et al.*, 2009). These cell lines were used to compare Notch- and EBNA2-regulated genes in B cells.

7.4 Mouse strains

I) C57BL/6 (Charles River Laboratories)

This mouse strain was used for blastocyst injection and for crossings to obtain germline transmission of the *notch2IC* transgene.

II) CD19-*Cre* (Rickert *et al.*, 1997)

C57BL/6 mouse strain with the *Cre* recombinase gene placed into the *CD19* locus, thereby destructing the *CD19* gene. The expression of the *Cre* gene is regulated by the CD19 promoter.

III) Igβ$^{\Delta c}$ (Reichlin *et al.*, 2001)

C57BL/6 mouse strain with deleted exons 5 and 6 of the *Igß* gene.

IV) Igβ$^{fl(GFP)}$ (Casola *et al.*, 2006)

C57BL/6 mouse strain with loxP sites-flanked exons 5 and 6 of the *Igß* gene and a downstream IRES-GFP sequence. Only in the presence of *Cre*, the flanked region is excised and GFP is concomitantly expressed (ΔGFP).

V) LMP1/CD40^{flSTOPP} (Homig-Holzel *et al.*, 2008)

Balb/C mouse strain that is conditional transgenic for the chimeric *LMP1/CD40* gene placed into the *rosa26* locus. A loxP sites-flanked STOP cassette upstream of the *LMP1/CD40* gene prevents transgene expression. Only in the presence of *Cre*, the STOP cassette is excised and *LMP1/CD40* is expressed under the control of the endogenous rosa26 promoter.

VI) CD21-*Cre* (Kraus *et al.*, 2004)

C57BL/6 mouse strain with a randomly integrated BAC clone encoding *Cre* under the control of the CD21 promoter.

7.5 DNA probes for Southern blotting

I) Rosa26

698 bp DNA fragment that was isolated from pRosa26-5-pBS-KS (kindly provided by P. Soriano) using the restriction enzymes *EcoRI* and *Pac1*.

II) hCD2

424 bp DNA fragment that was isolated from pBS_hCD2 using the restriction enzymes *BmgBI* and *BsaI*.

III) Notch2IC

319 bp DNA fragment that was isolated from pSG5_N2IC using the restriction enzymes *XmaI* and *StuI*.

7.6 Oligonucleotides

I) Primers for PCR and sequencing reactions

Primer name	Primer sequence (5´ to 3´)
B29-9R	CTTGTCAAGTAGCAGGAAGA
B29-18F	GTGGCACGGAACTTCTAGTC
CD19c	AACCAGTCAACACCCTTCC
CD19d	CCAGACTAGATACAGACCAG
CD21 Cre rev	GAACCTCATCACTCGTCGTTGCAT C
CD21 NDE	TCTGGC ATACTTATTCCCTGAAG
CD40 PCR3	CTGAGATGCGACTCTCTTTGCCAT
Cre 7	TCAGCTACACCAGAGACGG
Ex1Fw1 LMP1	AGGAGCCCTCCTTGTCCTCTA
Notch2IC 18 seq	ATCTACCTGCAGGGGTCATC
Notch2IC 21 seq	GGGATGTGATCATGGGAGAG
Notch2IC 22 seq	TCTTGACTTCTGCGCTCTCA
Notch2IC 25 rev (T)	ATCCCGGTCTCCGTATAGTG
Notch2IC 33 fw (T)	CCCTTGCCCTCTATGTACCA
Mb1-Cre P54	GGAGATGTCCTTCACTCTGATTCT
Mb1-Cre P55	ACCTCTGATGAAGTCAGGAAG AAC
Rosa fw1 (60)	CTCTCCCAAAGTCGCTCTG
Rosa rev2 (62)	TACTCCGAGGCGGATCACAAGC
TV fw 3	GTCCAGGGTTTCCTTGATGA
TV fw 4	TGACGTCAATGGGTGGAGTA
TV fw 5	GCTAACCATGTTCATGCCTTC
TV fw 6	ATGCGATGTTTCGCTTGGT
TV fw 7	TAAAGTCGACTCGGGGACAC
TV fw 8	TGCCATCTAGTGATGATGAGG
TV fw 9	CGCCATCATGCCTACATTCT
TV fw 10	ACTCCTGGAGGTGGTGGAG
TV fw 11	GGACGTGGTTTTCCTTTGAA
TV fw 12	GAGGAGTCGGAGAAATGATGA

II) Primers for qPCR

Transcript	Primer sequence (5´ to 3´)
Bcl2l1 seq	GTAAACTGGGGTCGCATTGT
Bcl2l1 rev	TGTCTGGTCATTTCCGACTG
Bfl-1 seq	CCGTAGACACTGCCAGAACA
Bfl-1 rev	AAAATTAGGCCGGTTTCACA
Birc5 seq	GGACCACCGCATCTCTACAT
Birc5 rev	TCTCCGCAGTTTCCTCAAAT
Casp1 seq	TTTGAAGGACAAACCGAAGG
Casp1 rev	CATCTGGCTGCTCAAATGAA

CD21 seq	AGATCCTAAGAGGCCGAATGG
CD21 rev	CACATAGCCAGGGTTACAGC
Cdk2 seq	TCCTCCACCGAGACCTTAAA
Cdk2 rev	CATCCTGGAAGAAAGGGTGA
Cdk4 seq	CCGAAGTTCTTCTGCAGTCC
Cdk4 rev	AGGCAGAGATTCGCTTGTGT
Cdk6 seq	TGTTTCAGCTTCTCCGAGGT
Cdk6 rev	TCTCCTGGGAGTCCAATCAC
c-Myc seq	CTTGTACCTGCAGGATCTGA
c-Myc rev	AGTTGTGCTGATGTGTGGAG
CyclinA2 seq	CCTGCAAACTGCAAAGTTGA
CyclinA2 rev	CTCTGGTGGGTTGAGGAGAG
CyclinE1 seq	CAGATTGCAGAGCTGTTGGA
CyclinE1 rev	GGGGAGAGGAGAAGCCCTAT
CyclinE2 seq	TACTGACTGCTGCTGCCTTG
CyclinE2 rev	CCTGGTGGTTTTTCAGTGCT
CyclinD1 seq	CTTCAAATGTGTGCAGAAGG
CyclinD1 rev	GCATTTTGGAGAGGAAGTGT
CyclinD2 seq	CATTTACACCGACAACTCCA
CyclinD2 rev	CACGTCTGTGTTGGTGATC
CyclinD3 seq	TGACCATCGAAAAACTGTGC
CyclinD3 rev	AGCTTCGATCTGCTCCTGAC
Deltex1 seq	GCCATCTACGGGGAGAAGA
Deltex1 rev	AGCCAGCACGTTGTCTAGGT
G1toS seq	CCCAGGTGAAAACCTCAAAA
G1toS rev	AAGGTGAAACGACCCATCTG
Hes1 seq	GAAAAGACGAAGAGCAAGAATAA
Hes1 rev	ATTGATCTGGGTCATGCAGT
Hey1 seq	GCTAGAAAAAGCCGAGATCC
Hey1 rev	CGGGTGATGTCCGAAGAC
Igμ seq	GAGGACACAGCCGTGTATTACTG
Igμ rev	CCGAATTCAGACGAGGGGGAAAAGGGTT
LMP1 seq	TGTTCATCACTGTGTCGTTGTCC
LMP1 rev	AGAAGAGACCTTCTCTGTCCACT
LMP2A seq	ATGACTCATCTCAACACATA
LMP2A rev	CATGTTAGGCAAATTGCAAA
PIK3R1 seq	TTGTGGCACAGACTTGATGTT
PIK3R1 rev	AAGCCATATTTCCCATCTCG
ribosomal protein L23a seq	CTCCTAAAGCTGAAGCCAAA
ribosomal protein L23a rev	GCCTGTTTAATCTGGTGCTT

III) Oligonucleotide used for cloning

Name	**Oligonucleotide sequence (5´ to 3´)**
Oligo 1 (puc18)	GGAAGCGGAAGAGCGGCGCGCCGTTTAAACTTGGCTCATTCTGAT CTACCTGCAGGGGGCGCGCCAAGCTTAAG

Oligonucleotides were synthesized by Metabion, Martinsried.

7.7 Enzymes

Restriction endonucleases were purchased from New England BioLabs and MBI Fermentas. Taq DNA polymerase was purchased from Invitrogen Life Technologies.

7.8 Antibodies

I) Antibodies for immunoblotting

Antigen	Manufacturer	Source	kDa	Dilution	Diluent
Akt	Cell Signaling	rabbit	60	1:1000	TBST, 5 % (w/v) BSA
pAkt (Ser)	Cell Signaling	rabbit	60	1:1000	TBST, 5 % (w/v) BSA
Bcl3	Santa Cruz	rabbit	60	1:500	TBST, 5 % (w/v) BSA
c-Rel	Santa Cruz	mouse	75	1:500	TBST, 5 % (w/v) BSA
Deltex1	Santa Cruz	rabbit	67	1:1000	TBST, 5 % (w/v) BSA
Erk	Cell Signaling	rabbit	42, 44	1:1000	TBST, 5 % (w/v) BSA
pErk	Cell Signaling	rabbit	42, 44	1:1000	TBST, 5 % (w/v) BSA
Hes1	Santa Cruz	rabbit	34	1:1000	TBST, 5 % (w/v) BSA
IκBα	Santa Cruz	rabbit	40	1:1000	TBST, 5 % (w/v) BSA
pIκBα	Cell Signaling	mouse	40	1:1000	TBST, 5 % (w/v) milk powder
Jnk	Cell Signaling	rabbit	46, 54	1:1000	TBST, 5 % (w/v) BSA
pJnk	Cell Signaling	rabbit	46, 54	1:1000	TBST, 5 % (w/v) BSA
c-Myc	Cell Signaling	rabbit	64	1:1000	TBST, 5 % (w/v) BSA
c-Myc (h)	Santa Cruz	rabbit	64, 67	1:2000	TBS, 5 % (w/v) milk powder
p50p105	Santa Cruz	goat	50, 100	1:500	TBST, 5 % (w/v) BSA
p52p100	Cell Signaling	rabbit	52, 100	1:1000	TBST, 5 % (w/v) BSA
p65	Santa Cruz	rabbit	65	1:1000	TBST, 5 % (w/v) BSA
PI3K p55	Upstate	rabbit	55	1:2000	PBS, 3 % (w/v) milk powder
RelB	Cell Signaling	rabbit	70	1:1000	TBST, 5 % (w/v) BSA
Tubulin	Cell Signaling	mouse	55	1:1000	TBST, 5 % (w/v) BSA

The hybridoma for the Notch2 antibody (C651.6DbHN), developed by Dr. Artavanis-Tsakonas, was obtained from the Developmental Studies Hybridoma Bank (University of Iowa) and was diluted in TBS, containing 5 % (w/v) milk powder.

II) Antibodies for immunohistochemistry

Antigen	Source	Coupled to	Dilution	Manufacturer
Human CD2	Rat	Biotin	1:50	BD Bioscience
Mouse CD3	Dog		1:2	By courtesy of E. Kremmer
Mouse IgM	Goat	Peroxidase	1:100	Sigma
Mouse MOMA-1	Rat		1:100	Biomedicals
PNA	Rat	Biotin	1:2000	Vector
Rat IgG2	Mouse	Biotin	1:250	Jackson Laboratories

7.9 Software

Adobe Illustrator CS3

Adobe Photoshop CS3

Basic Local Alignment Search Tool (BLAST)

Clone Manager 9

CELLQuest Becton Dickinson

Endnote 9

Epson Scanner program

Microsoft Excel

Microsoft Word

OpenLab Improvision

Primer3

Roche LightCycler Software 3

8 Methods

8.1 Cell culture methods

8.1.1 Culture of EREB2.5 cells

Notch1IC/EREB, Notch2IC/EREB, and CAT/EREB cells (Kohlhof *et al.*, 2009) were grown in 1x RPMI (Gibco), supplemented with 10 % (v/v) heat-inactivated FCS (Biochrom KG), 1 % (v/v) L-glutamine, 1 % (v/v) sodium pyruvate, 1 % (v/v) penicillin-streptomycin (all purchased from Gibco), 75 µg/ml hygromycin (Invitrogen), and 1 µM 1.2-estrogen (Sigma). In general, EREB2.5 cells were centrifuged at 300 x g for 10 minutes. In order to deprive estrogen, cells were washed three times in cold 1x RPMI, 10 % (v/v) FCS. Between the second and the third washing step, cells were incubated in 1x RPMI, 10 % (v/v) FCS for 20 minutes at RT, to increase the efficiency of the estrogen removal. $4x10^5$ cells per ml were plated again in 1x RPMI, supplemented as described before, but not containing estrogen. In order to activate EBNA2 function, 1.2-estrogen was added to the culture medium in a concentration of 1 µM. Expression of Notch1/2IC and CAT was induced by adding 100 ng doxycycline per ml medium.

8.1.2 Preparation of embryonic fibroblasts

IDG2.3 ES cells (Hitz *et al.*, 2007) have to be cultured on a layer of embryonic fibroblasts (EF cells) to prevent differentiation. EF cells were dissected from pSV2neo, PEP-IL4 C57BL/6 embryos at day 13.5. Pregnant mice were killed by neck breaking and the belly was moistened with 70 % (v/v) ethanol before uteri were dissected. For washing, uteri were transferred twice to a new falcon tube containing sterile PBS. Uteri were subsequently placed on a Petri dish underneath a laminar front flow bench to dissect the embryos and to remove all membranes. Embryos were collected in a Petri dish containing PBS (Gibco) and heads were removed from the embryos by cutting straight above the arms. Each embryonic body was laid on its back in a new Petri dish placed under a stereomicroscope (Nikon) to remove all internal organs. Carcasses were collected in a 50 ml falcon tube containing PBS while continuing with the other embryos. Around 25 carcasses were washed in 35 ml PBS three times to remove the blood as efficient as possible. After sucking off the PBS, carcasses were transferred to a Petri dish placed on ice and were minced with a scalpel not longer than five minutes. Minced bodies were collected in 10 ml trypsin (Gibco) containing 0.2 mg/ml DNAse I (Invitrogen) and were incubated for 15 minutes at 37 °C. Meanwhile, a sterile mesh was washed once with trypsin and placed on an Erlenmeyer flask. Embryos were subsequently placed on the mesh and pressed through using a syringe plunger. To flush remaining clumps from the mesh, trypsin was continuously added during the

procedure (50 ml in total). In case the solution had become too viscous due to released DNA, more DNAse I in a concentration of 10 mg/ml was added (200 to 600 µl). Off note, total trypsin treatment should not exceed 30 minutes. The suspension was carefully decanted in four falcon tubes each containing 25 ml DMEM (Gibco) and was spun down at 250 x g at RT for five minutes. The cell pellet was washed twice in medium. If the pellet was too viscous, another 500 µl DNAse I were added and the pellet was incubated for 30 minutes at RT. Finally, cells were resuspended in 10 ml EF cell medium (see 8.1.3) and were counted using Trypan blue. $3x10^7$ cells can be expected per 10 embryos. $5x10^6$ cells were plated per 15 cm dish and were cultured over night. The next day, the medium was changed to remove all cell debris. When cells had grown to 80 % confluence after two to three days, cells were brought in suspension by trypsin treatment and $5x10^6$ cells were frozen per vial. At that point, cells are referred to as "F0".

8.1.3 Culture of embryonic fibroblasts

EF cells were cultured until the third passage ("FIII") in DMEM containing 10 % (v/v) heat-inactivated FCS (Biochrom KG), 1 % (v/v) L-glutamine, and 1 % (v/v) non-essential amino acids (both purchased from Gibco). One vial EF cells was plated on five 10 cm dishes after thawing and EF cells were split in a ratio of 1:5 every three to four days. For culture with ES cells, EF cells were mitotically inactivated by incubation with Mitomycin C (Sigma), a *Streptomyces caespitosus*-derived cell toxin. Adherently grown EF cells were washed once with PBS, incubated with 10 µg/ml Mitomycin C for three hours at 37 °C, and washed again three times with PBS. EF cells were subsequently brought in suspension by incubation with 1x trypsin (Gibco) at 37 °C for five minutes before the reaction was stopped by adding two volumes of FCS-containing medium. A single cell suspension was obtained by cautiously pipetting the cells up and down. Cells were subsequently centrifuged, counted, and plated on freshly gelatinized plates (15 minutes incubation with 0.1 % (v/v) gelatin PBS solution) in an average density of $1.5x10^6$ cells per 10 cm dish. ES cells were seeded on the EF cell layer after 12 hours.

8.1.4 Culture of embryonic stem cells (ES cells)

IDG2.3 ES cells were cultured on a layer of Mitomycin C treated EF cells in DMEM (Gibco) containing 15 % (v/v) ES cell-tested FCS (PAN Biotech), 2 % HEPES, 1.5 % (v/v) L-glutamine, 1 % (v/v) sodium pyruvate, 1 % (v/v) non-essential amino acids, and 50 mM β-mercaptoethanol (all purchased from Gibco). 0.1 % (v/v) LIF (Leukemia inhibitory factor, Chemicon International) was added freshly to prevent ES cell differentiation. Medium was changed every day and the culture was split every other day. In general, ES cells were centrifuged at 250 x g for five minutes. As ES cells grow in adherent colonies on the EF cell layer, trypsinization was

required for passaging. For that purpose, cells were rinsed once with PBS and subsequently incubated with half the volume of culture medium of 1x trypsin, supplemented with 1 % (v/v) chicken serum (Gibco) for 10 minutes at 37 °C before the reaction was stopped by adding two volumes of serum-containing culture medium. Single cells were obtained by pipetting the suspension up and down 10 times. Cells were subsequently centrifuged, counted, and plated on an EF cell layer in the appropriate density (in general $7.5x10^5$ cells per 10 cm dish).

8.1.5 Freezing and thawing of cells

For freezing, 500 µl cell suspension containing $1x10^6$ ES or EF cells and $5x10^6$ EREB2.5 cells, respectively were pipetted to a cryovial tube (Nunc) before adding 500 µl 2x freezing medium, containing 50 % (v/v) respective FCS, 30 % respective culture medium, and 20 % (v/v) DMSO (Sigma). Vials were immediately placed in a pre-chilled freezing box (Nalgene), filled with isopropyl alcohol to allow slow freezing of the cells in a rate of -1 °C per minute in a -80 °C freezer. After two days, vials were transferred to liquid nitrogen (-196 °C) for long-term storage. In order to thaw frozen cells quickly, cryovial tubes were placed at 37 °C until the still frozen, major part of cells could be mixed with 1 ml pre-warmed medium. After washing cells in 10 volumes of culture medium to remove DMSO, cells were plated immediately in fresh culture medium.

8.1.6 Transfection of ES cells

ES cells were either stably transfected to establish ES cell clones carrying the *notch2IC* transgene within their genome or were transiently transfected for transgene expression analysis. In both cases, ES cells were grown to a density of $5x10^6$ to $1x10^7$ cells per 10 cm dish and the culture medium was changed three hours before transfection to obtain highly proliferating cells. ES cells were then trypsin-treated as described above, washed once with PBS, and resuspended in transfection medium (RPMI w/o phenol red, PAA). $7x10^6$ ES cells in 700 µl transfection medium were transfected with 20 µg of linearized plasmid DNA in case of stable transfection or of circular plasmid DNA in case of transient transfection. DNA resolved in 100 µl transfection medium was pipetted to a transfection cuvette (Gene Pulser cuvette, 0.4 cm electrode, Bio-Rad), and subsequently cells were added. Cells and DNA were incubated for 10 to 20 minutes on ice before transfection was performed with an electroporator (Gene Pulser, Bio-Rad) at 230 V, 500 µF. After the pulse, cells were left at RT for 10 minutes. $7x10^6$ transfected ES cells were diluted in 40 ml culture medium and then plated on four 10 cm dishes. Cells were plated on an EF cell layer in case of stable transfection and on gelatin in case of transient transfection.

In case of stable transfection, $1x10^5$ non-transfected cells were plated as control on a 10 cm dish on an EF cell layer to be treated later with G418 (Gibco) containing medium, in order to monitor cell death due to the G418 treatment. As further controls, $1x10^3$ transfected and non-transfected cells were plated each on gelatinized 6 cm plates with normal medium to determine the cell loss due to the transfection.

8.1.7 Selection and expansion of stably transfected ES cell clones

After stable transfection with the targeting vector DCR26CAGp-IRESCD2-Notch2IC, ES cells were grown in normal culture medium for 24 hours. Subsequently, the medium was replaced by G418 selection medium (culture medium with 140 µg active G418 per ml medium). The used targeting construct contains a neomycin-geneticin-resistance gene, mediating resistance against G418. The amino-glycoside antibiotics G418 is toxic for eukaryotic cells besides other, since it blocks protein biosynthesis. Therefore, only cells that have successfully integrated parts of the construct and have thus acquired geneticin-resistance can grow in G418 selection medium. The selection medium was renewed every day and the G418 concentration was increased in the beginning every day by 10 µg/ml up to 170 µg/ml medium. After seven days, non-recombined cells had died as controlled by the non-transfected cells treated with G418, and thus selection had occurred. At that day, colonies appeared to be nicely formed as well as appropriate for picking and transferring to 96-well plates. The medium was exchanged by PBS and colonies were picked with a 200 µl tip in a laminar front flow under a stereomicroscope (Nikon) and were transferred in 25 µl PBS to a 96-well plate (round bottom). To each well containing a colony, 50 µl trypsin were added and the plate was incubated at 37 °C for 10 minutes. 50 µl G418 selection medium were added to stop the reaction and single cells were obtained by pipetting up and down 10 times. The cell suspensions were then transferred to a 96-well plate (flat bottom) containing a Mitomycin C-treated EF cell layer and 100 µl G418 selection medium. Cells were cultured for two or three days, with medium change each day, before splitting to three 96-well plates. Two of these plates contained EF cells to expand the ES cell clones for freezing and later injection into blastocysts, whereas the other one was only gelatinized to expand the ES cell clones for DNA preparation and subsequent Southern blot analysis. The two 96-well plates containing ES cell clones on the EF cell layer were frozen one and two days, respectively after the splitting to obtain the optimal proliferation state of each clone. Plates were frozen after trypsinization, the addition of 50 µl ES cell freezing medium (20 % (v/v) DMSO, 80 % (v/v) FCS), and covering with 50 µl mineral oil (Sigma). The plates were wrapped into several layers of cellulose towels to allow slow freezing in a -80 °C freezer, where frozen ES cells can be stored up to two months. Two days after first passaging, cells on the 96-well plate for DNA preparation were split onto two

gelatinized plates, to have one backup. Cells were grown to full density for four to five days to receive enough cells for DNA extraction for Southern blot analysis.

8.1.8 Thawing and expansion of homologous recombined ES cell clones

ES cell clones showing homologous instead of random recombination were identified by Southern blot. To preserve these clones for long-term, the cells have to be thawed from the 96-well plate, expanded in culture, and frozen in cryovial tubes in liquid nitrogen at -196 °C. For that purpose, 96-well plates were thawed in a semi-sterile water bath of 37 °C and each positive clone was transferred without the covering oil to a 24-well, containing a mitotically inactive EF cell layer and 1 ml G418 selection medium. The medium was exchanged after eight hours to remove DMSO. After three days, cells were trypsin-treated and transferred to 6-well plates without centrifugation, and from there after two days to a 10 cm plate by the same procedure. When cells had been properly growing on a 10 cm dish, cells from one plate were frozen in four cryovial tubes for long-term storage. G418 selection medium was used until one passage before blastocyst injection.

8.1.9 Induction of transgene expression in transiently transfected ES cell clones

Correctly targeted ES cell clones were chosen for testing transgene expression. For this purpose, cells were transfected with the *Cre* expression plasmid pGK-Cre-bpA, encoding *Cre* recombinase to delete the loxP sites-flanked STOP cassette upstream of the *notch2IC-IRES-hCD2* transgene and to allow its expression. Cells were cultivated in medium containing 1 % (v/v) penicillin-streptomycin. As control, non-transfected ES cells were grown to monitor leaky expression. The next day, the medium was changed. After 48 hours, cells were brought in suspension by the same procedure as trypsinization, but using versene (Gibco) instead, to protect surface expression of the hCD2 molecule. hCD2 expression was analyzed by flow cytometry after staining cells with a hCD2-specific antibody.

8.1.10 Preparation of stably transfected ES cell clones for blastocyst injection

After verification of correctly integrated *notch2IC* cDNA by Southern blot and testing for transgene expression, three clones were chosen for injection into blastocysts. For this purpose, cells were thawed and cultured on Mitomycin C-treated EF cells. From now on, normal culture medium without G418 was used. Medium was renewed every day and cells were trypsinized for passaging two or three days after thawing. After 36 hours, cells displayed a highly proliferative state. Thus, cells were trypsin-treated again, resuspended in culture medium, and subsequently injected into blastocysts (in cooperation with the Institute of Developmental Genetics at the

Helmholtz Center Munich). Blastocysts were derived from pregnant C57BL/6 mice to obtain visible chimerism in the offspring. IDG2.3 ES cells are F1 chimeras out of black C57BL/6 and brown 129/SV mice, and thus give rise to mice with a coat color mixed out of black and brown. Therefore, chimeras can be identified by the occurrence of brown coat on the black C57BL/6 background.

8.2 Mice-associated methods

8.2.1 Mouse breeding

Mice carrying the *notch2IC*^{flSTOP} allele were crossed to the CD19-*Cre* mouse strain (on a C57BL/6 background) to generate mice expressing the transgene from the pro-B cell stage with a gradual increase in *Cre*-mediated recombination during proceeding B cell differentiation (Rickert *et al.*, 1997) (Notch2IC//CD19Cre$^{+/-}$). Notch2IC//CD19Cre$^{+/+}$ mice were generated by crossing Notch2IC//CD19Cre$^{+/-}$ and CD19-*Cre* (C57BL/6) mice. Notch2IC^{flSTOP} mice were crossed to the mb1-*Cre* mouse strain (on a C57BL/6 background) to generate mice expressing Notch2IC from the early pro-B cell stage in the bone marrow (Notch2IC//mb1Cre$^{+/-}$). LMP1/CD40//Igβ$^{fl(GFP)/\Delta c}$//CD21Cre (referred to as LMP1/CD40//Igβ$^{\Delta GFP/\Delta}$) mice were generated by crossing LMP1/CD40^{flSTOP} (Balb/C), Igβ$^{fl(GFP)/\Delta c}$ (C57BL/6), and CD21-*Cre* (C57BL/6) mice (Kraus *et al.*, 2004).

Consequently, analyses were performed on a mixed background. Mice were analyzed at eight to 16 weeks of age, unless otherwise stated. Mice that were monitored for the development of lymphomas or leukemic disease were kept under special observation. All mice were bred and maintained in specific pathogen-free conditions. All experiments were performed in compliance with the German animal welfare law and have been approved by the Institutional Committee on Animal Experimentation and the government of Upper Bavaria.

8.2.2 Isolation of primary lymphocytes

Mice were euthanized by CO_2 gassing for five minutes and were subsequently dissected. Peritoneal cells were harvested by rinsing the peritoneal cavity with B cell medium (1x RPMI 1640 (Gibco), containing 5 % (v/v) heat-inactivated FCS (Biochrom KG), 1 % (v/v) penicillin-streptomycin, 1 % (v/v) sodium pyruvate, 1 % (v/v) L-glutamine, and 50 mM β-mercaptoethanol (all purchased from Gibco)) and draining it with a syringe. Spleen, thymus, and lymph nodes were taken out as whole organs and were maintained in medium until further procedures. To isolate cells from the bone marrow, tibia bones were dissected and cut and the cavity was rinsed with medium. To receive single cell suspensions, tissues were passed through a capillary cell strainer

(Becton Dickinson). Single cell suspensions from spleen and bone marrow were depleted from erythrocytes by lysis with a hypotonic buffer (1 part of 170 mM Tris/HCl, pH 7.65, 9 parts of 155 mM NH_4Cl) for three minutes. Cells were kept on ice during the entire procedures and were generally centrifuged for 10 minutes at 300 x g at 4 °C.

Isolation of splenic B cells was performed by depletion of $CD43^+$ non-B cells by magnetic cell separation (MACS), using α-CD43 beads and LS columns according to the manufacturer's specifications (Miltenyi Biotec). This resulted in a purity of 85 to 95 % B cells.

For Western blot analyses, splenic cells were maintained from the beginning in B cell medium containing only 1 % (v/v) FCS.

8.2.3 Flow Cytometry (FACS)

Single cell suspension prepared from various lymphoid organs were surface-stained with a combination of FITC-, PE-, PerCP- and APC-conjugated monoclonal antibodies, diluted in FACS buffer. Antibodies specific for AA4.1, B220, CD1d, CD2 (human), CD3, CD5, CD9, CD19, CD21, CD23, CD25, CD36, CD43, CD80, CD86, CD95, ICAM-1, IgD, IgM, and MHCII were purchased from BD Biosciences. The monoclonal antibody to Thy1.2 was kindly provided by J. Mysliwietz. Data were analyzed from $3x10^4$ viable, lymphocyte-gated cells as determined from forward and side scatter as well as TOPRO-3 or propidium iodide (PI) staining (both Molecular Probes). TOPRO-3 and PI are intercalating fluorescent dyes that bind DNA and thus only stain dead cells that are permeable for the dye to diffuse into the nucleus. All analyses were performed with a FACSCalibur™ flow cytometer (BD Biosciences) and results were analyzed using CELLQuest software.

8.2.4 *In vitro* culture of primary lymphocytes

Splenic, MACS-purified B cells were cultured in B cell medium with 10 % (v/v) FCS with or without stimuli up to five days in 96-well plates ($5x10^5$ cells/well). Stimuli included lipopolysaccharide (10 to 25 μg/ml; E. coli 055:B5; Sigma), IL4 (10 ng/ml; mouse recombinant; Sigma), α-CD40 antibody (2.5 μg/ml; eBioscience (HM40-3)), and anti-IgM $F(ab')_2$ (5 μg/ml, AffiniPure $F(ab')_2$ goat α-mouse IgM, μ-chain, Dianova). At different time points, cells were surface-stained with various antibodies and were analyzed or counted with a FACSCalibur™. The percentage of living cells was determined by staining and excluding dead cells by TOPRO-3 or PI that binds to DNA. For proliferation assays, splenic B cells ($5x10^6$ cells/ml) were labeled for five minutes by incubation in serum-free B cell medium containing 5-(and 6)-carboxyfluorescein diacetate N-succinimidyl ester (CFSE, Molecular Probes, final concentration 5 μM) at 37 °C. CFSE binds to proteins on the inner cell membrane and is consequently transferred equally to

each daughter cell upon cell division, leading to declining fluorescence intensity. CFSE-labeled cells were cultured for up to five days in 96-well plates ($5x10^5$ cells/well) in 200 µl B cell medium per well with 10 % (v/v) FCS and were analyzed by flow cytometry every day.
For Western blot analyses, MACS-purified B cells were left untreated for one hour in B cell medium with 1 % (v/v) FCS at 37 °C before proteins were isolated.

8.2.5 *In vivo* 5-bromo-2′-deoxyuridine (BrdU) assay

Mice were fed with 0.8 mg/ml BrdU (Sigma) in the drinking water for 14 days, while the water was exchanged every three to four days. Mice were maintained up to day 70 after the start of the BrdU feeding. Mice were analyzed at day 14, 42, and 70 during the assay. Thereby, the spleen was dissected and splenocytes were isolated as described above. BrdU incorporation into the DNA of splenic B cells was analyzed by using the APC BrdU Flow Kit (BD Biosciences) according to manufacturer's instructions.

8.2.6 Immunization of mice

Mice at the age of eight to 12 weeks were immunized with 50 µg NP-Lipopolysaccharide (LPS), 50 µg NP-Ficoll, or 100 µg NP-chicken gamma globulin (CGG) (4-hydroxy-3-nitrophenylacetyl hapten, all Biosearch Technologies). The latter was precipitated by potassium aluminum sulfate to enhance the immune response in mice. For precipitation, one volume of antigen was mixed with one volume of 10 % (w/v) $KAl(SO_4)_2$ and the pH was adjusted to pH 6.5 with 1 N NaOH. After 30 minutes incubation on ice, the antigen was centrifuged for 10 minutes at 2.300 x g and washed three times in sterile PBS. NP-LPS and NP-Ficoll antigen stocks were quickly centrifuged before usage and the supernatant was transferred to a new tube to remove any precipitation. Finally, 50 µg of each antigen were resuspended in 200 µl sterile PBS for intraperitoneal injection.

8.2.7 Enzyme-linked immunosorbent assay (ELISA)

To determine the serum concentration of secreted antibodies that offer a certain antigen specificity and/or are from a certain immunoglobulin isotype, the serum was collected and an ELISA was performed.

8.2.7.1 Preparation of serum from murine blood

Before and seven days after immunization, blood was collected from mice from the caudal vein using a glass capillary. Dissecting the mice seven or 14 days after immunization or in a regular analysis without immunization, blood was collected directly from the heart. Afterwards, the blood was incubated on ice for at least three hours and was subsequently centrifuged at 9.000 x g

and 4 °C for 10 minutes. The supernatant was transferred to a new tube and the procedure was repeated once to guarantee pure serum.

8.2.7.2 Detection of specific standard immunoglobulin titers

Maxisorb 96-well plates (Nunc) were coated over night at 4 °C with 5 µg/ml of immunoglobulin isotype-specific rat α-mouse antibodies (depending on the isotype: IgM, II/41; IgG1, A85-3; IgG2a, R11-8; IgG2b, R9-91; IgG3, R2-38; IgA, C11-3, all from BD Bioscience), diluted in 0.1 M $NaHCO_3$ (pH 9.2). All the following procedures were performed at RT. Wells were blocked with PBS, 1 % (w/v) milk powder solution for 30 minutes. Subsequently, different dilutions of serum were applied to the wells and were incubated for one hour, then incubated one hour with biotin-conjugated secondary antibodies specific for the different antibody isotypes (depending on the isotype: IgM-Bio, R6-60.2; IgG1-Bio, A85-1; IgG2a-Bio, R19-15; IgG2b-Bio, R12-3; IgG3-Bio, R40-82; IgA-Bio, C10-1, all from BD Bioscience), followed by a 30 minutes incubation with streptavidin-coupled alkaline phosphatase (SA-AP), diluted in 0.1 M $NaHCO_3$ (pH 9.2) (1:2000). The amount of bound SA-AP was detected by incubation with O-phenyldimine (Sigma) in 0.1 M citric acid buffer containing 0.015 % (v/v) H_2O_2 that serves as substrate for the reaction. Following each incubation step, plates were washed three times with PBS. The absorbance was determined at 405 nm, using a microplate reader (Photometer Sunrise RC, Tecan) and antibody concentrations were determined by comparing with isotype-specific standards (IgM, G155-228; IgG1, MOPC-31-C; IgG2a, G155-178; IgG2b, MPC-11; IgG3, A112-3; IgA, M18-254).

8.2.7.3 Detection of NP-specific immunoglobulin titers

α-NP immunoglobulin titers of the different isotypes were determined by ELISA with the same procedure as described above, but using NP-BSA as capture antigen. Plates were coated with 5 µg/ml NP_{17}-BSA or NP_3-BSA (both Biosearch Technologies) to detect low and high affinity NP-specific IgG1 antibodies, respectively. After serum incubation, plates were subsequently incubated with the IgG1-specific rat α-mouse antibody A85-3 (BD Bioscience). To detect NP-specific antibodies of the different isotypes, plates were coated with 5 µg/ml NP_{17}-BSA and were incubated with the different immunoglobulin isotype-specific rat α-mouse antibodies (see above) after serum incubation.

8.2.8 Immunohistochemistry

Spleens were embedded in O.C.T. Tissue Tek (Sakura) and were frozen in liquid nitrogen for some seconds. Embedded organs were stored at -20 °C, wrapped in aluminum foil to avoid air contact. Sections of 4 to 8 µm in thickness were cut, using a cryostat (Leica Microsystems) and

were air-dried over night. Sections were fixed for five minutes in 100 % (v/v) acetone. Subsequently, sections were dried again at RT and stored at -20 °C wrapped in aluminum foil until analysis. For immunohistochemistry, sections were thawed 30 minutes at RT, washed with PBS, and incubated for 20 minutes in quenching buffer (PBS containing 10 % (v/v) goat serum, 0.1 % (v/v) H_2O_2, 1 % (w/v) BSA) to block non-specific binding sites. Afterwards, sections were incubated for each 15 minutes in two different blocking buffers (Avidin/Biotin Blocking Kit; Vector Laboratories). Between procedures for blocking, sections were washed for five minutes in PBS, whereas before and after labeling procedures, sections were washed with PBS each three times for five minutes. Subsequently, labeling was performed by incubating sections with different antibodies and streptavidin-conjugated Phosphatase (Sigma), diluted 1:400 in PBS, each for one hour.

Antibodies conjugated to streptavidin were detected in blue using Blue Alkaline Phosphatase Substrate Kit III (Vector laboratories). Antibodies conjugated to peroxidase were stained in red due to a reaction with 3-amino-9-ethylcarbazole (AEC) after treatment with Peroxidase Substrate Kit AEC (Vector laboratories). Staining reactions were stopped by washing with PBS. All incubation steps were performed at 22 °C in a wet chamber.

Sections were air-dried and subsequently embedded in gelatin before a coverslip was put on top. Slides were inspected using a fluorescent microscope (Zeiss). Pictures were obtained with a digital camera (RS Photometrics) and edited using Adobe Photoshop software.

8.3 Standard methods of molecular biology

8.3.1 DNA isolation

8.3.1.1 Plasmid isolation from bacteria and preparation for ES cell transfection

Plasmids were isolated from bacteria with the Jetstar Kit (Genomed) for cloning or with the endotoxin-free Qiagen Maxi Kit (Qiagen) for transfection into ES cells. The targeting plasmid was linearized with *SgfI* according to the manufacturer's protocol overnight at 37 °C and was purified by phenol-chloroform extraction. One volume of phenol-chloroform-isoamyl alcohol (ratio of components: 25:24:1, Roth) was added to the restriction mix and the tube was inverted. After centrifugation at 20.000 x g for five minutes, the upper phase containing genomic DNA was saved, one volume of chloroform-isoamyl alcohol (24:1) was added, and the tube was inverted. After the same centrifugation procedure, 1/10 volume 3 M NaAc and 2.5 volumes 100 % ethanol (v/v) were added to the upper phase and the tube was inverted each time. To precipitate DNA efficiently, the tube was kept at -20 °C for 30 minutes. DNA was then spun

down by high speed centrifugation for 20 minutes. The pellet was washed and at the same time, the tube was sterilized by filling it completely with 70 % (v/v) ethanol. DNA was stored in this way until the day of transfection. For usage, the tube was centrifuged as described before and the DNA pellet was air-dried underneath the ES cell laminar flow bench. The dried pellet was resolved in 100 µl transfection medium (RPMI w/o phenol red, PAA) by incubation at RT for one hour and its density was subsequently measured to determine DNA concentration.

8.3.1.2 Isolation of genomic DNA from ES cells

To isolate DNA from ES cells growing on a 96-well plate, cells were grown to 90 % confluence in medium without LIF, and were washed twice with PBS before cells were incubated with lysis buffer (10 mM Tris pH 7.5, 10 mM EDTA, 10 mM NaCl, 0.5 % (w/v) sarcosyl, 0.4 mg/ml proteinase K) at 56 °C overnight. During this procedure, the 96-well plate was wrapped into plastic foil and put into a wet chamber (Tupperware®) to prevent drying out. Following, the Tupper box was cooled down at RT for one hour. After eight minutes centrifugation at 400 x g, 100 µl 100 % (v/v) ethanol were added to each well to precipitate DNA. After incubation for one hour at RT and centrifugation as described above, the liquid was decanted and the DNA was washed with 150 µl of 70 % (v/v) ethanol three times before drying at RT up to one hour. 35 µl of the restriction buffer mix was directly added.

To isolate DNA from ES cells growing on a 10 cm dish, cells were brought in suspension when grown to approximately 90 % of confluence. Cells were portioned in three 2 ml Eppendorf tubes, pelletized, and stored at -20 °C until DNA extraction. Cells of one tube were lysed over night in 750 µl of abovementioned cell lysis buffer. 305 µl of a saturated (> 5 M) NaCl solution were added and the sample was centrifuged at 9.000 x g. The supernatant was transferred to a new reaction tube and the DNA was purified by phenol-chloroform extraction as described in 8.3.1.1. The DNA pellet was air-dried and resolved in TE buffer (10 mM Tris, pH 7.9, 1 mM EDTA) by shaking the tube for four hours at 37 °C.

8.3.1.3 Isolation of genomic DNA from murine tails

DNA from murine tails was isolated according to a slightly modified procedure derived from Laird (Laird *et al.*, 1991). A small piece of murine tail was incubated shaking over night at 56 °C in 500 µl lysis buffer (100 mM Tris/HCl pH 8, 5 mM EDTA, 0.2 % (w/v) SDS, 200 mM NaCl, 100 µg/ml proteinase K). 170 µl of a saturated (> 5 M) NaCl were added to precipitate proteins and the sample was centrifuged at 10.000 x g. The supernatant was transferred into a new tube and the DNA was precipitated by adding 600 µl 100 % (v/v) isopropyl alcohol and inverting the tube. Samples were centrifuged as described above. The DNA was washed once by adding 1 ml 70 %

(v/v) ethanol, air-dried afterwards, and ultimately dissolved in 100 µl TE by shaking for several hours at 37 °C.

8.3.2 DNA analysis

8.3.2.1 Polymerase Chain Reaction (PCR)

PCR (Saiki *et al.*, 1985; Saiki *et al.*, 1988) was applied to amplify *notch2IC* cDNA from the genomic DNA of targeted ES cells for sequencing or to detect specific regions in the DNA of transgenic mice for genotyping by analyzing their tail DNA. The following reaction mixture was used in different variations:

Reaction batch	**1x**
Taq (10x)/Phusion (5x) buffer	2.5/5 µl
$MgCl_2$ (50 mM)/$MgSO_4$ (25 mM)	1-2 µl
dNTP mixture (10 mM)	0.5 µl
Primer sense	0.1-0.25 µl
Primer antisense	0.1-0.25 µl
TaqPol (5 U/µl), Phusion (2 U/µl)	0.15-0.75 µl
DNA (about 5 ng)	1.5 µl
DMSO (100 %)	0.25 µl
H_2O	To 25 µl

Reaction cycle		
Starting temperature	94 °C	5’
Cyclic denaturation	94 °C	45”
Cyclic annealing	55-63 °C	45”
Cyclic elongation	72 °C	1-3’
Final elongation	72 °C	10’
# cycles	30-35	

8.3.2.2 Agarose gel electrophoresis of DNA

Agarose gel electrophoresis was performed according to Sambrook (2001), to determine the yield of a DNA isolation or PCR reaction, and to size-fractionate restriction-digested DNA molecules, which were then eluted from the gel. Gels contained 1x TAE (40 mM Tris/HCl, 20 mM acetic acid, 1 mM EDTA pH 8.5), 5 µg/ml ethidium bromide, and 0.8 to 2 % (w/v) agarose. Electrophoresis was performed in a gel electrophoresis chamber (Peqlab) with 1x TAE buffer at 80 to 100 V for one to two hours. Specific DNA fragments of interest were excised from the gel with a clean scalpel and DNA was isolated using QIAquick Gel Extraction Kit (Qiagen) according to manufacturer’s suggestions.

8.3.2.3 Sequencing

DNA fragments were sequenced by Sequiserve, Vaterstetten, Germany, utilizing the chain termination method according to Sanger (Sanger *et al.*, 1977) slightly modified.

8.3.2.4 Restriction digest of DNA

Restriction digest of plasmid DNA was accomplished using specific restriction enzymes according to manufacturer’s recommendations for reaction conditions and buffers.

Genomic DNA from ES cells was restricted by specific enzymes for the subsequent performance of Southern blotting. An efficient restriction buffer mix, containing 1 mM Spermidin, 1 mM DTT, 100 µg/ml BSA, 50 µg/ml RNase, respective 1x buffer, and 100 to 150 U of the respective enzyme, was either added directly to undissolved ES cell DNA (96-well) or to DNA from ES cells dissolved in TE buffer. DNA was digested for 16 hour at 37 °C.

8.3.3 Southern blotting (Southern *et al.*, 1997)

This method was used for the identification of homologous recombined ES cell clones. Thereby, electrophoretically separated DNA is transferred from the agarose gel to a nitrocellulose membrane, and the hybridization of a radioactively labeled DNA probe to the denatured DNA on the membrane allows the detection of specific DNA fragments as definite bands on the membrane.

After digestion as described in 8.3.2.4, the samples were electrophoretically separated on a 0.8 % (w/v) agarose gel together with a standard 1 kb DNA ladder (Invitrogen) and a λ DNA-Mono Cut Mix ladder (1.5 to 48.5 kb fragments, New England Biolabs) overnight. Having recorded the separated DNA in the gel on a UV luminescent screen together with a ruler, the gel was incubated in 0.25 N HCl for 25 minutes to denature and fragment the DNA. To equilibrate the gel for the following DNA transfer, the gel was shortly rinsed in water and subsequently incubated for 40 minutes in alkaline transfer buffer (0.4 M NaOH, 0.6 M NaCl). Afterwards, the DNA was blotted from the gel to a nylon membrane (Immobilon™ Ny+ membrane, Millipore) over night from top to bottom by capillary pressure of the transfer buffer. After transfer, the slots of the gel were marked on the membrane and the membrane was rinsed shortly in 2x SSC (0.3 M NaCl, 0.03 M NaCitrate, pH 6.5) for neutralization. Then, DNA was cross-linked to the membrane by baking for one hour at 80 °C. In order to prevent unspecific binding, the membrane was pre-hybridized in pre-heated hybridization solution (1 M NaCl, 50 mM Tris, pH 7.5, 10 % (w/v) dextran sulfate, 1 % (w/v) SDS, 250 µg salmon sperm DNA/ml) for at least six hours at 65 °C, before incubation with the radioactively labeled probe.

Applying Random Prime Labeling Kit (GE Healthcare) according to manufacturer's instructions, 100 ng DNA probe were labeled with 50 µCi α32-dCTP (Hartmann Analytic). Subsequently, the labeled probe fraction was purified using a G50 sephadex column (GE Healthcare) according to manufacturer's specifications. For denaturation, the probe was incubated for five minutes at 100 °C and was quenched for two minutes on ice. The membrane was incubated for another 16 hours at 65 °C in the hybridization solution, containing pre-hybridization buffer with labeled probe.

Afterwards, the membrane was rinsed three times each for 10 minutes in pre-heated washing buffer (0.2x SSC, 0.5 % (w/v) SDS) at 58 °C to wash off unbound probe. Washing was stopped when radioactivity reached 30 counts. Radioactivity was visualized by autoradiography, using radiosensitive films (Biomax MS PE Applied Biosystems 35x43 cm, KODAK), exposed for one day at -80 °C in a Biomax cassette.

8.3.4 Cloning

Cloning of the DCR26CAGp-IRESCD2-Notch2IC vector was performed as follows: To obtain suitable restriction sites, the multiple cloning site of the puc18 vector was exchanged with a fragment containing *SapI – AscI – SbfI – AscI – HindIII* restriction sites (puc18_Oligo1). The *notch2IC* cDNA, corresponding to cDNA 5253 to 7583 (NCBI NM_010928) and thus encoding the full length murine *notch2IC* cDNA, was isolated from vector pHprt_Notch2IC by *SbfI* restriction and was then sub-cloned into the puc18 vector (puc18_Oligo1_Notch2IC). The *notch2IC* cDNA was then inserted into the DCR26CAGp-IRESCD2 targeting vector by *AscI* restriction of puc18_Oligo1_Notch2IC and DCR26CAGp-IRESCD2 (DCR26CAGp-IRESCD2-Notch2IC). After plasmid propagation and isolation, the sequence integrity of important elements of this vector, including the CAGGS promoter, the loxP sites, the STOP cassette with neomycin-resistance gene, and the sequence encoding *notch2IC-IRES-hCD2* was verified by sequencing. The targeting vector was linearized by *SgfI* digest for transfection into ES cells.

8.3.5 RNA analysis

8.3.5.1 Resolving of RNA

Total RNA that had been isolated before using TRIzol reagent according to manufacturer's specifications (Invitrogen), and had been stored precipitated in 100 % (v/v) isopropyl alcohol at -80 °C was pelletized by centrifugation at 12.000 x g for eight minutes at 4 °C. Having washed the RNA pellet with 75 % (v/v) ethanol, it was briefly air-dried and the RNA was dissolved in 15 µl DEPC-H_2O by passing the solution a few times through a pipette tip and incubating for 15 minutes at 55 to 60 °C.

To employ a definite amount of total RNA for cDNA synthesis, 2 µl RNA were diluted in 198 µl DEPC-H_2O in a mini-cuvette (UVette, Eppendorf) and its absorbance at 260 nm was determined, using a Bio-Photometer (Eppendorf) to calculate RNA concentration. Additionally, the ratio of the readings at 260 nm and 280 nm (OD_{260}/ OD_{280}) provides an estimation of the purity of the RNA preparation, with respect to contaminants that absorb UV, such as proteins. Pure RNA has an OD_{260}/OD_{280} ratio of > 1.95.

8.3.5.2 cDNA synthesis

RNA can be reversely transcribed into a single-stranded DNA intermediate, called copy or complementary DNA (cDNA). Using oligo-dT primers, reverse transcriptase synthesizes the new cDNA strand starting at the 3´-end of the poly(A)-mRNA. 1 µg total RNA was reversely transcribed with > 10 U of viral AMV Reverse Transkriptase, using 1st Strand cDNA Synthesis Kit for RT-PCR [AMV] (Roche Diagnostics) with 0.02 A_{260} units (0.8 µg) Oligo-p$(dT)_{15}$ primers according to manufacturer's instructions, whereas each reaction was performed in a final volume of 10 µl. The resulting first strand cDNA was stored at -20 °C and was used as a template for qPCR.

8.3.5.3 Quantitative real-time PCR (qPCR)

Principle

The technique of quantitative real-time PCR (qPCR) allows studying mRNA expression in a comparative manner and can be performed using the LightCycler system (Roche Diagnostics). Within the LightCycler instrument, a fluorescence-coupled PCR, working with FastStart Taq polymerase and SYBR green fluorescent dye, occurs in special glass capillaries and is monitored on-line by the instrument by means of fluorescence detection. SYBR green intercalates specifically into the minor groove of double-stranded DNA (Morrison *et al.*, 1998). Whereas the unbound dye exhibits very little fluorescence, fluorescence is dramatically increased upon DNA binding. Therefore, the intensity of the fluorescence signal is directly proportional to the amount of double-stranded DNA generated by PCR. The fluorescence is measured at the end of each elongation phase, what allows monitoring the increase in the amount of amplified DNA in real time. In turn, the amount of amplified DNA provides an estimate of the amount of cDNA present in the sample that is specifically recognized by the used primers.

Performance

qPCR was performed using LightCycler FastStart DNA Master SYBER Green. cDNA was diluted in a ratio of 1:10 before use. For LightCycler reaction, a mastermix was prepared as listed below and the mixture was filled in the LightCycler glass capillaries after adding the cDNA. Capillaries were centrifuged before qPCR was carried out with the LightCycler instrument (all purchased from Roche Diagnostics), using the protocol as stated below. Dilution series (10^{-3}, 10^{-5}, 10^{-7}, and 10^{-9}) of former LightCycler amplification products were prepared to generate calibration curves, needed to determine PCR efficiencies later on. As negative control, template DNA was replaced by PCR-grade water. To document the specificity of the desired PCR products, samples were electrophoretically separated on a 2 % (w/v) agarose gel and analyzed on a UV luminescent

screen. As the specificity of a particular DNA product can also be assessed by monitoring the melting temperature of the amplified PCR products, LightCycler melting curve analysis was performed in addition according to manufacturer's instructions.

Mastermix	**1x**
Roche SYBER green mix	1 µl
$MgCl_2$ (25 µM))	0.8 µl
Primer 1 (10 µM)	0.5 µl
Primer 2 (10 µM)	0.5 µl
H_2O	6.2 µl
cDNA	1 µl
Volume per Capillary	10 µl

LightCycler run protocol		
Starting temperature	95 °C	10'
Cyclic denaturation	95 °C	1"
Cyclic annealing	54-65 °C	10"
Cyclic elongation	72 °C	16"
Melting	70-97 °C	10'
Cooling	40 °C	15'
Transitionrate	0.1 °C/sec.	
# cycles	40	

Primers

Using Primer3 software, primers were designed to produce amplification products with the length of 300 to 400 bp. In addition, primers spanned always two flanked exons, to eliminate the possibility that contaminating genomic DNA would be amplified. Primers are listed in 7.6.

Data normalization and processing

In order to correlate the initial number of template molecules with real-time fluorescent curves, a certain quantity that is referred to as the crossing point (CP) needs to be determined for each transcript. The CP is defined as the point at which the fluorescence signal appreciably exceeds the background fluorescence (Higuchi *et al.*, 1992). Thereby, the CP indicates the fractional cycle number at which the fluorescence signal reaches this fixed threshold. At the CP, the number of formed amplification products is supposed to be the same in all samples that are being compared. This number is assumed to be about 10^{10} copies. Furthermore, the PCR efficiency of each run has to be determined for the correlation. Therefore, serial dilutions of LightCycler products were carried out for each run. By plotting the CP cycles versus the logarithm of the dilution factor of product input, a standard curve is obtained. The corresponding PCR efficiency (E) of one run was calculated from the given slope of the standard curve according to the equation

$$E = 10^{(1/slope)} \qquad \text{(Rasmussen, 2001)} \qquad (1)$$

In order to quantify the amount of a target transcript present in one sample, the relative quantification method was applied, which is based on the relative mRNA expression of a target gene versus a reference gene. Therefore, a stable and securely unregulated gene, such as a housekeeping gene, is applicable. The gene encoding human ribosomal protein L23a, which is a component of the 60S subunit of the ribosome, was employed as reference gene, since its mRNA expression is considered to be stable, even under experimental treatment.

Based on the following mathematical assumptions, the amount of a target transcript that is initially present can be quantified. Assuming that $X(target)_{CP}$ is the number of target molecules present at the crossing point CP_{target}, $X(target)_0$ is the initial number of target molecules, and E_{target} is the PCR efficiency of target amplification, an equation can be set up as follows:

$$X(target)_{CP} = X(target)_0 \cdot (E_{target})^{CP_{target}} \qquad (2)$$

A similar equation for the reference reaction is

$$X(ref)_{CP} = X(ref)_0 \cdot (E_{ref})^{CP_{ref}} \qquad (3)$$

where $X(ref)_{CP}$ is the number of reference molecules present at the crossing point CP_{ref}, $X(ref)_0$ is the number of reference molecules initially present, and E_{ref} is the PCR efficiency of reference amplification. Presuming that the number of molecules present at the crossing point is the same both in the target and the reference amplification reaction, the following equation can be arranged:

$$X(target)_0 \cdot (E_{target})^{CP_{target}} = X(ref)_0 \cdot (E_{ref})^{CP_{ref}} \qquad (4)$$

Setting $X(ref)_0$ equal to 1, the initial number of target molecules can be calculated as follows:

$$X(target)_0 = \frac{(E_{ref})^{CP_{ref}}}{(E_{target})^{CP_{target}}} \qquad (5)$$

This is referred to as the relative concentration of target molecules compared to the number of reference molecules, initially present in the sample. In the majority of cases, the comparison of the relative concentration in one sample with the relative concentration in a corresponding control, for instance in respect of a special kind of treatment, the time, or the genotype, is especially necessary. Therefore, the relative expression ratio of target mRNA compared to the reference mRNA is calculated from the PCR efficiencies and the crossing point of the sample versus a control.

$$ratio = \frac{(X(target)_0)_{sample}}{(X(target)_0)_{control}} = \left(\frac{(E_{ref})^{CP_{ref}}}{(E_{target})^{CP_{target}}}\right)_{sample} \div \left(\frac{(E_{ref})^{CP_{ref}}}{(E_{target})^{CP_{target}}}\right)_{control}$$

This can be simplified to the equation as follows:

$$ratio = \frac{(E_{target})^{\Delta CP_{target}(control-sample)}}{(E_{ref})^{\Delta CP_{ref}(control-sample)}} \quad \text{(Pfaffl, 2001b)} \quad (6)$$

with ΔCP_{target} is the CP derivation of (control – sample) of the target gene transcript and ΔCP_{ref} is the CP derivation of (control – sample) of the reference gene transcript. Having generated three biological replicates, one experimental run was performed from each cDNA and the E^{CP} mean value was determined to calculate the relative expression ratio (*R*) according to equation 6. EREB2.5 cells were sampled at different time points *(t = 0, 8, 24, 72 hours)* to monitor the mRNA expression of target genes over a period of time. In order to calculate R_{time}, values obtained at the time point *t = 0 hours* were set as control, and thus all residuals values are normalized to *t = 0 hours*. R_{time} of each biological repeat was determined separately before averaging the results. Data analyses were carried out using Excel software (Microsoft).

8.3.6 Protein detection

8.3.6.1 Protein isolation

Following MACS purification, B cells were subsequently rested for one hour in B cell medium containing 1 % (v/v) FCS at 37 °C before proteins were isolated. Cells were washed twice with ice-cold PBS before protein extraction. To prepare whole-cell extracts, 20 µl of 2x NP40 lysis buffer (100 mM Tris pH 7.4, 300 mM NaCl, 4 mM EDTA, 2 % (v/v) NP40) containing freshly added phosphatase inhibitors (Halt phosphatase inhibitor cocktail, Pierce) and protease inhibitors (Mini Complete, Roche Diagnostics) were added to a pellet of $5x10^6$ B cells without resuspension and the tube was shaken on a vortexer at 4 °C for 20 minutes. Cell debris and DNA was separated from the protein supernatant by centrifugation at maximum speed for 15 minutes at 4 °C. For B cell fractionation, $2x10^7$ B cells were incubated in 100 µl buffer A (10 mM HEPES pH 7.9, 10 mM KCl, 0.1 mM EDTA, 0.1 mM EGTA, 1 mM DTT, 1x protease inhibitors) for 15 minutes on ice. After the addition of 6.75 µl 10 % (v/v) NP40 and shaking for five minutes at 4 °C, nuclei were spun down at maximum speed for 15 minutes, and the supernatant containing the cytoplasmic fraction was saved. Nuclei were washed once with buffer A before lysis in 40 µl buffer C (20 mM HEPES pH 7.9, 0.4 M NaCl, 1 mM EDTA, 1 mM EGTA, 1 mM DTT, 1x protease inhibitors). After shaking at 4 °C for 30 minutes and centrifugation at maximum speed for 15 minutes, the supernatant containing the nuclear fraction was saved. Protein samples were subsequently frozen at -80 °C.

8.3.6.2 SDS polyacrylamide gel electrophoresis (PAGE)

The protein concentration of each sample was quantified using a Bradford reagent (DC protein assay, Bio-Rad) according to manufacturer's instructions and a bovine serum albumin standard slope. Protein mixtures were separated by discontinuous SDS PAGE (Laemmli, 1970). In

discontinuous PAGE, the acrylamide gel is composed of a stacking gel (5 % (v/v) acrylamide, 0.625 mM Tris pH 6.8, 0.1 % (w/v) SDS, 0.1 % (w/v) APS, 0.006 % (w/v) TEMED), in which negatively charged proteins are focused at the separation line, and a resolving gel (10 to 12 % (v/v) acrylamide, 3.75 mM Tris pH 6.8, 0.1 % (w/v) SDS, 0.1 % (w/v) APS, 0.004 % (w/v) TEMED), in which proteins are separated according to molecular weight. 5x Laemmli buffer (300 mM Tris pH 6.8, 7.5 % (w/v) SDS, 50 % (v/v) glycerin, 0.01 % (v/v) bromphenol blue, 1 % (v/v) β-mercaptoethanol) was added to the samples to a concentration of 1x before heating the samples at 70 °C for 10 minutes and loading denatured proteins onto a SDS polyacrylamide gel together with a protein standard (Benchmark™, Invitrogen). Electrophoresis was accomplished in Laemmli running buffer (25 mM Tris base, 0.2 M glycine, 0.1 % (v/v) SDS) at 20 to 40 mA per gel, using a Bio-Rad electrophoresis chamber.

8.3.6.3 Western blotting

After having separated proteins by SDS PAGE, proteins were transferred onto a polyvinyliden fluoride (PVDF) membrane by using electrical current (Western blotting, Towbin *et al.*, 1979). Proteins were blotted to the PVDF membrane (Immobilon™ P membrane, Millipore) by wet transfer for three hours at 250 mA in transfer buffer (25 mM Tris base, 0.2 M glycine, 20 % (v/v) methanol), utilizing a Bio-Rad mini tank blotting chamber on a magnetic stirrer in the cold room. To verify protein transfer and equal loading, the membrane was incubated for five minutes in Ponceau S solution (Sigma) to stain proteins non-specifically.

8.3.6.4 Immunostaining

To block non-specific binding sites, membranes were incubated for one hour in TBST (0.1 M Tris/HCl pH 7.5, 0.1 M NaCl, 0.02 % (v/v) tween), containing 5 % (w/v) milk powder, with slight shaking. Incubation with the primary antibody was performed over night at 4 °C in TBST, containing 5 % (w/v) BSA, unless stated otherwise in chapter 7.8. The membrane was incubated with the secondary antibody, conjugated to HRP, diluted in TBST, containing 1 % (w/v) milk powder, for two hours at RT. Antibody incubation was always performed on a roller and the membranes were washed three times in between and afterwards with TBST for seven minutes with vigorous shaking. Proteins were visualized using Enhanced Chemiluminescence ECL™ (GE Healthcare) according to manufacturer's instructions. Signals were detected by the exposition of photosensitive films (CEA RP new) using a Cawomat 2000 IR processor (both ErnstChristiansen). For reprobing with further antibodies, bound antibodies were stripped from the membrane by incubating in stripping buffer (62.5 mM Tris/HCl pH 6.8, 2 % (w/v) SDS, 100 mM β-mercaptoethanol) at 56 °C for 30 minutes with slightly shaking.

9 References

Adams, J. M., Harris, A. W., Pinkert, C. A., Corcoran, L. M., Alexander, W. S., Cory, S., Palmiter, R. D. &Brinster, R. L. (1985). The c-myc oncogene driven by immunoglobulin enhancers induces lymphoid malignancy in transgenic mice. *Nature* 318(6046): 533-538.

Allman, D. &Calamito, M. (2009). Instructing B cell fates on the fringe. *Immunity* 30(2): 175-177.

Allman, D., Karnell, F. G., Punt, J. A., Bakkour, S., Xu, L., Myung, P., Koretzky, G. A., Pui, J. C., Aster, J. C. &Pear, W. S. (2001a). Separation of Notch1 promoted lineage commitment and expansion/transformation in developing T cells. *J Exp Med* 194(1): 99-106.

Allman, D., Lindsley, R. C., DeMuth, W., Rudd, K., Shinton, S. A. &Hardy, R. R. (2001b). Resolution of three nonproliferative immature splenic B cell subsets reveals multiple selection points during peripheral B cell maturation. *J Immunol* 167(12): 6834-6840.

Alt, F. W., Yancopoulos, G. D., Blackwell, T. K., Wood, C., Thomas, E., Boss, M., Coffman, R., Rosenberg, N., Tonegawa, S. &Baltimore, D. (1984). Ordered rearrangement of immunoglobulin heavy chain variable region segments. *EMBO J* 3(6): 1209-1219.

Amsen, D., Antov, A., Jankovic, D., Sher, A., Radtke, F., Souabni, A., Busslinger, M., McCright, B., Gridley, T. &Flavell, R. A. (2007). Direct regulation of Gata3 expression determines the T helper differentiation potential of Notch. *Immunity* 27(1): 89-99.

Anzelon, A. N., Wu, H. &Rickert, R. C. (2003). Pten inactivation alters peripheral B lymphocyte fate and reconstitutes CD19 function. *Nat Immunol* 4(3): 287-294.

Attanavanich, K. &Kearney, J. F. (2004). Marginal zone, but not follicular B cells, are potent activators of naive CD4 T cells. *J Immunol* 172(2): 803-811.

Bannish, G., Fuentes-Panana, E. M., Cambier, J. C., Pear, W. S. &Monroe, J. G. (2001). Ligand-independent signaling functions for the B lymphocyte antigen receptor and their role in positive selection during B lymphopoiesis. *J Exp Med* 194(11): 1583-1596.

Bargou, R. C., Emmerich, F., Krappmann, D., Bommert, K., Mapara, M. Y., Arnold, W., Royer, H. D., Grinstein, E., Greiner, A., Scheidereit, C. &Dorken, B. (1997). Constitutive nuclear factor-kappaB-RelA activation is required for proliferation and survival of Hodgkin's disease tumor cells. *J Clin Invest* 100(12): 2961-2969.

Bellavia, D., Campese, A. F., Alesse, E., Vacca, A., Felli, M. P., Balestri, A., Stoppacciaro, A., Tiveron, C., Tatangelo, L., Giovarelli, M., Gaetano, C., Ruco, L., Hoffman, E. S., Hayday, A. C., Lendahl, U., Frati, L., Gulino, A. &Screpanti, I. (2000). Constitutive activation of NF-kappaB and T-cell leukemia/lymphoma in Notch3 transgenic mice. *EMBO J* 19(13): 3337-3348.

Besseyrias, V., Fiorini, E., Strobl, L. J., Zimber-Strobl, U., Dumortier, A., Koch, U., Arcangeli, M. L., Ezine, S., Macdonald, H. R. &Radtke, F. (2007). Hierarchy of Notch-Delta interactions promoting T cell lineage commitment and maturation. *J Exp Med* 204(2): 331-343.

Blaumueller, C. M., Qi, H., Zagouras, P. &Artavanis-Tsakonas, S. (1997). Intracellular cleavage of Notch leads to a heterodimeric receptor on the plasma membrane. *Cell* 90(2): 281-291.

Bonizzi, G., Bebien, M., Otero, D. C., Johnson-Vroom, K. E., Cao, Y., Vu, D., Jegga, A. G., Aronow, B. J., Ghosh, G., Rickert, R. C. &Karin, M. (2004). Activation of IKKalpha target genes depends on recognition of specific kappaB binding sites by RelB:p52 dimers. *EMBO J* 23(21): 4202-4210.

Bonizzi, G. &Karin, M. (2004). The two NF-kappaB activation pathways and their role in innate and adaptive immunity. *Trends Immunol* 25(6): 280-288.

Bornkamm, G. W., Berens, C., Kuklik-Roos, C., Bechet, J. M., Laux, G., Bachl, J., Korndoerfer, M., Schlee, M., Holzel, M., Malamoussi, A., Chapman, R. D., Nimmerjahn, F., Mautner, J., Hillen, W., Bujard, H. &Feuillard, J. (2005). Stringent doxycycline-dependent control of gene activities using an episomal one-vector system. *Nucleic Acids Res* 33(16): e137.

Bossy, D., Milili, M., Zucman, J., Thomas, G., Fougereau, M. &Schiff, C. (1991). Organization and expression of the lambda-like genes that contribute to the mu-psi light chain complex in human pre-B cells. *Int Immunol* 3(11): 1081-1090.

Brazil, D. P., Park, J. &Hemmings, B. A. (2002). PKB binding proteins. Getting in on the Akt. *Cell* 111(3): 293-303.

Buhl, A. M., Pleiman, C. M., Rickert, R. C. &Cambier, J. C. (1997). Qualitative regulation of B cell antigen receptor signaling by CD19: selective requirement for PI3-kinase activation, inositol-1,4,5-trisphosphate production and Ca2+ mobilization. *J Exp Med* 186(11): 1897-1910.

Busslinger, M. (2004). Transcriptional control of early B cell development. *Annu Rev Immunol* 22: 55-79.

Calamito, M., Juntilla, M. M., Thomas, M., Northrup, D. L., Rathmell, J., Birnbaum, M. J., Koretzky, G. &Allman, D. (2009). Akt1 and Akt2 promote peripheral B cell maturation and survival. *Blood*.

Cannell, E. J., Farrell, P. J. &Sinclair, A. J. (1996). Epstein-Barr virus exploits the normal cell pathway to regulate Rb activity during the immortalisation of primary B-cells. *Oncogene* 13(7): 1413-1421.

Cariappa, A., Boboila, C., Moran, S. T., Liu, H., Shi, H. N. &Pillai, S. (2007). The recirculating B cell pool contains two functionally distinct, long-lived, posttransitional, follicular B cell populations. *J Immunol* 179(4): 2270-2281.

Carlyle, J. R. &Zuniga-Pflucker, J. C. (1998). Requirement for the thymus in alphabeta T lymphocyte lineage commitment. *Immunity* 9(2): 187-197.

Carter, R. H., Tuveson, D. A., Park, D. J., Rhee, S. G. &Fearon, D. T. (1991). The CD19 complex of B lymphocytes. Activation of phospholipase C by a protein tyrosine kinase-dependent pathway that can be enhanced by the membrane IgM complex. *J Immunol* 147(11): 3663-3671.

Casola, S., Cattoretti, G., Uyttersprot, N., Koralov, S. B., Seagal, J., Hao, Z., Waisman, A., Egert, A., Ghitza, D. &Rajewsky, K. (2006). Tracking germinal center B cells expressing germ-line immunoglobulin gamma1 transcripts by conditional gene targeting. *Proc Natl Acad Sci U S A* 103(19): 7396-7401.

Cazac, B. B. &Roes, J. (2000). TGF-beta receptor controls B cell responsiveness and induction of IgA in vivo. *Immunity* 13(4): 443-451.

Chen, L., Monti, S., Juszczynski, P., Daley, J., Chen, W., Witzig, T. E., Habermann, T. M., Kutok, J. L. &Shipp, M. A. (2008). SYK-dependent tonic B-cell receptor signaling is a rational treatment target in diffuse large B-cell lymphoma. *Blood* 111(4): 2230-2237.

Chiang, M. Y., Xu, L., Shestova, O., Histen, G., L'Heureux, S., Romany, C., Childs, M. E., Gimotty, P. A., Aster, J. C. &Pear, W. S. (2008). Leukemia-associated NOTCH1 alleles are weak tumor initiators but accelerate K-ras-initiated leukemia. *J Clin Invest* 118(9): 3181-3194.

Chung, J. B., Silverman, M. &Monroe, J. G. (2003). Transitional B cells: step by step towards immune competence. *Trends Immunol* 24(6): 343-349.

Ciofani, M., Knowles, G. C., Wiest, D. L., von Boehmer, H. &Zuniga-Pflucker, J. C. (2006). Stage-specific and differential notch dependency at the alphabeta and gammadelta T lineage bifurcation. *Immunity* 25(1): 105-116.

Clayton, E., Bardi, G., Bell, S. E., Chantry, D., Downes, C. P., Gray, A., Humphries, L. A., Rawlings, D., Reynolds, H., Vigorito, E. &Turner, M. (2002). A crucial role for the p110delta subunit of phosphatidylinositol 3-kinase in B cell development and activation. *J Exp Med* 196(6): 753-763.

Cully, M., You, H., Levine, A. J. &Mak, T. W. (2006). Beyond PTEN mutations: the PI3K pathway as an integrator of multiple inputs during tumorigenesis. *Nat Rev Cancer* 6(3): 184-192.

Dal Porto, J. M., Gauld, S. B., Merrell, K. T., Mills, D., Pugh-Bernard, A. E. &Cambier, J. (2004). B cell antigen receptor signaling 101. *Mol Immunol* 41(6-7): 599-613.

Dallman, C., Johnson, P. W. &Packham, G. (2003). Differential regulation of cell survival by CD40. *Apoptosis* 8(1): 45-53.

Daly, T. M., Okuyama, T., Vogler, C., Haskins, M. E., Muzyczka, N. &Sands, M. S. (1999a). Neonatal intramuscular injection with recombinant adeno-associated virus results in prolonged beta-glucuronidase expression in situ and correction of liver pathology in mucopolysaccharidosis type VII mice. *Hum Gene Ther* 10(1): 85-94.

Daly, T. M., Vogler, C., Levy, B., Haskins, M. E. &Sands, M. S. (1999b). Neonatal gene transfer leads to widespread correction of pathology in a murine model of lysosomal storage disease. *Proc Natl Acad Sci U S A* 96(5): 2296-2300.

Dammers, P. M., de Boer, N. K., Deenen, G. J., Nieuwenhuis, P. &Kroese, F. G. (1999). The origin of marginal zone B cells in the rat. *Eur J Immunol* 29(5): 1522-1531.

Dejardin, E., Droin, N. M., Delhase, M., Haas, E., Cao, Y., Makris, C., Li, Z. W., Karin, M., Ware, C. F. &Green, D. R. (2002). The lymphotoxin-beta receptor induces different patterns of gene expression via two NF-kappaB pathways. *Immunity* 17(4): 525-535.

Derudder, E., Dejardin, E., Pritchard, L. L., Green, D. R., Korner, M. &Baud, V. (2003). RelB/p50 dimers are differentially regulated by tumor necrosis factor-alpha and lymphotoxin-beta receptor activation: critical roles for p100. *J Biol Chem* 278(26): 23278-23284.

Dirmeier, U., Hoffmann, R., Kilger, E., Schultheiss, U., Briseno, C., Gires, O., Kieser, A., Eick, D., Sugden, B. &Hammerschmidt, W. (2005). Latent membrane protein 1 of Epstein-Barr virus coordinately regulates proliferation with control of apoptosis. *Oncogene* 24(10): 1711-1717.

DiSanto, J. P., Bonnefoy, J. Y., Gauchat, J. F., Fischer, A. &de Saint Basile, G. (1993). CD40 ligand mutations in x-linked immunodeficiency with hyper-IgM. *Nature* 361(6412): 541-543.

Edry, E. &Melamed, D. (2004). Receptor editing in positive and negative selection of B lymphopoiesis. *J Immunol* 173(7): 4265-4271.

Elgueta, R., Benson, M. J., de Vries, V. C., Wasiuk, A., Guo, Y. &Noelle, R. J. (2009). Molecular mechanism and function of CD40/CD40L engagement in the immune system. *Immunol Rev* 229(1): 152-172.

Ellisen, L. W., Bird, J., West, D. C., Soreng, A. L., Reynolds, T. C., Smith, S. D. &Sklar, J. (1991). TAN-1, the human homolog of the Drosophila notch gene, is broken by chromosomal translocations in T lymphoblastic neoplasms. *Cell* 66(4): 649-661.

Engel, P., Zhou, L. J., Ord, D. C., Sato, S., Koller, B. &Tedder, T. F. (1995). Abnormal B lymphocyte development, activation, and differentiation in mice that lack or overexpress the CD19 signal transduction molecule. *Immunity* 3(1): 39-50.

Fang, T. C., Yashiro-Ohtani, Y., Del Bianco, C., Knoblock, D. M., Blacklow, S. C. &Pear, W. S. (2007). Notch directly regulates Gata3 expression during T helper 2 cell differentiation. *Immunity* 27(1): 100-110.

Forster, I. &Rajewsky, K. (1990). The bulk of the peripheral B-cell pool in mice is stable and not rapidly renewed from the bone marrow. *Proc Natl Acad Sci U S A* 87(12): 4781-4784.

Gay, D., Saunders, T., Camper, S. &Weigert, M. (1993). Receptor editing: an approach by autoreactive B cells to escape tolerance. *J Exp Med* 177(4): 999-1008.

Gilfillan, S., Dierich, A., Lemeur, M., Benoist, C. &Mathis, D. (1993). Mice lacking TdT: mature animals with an immature lymphocyte repertoire. *Science* 261(5125): 1175-1178.

Gold, M. R. (2003). Akt is TCL-ish: implications for B-cell lymphoma. *Trends Immunol* 24(3): 104-108.

Gordadze, A. V., Peng, R., Tan, J., Liu, G., Sutton, R., Kempkes, B., Bornkamm, G. W. &Ling, P. D. (2001). Notch1IC partially replaces EBNA2 function in B cells immortalized by Epstein-Barr virus. *J Virol* 75(13): 5899-5912.

Gray, D., Siepmann, K., van Essen, D., Poudrier, J., Wykes, M., Jainandunsing, S., Bergthorsdottir, S. &Dullforce, P. (1996). B-T lymphocyte interactions in the generation and survival of memory cells. *Immunol Rev* 150: 45-61.

Grossman, S. R., Johannsen, E., Tong, X., Yalamanchili, R. &Kieff, E. (1994). The Epstein-Barr virus nuclear antigen 2 transactivator is directed to response elements by the J kappa recombination signal binding protein. *Proc Natl Acad Sci U S A* 91(16): 7568-7572.

Grumont, R. J., Strasser, A. &Gerondakis, S. (2002). B cell growth is controlled by phosphatidylinosotol 3-kinase-dependent induction of Rel/NF-kappaB regulated c-myc transcription. *Mol Cell* 10(6): 1283-1294.

Guan, E., Wang, J., Laborda, J., Norcross, M., Baeuerle, P. A. &Hoffman, T. (1996). T cell leukemia-associated human Notch/translocation-associated Notch homologue has I kappa B-like activity and physically interacts with nuclear factor-kappa B proteins in T cells. *J Exp Med* 183(5): 2025-2032.

Guo, B., Kato, R. M., Garcia-Lloret, M., Wahl, M. I. &Rawlings, D. J. (2000). Engagement of the human pre-B cell receptor generates a lipid raft-dependent calcium signaling complex. *Immunity* 13(2): 243-253.

Gururajan, M., Jennings, C. D. &Bondada, S. (2006). Cutting edge: constitutive B cell receptor signaling is critical for basal growth of B lymphoma. *J Immunol* 176(10): 5715-5719.

Gutierrez, A. &Look, A. T. (2007). NOTCH and PI3K-AKT pathways intertwined. *Cancer Cell* 12(5): 411-413.

Han, H., Tanigaki, K., Yamamoto, N., Kuroda, K., Yoshimoto, M., Nakahata, T., Ikuta, K. &Honjo, T. (2002). Inducible gene knockout of transcription factor recombination signal binding protein-J reveals its essential role in T versus B lineage decision. *Int Immunol* 14(6): 637-645.

Hanissian, S. H. &Geha, R. S. (1997). Jak3 is associated with CD40 and is critical for CD40 induction of gene expression in B cells. *Immunity* 6(4): 379-387.

Hao, Z. &Rajewsky, K. (2001). Homeostasis of peripheral B cells in the absence of B cell influx from the bone marrow. *J Exp Med* 194(8): 1151-1164.

Harnett, M. M. (2004). CD40: a growing cytoplasmic tale. *Sci STKE* 2004(237): pe25.

Harnett, M. M., Katz, E. &Ford, C. A. (2005). Differential signalling during B-cell maturation. *Immunol Lett* 98(1): 33-44.

Hay, N. (2005). The Akt-mTOR tango and its relevance to cancer. *Cancer Cell* 8(3): 179-183.

Henkel, T., Ling, P. D., Hayward, S. D. &Peterson, M. G. (1994). Mediation of Epstein-Barr virus EBNA2 transactivation by recombination signal-binding protein J kappa. *Science* 265(5168): 92-95.

Higuchi, R., Dollinger, G., Walsh, P. S. &Griffith, R. (1992). Simultaneous amplification and detection of specific DNA sequences. *Biotechnology (N Y)* 10(4): 413-417.

Hitz, C., Wurst, W. &Kuhn, R. (2007). Conditional brain-specific knockdown of MAPK using Cre/loxP regulated RNA interference. *Nucleic Acids Res* 35(12): e90.

Hobeika, E., Thiemann, S., Storch, B., Jumaa, H., Nielsen, P. J., Pelanda, R. &Reth, M. (2006). Testing gene function early in the B cell lineage in mb1-cre mice. *Proc Natl Acad Sci U S A* 103(37): 13789-13794.

Hofelmayr, H., Strobl, L. J., Marschall, G., Bornkamm, G. W. &Zimber-Strobl, U. (2001). Activated Notch1 can transiently substitute for EBNA2 in the maintenance of proliferation of LMP1-expressing immortalized B cells. *J Virol* 75(5): 2033-2040.

Homig-Holzel, C., Hojer, C., Rastelli, J., Casola, S., Strobl, L. J., Muller, W., Quintanilla-Martinez, L., Gewies, A., Ruland, J., Rajewsky, K. &Zimber-Strobl, U. (2008). Constitutive CD40 signaling in B cells selectively activates the noncanonical NF-kappaB pathway and promotes lymphomagenesis. *J Exp Med* 205(6): 1317-1329.

Hozumi, K., Negishi, N., Suzuki, D., Abe, N., Sotomaru, Y., Tamaoki, N., Mailhos, C., Ish-Horowicz, D., Habu, S. &Owen, M. J. (2004). Delta-like 1 is necessary for the generation of marginal zone B cells but not T cells in vivo. *Nat Immunol* 5(6): 638-644.

Hsu, B. L., Harless, S. M., Lindsley, R. C., Hilbert, D. M. &Cancro, M. P. (2002). Cutting edge: BLyS enables survival of transitional and mature B cells through distinct mediators. *J Immunol* 168(12): 5993-5996.

Hubmann, R., Schwarzmeier, J. D., Shehata, M., Hilgarth, M., Duechler, M., Dettke, M. &Berger, R. (2002). Notch2 is involved in the overexpression of CD23 in B-cell chronic lymphocytic leukemia. *Blood* 99(10): 3742-3747.

Inui, S., Maeda, K., Hua, D. R., Yamashita, T., Yamamoto, H., Miyamoto, E., Aizawa, S. &Sakaguchi, N. (2002). BCR signal through alpha 4 is involved in S6 kinase activation and required for B cell maturation including isotype switching and V region somatic hypermutation. *Int Immunol* 14(2): 177-187.

Jacob, J. &Kelsoe, G. (1992). In situ studies of the primary immune response to (4-hydroxy-3-nitrophenyl)acetyl. II. A common clonal origin for periarteriolar lymphoid sheath-associated foci and germinal centers. *J Exp Med* 176(3): 679-687.

Janeway, C., Murphy, K., Travers, P., Walport, M. (2007). Janeway´s immunobiology. *Garland Science, Taylor & Francies Group, LCC, New York and London*, 7th ed.

Jang, M. S., Miao, H., Carlesso, N., Shelly, L., Zlobin, A., Darack, N., Qin, J. Z., Nickoloff, B. J. &Miele, L. (2004). Notch-1 regulates cell death independently of differentiation in murine erythroleukemia cells through multiple apoptosis and cell cycle pathways. *J Cell Physiol* 199(3): 418-433.

Jumaa, H., Wollscheid, B., Mitterer, M., Wienands, J., Reth, M. &Nielsen, P. J. (1999). Abnormal development and function of B lymphocytes in mice deficient for the signaling adaptor protein SLP-65. *Immunity* 11(5): 547-554.

Jundt, F., Acikgoz, O., Kwon, S. H., Schwarzer, R., Anagnostopoulos, I., Wiesner, B., Mathas, S., Hummel, M., Stein, H., Reichardt, H. M. &Dorken, B. (2008). Aberrant expression of Notch1 interferes with the B-lymphoid phenotype of neoplastic B cells in classical Hodgkin lymphoma. *Leukemia* 22(8): 1587-1594.

Jundt, F., Anagnostopoulos, I., Forster, R., Mathas, S., Stein, H. &Dorken, B. (2002a). Activated Notch1 signaling promotes tumor cell proliferation and survival in Hodgkin and anaplastic large cell lymphoma. *Blood* 99(9): 3398-3403.

Jundt, F., Kley, K., Anagnostopoulos, I., Schulze Probsting, K., Greiner, A., Mathas, S., Scheidereit, C., Wirth, T., Stein, H. &Dorken, B. (2002b). Loss of PU.1 expression is associated with defective immunoglobulin transcription in Hodgkin and Reed-Sternberg cells of classical Hodgkin disease. *Blood* 99(8): 3060-3062.

Jundt, F., Probsting, K. S., Anagnostopoulos, I., Muehlinghaus, G., Chatterjee, M., Mathas, S., Bargou, R. C., Manz, R., Stein, H. &Dorken, B. (2004). Jagged1-induced Notch signaling drives proliferation of multiple myeloma cells. *Blood* 103(9): 3511-3515.

Kaiser, C., Laux, G., Eick, D., Jochner, N., Bornkamm, G. W. &Kempkes, B. (1999). The proto-oncogene c-myc is a direct target gene of Epstein-Barr virus nuclear antigen 2. *J Virol* 73(5): 4481-4484.

Kanzler, H., Kuppers, R., Hansmann, M. L. &Rajewsky, K. (1996). Hodgkin and Reed-Sternberg cells in Hodgkin's disease represent the outgrowth of a dominant tumor clone derived from (crippled) germinal center B cells. *J Exp Med* 184(4): 1495-1505.

Katso, R., Okkenhaug, K., Ahmadi, K., White, S., Timms, J. &Waterfield, M. D. (2001). Cellular function of phosphoinositide 3-kinases: implications for development, homeostasis, and cancer. *Annu Rev Cell Dev Biol* 17: 615-675.

Kawabe, T., Naka, T., Yoshida, K., Tanaka, T., Fujiwara, H., Suematsu, S., Yoshida, N., Kishimoto, T. &Kikutani, H. (1994). The immune responses in CD40-deficient mice: impaired immunoglobulin class switching and germinal center formation. *Immunity* 1(3): 167-178.

Kempkes, B., Pawlita, M., Zimber-Strobl, U., Eissner, G., Laux, G. &Bornkamm, G. W. (1995b). Epstein-Barr virus nuclear antigen 2-estrogen receptor fusion proteins transactivate viral and cellular genes and interact with RBP-J kappa in a conditional fashion. *Virology* 214(2): 675-679.

Kempkes, B., Spitkovsky, D., Jansen-Durr, P., Ellwart, J. W., Kremmer, E., Delecluse, H. J., Rottenberger, C., Bornkamm, G. W. &Hammerschmidt, W. (1995a). B-cell proliferation and induction of early G1-regulating proteins by Epstein-Barr virus mutants conditional for EBNA2. *Embo J* 14(1): 88-96.

Khan, W. N., Sideras, P., Rosen, F. S. &Alt, F. W. (1995). The role of Bruton's tyrosine kinase in B-cell development and function in mice and man. *Ann N Y Acad Sci* 764: 27-38.

Khwaja, A. (1999). Akt is more than just a Bad kinase. *Nature* 401(6748): 33-34.

Kidd, S., Kelley, M. R. &Young, M. W. (1986). Sequence of the notch locus of Drosophila melanogaster: relationship of the encoded protein to mammalian clotting and growth factors. *Mol Cell Biol* 6(9): 3094-3108.

Kilger, E., Kieser, A., Baumann, M. &Hammerschmidt, W. (1998). Epstein-Barr virus-mediated B-cell proliferation is dependent upon latent membrane protein 1, which simulates an activated CD40 receptor. *EMBO J* 17(6): 1700-1709.

Kilpinen, S., Autio, R., Ojala, K., Iljin, K., Bucher, E., Sara, H., Pisto, T., Saarela, M., Skotheim, R. I., Bjorkman, M., Mpindi, J. P., Haapa-Paananen, S., Vainio, P., Edgren, H., Wolf, M., Astola, J., Nees, M., Hautaniemi, S. &Kallioniemi, O. (2008). Systematic bioinformatic analysis of expression levels of 17,330 human genes across 9,783 samples from 175 types of healthy and pathological tissues. *Genome Biol* 9(9): R139.

Koch, U. &Radtke, F. (2007). Notch and cancer: a double-edged sword. *Cell Mol Life Sci* 64(21): 2746-2762.

Kohlhof, H., Hampel, F., Hoffmann, R., Burtscher, H., Weidle, U. H., Holzel, M., Eick, D., Zimber-Strobl, U. &Strobl, L. J. (2009). Notch1, Notch2 and EBNA2 signaling differentially affects proliferation and survival of EBV-infected B cells. *Blood*.

Kopan, R. &Ilagan, M. X. (2009). The canonical Notch signaling pathway: unfolding the activation mechanism. *Cell* 137(2): 216-233.

Korthauer, U., Graf, D., Mages, H. W., Briere, F., Padayachee, M., Malcolm, S., Ugazio, A. G., Notarangelo, L. D., Levinsky, R. J. &Kroczek, R. A. (1993). Defective expression of T-cell CD40 ligand causes X-linked immunodeficiency with hyper-IgM. *Nature* 361(6412): 539-541.

Kraus, M., Alimzhanov, M. B., Rajewsky, N. &Rajewsky, K. (2004). Survival of resting mature B lymphocytes depends on BCR signaling via the Igalpha/beta heterodimer. *Cell* 117(6): 787-800.

Kuppers, R. (2009). The biology of Hodgkin's lymphoma. *Nat Rev Cancer* 9(1): 15-27.

Kuppers, R., Schmitz, R., Distler, V., Renne, C., Brauninger, A. &Hansmann, M. L. (2005). Pathogenesis of Hodgkin's lymphoma. *Eur J Haematol Suppl* (66): 26-33.

Kuroda, K., Han, H., Tani, S., Tanigaki, K., Tun, T., Furukawa, T., Taniguchi, Y., Kurooka, H., Hamada, Y., Toyokuni, S. &Honjo, T. (2003). Regulation of marginal zone B cell development by MINT, a suppressor of Notch/RBP-J signaling pathway. *Immunity* 18(2): 301-312.

Kurosaki, T. (1999). Genetic analysis of B cell antigen receptor signaling. *Annu Rev Immunol* 17: 555-592.

Laemmli, U. K. (1970). Cleavage of structural proteins during the assembly of the head of bacteriophage T4. *Nature* 227(5259): 680-685.

Laird, P. W., Zijderveld, A., Linders, K., Rudnicki, M. A., Jaenisch, R. &Berns, A. (1991). Simplified mammalian DNA isolation procedure. *Nucleic Acids Res* 19(15): 4293.

Lam, K. P., Kuhn, R. &Rajewsky, K. (1997). In vivo ablation of surface immunoglobulin on mature B cells by inducible gene targeting results in rapid cell death. *Cell* 90(6): 1073-1083.

Lee, S. Y., Kumano, K., Nakazaki, K., Sanada, M., Matsumoto, A., Yamamoto, G., Nannya, Y., Suzuki, R., Ota, S., Ota, Y., Izutsu, K., Sakata-Yanagimoto, M., Hangaishi, A., Yagita, H., Fukayama, M., Seto, M., Kurokawa, M., Ogawa, S. &Chiba, S. (2009). Gain-of-function mutations and copy number increases of Notch2 in diffuse large B-cell lymphoma. *Cancer Sci* 100(5): 920-926.

Li, X. &Carter, R. H. (1998). Convergence of CD19 and B cell antigen receptor signals at MEK1 in the ERK2 activation cascade. *J Immunol* 161(11): 5901-5908.

Liu, Y. J., de Bouteiller, O. &Fugier-Vivier, I. (1997). Mechanisms of selection and differentiation in germinal centers. *Curr Opin Immunol* 9(2): 256-262.

Logeat, F., Bessia, C., Brou, C., LeBail, O., Jarriault, S., Seidah, N. G. &Israel, A. (1998). The Notch1 receptor is cleaved constitutively by a furin-like convertase. *Proc Natl Acad Sci U S A* 95(14): 8108-8112.

Maillard, I., Tu, L., Sambandam, A., Yashiro-Ohtani, Y., Millholland, J., Keeshan, K., Shestova, O., Xu, L., Bhandoola, A. &Pear, W. S. (2006). The requirement for Notch signaling at the beta-selection checkpoint in vivo is absolute and independent of the pre-T cell receptor. *J Exp Med* 203(10): 2239-2245.

Marshall, A. J., Niiro, H., Yun, T. J. &Clark, E. A. (2000). Regulation of B-cell activation and differentiation by the phosphatidylinositol 3-kinase and phospholipase Cgamma pathway. *Immunol Rev* 176: 30-46.

Martin, F. &Kearney, J. F. (2000). B-cell subsets and the mature preimmune repertoire. Marginal zone and B1 B cells as part of a "natural immune memory". *Immunol Rev* 175: 70-79.

Martin, F. &Kearney, J. F. (2002). Marginal-zone B cells. *Nat Rev Immunol* 2(5): 323-335.

Martin, F., Oliver, A. M. &Kearney, J. F. (2001). Marginal zone and B1 B cells unite in the early response against T-independent blood-borne particulate antigens. *Immunity* 14(5): 617-629.

McCubrey, J. A., Steelman, L. S., Chappell, W. H., Abrams, S. L., Wong, E. W., Chang, F., Lehmann, B., Terrian, D. M., Milella, M., Tafuri, A., Stivala, F., Libra, M., Basecke, J., Evangelisti, C., Martelli, A. M. &Franklin, R. A. (2007). Roles of the Raf/MEK/ERK pathway in cell growth, malignant transformation and drug resistance. *Biochim Biophys Acta* 1773(8): 1263-1284.

Meyer-Bahlburg, A., Bandaranayake, A. D., Andrews, S. F. &Rawlings, D. J. (2009). Reduced c-myc expression levels limit follicular mature B cell cycling in response to TLR signals. *J Immunol* 182(7): 4065-4075.

Michie, A. M., Chan, A. C., Ciofani, M., Carleton, M., Lefebvre, J. M., He, Y., Allman, D. M., Wiest, D. L., Zuniga-Pflucker, J. C. &Izon, D. J. (2007). Constitutive Notch signalling promotes CD4 CD8 thymocyte differentiation in the absence of the pre-TCR complex, by mimicking pre-TCR signals. *Int Immunol* 19(12): 1421-1430.

Moloney, D. J., Panin, V. M., Johnston, S. H., Chen, J., Shao, L., Wilson, R., Wang, Y., Stanley, P., Irvine, K. D., Haltiwanger, R. S. &Vogt, T. F. (2000). Fringe is a glycosyltransferase that modifies Notch. *Nature* 406(6794): 369-375.

Moore, P. A., Belvedere, O., Orr, A., Pieri, K., LaFleur, D. W., Feng, P., Soppet, D., Charters, M., Gentz, R., Parmelee, D., Li, Y., Galperina, O., Giri, J., Roschke, V., Nardelli, B., Carrell, J., Sosnovtseva, S., Greenfield, W., Ruben, S. M., Olsen, H. S., Fikes, J. &Hilbert, D. M. (1999). BLyS: member of the tumor necrosis factor family and B lymphocyte stimulator. *Science* 285(5425): 260-263.

Moran, S. T., Cariappa, A., Liu, H., Muir, B., Sgroi, D., Boboila, C. &Pillai, S. (2007). Synergism between NF-kappa B1/p50 and Notch2 during the development of marginal zone B lymphocytes. *J Immunol* 179(1): 195-200.

Morgan, T.H. (1917). The theory of the gene. *Am Nat* 51(609):513–544.

Morimura, T., Goitsuka, R., Zhang, Y., Saito, I., Reth, M. &Kitamura, D. (2000). Cell cycle arrest and apoptosis induced by Notch1 in B cells. *J Biol Chem* 275(47): 36523-36531.

Morrison, T. B., Weis, J. J. &Wittwer, C. T. (1998). Quantification of low-copy transcripts by continuous SYBR Green I monitoring during amplification. *Biotechniques* 24(6): 954-958, 960, 962.

Muramatsu, M., Kinoshita, K., Fagarasan, S., Yamada, S., Shinkai, Y. &Honjo, T. (2000). Class switch recombination and hypermutation require activation-induced cytidine deaminase (AID), a potential RNA editing enzyme. *Cell* 102(5): 553-563.

Niwa, H., Yamamura, K. &Miyazaki, J. (1991). Efficient selection for high-expression transfectants with a novel eukaryotic vector. *Gene* 108(2): 193-199.

O'Grady, J. T., Stewart, S., Lowrey, J., Howie, S. E. &Krajewski, A. S. (1994). CD40 expression in Hodgkin's disease. *Am J Pathol* 144(1): 21-26.

Oakley, F., Mann, J., Ruddell, R. G., Pickford, J., Weinmaster, G. &Mann, D. A. (2003). Basal expression of IkappaBalpha is controlled by the mammalian transcriptional repressor RBP-J (CBF1) and its activator Notch1. *J Biol Chem* 278(27): 24359-24370.

Oliver, A. M., Martin, F., Gartland, G. L., Carter, R. H. &Kearney, J. F. (1997). Marginal zone B cells exhibit unique activation, proliferative and immunoglobulin secretory responses. *Eur J Immunol* 27(9): 2366-2374.

Oliver, A. M., Martin, F. &Kearney, J. F. (1999). IgMhighCD21high lymphocytes enriched in the splenic marginal zone generate effector cells more rapidly than the bulk of follicular B cells. *J Immunol* 162(12): 7198-7207.

Osipo, C., Golde, T. E., Osborne, B. A. &Miele, L. A. (2008). Off the beaten pathway: the complex cross talk between Notch and NF-kappaB. *Lab Invest* 88(1): 11-17.

Otero, D. C., Omori, S. A. &Rickert, R. C. (2001). Cd19-dependent activation of Akt kinase in B-lymphocytes. *J Biol Chem* 276(2): 1474-1478.

Palomero, T., Lim, W. K., Odom, D. T., Sulis, M. L., Real, P. J., Margolin, A., Barnes, K. C., O'Neil, J., Neuberg, D., Weng, A. P., Aster, J. C., Sigaux, F., Soulier, J., Look, A. T., Young, R. A., Califano, A. &Ferrando, A. A. (2006). NOTCH1 directly regulates c-MYC and activates a feed-forward-loop transcriptional network promoting leukemic cell growth. *Proc Natl Acad Sci U S A* 103(48): 18261-18266.

Palomero, T., Sulis, M. L., Cortina, M., Real, P. J., Barnes, K., Ciofani, M., Caparros, E., Buteau, J., Brown, K., Perkins, S. L., Bhagat, G., Agarwal, A. M., Basso, G., Castillo, M., Nagase, S., Cordon-Cardo, C., Parsons, R., Zuniga-Pflucker, J. C., Dominguez, M. &Ferrando, A. A. (2007). Mutational loss of PTEN induces resistance to NOTCH1 inhibition in T-cell leukemia. *Nat Med* 13(10): 1203-1210.

Pear, W. S., Aster, J. C., Scott, M. L., Hasserjian, R. P., Soffer, B., Sklar, J. &Baltimore, D. (1996). Exclusive development of T cell neoplasms in mice transplanted with bone marrow expressing activated Notch alleles. *J Exp Med* 183(5): 2283-2291.

Pezzutto, A., Dorken, B., Rabinovitch, P. S., Ledbetter, J. A., Moldenhauer, G. &Clark, E. A. (1987). CD19 monoclonal antibody HD37 inhibits anti-immunoglobulin-induced B cell activation and proliferation. *J Immunol* 138(9): 2793-2799.

Pfaffl, M. W. (2001b). A new mathematical model for relative quantification in real-time RT-PCR. *Nucleic Acids Res* 29(9): e45.

Phan, T. G., Gardam, S., Basten, A. &Brink, R. (2005). Altered migration, recruitment, and somatic hypermutation in the early response of marginal zone B cells to T cell-dependent antigen. *J Immunol* 174(8): 4567-4578.

Pillai, S. &Cariappa, A. (2009). The follicular versus marginal zone B lymphocyte cell fate decision. *Nat Rev Immunol* 9(11): 767-777.

Pillai, S., Cariappa, A. &Moran, S. T. (2005). Marginal zone B cells. *Annu Rev Immunol* 23: 161-196.

Pui, J. C., Allman, D., Xu, L., DeRocco, S., Karnell, F. G., Bakkour, S., Lee, J. Y., Kadesch, T., Hardy, R. R., Aster, J. C. &Pear, W. S. (1999). Notch1 expression in early lymphopoiesis influences B versus T lineage determination. *Immunity* 11(3): 299-308.

Radic, M. Z., Erikson, J., Litwin, S. &Weigert, M. (1993). B lymphocytes may escape tolerance by revising their antigen receptors. *J Exp Med* 177(4): 1165-1173.

Radtke, F., Wilson, A., Stark, G., Bauer, M., van Meerwijk, J., MacDonald, H. R. &Aguet, M. (1999). Deficient T cell fate specification in mice with an induced inactivation of Notch1. *Immunity* 10(5): 547-558.

Rajewsky, K. (1996). Clonal selection and learning in the antibody system. *Nature* 381(6585): 751-758.

Rasmussen, R. (2001). Quantification on the LightCycler. *In Meuer, S., Wittwer, C. and Nakagawara, K. (eds), Rapid Cycle Real-time PCR, Methods and Applications* Springer Press, Heidelberg, Germany: 21-34.

Reichlin, A., Hu, Y., Meffre, E., Nagaoka, H., Gong, S., Kraus, M., Rajewsky, K. &Nussenzweig, M. C. (2001). B cell development is arrested at the immature B cell stage in mice carrying a mutation in the cytoplasmic domain of immunoglobulin beta. *J Exp Med* 193(1): 13-23.

Revy, P., Muto, T., Levy, Y., Geissmann, F., Plebani, A., Sanal, O., Catalan, N., Forveille, M., Dufourcq-Labelouse, R., Gennery, A., Tezcan, I., Ersoy, F., Kayserili, H., Ugazio, A. G., Brousse, N., Muramatsu, M., Notarangelo, L. D., Kinoshita, K., Honjo, T., Fischer, A. &Durandy, A. (2000). Activation-induced cytidine deaminase (AID) deficiency causes the autosomal recessive form of the Hyper-IgM syndrome (HIGM2). *Cell* 102(5): 565-575.

Rickert, R. C., Rajewsky, K. &Roes, J. (1995). Impairment of T-cell-dependent B-cell responses and B-1 cell development in CD19-deficient mice. *Nature* 376(6538): 352-355.

Rickert, R. C., Roes, J. &Rajewsky, K. (1997). B lymphocyte-specific, Cre-mediated mutagenesis in mice. *Nucleic Acids Res* 25(6): 1317-1318.

Rohn, J. L., Lauring, A. S., Linenberger, M. L. &Overbaugh, J. (1996). Transduction of Notch2 in feline leukemia virus-induced thymic lymphoma. *J Virol* 70(11): 8071-8080.

Romer, S., Saunders, U., Jack, H. M. &Jehn, B. M. (2003). Notch1 enhances B-cell receptor-induced apoptosis in mature activated B cells without affecting cell cycle progression and surface IgM expression. *Cell Death Differ* 10(7): 833-844.

Ronchini, C. &Capobianco, A. J. (2001). Induction of cyclin D1 transcription and CDK2 activity by Notch(ic): implication for cell cycle disruption in transformation by Notch(ic). *Mol Cell Biol* 21(17): 5925-5934.

Rosati, E., Sabatini, R., Rampino, G., Tabilio, A., Di Ianni, M., Fettucciari, K., Bartoli, A., Coaccioli, S., Screpanti, I. &Marconi, P. (2009). Constitutively activated Notch signaling is involved in survival and apoptosis resistance of B-CLL cells. *Blood* 113(4): 856-865.

Rowley, R. B., Burkhardt, A. L., Chao, H. G., Matsueda, G. R. &Bolen, J. B. (1995). Syk protein-tyrosine kinase is regulated by tyrosine-phosphorylated Ig alpha/Ig beta immunoreceptor tyrosine activation motif binding and autophosphorylation. *J Biol Chem* 270(19): 11590-11594.

Ruland, J., Duncan, G. S., Wakeham, A. &Mak, T. W. (2003). Differential requirement for Malt1 in T and B cell antigen receptor signaling. *Immunity* 19(5): 749-758.

Saiki, R. K., Gelfand, D. H., Stoffel, S., Scharf, S. J., Higuchi, R., Horn, G. T., Mullis, K. B. &Erlich, H. A. (1988). Primer-directed enzymatic amplification of DNA with a thermostable DNA polymerase. *Science* 239(4839): 487-491.

Saiki, R. K., Scharf, S., Faloona, F., Mullis, K. B., Horn, G. T., Erlich, H. A. &Arnheim, N. (1985). Enzymatic amplification of beta-globin genomic sequences and restriction site analysis for diagnosis of sickle cell anemia. *Science* 230(4732): 1350-1354.

Saito, T., Chiba, S., Ichikawa, M., Kunisato, A., Asai, T., Shimizu, K., Yamaguchi, T., Yamamoto, G., Seo, S., Kumano, K., Nakagami-Yamaguchi, E., Hamada, Y., Aizawa, S. &Hirai, H. (2003). Notch2 is preferentially expressed in mature B cells and indispensable for marginal zone B lineage development. *Immunity* 18(5): 675-685.

Samardzic, T., Gerlach, J., Muller, K., Marinkovic, D., Hess, J., Nitschke, L. &Wirth, T. (2002). CD22 regulates early B cell development in BOB.1/OBF.1-deficient mice. *Eur J Immunol* 32(9): 2481-2489.

Sambrook, J. &Russel, D. W. (2001). Molecular Cloning: A Laboratory Manual. 3rd Vol. Cold Spring Harbour Laboratory Press, Cold Spring Harbour, NY.

Samuels, Y. &Ericson, K. (2006). Oncogenic PI3K and its role in cancer. *Curr Opin Oncol* 18(1): 77-82.

Sanger, F., Air, G. M., Barrell, B. G., Brown, N. L., Coulson, A. R., Fiddes, C. A., Hutchison, C. A., Slocombe, P. M. &Smith, M. (1977). Nucleotide sequence of bacteriophage phi X174 DNA. *Nature* 265(5596): 687-695.

Santos, M. A., Sarmento, L. M., Rebelo, M., Doce, A. A., Maillard, I., Dumortier, A., Neves, H., Radtke, F., Pear, W. S., Parreira, L. &Demengeot, J. (2007). Notch1 engagement by Delta-like-1 promotes differentiation of B lymphocytes to antibody-secreting cells. *Proc Natl Acad Sci U S A* 104(39): 15454-15459.

Sarbassov, D. D., Guertin, D. A., Ali, S. M. &Sabatini, D. M. (2005). Phosphorylation and regulation of Akt/PKB by the rictor-mTOR complex. *Science* 307(5712): 1098-1101.

Schmidt-Supprian, M. &Rajewsky, K. (2007). Vagaries of conditional gene targeting. *Nat Immunol* 8(7): 665-668.

Schmitt, T. M., Ciofani, M., Petrie, H. T. &Zuniga-Pflucker, J. C. (2004). Maintenance of T cell specification and differentiation requires recurrent notch receptor-ligand interactions. *J Exp Med* 200(4): 469-479.

Schuhmacher, M., Staege, M. S., Pajic, A., Polack, A., Weidle, U. H., Bornkamm, G. W., Eick, D. &Kohlhuber, F. (1999). Control of cell growth by c-Myc in the absence of cell division. *Curr Biol* 9(21): 1255-1258.

Sharma, V. M., Calvo, J. A., Draheim, K. M., Cunningham, L. A., Hermance, N., Beverly, L., Krishnamoorthy, V., Bhasin, M., Capobianco, A. J. &Kelliher, M. A. (2006). Notch1 contributes to mouse T-cell leukemia by directly inducing the expression of c-myc. *Mol Cell Biol* 26(21): 8022-8031.

Shimizu, K., Chiba, S., Hosoya, N., Kumano, K., Saito, T., Kurokawa, M., Kanda, Y., Hamada, Y. &Hirai, H. (2000). Binding of Delta1, Jagged1, and Jagged2 to Notch2 rapidly induces cleavage, nuclear translocation, and hyperphosphorylation of Notch2. *Mol Cell Biol* 20(18): 6913-6922.

Shin, H. M., Minter, L. M., Cho, O. H., Gottipati, S., Fauq, A. H., Golde, T. E., Sonenshein, G. E. &Osborne, B. A. (2006). Notch1 augments NF-kappaB activity by facilitating its nuclear retention. *Embo J* 25(1): 129-138.

Sinclair, A. J., Palmero, I., Peters, G. &Farrell, P. J. (1994). EBNA-2 and EBNA-LP cooperate to cause G0 to G1 transition during immortalization of resting human B lymphocytes by Epstein-Barr virus. *EMBO J* 13(14): 3321-3328.

Song, H. &Cerny, J. (2003). Functional heterogeneity of marginal zone B cells revealed by their ability to generate both early antibody-forming cells and germinal centers with hypermutation and memory in response to a T-dependent antigen. *J Exp Med* 198(12): 1923-1935.

Southern, E. M., Milner, N. &Mir, K. U. (1997). Discovering antisense reagents by hybridization of RNA to oligonucleotide arrays. *Ciba Found Symp* 209: 38-44; discussion 44-36.

Srinivasan, L., Sasaki, Y., Calado, D. P., Zhang, B., Paik, J. H., DePinho, R. A., Kutok, J. L., Kearney, J. F., Otipoby, K. L. &Rajewsky, K. (2009). PI3 kinase signals BCR-dependent mature B cell survival. *Cell* 139(3): 573-586.

Srivastava, B., Quinn, W. J., 3rd, Hazard, K., Erikson, J. &Allman, D. (2005). Characterization of marginal zone B cell precursors. *J Exp Med* 202(9): 1225-1234.

Stahl, M., Ge, C., Shi, S., Pestell, R. G. &Stanley, P. (2006). Notch1-induced transformation of RKE-1 cells requires up-regulation of cyclin D1. *Cancer Res* 66(15): 7562-7570.

Starr, T. K., Jameson, S. C. &Hogquist, K. A. (2003). Positive and negative selection of T cells. *Annu Rev Immunol* 21: 139-176.

Strobl, L. J., Hofelmayr, H., Marschall, G., Brielmeier, M., Bornkamm, G. W. &Zimber-Strobl, U. (2000). Activated Notch1 modulates gene expression in B cells similarly to Epstein-Barr viral nuclear antigen 2. *J Virol* 74(4): 1727-1735.

Sudo, T., Nishikawa, S., Ohno, N., Akiyama, N., Tamakoshi, M., Yoshida, H. &Nishikawa, S. (1993). Expression and function of the interleukin 7 receptor in murine lymphocytes. *Proc Natl Acad Sci U S A* 90(19): 9125-9129.

Sulis, M. L. &Parsons, R. (2003). PTEN: from pathology to biology. *Trends Cell Biol* 13(9): 478-483.

Suzuki, A., Kaisho, T., Ohishi, M., Tsukio-Yamaguchi, M., Tsubata, T., Koni, P. A., Sasaki, T., Mak, T. W. &Nakano, T. (2003). Critical roles of Pten in B cell homeostasis and immunoglobulin class switch recombination. *J Exp Med* 197(5): 657-667.

Taghon, T., Yui, M. A., Pant, R., Diamond, R. A. &Rothenberg, E. V. (2006). Developmental and molecular characterization of emerging beta- and gammadelta-selected pre-T cells in the adult mouse thymus. *Immunity* 24(1): 53-64.

Tan, J. B., Xu, K., Cretegny, K., Visan, I., Yuan, J. S., Egan, S. E. &Guidos, C. J. (2009). Lunatic and manic fringe cooperatively enhance marginal zone B cell precursor competition for delta-like 1 in splenic endothelial niches. *Immunity* 30(2): 254-263.

Tanigaki, K., Han, H., Yamamoto, N., Tashiro, K., Ikegawa, M., Kuroda, K., Suzuki, A., Nakano, T. &Honjo, T. (2002). Notch-RBP-J signaling is involved in cell fate determination of marginal zone B cells. *Nat Immunol* 3(5): 443-450.

Tarakhovsky, A. (1997). Antigen receptor signalling in B cells. *Res Immunol* 148(7): 457-460.

Thomas, M., Calamito, M., Srivastava, B., Maillard, I., Pear, W. S. &Allman, D. (2007). Notch activity synergizes with B-cell-receptor and CD40 signaling to enhance B-cell activation. *Blood* 109(8): 3342-3350.

Tiegs, S. L., Russell, D. M. &Nemazee, D. (1993). Receptor editing in self-reactive bone marrow B cells. *J Exp Med* 177(4): 1009-1020.

Tonegawa, S. (1993). The Nobel Lectures in Immunology. The Nobel Prize for Physiology or Medicine, 1987. Somatic generation of immune diversity. *Scand J Immunol* 38(4): 303-319.

Towbin, H., Staehelin, T. &Gordon, J. (1979). Electrophoretic transfer of proteins from polyacrylamide gels to nitrocellulose sheets: procedure and some applications. *Proc Natl Acad Sci U S A* 76(9): 4350-4354.

Troen, G., Wlodarska, I., Warsame, A., Hernandez Llodra, S., De Wolf-Peeters, C. &Delabie, J. (2008). NOTCH2 mutations in marginal zone lymphoma. *Haematologica* 93(7): 1107-1109.

Tsuruta, F., Masuyama, N. &Gotoh, Y. (2002). The phosphatidylinositol 3-kinase (PI3K)-Akt pathway suppresses Bax translocation to mitochondria. *J Biol Chem* 277(16): 14040-14047.

van Kooten, C. &Banchereau, J. (2000). CD40-CD40 ligand. *J Leukoc Biol* 67(1): 2-17.

Wade, M. &Wahl, G. M. (2006). c-Myc, genome instability, and tumorigenesis: the devil is in the details. *Curr Top Microbiol Immunol* 302: 169-203.

Walker, L., Carlson, A., Tan-Pertel, H. T., Weinmaster, G. &Gasson, J. (2001). The notch receptor and its ligands are selectively expressed during hematopoietic development in the mouse. *Stem Cells* 19(6): 543-552.

Wang, J., Shelly, L., Miele, L., Boykins, R., Norcross, M. A. &Guan, E. (2001). Human Notch-1 inhibits NF-kappa B activity in the nucleus through a direct interaction involving a novel domain. *J Immunol* 167(1): 289-295.

Wang, Y., Brooks, S. R., Li, X., Anzelon, A. N., Rickert, R. C. &Carter, R. H. (2002). The physiologic role of CD19 cytoplasmic tyrosines. *Immunity* 17(4): 501-514.

Washburn, T., Schweighoffer, E., Gridley, T., Chang, D., Fowlkes, B. J., Cado, D. &Robey, E. (1997). Notch activity influences the alphabeta versus gammadelta T cell lineage decision. *Cell* 88(6): 833-843.

Weng, A. P., Millholland, J. M., Yashiro-Ohtani, Y., Arcangeli, M. L., Lau, A., Wai, C., Del Bianco, C., Rodriguez, C. G., Sai, H., Tobias, J., Li, Y., Wolfe, M. S., Shachaf, C., Felsher, D., Blacklow, S. C., Pear, W. S. &Aster, J. C. (2006). c-Myc is an important direct target of Notch1 in T-cell acute lymphoblastic leukemia/lymphoma. *Genes Dev* 20(15): 2096-2109.

Westendorf, J. J., Ahmann, G. J., Armitage, R. J., Spriggs, M. K., Lust, J. A., Greipp, P. R., Katzmann, J. A. &Jelinek, D. F. (1994). CD40 expression in malignant plasma cells. Role in stimulation of autocrine IL-6 secretion by a human myeloma cell line. *J Immunol* 152(1): 117-128.

Wharton, K. A., Johansen, K. M., Xu, T. &Artavanis-Tsakonas, S. (1985). Nucleotide sequence from the neurogenic locus notch implies a gene product that shares homology with proteins containing EGF-like repeats. *Cell* 43(3 Pt 2): 567-581.

Wienands, J., Schweikert, J., Wollscheid, B., Jumaa, H., Nielsen, P. J. &Reth, M. (1998). SLP-65: a new signaling component in B lymphocytes which requires expression of the antigen receptor for phosphorylation. *J Exp Med* 188(4): 791-795.

Witt, C. M., Hurez, V., Swindle, C. S., Hamada, Y. &Klug, C. A. (2003a). Activated Notch2 potentiates CD8 lineage maturation and promotes the selective development of B1 B cells. *Mol Cell Biol* 23(23): 8637-8650.

Witt, C. M., Won, W. J., Hurez, V. &Klug, C. A. (2003b). Notch2 haploinsufficiency results in diminished B1 B cells and a severe reduction in marginal zone B cells. *J Immunol* 171(6): 2783-2788.

Wolfer, A., Wilson, A., Nemir, M., MacDonald, H. R. &Radtke, F. (2002). Inactivation of Notch1 impairs VDJbeta rearrangement and allows pre-TCR-independent survival of early alpha beta Lineage Thymocytes. *Immunity* 16(6): 869-879.

Wu, L., Maillard, I., Nakamura, M., Pear, W. S. &Griffin, J. D. (2007). The transcriptional coactivator Maml1 is required for Notch2-mediated marginal zone B-cell development. *Blood* 110(10): 3618-3623.

Xu, J., Foy, T. M., Laman, J. D., Elliott, E. A., Dunn, J. J., Waldschmidt, T. J., Elsemore, J., Noelle, R. J. &Flavell, R. A. (1994). Mice deficient for the CD40 ligand. *Immunity* 1(5): 423-431.

Yamazaki, T., Takeda, K., Gotoh, K., Takeshima, H., Akira, S. &Kurosaki, T. (2002). Essential immunoregulatory role for BCAP in B cell development and function. *J Exp Med* 195(5): 535-545.

Yashiro-Ohtani, Y., He, Y., Ohtani, T., Jones, M. E., Shestova, O., Xu, L., Fang, T. C., Chiang, M. Y., Intlekofer, A. M., Blacklow, S. C., Zhuang, Y. &Pear, W. S. (2009). Pre-TCR signaling inactivates Notch1 transcription by antagonizing E2A. *Genes Dev* 23(14): 1665-1676.

Yoon, S. O., Zhang, X., Berner, P., Blom, B. &Choi, Y. S. (2009). Notch ligands expressed by follicular dendritic cells protect germinal center B cells from apoptosis. *J Immunol* 183(1): 352-358.

Young, R. M., Hardy, I. R., Clarke, R. L., Lundy, N., Pine, P., Turner, B. C., Potter, T. A. &Refaeli, Y. (2009). Mouse models of non-Hodgkin lymphoma reveal Syk as an important therapeutic target. *Blood* 113(11): 2508-2516.

Zambrowicz, B. P., Imamoto, A., Fiering, S., Herzenberg, L. A., Kerr, W. G. &Soriano, P. (1997). Disruption of overlapping transcripts in the ROSA beta geo 26 gene trap strain leads to widespread expression of beta-galactosidase in mouse embryos and hematopoietic cells. *Proc Natl Acad Sci U S A* 94(8): 3789-3794.

Zhang, P., Li, W., Wang, Y., Hou, L., Xing, Y., Qin, H., Wang, J., Liang, Y. &Han, H. (2007). Identification of CD36 as a new surface marker of marginal zone B cells by transcriptomic analysis. *Mol Immunol* 44(4): 332-337.

Zimber-Strobl, U. &Strobl, L. J. (2001). EBNA2 and Notch signalling in Epstein-Barr virus mediated immortalization of B lymphocytes. *Semin Cancer Biol* 11(6): 423-434.

Zimber-Strobl, U., Strobl, L. J., Meitinger, C., Hinrichs, R., Sakai, T., Furukawa, T., Honjo, T. &Bornkamm, G. W. (1994). Epstein-Barr virus nuclear antigen 2 exerts its transactivating function through interaction with recombination signal binding protein RBP-J kappa, the homologue of Drosophila Suppressor of Hairless. *EMBO J* 13(20): 4973-4982.

Zweidler-McKay, P. A., He, Y., Xu, L., Rodriguez, C. G., Karnell, F. G., Carpenter, A. C., Aster, J. C., Allman, D. &Pear, W. S. (2005). Notch signaling is a potent inducer of growth arrest and apoptosis in a wide range of B-cell malignancies. *Blood* 106(12): 3898-3906.

10 Appendix

Supplementary Data

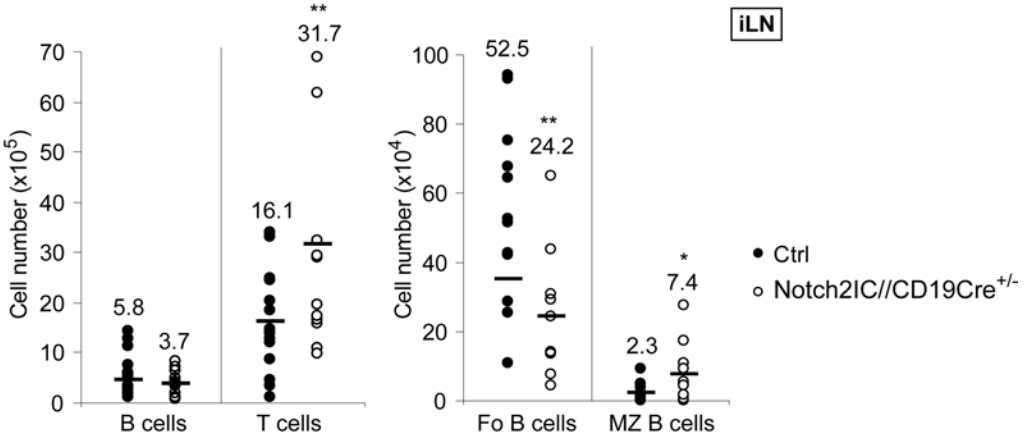

Figure S1 Increased T cell numbers and more MZ-like B cells in the inguinal lymph nodes of Notch2IC//CD19Cre$^{+/-}$ mice. Absolute numbers of lymphocyte-gated, B220^{+} B cells, CD3^{+} T cells, B220^{+}CD21^{int}CD23^{+} Fo B cells, and B220^{+}CD21^{high}CD23^{-} MZ B cells in the inguinal lymph nodes (iLN) of Notch2IC//CD19Cre$^{+/-}$ (blank circle) and control (filled circle) mice. Points represent data from individual mice and horizontal bars mark the mean value, indicated in numbers above each point column. * P < 0.1 ** P < 0.05, in comparison to control, as calculated by the two-tailed student's t-test.

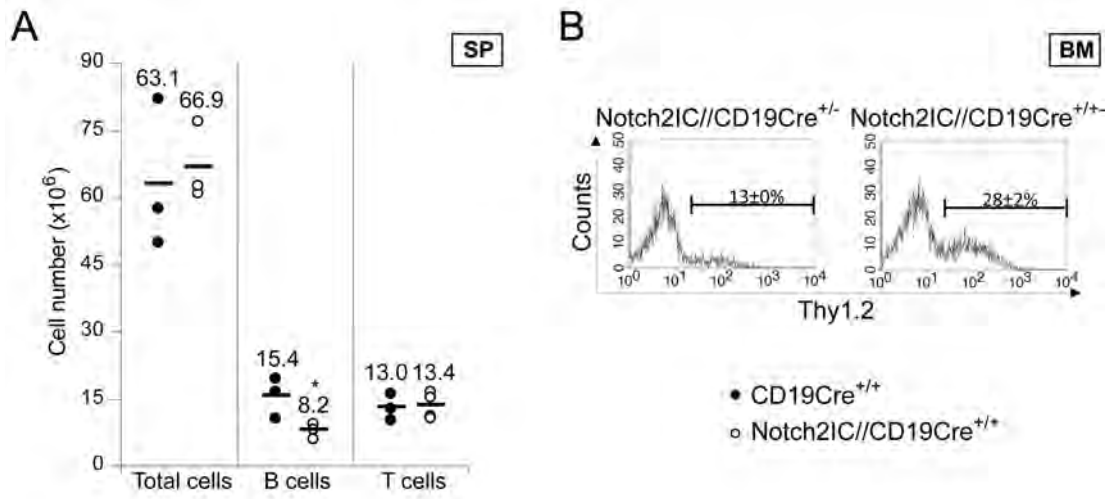

Figure S2 Reduced B cell numbers in the spleen and more Thy1.2^{+} Notch2IC-expressing cells in the bone marrow of Notch2IC//CD19Cre$^{+/+}$ mice. (A) Notch2IC//CD19Cre$^{+/+}$ mice have reduced splenic B cell numbers compared to CD19Cre$^{+/+}$ control mice. Absolute numbers of total counted cells, lymphocyte-gated, B220^{+} B cells, and CD3^{+} T cells in the spleen of Notch2IC//CD19Cre$^{+/+}$ (blank circle) and CD19Cre$^{+/+}$ control (filled circle) mice are displayed. Points represent data from individual mice and horizontal bars mark the mean value, indicated in numbers above each point column. * P < 0.05, in comparison to control, as calculated by the two-tailed student's t-test. **(B)** Higher percentages of Thy1.2^{+} cells within the hCD2^{+} cell population in the bone marrow of Notch2IC//CD19Cre$^{+/+}$ mice compared to Notch2IC//CD19Cre$^{+/-}$ mice. Mean percentages and SD of Thy1.2 expression on lymphocyte-gated, hCD2^{+} cells in the bone marrow of Notch2IC//CD19Cre$^{+/-}$ (left) and Notch2IC//CD19Cre$^{+/+}$ (right) mice are illustrated. Data are representative for two independent experiments.

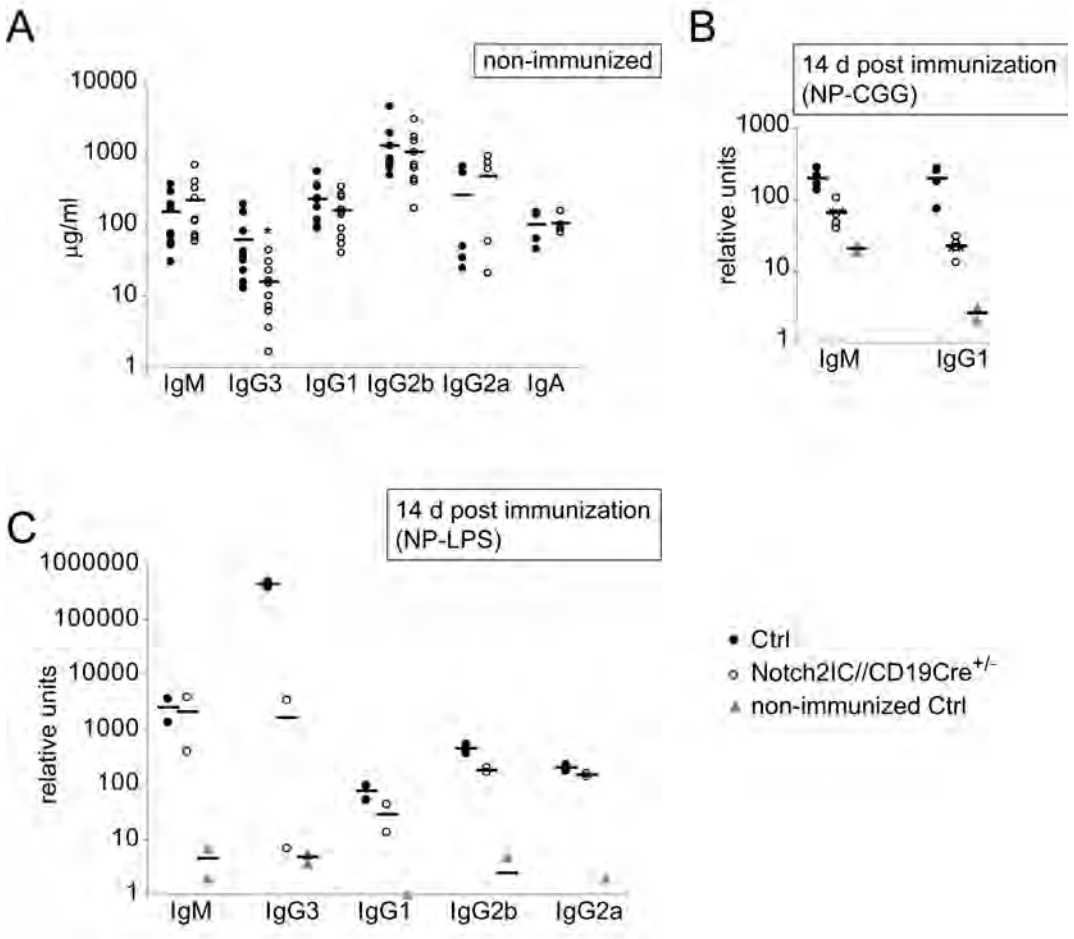

Figure S3 Immunoglobulin titers in non-immunized and immunized Notch2IC//CD19Cre$^{+/-}$ mice. Points represent data from individual mice and horizontal bars mark the mean value. Control (filled circle); Notch2IC//CD19Cre$^{+/-}$ (blank circle); Non-immunized control (filled triangle); * P<0.1, ** P<0.01, in comparison to control. **(A)** Serum concentrations of total immunoglobulin titers of indicated isotypes from 10 to 12 week-old non-immunized mice were determined by ELISA. **(B)** NP-specific antibody response to T cell-dependent antigen. Mice were injected intraperitoneally with 100 µg NP-CGG and concentrations of NP-specific antibodies of the indicated isotypes were measured by ELISA at day 14 after immunization. Four mice were analyzed per group. **(C)** NP-specific antibody response to T cell-independent antigen. Mice were injected intraperitoneally with 50 µg NP-LPS and concentrations of NP-specific antibodies of the indicated isotypes were measured by ELISA at day 14 after immunization. Two mice were analyzed per group.

Table S1

Cell populations in the thymus and inguinal lymph nodes of Notch2IC//mb1Cre$^{+/-}$ and control mice.

	Mice (n)			
Organ:		Thymus	iLN	iLN
Gated on:		Thy1.2^{+} T cells	B220^{+} B cells	Thy1.2^{+} T cells
[x 10^6]				
Ctrl	8	43.8±63.7	0.43±0.30	1.27±0.86
Notch2IC//CD19Cre$^{+/-}$	14	39.4±47.2	0.03±0.02***	1.59±1.23

Percentages within the lymphocyte gate are shown.Values represent the mean ± SD.
*** P<0.001, in comparison to Ctrl.

Acknowledgement

Many people have contributed to the success of this work. Therefore, I would like to mention at least the most important ones (although I could mention many more), and thus I sincerely thank…

…my advisor *PD Ursula Zimber-Strobl*, for giving me the opportunity to pursue my PhD thesis in her laboratory and to work on this interesting project, which made me enthusiastic about research in an unexpected manner…for allowing me such freedom for decision-making, and letting me work very independently, which encouraged me and enabled me to learn a lot…for being willing to listen to problems at any time and for offering her advice as well as constant support at all stages of my work.

…*Prof. Dirk Eick*, for supervising my PhD thesis as well as for his feedback and his scientific support during my PhD time.

…*Prof. Elisabeth Weiß*, for evaluating this work as second examiner.

…*Prof. Wolfgang Hammerschmidt* and *Prof. Georg W. Bornkamm*, for the ability to perform research in the motivating environment and pleasant atmosphere of their institute.

…all members of our research group, especially *Caroline Hojer*, for teaching me a lot of techniques, for exciting discussions about data, and for always supporting me...particularly *Gabrielle Marschall*, for her excellent technical assistance, mainly in mouse immunizations assays and histology, but also for her encouragement during frustrating times…*Cornelia Hömig-Hölzel, Hella Kohlhof* and *Lothar Strobl* for their helpful advice during my work….the new generation of our laboratory for great support during daily lab routine as well as for the enjoyable and cooperative atmosphere in our lab…namely *Petra Fiedler* and *Anne Draeseke,* for nice coffe breaks…*Samantha Feicht*, for nice South American dinners and sharing tjmaxx dreams…*Sabine Schmidl*, for her down-to-earth nature, helping a lot in many cases…*Kristina Djermanovic*, for making my daily life so sparkling.

…all apprentices of our laboratory, who worked with me during the last three years, most notably *Katrin Schlien*, *Franziska Bott* (intern), and *Angela Mieth*, for excellently managing mice genotyping as well as for their interested and motivated nature…*Gerhard Laux* for kindly helping me with any kind of computer problem…*Prof. Berit Jungnickel* for enriching discussions about my project.

…all members of the animal facility, particularly *Michael Hageman*, *Martina Münichsdorfer*, and *Monique Röthig* for taking care of my mice, carefully managing my enormous breeding of various mouse strains, and thus for significantly contributing to this work.

…all collaboration partners, who helped me with the generation of my transgenic mouse line…especially *Susann Bourier*, who taught me not only how to prepare EF cells, but who also offered me via email and phone her excellent expertise in ES cell culture techniques…*Marc Schmidt-Supprian*, not only for providing the targeting vector, but also for helpfully sharing ideas and expertise as well as critical thoughts on my data…*Ralf Kühn* for making the IDG2.3 ES cell line and the associated protocol available…*Adrianne Tasdemir* as well as *Susanne Weidemann*, for their good work when they performed blastocyst injection of my ES cell clones.

…*Brigitte Mack*, who excellently performed all immunohistochemical stainings for hCD2 of this work…*Olivier Gires* for critical project discussions…*Nathalie Uyttersprot* and *Elias Hobeika* for providing the $Ig\beta^{fl(GFP)/\Delta c}$ and mb1-*Cre* mouse strains, respectively…*Silke Raffegerst,* for offering me antibodies at any time…*Petra Prinz* as well as *Josef Myslivietz,* for their patient introduction in the usage of the LSRII FACS.

…all members of the doctoral students initiative DINI, for the enjoyable, productive, and great collaboration within the last three years, most notably the founding members of the "new DINI era", *Sibylle Gündisch*, *Luise Weigand*, *Claudia Brunner*, *Christoph Brenner*, and *Tilman Janzen.*

…on a more personal note, my friends *Petra*, *Beate*, *Kerstin*, and *Micha*, for coming along with me over the last nine years of education and for innumerable lovely moments in private life...*Kerstin*, moreover for kindly proofreading this manuscript…*Petra*, for her friendship in any circumstance, no matter from where in the world…*Rosi* and *Herbert*, for being such great parents-in-law.

…my *beloved parents*, for giving me so many opportunities in life, for their constant support, and for having perpetually believed in my skills.

…my husband *Thomas*, for his everlasting encouragement, his understanding, and his humor… for having been there for me unconditionally and for his infectious positive frame of mind.

Curriculum Vitae

FRANZISKA BARBARA HAMPEL

PERSONAL DATA

Date of Birth	7th April 1982
Place of Birth	Fürstenfeldbruck, Germany
Nationality	German
Marital status	Married
Contact	franziska.hampel@helmholtz-muenchen.de

EDUCATION

10/2004 – 04/2006	Master of Science in Molecular Biotechnology, Technical University of Munich, passed with distinction
10/2001 – 07/2004	Bachelor of Science in Molecular Biotechnology, Technical University of Munich, passed with merit
09/ 1992 – 06/2001	Abitur (general qualification for university entry), Städt. Elsa-Brändström-Gymnasium, Munich, passed with distinction

PRACTICAL EXPERIENCE

Since 05/2007	PhD Thesis at the Helmholtz Center Munich, Institute of Clinical Molecular Biology and Tumor Genetics, as a student of the Ludwig-Maximilians-University Munich, Biology Faculty, Supervisors: PD Dr. Ursula Zimber-Strobl, Prof. Dr. Dirk Eick
10/2006 – 04/2007	Scientific employee at Bio-Rad Laboratories GmbH, Munich, R&D Expression Proteomics
09/2005 – 03/2006	Master Thesis at the Helmholtz Center Munich, Institute of Clinical Molecular Biology and Tumor Genetics, Supervisors: PD Dr. Ursula Zimber-Strobl, PD Dr. Michael Pfaffl
08/2004 – 10/2004	Volunteer Scientist at the National Institutes of Health (NIH), Bethesda, MD, USA, National Institute of Diabetes and Digestive and Kidney Diseases, Supervisor: Dr. Lothar Hennighausen
03/2004 – 06/2004	Bachelor Thesis at the Max-Planck-Institute of Biochemistry, Martinsried, Department of Cellular Biochemistry, Supervisor: Prof. Dr. Jörg Tatzelt

Publications

ARTICLES

Kohlhof H, **Hampel F**, Hoffmann R, Burtscher H, Weidle UH, Eick D, Hölzel M, Zimber-Strobl U, Strobl JL.
Notch1, Notch2 and EBNA2 signaling differentially affects proliferation and survival of EBV-infected B cells.
Blood. 2009 May 28;113(22):5506-15.

Hampel F, Ehrenberg S, Hojer C, Marschall G, Kühn R, Mack B, Gires O, Schmidt-Supprian M, Strobl LJ, Zimber-Strobl U.
CD19 independent instruction of Marginal Zone B cell development by constitutive Notch2 signaling.
Manuscript to be submitted

Hojer C, **Hampel F**, Hömig-Hölzel C, Uyttersprot N, Ferch U, Strobl LJ, Ruland J, Rajewsky K, Zimber-Strobl U.
A new role for CD19 in B cell activation and lymphomagenesis**.**
Manuscript in preparation

POSTER AND ABSTRACTS

Hampel F, Marschall G, Kühn R, Mack B, Gires O, Hobeika E, Strobl LJ, Zimber-Strobl U.
Notch2 signaling is instructive in marginal zone B cell differentiation *in vivo*.
Accepted at Gene Expression & Signaling in the Immune System Meeting of the Cold Spring Harbor Laboratory, Cold Spring Harbor, NY, USA, 04/2010

Schmidl S, Djermanovic K, Hojer C, Hömig-Hölzel C, **Hampel F**, Weih F, Schmidt-Supprian M, Zimber-Strobl U.
The role of NF-κB under the influence of a constant CD40 signal**.**
7th B cell Biology Forum of the Study Group "Biology of B Lymphocytes" of the German Society of Immunology, Salzburg, Austria, 05/2009

Hampel F, Kühn R, Strobl LJ, Zimber-Strobl U.
Generation of a conditional transgenic mouse strain for Notch2IC.
2nd Interact Symposium, Munich, Germany, 04/2009

Kohlhof H, **Hampel F**, Hoffmann R, Burtscher H, Weidle UH, Eick D, Zimber-Strobl U, Strobl JL.
Comparison of Notch and EBNA2 target genes in B cells.
6th B cell Biology Forum of the Study Group "Biology of B Lymphocytes" of the German Society of Immunology, Eibsee, Germany, 04/2008

Paulus A, Posch A, Hausmann M, **Hampel F**, Blankenstein G, Duong TT, Kentsch J, Angres B, Stoll D, Stelzle M.
Subzelluläre Fraktionierung in fluidischem Mikrosystem.
Congress of Microsystems Technologies 2007 of VDE and BMBF, Dresden, Germany, 10/2007

Kohlhof H, **Hampel F**, Hoffmann R, Burtscher H, Weidle UH, Eick D, Zimber-Strobl U, Strobl JL.
The role of Notch and EBNA2 in B cell development and activation.
4th B cell Biology Forum of the Study Group "Biology of B Lymphocytes" of the German Society of Immunology, Bad Staffelstein, Germany, 03/2006